2018

Optimisation of stand-alone hybrid energy systems for power and thermal loads

Barun Kumar Das
Edith Cowan University

Edith Cowan University

Copyright Warning

Optimisation of Stand-alone Hybrid Energy Systems for Power and Thermal Loads

This thesis is presented for the degree of

Doctor of Philosophy

Barun Kumar Das

Edith Cowan University

School of Engineering

2018

USE OF THESIS

The Use of Thesis statement is not included in this version of the thesis.

Abstract

Stand-alone hybrid energy systems are an attractive option for remote communities without a connection to a main power grid. However, the intermittent nature of solar and other renewable sources adversely affects the reliability with which these systems respond to load demands. Hybridisation, achieved by combining renewables with combustion-based supplementary prime movers, improves the ability to meet electric load requirements. In addition, the waste heat generated from backup Internal Combustion Engines or Micro Gas Turbines can be used to satisfy local heating and cooling loads. As a result, there is an expectation that the overall efficiency and Greenhouse Gas Emissions of stand-alone systems can be significantly improved through waste heat recovery.

The aims of this PhD project are to identify how incremental increases to the hardware complexity of hybridised stand-alone energy systems affect their cost, efficiency, and CO_2 footprint. The research analyses a range of systems, from those designed to meet only power requirements to others satisfying power and heating (Combined Heat and Power), or power plus both heating and cooling (Combined Cooling, Heating, and Power). The majority of methods used focus on MATLAB-based Genetic Algorithms (GAs). The modelling deployed finds the optimal selection of hardware configurations which satisfy single- or multi-objective functions (i.e. Cost of Energy, energy efficiency, and exergy efficiency). This is done in the context of highly dynamic meteorological (e.g. solar irradiation) and load data (i.e. electric, heating, and cooling).

Results indicate that the type of supplementary prime movers (ICEs or MGT) and their minimum starting thresholds have insignificant effects on COE but have some effects on Renewable Penetration (RP), Life Cycle Emissions (LCE), CO_2 emissions, and waste heat generation when the system is sized meeting electric load only. However, the transient start-up time of supplementary prime movers and temporal resolution have no significant effects on sizing optimisation. The type of Power Management Strategies (Following Electric Load-FEL, and Following Electric and Following Thermal Load-FEL/FTL) affect overall Combined Heating and Power (CHP) efficiency and meeting thermal demand through recovered heat for a system meeting electric and heating load with response to a specific load meeting reliability (Loss of Power Supply Probability-LPSP). However, the PMS has marginal effects on COE. The Electric to Thermal Load Ratio (ETLR) has no effects on COE for PV/Batt/ICE but strongly affects PV/Batt/MGT-based hybridised CHP systems. The higher thermal than the electric loads lead to higher efficiency and better environmental footprint.

Results from this study also indicate that for a stand-alone hybridised system operating under FEL/FTL type PMS, the power only system has lower cost compared to the CHP and the Combined Cooling, Heating, and Power (CCHP) systems. This occurs at the expense of overall energy and exergy efficiencies. Additionally, the relative magnitude of heating and cooling loads have insignificant effects

on COE for PV/Batt/ICE-based system configurations, however this substantially affects PV/Batt/MGT-based hybridised CCHP systems. Although there are no significant changes in the overall energy efficiency of CCHP systems in relation to variations to heating and cooling loads, systems with higher heating demand than cooling demand lead to better environmental benefits and renewable penetration at the cost of Duty Factor. Results also reveal that the choice of objective functions do not affect the system optimisation significantly.

Keywords: Hybrid energy system; Power management strategy; Waste heat; Cost of energy; Load reliability; Energy efficiency; Exergy efficiency; Renewable penetration; Duty factor.

Declaration

I, Barun Kumar Das, hereby declare that this thesis does not, to the best of my knowledge and belief:

i. Incorporate without acknowledgement any material previously submitted for a degree or diploma in any institution of higher education;

ii. Contain any material previously published or written by another person except where due reference is made in the text; or contain any defamatory material.

Signed 

Barun Kumar Das,

Dated: 14.12.2018

Acknowledgements

I would like to express my sincere gratitude to numerous people who have contributed to this PhD program both technically and emotionally. I am grateful to my principal supervisor A/Prof. Dr. Yasir M Al-Abdeli and associate supervisor Dr. Ganesh Kothapalli for their invaluable guidance, constructive criticism, and continuous support in every aspect throughout this journey at Edith Cowan University. The valuable suggestions, recommendations, and scholarly comments of anonymous reviewers and editors from the various international journals are gratefully acknowledged. These individuals and organisations have helped to improve the quality of the manuscript and to identify future research directions.

The research is facilitated with an Edith Cowan University (ECU) research infrastructure block grant. I would like to acknowledge ECU for awarding me an Australian Government Research Training Program Scholarship (RTP) to enable me to pursue my PhD study program. The generous support from the technical and administration staff of School of Engineering at ECU is highly appreciated.

I am also thankful to the Western Power, a Western Australian State Government-owned corporation, for assisting in relation to the electric load data for simulations undertaken. The Cummins South Pacific and the Optimal Group Australia Pty Ltd are also gratefully acknowledged for their technical support for combustion engines.

I am sincerely grateful to each of my family members, and in particular my parents, for their invaluable encouragement. This journey would never be possible without the endless love and unconditional support from my beautiful wife during this stressful time, even from a far. Finally, I would like to thank my friends, colleagues in Australia and Bangladesh who supported me in every aspect of this endeavour.

List of journal papers arising from this candidature

1. **Das, Barun K**., Al-Abdeli, Yasir M., and Kothapalli, Ganesh, 2017. *Optimisation of stand-alone hybrid energy systems supplemented by combustion-based prime movers.* **Applied Energy,** 196, p. 18-33. Impact Factor: **7.90.**
   doi.org/10.1016/j.apenergy.2017.03.119

2. **Das, Barun K**., and Al-Abdeli, Yasir M., 2017. *Optimisation of stand-alone hybrid CHP systems meeting electric and heating loads.* **Energy Conversion and Management,** 153, p. 391-408. Impact Factor: **6.377.**
   doi.org/10.1016/j.enconman.2017.09.078

3. **Das, Barun K**., Al-Abdeli, Yasir M., and Kothapalli, Ganesh, 2018. *Effect of load following strategies, hardware, and thermal load distribution on stand-alone hybrid CCHP systems.* **Applied Energy,** 220, p. 735-753. Impact Factor: **7.90.**
   doi.org/10.1016/j.apenergy.2018.03.068

4. **Das, Barun K**., Al-Abdeli, Yasir M., and Kothapalli, Ganesh, 2018. *Energy, exergy, and cost optimisation of stand-alone hybrid power, CHP, and CCHP systems.* **(Pending submission).**

5. **Das, Barun K**., Al-Abdeli, Yasir M., and Woolridge, Matthew, 2019. *Effects of battery technology and load scalability on stand-alone PV/ICE hybrid micro-grid system performance.* **Energy, 168, p. 57-69.** Impact Factor: **4.968.**
   doi.org/10.1016/j.energy.2018.11.033

Table of Contents

List of Tables

List of Figures

List of Symbols, Nomenclature

A	Total area of PV modules (m^2)
B_{SOC}	Battery state of charge (%)
$B_{SOC, max}$	Maximum battery state of charge (%)
$B_{SOC, min}$	Minimum battery state of charge (%)
C_A	Annualised cost ($)
C_{A_cap}	Annualised capital cost ($)
C_{A_fuel}	Annualised fuel cost ($)
$C_{A\_O\&M}$	Annualised operation and maintenance cost ($)
C_b	Nominal battery capacity (kWh)
C_{fuel_sup}	Fuel consumption rate for supplementary prime movers (kg/h)
C_{fuel_ICE}	Fuel consumption rate for ICE (l/h, kg/h)
C_{fuel_MGT}	Fuel consumption rate for MGT (l/h, kg/h)
C_0	Capital cost ($)
c_{pg}	Specific heat capacity of exhaust gas (kJ/kg K)
c_{pf}	Specific heat capacity of fuel (kJ/kg K)
COP_{AC}	Coefficient of performance of absorption chiller
COP_{EC}	Coefficient of performance of electric chiller
d	Discount rate (%)
$\dot{E}$	Exergy rate (kW)
E_L	Energy load demand (kWh)
EC_{cool}	Cooling energy output from electric chiller (kW)
E_s	Useful energy production from the system (kWh)
E_{cool}	Cooling energy demand (kWh)
E_{elec}	Electrical energy demand (kWh)
E_{heat}	Heating energy demand (kWh)
EWH_{heat}	Heating energy output from electric water heater (kW)
E_{ther}	Thermal energy demand (kW)
$\dot{E}_{dest}$	Exergy destruction rate (kW)
$\dot{E}_{heat}$	Exergy transfer rate by heat (kW)
$\dot{E}_{in}$	Input energy rate (kW)
$\dot{E}_{out}$	Output energy rate (kW)
E_{sup}	Energy generation by supplementary prime movers (kWh)
$\dot{E}_{system}$	System energy rate (kW)
$\dot{E}x_f$	Fuel exergy rate (kW)

$E_{x,in}$	Exergy rate of solar irradiance (kW)
$E_{x,out}$	Output exergy (kW)
$E_{x,elec}$	Electrical exergy of PV module (kW)
$E_{x,ther}$	Thermal exergy of PV module (kW)
F	Objective function (Genetic Algorithm)
F_{sup}	Fuel energy (kW)
F_{ICE}	Fuel energy to ICE (kW)
F_{MGT}	Fuel energy to MGT (kW)
G	Solar irradiation (kW/m^2), inequality constraints (Genetic Algorithm)
G_{ref}	Reference solar irradiation (kW/m^2)
H	Equality constraints (Genetic Algorithm)
h	Enthalpy (kJ/kg)
h	Enthalpy at reference temperature (kJ/kg)
h_{conv}	Convective heat transfer coefficient (W/m^{2}K)
h_{rad}	Radiative heat transfer coefficient (W/m^{2}K)
I_D	PV diode current (A)
I_{sh}	PV shunt current (A)
I_L	PV light current (A)
$I_{L,ref}$	PV short circuit current at reference temperature (A)
I_{mp}	PV maximum power point current (A)
I_o	PV diode reverse saturation current (A)
I_{PV}	PV saturation current (A)
I_{sc}	PV short circuit current (A)
LPS_{elec}	Loss of Power Supply, i.e reliability of meeting electric load (kWh)
LPS_{heat}	Loss of Power Supply, i.e reliability of meeting heating load (kWh)
LPS_{cool}	Loss of Power Supply, i.e reliability of meeting cooling load (kWh)
$LPSP_{comp}$	Computed loss of power supply probability
$LPSP_{max}$	Maximum loss of power supply probability
LPS_{ther}	Loss of Power Supply, i.e reliability of meeting thermal load (kWh)
$\dot{m}$	Mass flow rate (kg/s)
$\dot{m}_g$	Exhaust gas mass flow rate (kg/h)
$\dot{M}_{Exh\_ICE}$	Exhaust gas mass flow rate for ICE (kg/h)
$\dot{M}_{Exh\_MGT}$	Exhaust gas mass flow rate for MGT (kg/h)
N	Number of values
N_{batt}	Number of lead acid batteries
N_{PV}	Number of PV modules

N_{sup}	Number of supplementary prime movers (ICE or MGT)
$N_{s/s}$	Number of start-stop for supplementary prime movers
n	Components life time (yr)
P	Operating pressure (bar)
P_B	Power flow toward/out of battery (kW)
P_o	Atmospheric pressure (bar)
P_{cool}	Cooling load met by absorption chiller (kW)
P_{elec}	Electric load demand (kW)
P_{ICE}	Power generation by ICE (kW)
P_L	Total load demand (kW)
P_{MGT}	Power generation by MGT (kW)
P_{NET}	Net power generation (kW)
P_{PV}	Power generation by PV (kW)
P_{sup}	Power generation by supplementary prime movers (kW)
$P_{sup,max}$	Maximum power generation by supplementary prime movers (kW)
$P_{sup,min}$	Minimum starting threshold of supplementary prime movers (kW)
P_{ther}	Thermal load demand (kW)
$P_{ther,c}$	Cooling load demand (kW)
$P_{ther,h}$	Heating load demand (kW)
P_{heat}	Heating load met by heat exchanger (kW)
Q	Heat transfer for PV to atmosphere (kW)
$\dot{Q}$	Rate of heat transfer (kW)
Q_A	Absorber heat transfer (kW)
Q_C	Condenser heat transfer (kW)
Q_E	Evaporator heat transfer (kW)
Q_{cool}	Cooling demand met by recovered waste heat (kW)
Q_{heat}	Heating demand met by recovered waste heat (kW)
$Q_{Exh,avl}$	Available heat energy from exhaust gas (kW)
Q_{Exh}	Recoverable heat energy from exhaust gas (kW)
Q_T	Total recovered heat energy (kW)
R	Molar gas constant of fuel (kJ/kg K)
R_s	PV series resistance (Ω)
R_{sh}	PV shunt resistance (Ω)
S	Solar irradiation (W/m^2)
S_{ref}	Reference solar irradiation (W/m^2)
s	Entropy (kJ/kg K)

s_0	Entropy at reference temperature (kJ/kg K)
$\dot{S}_{gen}$	Entropy generation rate (kW/K)
S_{N-1}	Standard deviation
T	Temperature (˚C)
T_0	Reference temperature (25, ˚C)
$\bar{T}_c$	Average temperature of chilled water (˚C)
$\bar{T}_h$	Average temperature of hot water (˚C)
T_{amb}	Ambient temperature (˚C)
T_{Exh_MGT}	Exhaust outlet temperature from MGT (K)
T_{HE_in}	Exhaust inlet temperature to heat exchanger (K)
T_{HE_out}	Exhaust outlet temperature from heat exchanger (K)
T_{PV}	Cell temperature (˚C)
T_{ref}	Reference temperature (˚C)
T_{sky}	Effective temperature of sky (˚C)
T_{sun}	Sun temperature (K)
U	Overall heat transfer coefficient (W/m^2K)
V_{PV}	PV module voltage (V)
V_{oc}	Nominal open circuit voltage (V)
V_{mp}	Maximum power point voltage (V)
$\dot{W}$	Work rate (kW)
W_s	Wind speed (m/s)
$\dot{WH}_{MGT}$	Available heat energy from MGT (kW)
$\dot{WH}_{sup}$	Available heat energy from supplementary prime movers (kW)
x_i	Load demand at any time step (kW)
$\bar{x}$	Mean load (kW)
Δt	Time step (min)
ΔT_s	Transient start-up time (s)
Greek symbols	
α	Modified ideality factor
β	Lifetime equivalent CO2 emission (kg CO_2-eq/kWh)
∈	Emissivity of PV module
σ	Stefan Boltzmann constant (W/m^2K)
κ_t	Temperature coefficient of short circuit current (/˚C)
ε	Specific exergy flow (kJ/kg)
ε_{kn}	Kinetic exergy flow (kJ/kg)
ε_{pt}	Potential exergy flow (kJ/kg)

ε_{ph}	Physical exergy flow (kJ/kg)
ε_{ch}	Chemical exergy flow (kJ/kg)
η	Energy efficiency (%)
η_b	Battery efficiency (%)
η_{ex}	Exergy efficiency (%)
η_{inv}	Inverter efficiency (%)
η_{MGT}	MGT energy efficiency (%)
η_P	Overall energy efficiency (%)
η_{PV}	PV energy efficiency (%)
η_{CHP}	Overall CHP efficiency (%)
η_{CCHP}	Overall CCHP efficiency (%)
$\eta_{wh,sys}$	Overall process water heater efficiency (%)
$\eta_{ex,CHP}$	Overall CHP exergy efficiency (%)
$\eta_{ex,CCHP}$	Overall CCHP exergy efficiency (%)
$\eta_{ex,MGT}$	MGT exergy efficiency (%)
$\eta_{ex,P}$	Overall exergy efficiency (%)
$\eta_{ex,PV}$	PV exergy efficiency (%)

Abbreviations

ACC	Annualised capital cost ($/yr)
AFC	Annual fuel cost ($/yr)
AOM	Annual operation and maintenance cost ($/yr)
CCHP	Combined cooling, heating, and power
CHP	Combined heating and power
COE	Cost of energy ($/kWh)
CRF	Capital recovery factor
DF	Duty Factor (kWh/start-stop/yr)
EE	Excess Energy (kWh)
ETLR	Electric to thermal load ratio
FEL	Following electric load
FTL	Following thermal load
GA	Genetic algorithm
ICE	Internal Combustion Engine
IEA	International Energy Agency
LCE	Life cycle emissions (kg CO_2-eq/yr)
LHV	Lower heating value
LPS	Loss of power supply (kWh)

LPSP	Loss of power supply probability
MGT	Micro gas turbine
PV	Photovoltaic
PMS	Power management strategy
RP	Renewable penetration (%)
TER	Thermal to electric ratio
WHSP	Waste heat to supply power

Chapter 1: Topical Overview

1.1 Energy systems

The continuous depletion of fossil fuel reserves and the growing awareness of their environmental impact are driving the development of more sustainable energy supply options. Global energy demand is rising steadily as a consequence of population growth and higher living standards in many areas across the world. Over 85 % of global energy demand is supplied by fossil fuels [1], whilst more than 67 % of electricity is generated by using fossil fuels, as shown in Figure 1.1. The consequences are a strong link between greenhouse gas emissions (such as CO_2) and the fossil fuels which are largely responsible for power generation.

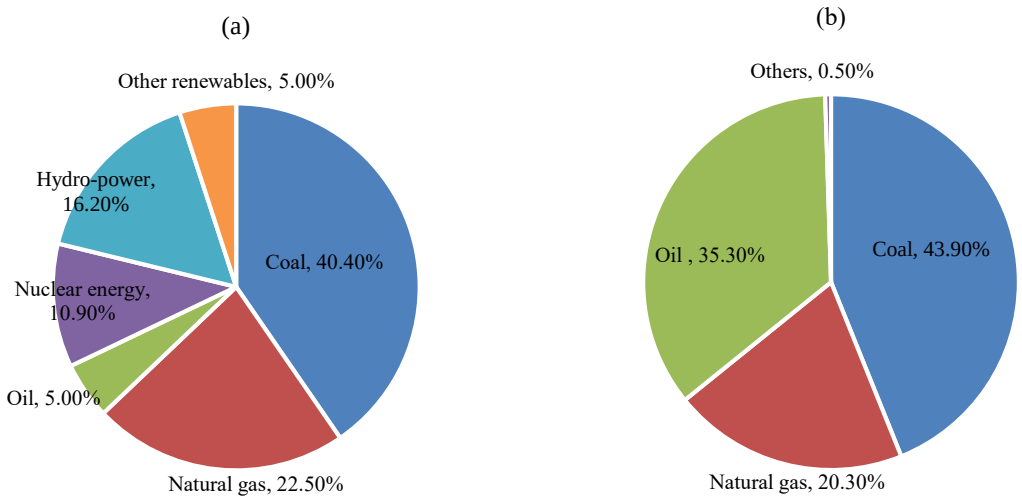

Fig 1.1 (a): Global electricity generation, and (b) CO_2 emission by fuel type in 2012 [1]

There are two pathways available to reduce dependency on fossil fuels: (i) increasing overall process efficiencies in different applications (industrial, domestic, agricultural, transport etc.), and (ii) to escalate the penetration of renewable energy instead of conventional energy resources. These two technical challenges are further complicated by the higher transmission and distribution costs associated with centralized power grids, particularly if supplying remote communities [2]. Although many stand-alone and distributed energy systems integrate renewable energy resources, the intermittent and seasonal nature of these resources means they are not reliable in meeting all utility demand if used without some form of energy storage. Additionally, to improve the performance and reliability of stand-alone and distributed energy systems, prime movers are used along with energy storage to supplement power if needed. The traditional prime mover Internal Combustion Engines (ICEs) have been used for back-up [3]. However, other prime movers such as Micro Gas Turbines (MGTs) can also be considered for decentralized power. The electric efficiencies of small scale (<100 kW) ICEs and MGTs are roughly 35 % and 25 %, respectively [4]. However, their inefficiency arises from waste heat, which is not

commonly recaptured. Whilst it is acknowledged that integrating waste heat recovery for cooling and heating applications into conventional power stations could increase overall efficiency by up to 90 % [4], the implementation of waste heat recovery into stand-alone energy systems is less researched.
Stand-alone energy systems produce electricity independently where it is not feasible to connect to the main utility grid. On the other hand, distributed power is characterised by the generation of power to meet local energy needs. Distributed energy generation systems run in the presence of a connection to a main grid to help supplement shortfalls or reduce peak power costs. Distributed energy systems typically include prime movers such as reciprocating Internal Combustion Engines (Compression Ignition or Spark Ignition), Micro Gas Turbines (small-scale combustion turbines that run on fossil fuels and biofuels), Fuel Cells (FCs), solar Photovoltaic (PV) panels, solar thermal power plants and wind turbines. In the context of stand-alone and distributed energy systems, a Combined Heat and Power system (CHP) is the integration of both electrical and thermal load to end users. There are potential benefits from the use of cogeneration systems including improved fuel efficiency and reduced overall CO_2 emissions compared to the single generation (power) system. On the other hand, trigeneration extends cogeneration to the cooling loads for the same energy input. This type of system is also known as Combined Cooling, Heating and Power (CCHP). Whilst CCHP is a proven and reliable technology, its use has mainly been confined to industrial applications and large-scale centralized power plants. However, stand-alone and distributed CCHP systems are receiving more attention because of improved overall process efficiencies. Despite this, the inclusion of additional hardware infrastructure in both CHP and CCHP systems means field deployment requires careful thermo-economic analysis. Well-designed CHP and CCHP systems should be cost-effective and could lead to long-term energy savings and less emission of pollutants through improved process efficiencies. This study focuses on the recovery of waste heat generated from the prime movers (i.e. ICEs, MGTs) when supplementing renewables (i.e. PV).

Solar-Photovoltaic (PV): Solar energy represents one of the energy options readily available for use in stand-alone systems without compromising or adding to global warming. PV systems, however, need storage to meet peak electric load demands through using surplus energy for power generation.

The IEA solar energy roadmap has set a target of 27 % of worldwide electricity generation from solar energy (PV and solar thermal) by 2050 and for it to be a leading source of global electricity production as early as 2040 [5]. This target will be achieved in two ways: firstly by reducing the cost of electricity generation from solar energy, and secondly, by developing cost effective energy storage technologies. Energy generation from PV technology has a number of advantages including: familiarity and durability with no operational CO_2 emissions and suitability for stand-alone applications. However, the limitations of photovoltaic efficiency and manufacturing costs have not reached the point where PV power generation is the default choice for stand-alone systems.

Internal Combustion Engines: ICEs are a widely used technology for stand-alone and distributed power generation, and are used all the way through remote facilities for power and thermal energy generation. These prime movers have higher efficiency compared to combustion gas turbines, quick transient start-up, decent efficiencies at part load, and are generally reliable. The thermal efficiency of a small size high-speed diesel engine is about 30 %; however, efficiency increases up to 42–48 % for larger size engines [4]. Diesel engines have higher part load efficiency compared to the spark ignition engines. Diesel engines show a comparatively flat efficiency curve between 50 and 100 % load whereas spark ignition engine efficiency drops by 15–25 % at half load conditions [4].

Micro Gas Turbines: MGTs are small-scale gas turbines that burn either liquid or gaseous fuels. These devices produce a high pressure gas stream which in turn drives an electrical generator to produce electricity. MGTs have slightly lower electrical efficiency than similarly sized diesel generators. However, MGTs have the potential for higher reliability, a lower installation and maintenance cost, and lower noise and vibration due to the design simplicity and the lower number of moving parts. The power output and efficiency of MGT largely depends on ambient temperature and pressure. As the temperature of air increases, the density of air declines, which in turn decreases the density and mass flow rate of air. This consequently reduces the output power and efficiency as the compressor needs more power to deliver the same mass flow rates, but for the less dense air. On the other hand, both the power and the efficiency of the MGT increase with lower inlet air temperature. The part load performance of an MGT is quite low as compared to the diesel engine and fuel cell. When operating at 50 % load, the electrical efficiency drops from approximately 30 % to 25 % [4].

Hybrid Systems: Hybrid energy systems combine two or more energy sources, which can include renewables or conventional fuels with energy storage devices. The main benefits of hybrid power systems may be used to reduce dependency on either conventional energy or renewable systems. These systems are usually more suitable than using an individual prime mover or energy source for stand-alone power applications load meeting if high reliability is needed. Over the last two decades, research has been conducted on the integration of combustion engines and MGTs with renewable energy sources such as PVs and/or wind [6-8]. Incorporating heat recovery (to facilitate CHP or CCHP) with diesel engines, MGTs and fuel cells can increase overall power plant efficiency.

The main disadvantage associated with stand-alone renewable energy systems is the reliability of the renewables (e.g. PV, wind) due to their unpredictable, seasonal, and time-dependent natures. Although renewable energy is considered to be an alternative to fossil fuels, due to its seasonal and temporal variations, neither a PV nor wind energy resources can fully satisfy the load requirements. However, combining PV and wind energy can satisfy the load demands in some areas. In this regard, one approach is to install a hybridised energy system and include some energy storage media (batteries, hydrogen, capacitors) in a stand-alone system since renewable energy resources are inherently intermittent in

character [9]. On the other hand, inefficiencies associated with prime movers result in significant amounts of waste heat alongside power production, particularly as some prime movers release as much as two thirds of their fuel energy through the tail pipes [10]. Capturing waste heat through a heat exchanger can increase overall efficiency, and it also creates fewer greenhouse gas emissions. Trigeneration, otherwise known as the combined production of cooling, heating, and power (CCHP) has high potential compared to a single generation system (e.g. power only) due to higher overall efficiencies as well as lower costs of energy and emissions per unit energy output. The main purpose of the trigeneration system is to improve overall efficiency, cost, and reliability, and to reduce environmental emissions. Table 1.1 presents the technical characteristics of supplementary prime movers used in CHP and CCHP systems.

Table 1.1: Characteristics of prime movers used in CCHP systems

Parameters	**Steam turbines**	**Internal Combustion Engine (ICE)**	**Combustion turbines**	**Micro Gas Turbine (MGT)**	**Fuel cells**
Capacity (kW) [11]	50–500,000	5–20,000	250–50,000	15–300	5–2,000
Fuels [11]	Any	Diesel, natural gas, propane, biogas	Natural gas, propane, biogas, HFO	Diesel, natural gas, propane, biogas	Hydrogen, fuels with hydrocarbon
Electrical efficiency (%) [11, 12]	7–20	27–45	25–42	15–30	37–60
Overall efficiency (%) [11, 12]	60–80	65–90	65–87	60–85	85–90
Power to heat ratio [11]	0.1–0.5	0.8–2.4	0.2–0.8	1.2–1.7	0.8–1.1
Part load performance [11]	Poor	Good	Fair	Moderate	Good
Output heat temperature (˚C) [11]	Up to 540	80–540	Up to 540	200–650	260–370
Start-up time (transient) [12]	1–24 h	10s	10 min–1 h	1 min	3–72 h
CO_2 emissions (kg/MWh) [11]	-	650	580–680	720	430–490
NO_x emissions (kg/MWh) [11]	-	10	0.3–0.5	0.1	0.005–0.01
Lifetime (yr) [11, 13]	20–35	10	10	20	10–20

1.2 Stand-alone energy systems

1.2.1 Power generation

Electricity is considered as the most extensively used energy carrier in our daily activities. A prime mover provides electrical energy by mechanical or chemical means as shown in Figure 1.2. A typical power plant converts around one third of the energy available from fuel into electric power [14]. The major portion of the energy content of fuel is lost through the release of waste heat from the power plant. It is possible to use the waste heat generated alongside the power generation from the prime mover to produce thermal load (heating or cooling). Hong and Lian [15] reported an optimized sizing of a stand-alone hybrid power system considering a 25 kW wind-turbine, 30 kW diesel generator, and 5 kW PV. Wang and Nehrir [16] proposed a hybrid (wind/PV/fuel cell) power generation system for stand-alone applications. They considered wind and PV as the primary energy sources and an FC–

electrolyser as a backup for the system. Due to limited reserves of conventional energy sources, increasing energy demands, and growing environmental concern, there has been intensive research into green power plants that use advanced technology [10]. Solar energy is the most readily available form of energy and it has been the focus of research attention. PV systems can produce electricity by directly transforming the abundant solar energy into electricity without emissions. In the near future, PV systems can play a promising role in power generation due to the continuous development of PV cells and reductions in cost. Fthenakis et al.[17] performed a feasibility study on the solar energy of the USA considering techno-economical and geographical conditions and reported that solar power and other renewables are fully capable of replacing the fossil fuels and reducing carbon emissions.

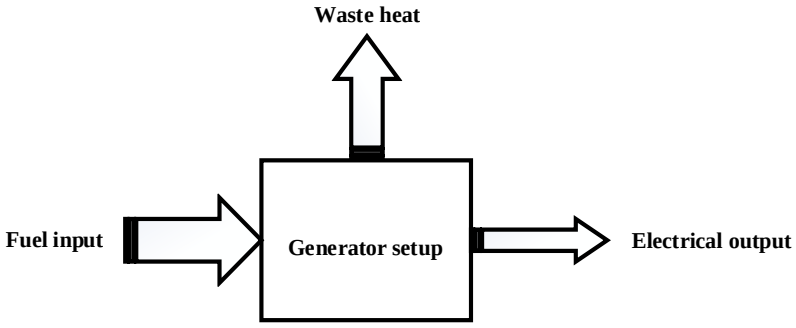

Fig. 1.2: System with power generation only

Internal Combustion Engines: ICEs are one of the most efficient power generation options for distributed power applications. The efficiency of a diesel engine increases with the increase in compression ratio and at low speed [18]. Power generation from combustion engines is widely used in different areas. Low speed diesel engines are more favoured for power generation in marine applications [19-21]. Diesel engine power generating sets are extensively used in telecommunications for distributed power generation, along with a battery bank and grid connection or off-grid applications [22]. Although diesel engine has lower efficiency compared to fuel cell, relatively lesser start-up time of diesel engine than fuel cell makes the diesel-based power generation system more suitable for off-grid and distributed power application (**Table 1.1**).

Micro Gas Turbines: Micro gas turbines (MGTs) are small gas turbines with a high-speed shaft and typical power range ~25–500 kW [23]. MGT has the potential to meet power, heating and cooling energy needs for both residential and small commercial applications due to its reliable, stable power generation, cost effectiveness, and low environmental pollution [24-27]. An MGT has a low installation and maintenance cost, less civil cost, requires less space, and are multi-fuelled combustion engines [28]. The part load efficiency of an MGT at 50 % load condition drops by around 15 % compared to an internal combustion engine in which the figure is only 5 %. An ICE-based power plant is advantageous compared to an MGT-based power plant in terms of part-load efficiency and for quick start-up time and higher overall efficiency. On the other hand, MGTs can be operated with different fuels including renewables, which adds flexibility to the operation.

1.2.2 Cogeneration (CHP)

Stand-alone cogeneration systems are usually installed close to end users. The utilisation of waste heat produced alongside electricity generation allows for the efficient utilisation of fuel energy and hence is more economical than the single generation systems (electricity or heat only). A typical Combined Heating and Power (CHP) system is shown in Figure 1.3.

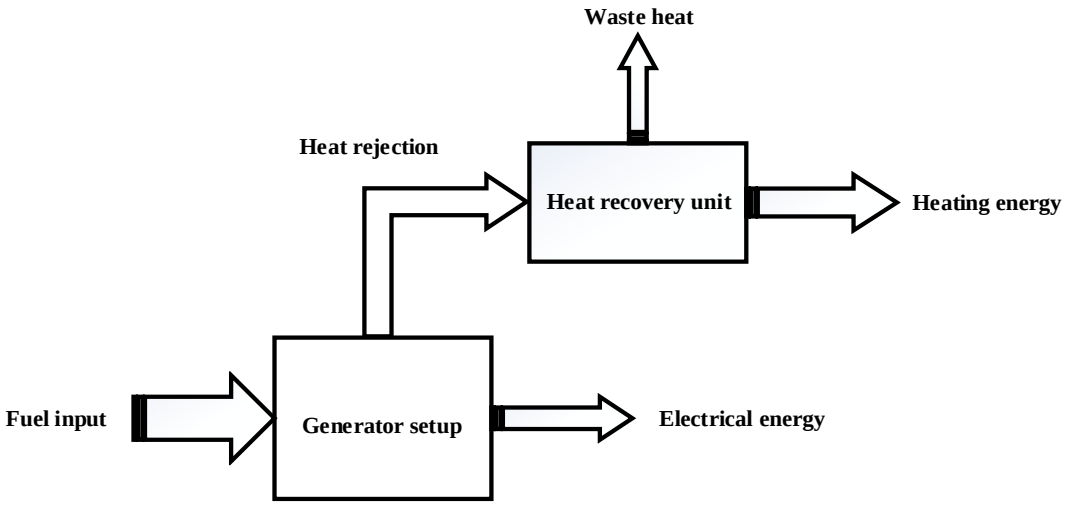

Fig. 1.3: System with Combined Heating and Power (CHP)

Internal Combustion Engines: Without waste heat recovery from ICE exhausts, the efficiency of ICE varies from 35 to 55 %; however, this can be increased to over 90 % as a result of CHP [29]. The CHP application could save around 20-30 % fuel compared to the amount of fuel needed to produce power and heat separately. Waste heat from ICEs can be recovered at different levels: from exhaust gases at temperature range 200–400 ºC and from jacket water cooling and lubricating oil cooling (at 90–125 º C)[30]. Compression ignition engine CHP systems are commonly used in educational institutions, health care centres, industrial facilities, and commercial and residential buildings.

Micro Gas Turbines: MGTs for CHP in stand-alone applications are receiving attention due to their low environmental pollution and low level of noise vibration. The higher range exhaust gas outlet temperatures (typically 450–550 ºC) make MGT very suitable for CHP applications. The major concern is low electrical efficiency (~30 %) which reduces significantly at part load. However, from an environmental point of view, MGT has a slight advantage compared to the ICE. Caresana et al.[31] performed an experimental study on 100 kW MGT with a cogeneration application and found electrical efficiency up to 29 % in the 80-100 kW range, and primary energy saving and overall efficiency about 74 % and 24 % respectively with substantially lower pollutants. An MGT cogeneration system is an efficient system and usage is increasing worldwide [32, 33]. Ehyaei and Mozafari [34] carried out an energy, economic, and environmental analysis of an MGT based on an on-site CHP application for a

10-storey residential building in Tehran. They reported that the energy management system and operational simplicity were the decisive factors for the system design and the system cost estimation. Most of the studies have been conducted by giving priority to energy and economic analysis. However, less attention has been paid to environmental, exergy, and exeroeconomic analyses of the CHP plant.

1.2.3 Trigeneration (CCHP)

The economic benefits of combustion engines in stand-alone power applications often depend on the effective use of the waste heat release, which accounts for almost two-thirds of the inlet fuel energy. Engine exhaust heat is the largest source of waste heat due to its high volumetric flow and temperature (up to 540 °C). It is quite feasible to use around 80 % of input fuel energy used for power generation by recovering waste generated by the combustion engine in the form of exhaust gas and cooling systems. Combined Cooling, Heating, and Power (CCHP) systems offer high overall efficiency and this leads to a reduction in the per energy output operating costs and environmental emissions. Figure 1.4 depicts the CCHP system.

The CCHP system can be operated with different possible operational modes. Usually, the two simplest operation strategies are: (i) to operate the prime mover to satisfy all electricity demand and to use the waste heat to meet part or all of the thermal demand and (ii) to operate the prime mover to meet all the thermal demand, while part or all of the electricity demand is met by the generating unit. The optimisation of small-scale CCHP systems is one of the most important issues in energy management due to the limited reserves of fossil fuel resources and the environmental concerns about using combustion fuel.

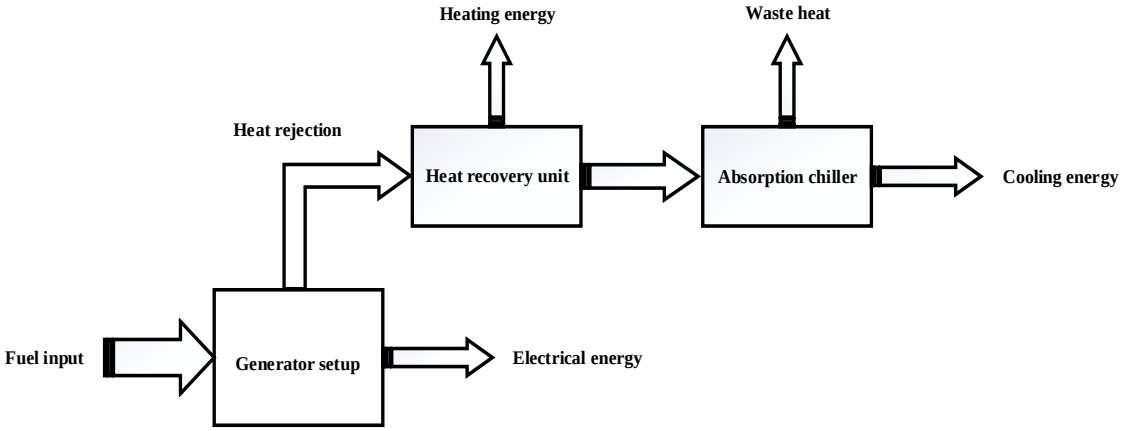

Fig. 1.4: System with combined cooling, heating, and power

Internal Combustion Engine: Rocha et al.[35] analysed the performance of two small-scale trigeneration plants based on a 30 kW MGT, and a 26 kW ICE as a prime mover, both the MGT and ICE natural gas fuelled and producing chilled water through an ammonia water absorption refrigeration. Khatri et al.[36] conducted an experimental investigation on a laboratory scale ICE-based CCHP system. They compared the performance of the power generation and the CCHP system and the results

showed that thermal efficiency increases from 33.7 % to 86.2 % when the engine is operating in CCHP mode. Also, CO_2 emissions from CCHP mode are 0.1211 kg CO_2/kWh whereas for a power generation system the emissions are of 0.308 kg CO_2/kWh. Lin et al. [37] also carried out a similar experimental test based on a diesel engine and the results showed that the building–sized CCHP system is feasible with a significant raising of the energy efficiency.

Micro Gas Turbines: Huang et al.[38] optimised an MGT using multi-objective genetic algorithms based on different load conditions. Moya et al.[28] investigated the performance analysis of an indirect–fired, air–cooled MGT of 28 kW capacity with an NH_3-H_2O absorption chiller trigeneration system. They conducted the parametric study at different load conditions, ambient temperatures for the absorption unit, cooling water temperature, and thermal oil temperature.

Different types of alternative energy sources like wind energy, PV, solar thermal power, geothermal, and hydro-energy are eco-friendly and have the potential to be extensively used. Combining these renewables with conventional sources like diesel engines, MGTs and fuel cells and with the battery sources to form a hybrid system can be utilised to supply power, cooling, and heating energy to the stand-alone community in a cost-effective and sustainable manner compared to the single generation system.

Optimisation of hybridised system: Simulation is considered one of the most favoured methods in solving the optimisation problems of trigeneration plants. Several studies on hybrid energy systems with various energy sources and components have been performed. However, very few of them are hybrid trigeneration systems. Mago and Chamra [39] optimised the primary energy, operational costs, and environmental emissions of a CCHP system based on the power demand, thermal demand, and power-thermal demand. Cardona and Piacentino [40] studied CCHP systems operating in Following Thermal Load (FTL) mode. Their work could not deliver an optimal CCHP system operating procedure in terms of cost, energy consumption, or emissions. In optimisation of a CCHP system, energy cost is commonly considered as an objective function. Most of the researchers worked on the optimisation of CCHP and CHP systems focus only on economy of the power plant [41-43]. However, Cho et al.[44] presented an optimisation of CCHP systems considering operational cost, primary energy consumption (PEC), and CO_2 emissions. Although there have been other prime movers such as steam turbines, gas engines, gas turbines, solid oxide fuel cells, etc, this PhD project study focuses on the small scale ($\leq$60 kWe) hybrid CCHP system with a diesel engine, and an MGT which is quite feasible for stand-alone energy generation.

Optimisation techniques refer to examining the optimal sizing of system components from a search space. The steps in these techniques are: (i) select the optimisation problem; (ii) find objective functions which can be either maximized or minimized based on the intentions of the decision-maker; and (iii)

identify a set of constraints with decision variables. There are a number of optimisation techniques for sizing hybrid energy systems reported in the literature, such as Genetic Algorithm (GA), Particle Swarm Optimisation (PSO), Fuzzy logic, Simulated Annealing (SA), and Artificial Neural Network (ANN).

GA is a search method for obtaining the optimal solution by natural evaluation [45]. Basic GA consists of random population generation with a fitness unit (based on objective functions) and a genetic operation unit (selection, crossover, and mutation). This procedure progresses toward the desired optimal point. When the optimisation process is dealing with two or more objective functions, then the procedure is considered as a multi-objective optimisation. This technique has been used to design a hybrid renewable energy system [46]. In multi-objective optimisation, there are two approaches: (i) to combine different objective functions into a single objective function, and (ii) to determine a Pareto optimal solution set. In this approach, a strategy is developed to balance or trade off each objective function relative to the others. This approach can successfully be applied to find the Pareto optimal solution set. Abdollahi et al. [47] optimised a small scale-scale CCHP system considering the objective functions (exergy efficiency, product cost, and environmental cost) using a multi-objective genetic algorithm. Bilal et al.[48] utilised a multi-objective genetic algorithm to find the optimal size of a stand-alone solar-wind-battery system in order to minimise the annualised cost system (ACS) and the loss of power supply probability (LPSP). Lagorse et al. [49] developed a genetic algorithm to economically design a hybrid energy system based on PV, wind, and fuel cell. In recent years, GA based on an evolutionary algorithm has been considered as a popular optimisation tool for energy systems. Ghaebi et al.[50] performed an optimisation technique of a CCHP system using a genetic algorithm based on total profit and the system product cost as the objective functions. Kavvadias and Maroulis [51] applied a multi-objective optimisation method using a genetic algorithm for the design of a CCHP system for a hospital. In this study, energy, cost, and environmental emissions were considered as objective functions and component size, operational strategy, and cost were the decision variables. A similar study was done by Wang et al. [52], where energy and cost savings and CO_2 emission reduction were considered as fitness functions.

PSO is another optimisation technique extensively used for the optimisation of hybrid energy technologies. Li et al.[53] instigated PSO for a CCHP plant based on solar energy in a commercial building. The objectives of this study were minimisation of cost, energy consumption, and CO_2 emissions. Wang et al. [54] performed a PSO technique to optimise a building's CCHP system to simultaneously measure the energy economy and environmental paybacks achieved by the building's CCHP system compared to a separate system. Kaviani et al.[55] proposed a PSO-based design methodology for a hybrid (Wind/PV/Fuel Cell) power generation system considering the annual cost as the objective function. Hakimi et al.[56] used a PSO algorithm for stand-alone hybrid system sizing considering total system costs as an objective function.

The Simulated Annealing (SA) optimisation technique is not a well-established procedure as compared to GA or PSO for sizing hybrid energy systems. Very few studies have covered this technique. Ekren et al. [57] performed an SA algorithm for hybrid (PV/wind with battery storage) energy system sizing in order to minimise of total system cost. Mellit et al.[58] proposed ANN to find the optimal sizing of stand-alone PV systems with a minimum of input data.

In this study, a MATLAB-based Genetic Algorithm (GA) is considered as an optimisation tool. The reliability of GAs is higher than other types of optimisation tools like PSO for finding the global optimum. In addition to this, it can handle a large number of parameters to find the optimal solution which makes it suitable for system design [45].

In summary, although a number of research projects have looked at using GAs for hybrid power supply applications, very few of these considered systems for power, heating, and cooling applications. This study uses highly dynamic load profiles and meteorological data. Moreover, the transient start-up for hybrid applications has not been considered. The detailed of Power Management Strategy is not widely reported in literature for hybridised CCHP systems. The effects of PMS, hardware components, and optimisation parameters are also reported in this study. Although LPSP is extensively used in designing hybrid power generation systems, this is not commonly used in CHP and CCHP sizing optimisations. The overall system energy and exergy efficiency of a stand-alone hybridised power, CHP, and CCHP system is analysed while the system is sized.

1.3 Project motivation

Around 17 % of the global population is not connected to the grid and this figure is even higher (22 %) in developing countries [59]. The major share of electricity (around 68 %, Figure 1.1) is generated using fossil fuels. However, the limited reserves of conventional fuels and the negative environmental consequences of using these fuels have triggered the use of sustainable energy resources, in particular in areas where grid connections are not readily available. There are two pathways to reduce the dependency on fossil fuels. Firstly, increasing the overall efficiency of prime movers in industrial and domestic applications. Secondly, escalating the integration of renewable energy (e.g. PV, wind etc.) in place of conventional energy sources. However, renewable energy resources are seasonal, unpredictable, and intermittent in nature [60, 61]; therefore, these systems require large-scale storage devices. In this context, one approach to reliably satisfy the load demand includes hybridisation supplemented by combustion-based prime movers (i.e. ICEs or MGTs) [62].

Numerous studies have been investigated on stand-alone hybrid power generation systems [63-73]; however, very little work is available in the literature which investigate the stand-alone hybridised CHP [74, 75], and CCHP [76, 77] systems. Around 60 % of fuel input energy is wasted through the exhaust

tail pipe (ICE and MGT) and cooling system (ICE). Recovering waste heat from supplementary prime movers to meet heating and cooling demands not only improves overall system efficiency [36] but also reduces environmental emissions [78]. In this regard, there is a need for further investigation into hybridised systems featuring CHP or CCHP systems.

The load-meeting reliability (Loss of Power Supply Probability-LPSP) is one of the most important constraints in the design of hybridised system components. Many studies have considered LPSP as a reliability index to meet electricity demands alone [60, 79, 80]; however, in CHP and CCHP systems design, an LPSP has not widely been reported in the literature. Additionally, Power Management Strategies (PMS) can significantly affect the outcome of the system sizing of hybridised power, CHP, and CCHP systems [81-83]. Therefore, design of detailed PMS needs extra attention to the optimisation of hybridised system configurations. CHP and CCHP systems with the grid connected use grid electricity and a back-up combustion boiler to meet the deficit of electricity and thermal demand, respectively [47, 84-86]. In this context, optimal sizing of stand-alone hybrid CHP and CCHP systems is a key challenge and requires the consideration of several parameters simultaneously. These parameters are choice of renewables, variations in load profiles (electric, heating, and cooling), hardware component characteristics, and the optimisation methods used along with their constraints and parameters.

Considering the facts discussed above, the research described in this thesis addresses the research gaps by meeting highly dynamic load demand and meteorological conditions. The study considered the LPSP as a reliability constraint and details of the PMS are developed for all three stand-alone (power, CHP, and CCHP) systems. A comparative analysis of stand-alone power, CHP, and CCHP systems using a multi-objective Genetic Algorithm is carried out to size the optimal system configurations considering the Cost of Energy (COE), overall energy efficiency, and overall exergy efficiency. The analyses of stand-alone power, CHP, and CCHP systems are also reported based on several key consequential (post optimisation) performance indicators such as LCE, CO_2, NO_x, Duty Factor (DF), Recovered Waste Heat to Power (RWHP), and Renewable Penetration (RP). The study is further extended to investigate the sensitivity of using different starting thresholds of supplementary prime movers, different types of resolutions, different numbers of objective functions, different relative distributions of load demand, and variations in the costs of components on the performance indicators.

1.4 Research objectives

The present research project focuses on sizing and optimisation of a PV/combustion engine-based hybridised system which is an essential part before installation for stand-alone application. The system is designed using intelligent techniques (GA) to meet highly dynamic loads (electric, heating, and cooling) and widely used optimisation tool HOMER to satisfy electric load only with greater reliability.

Power management strategies are developed for system sizing using GA. The main challenge is to design a hybridised system which would be able to meet a highly dynamic electric load, hot water (heating load), and chilled water (cooling load) with a specified load meeting reliability. In order to achieve this, single- and multi-objectives function are considered along with some acceptable performance indicators. The research is also extended to carry out a comparative analysis of a hybridised micro-grid system with different battery technologies and scalability of load demand. Although, the specific objectives are discussed at the end of Introduction Section of each chapter (chapters 2, 3, 4, 5, and 6), the overall objectives of this PhD project are listed below:

- To perform a sizing optimisation of a hybridised stand-alone system based on the single objective function while meeting a dynamic electric load demand. This system sizing also incorporates the effects of temporal resolution, minimum starting threshold of supplementary prime movers, transient start-up, and sensitivity analysis on the COE and other performance indicators (Chapter 2).
- To investigate a comparative analysis of using different battery technologies and scalability of load demand while sizing a hybridised micro-grid system using HOMER meeting power demand only. Apart from the economic analysis, several performance indicators also are considered for sizing optimisation (Chapter 6).
- To analyse the effects of various parameters (e.g. relative magnitude of load profiles, Following Electric Load (FEL) and, Following Electric Load to Thermal Load (FEL/FTL) management strategies, single- and double objective functions) on optimal sizing of hybridised CHP system (Chapter 3).
- To design a CCHP system meeting a highly dynamic simultaneously electric, heating, and cooling load considering the effects of relative load distribution, hardware components, and optimisations techniques on system sizing (Chapter 4).
- To carry out a sizing optimisation of hybridised power, CHP, and CCHP systems considering three objective functions (COE, overall energy efficiency, and overall exergy efficiency) and investigates the effects of scalability of prime movers, relative magnitude of load demands, and number of objective functions (Chapter 5).

1.5 Research scope

The main focus of this research is to design an optimal hybridised system configuration reliably meeting a highly dynamic electric, heating, and cooling loads in an off-grid area. This system includes Internal Combustion Engine (ICE), Micro Gas Turbine (MGT), PV module, battery bank, heat exchangers, and absorption chillers. The study also extends to analyse the effects of different battery technologies (i.e lead acid, Li-ion, and vanadium redox flow battery) on sizing and system performance. Among the various renewable sources, solar PV is only considered in this study. Although wind energy is a good contender for stand-alone application, due to the more intermittent nature than solar, it is out of scope

in this research. Another potential source Fuel cell is also excluded from this study which requires higher capital investment and has higher transient start-up time compared to the prime movers considered in this study. This system configuration is fully stand-alone; thus grid-connection is out of the scope. No solar tracking system and Maximum Power Point Tracking (MMPT) are used in this research. Moreover, it does include the auxiliary boiler meeting the heating demand. In this work, hot water driven absorption chiller (single effect chiller) is used for meeting cooling demand and thus, double or triple effect chiller is not considered which requires high temperature steam or exhaust gas. Costs associated with installation, instrumentation and control, wiring, civil structure and land are not considered for economic analysis. Studying the predictive power management system is beyond the scope of the present research. The study includes theoretical modelling using manufacturer technical characteristics of hardware components and develops simulation modelling for optimal sizing of the system components. Given the complexity of the system considered in this study, experimental part is out of scope of the PhD project. However, the outcome of this study is compared to the research found in the literature. This PhD thesis is to investigate the effects of incrementally increase the complexity of systems and load following strategies (i.e. Power Management Strategies) on the optimised system configuration. The system sizing is based on the Cost of Energy, overall energy and exergy efficiency, some widely acceptable performance indicators (e.g. Life Cycle Emissions, Excess Energy, Renewable Penetration, CO2, NOx emissions, etc.). This conceptual system develop can be applied with the integration of other renewable sources and supplementary prime movers. Although the system is developed under Australian conditions, the same can be used for the application of remote areas all over the world considering the meteorological data, load profiles, and economic input of the studied areas.

1.6 Research questions

On the basis of the challenges and unsettled issues identified above in relation to optimise the stand-alone power, CHP, and CCHP systems based on several key performance indicators, the present study is carried out by addressing the following research questions as shown in Figure 1.5:

RQ 1: In optimally sizing stand-alone hybrid systems meeting electric load only, how are the Cost of Energy and the consequential performance indicators affected by the following:

- **Hardware components:** start-up thresholds, type of supplementary prime movers, transient start-up periods, and scalability of prime movers
- **Load characteristics:** temporal resolutions, reliability constraints
- **Simulation methods:** GA parameters (e.g. population size, number of generations etc.).

RQ 2: In optimally sizing stand-alone hybrid systems meeting electric and heating loads, how are the Cost of Energy, overall CHP efficiency, and consequential performance indicators affected by the following:

- **Hardware components:** type of supplementary prime movers
- **Load characteristics and Power Management Strategies:** reliability constraints; relative magnitudes of load profiles, Electric-vs-Electric and Thermal Load Following strategies
- **Simulation methods:** GA parameters (e.g. population size, single-vs-double-objectives etc.).

RQ 3: In optimally sizing stand-alone hybrid systems meeting electric, heating, and cooling loads, how are the Cost of Energy, overall CHP/CCHP efficiency, and consequential performance indicators affected by the following:

- **Hardware components:** type of supplementary prime movers, adding absorption chiller to CHP systems
- **Load characteristics and Power Management Strategies:** reliability constraints, relative magnitudes of load profiles, Electric-vs-Electric and Thermal Load Following strategies.

RQ 4: In optimally sizing stand-alone hybrid systems meeting electric, heating, and cooling loads, how are the Cost of Energy, overall system CCHP energy efficiency, overall system CCHP exergy efficiency, and consequential performance indicators affected by the following:

- **Hardware components:** scalability of prime movers, type of absorption chillers
- **Load characteristics:** reliability constraints; relative magnitudes of load profiles
- **Simulation methods:** double-vs-triple-objectives.

RQ 5: In optimally sizing stand-alone hybrid systems meeting electric load only, how are the Cost of Energy, Net Present Cost, and consequential performance indicators affected by the following:

- **Hardware components:** type of battery technologies
- **Load characteristics:** reliability constraints; magnitudes of load profile

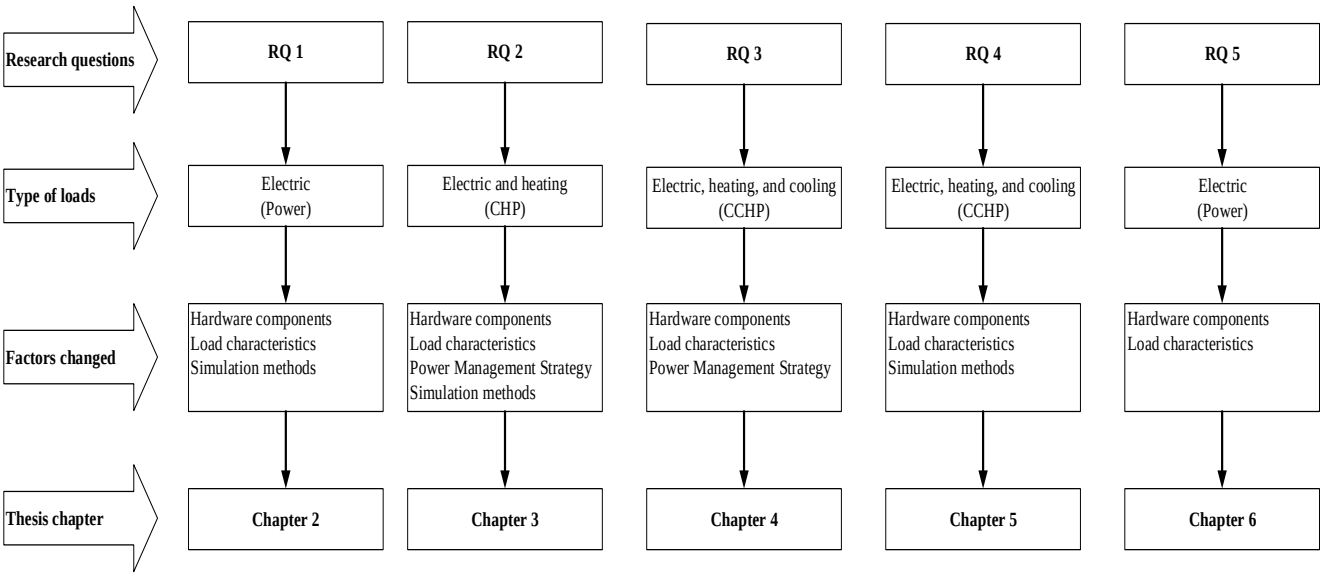

Fig. 1.5: Project research structure

1.7 Research methodologies

The above research questions are addressed using the MATLAB optimisation toolbox to implement single- and multi-objective functions. A commercial software package, MATLAB 2015b, operating on a desktop PC (processor: Intel Core i5-4570 CPU@ 3.20GHz, 32-bit operating system) is used to determine the stand-alone system performances based on the system architecture.

Figure 1.6 shows the work flow diagram for this research project. In this study, load profile associated with electrical demand is collected from Western Power (a Western Australian state government-owned corporation for a stand-alone system) and then scaled up to meet the community-based load demand. On the other hand, heating and cooling load demands are accumulated from Edith Cowan University (ECU) building. These load profiles are presented in Chapters 2, 3, and 4 and as supplementary materials in Appendix C. Time-resolved meteorological data (i.e. solar irradiation, wind velocity, and temperature) is taken for the stand-alone area in Western Australia (Broome: 17˚56'S latitude and 122˚14'E longitude) from the Bureau of Meteorology, Australia. The study area Broome is chosen as it is not connected to the Australian National Grid. Operational characteristics related to the combustion engines used in this research have been obtained from the manufacturer's datasheet and literature (Appendix D). The economical, technical, and environmental information about the hardware components is also obtained from manufacturer's websites and literature.

In this research work, the hybridisation power, CHP, and CCHP systems are performed using MATLAB-based Genetic Algorithm (GA) using an optimisation toolbox. The technical and economic details of the hybridised system components are incorporated into the objective function in an M-file

and the constraints (non-linear constraints) are incorporated into another M-file according to the type of system configurations. In the process of optimisation, GA population size has significant effects on the time required to obtain an optimal solution as presented in Appendix E. The MATLAB scripts related to the objective functions and constraints are presented in Appendix F. Another MATLAB script (Appendix F) is developed to determine the final solution for multi-objective optimisation. More details about GA optimisation are provided in Chapter 3 and the method used to select the final solution is described in Chapter 4. In post optimisation analysis, a MATLAB script is developed to determine the engine transient time and running time. The consequential performance indicators are also analysed in post-optimisation phases.

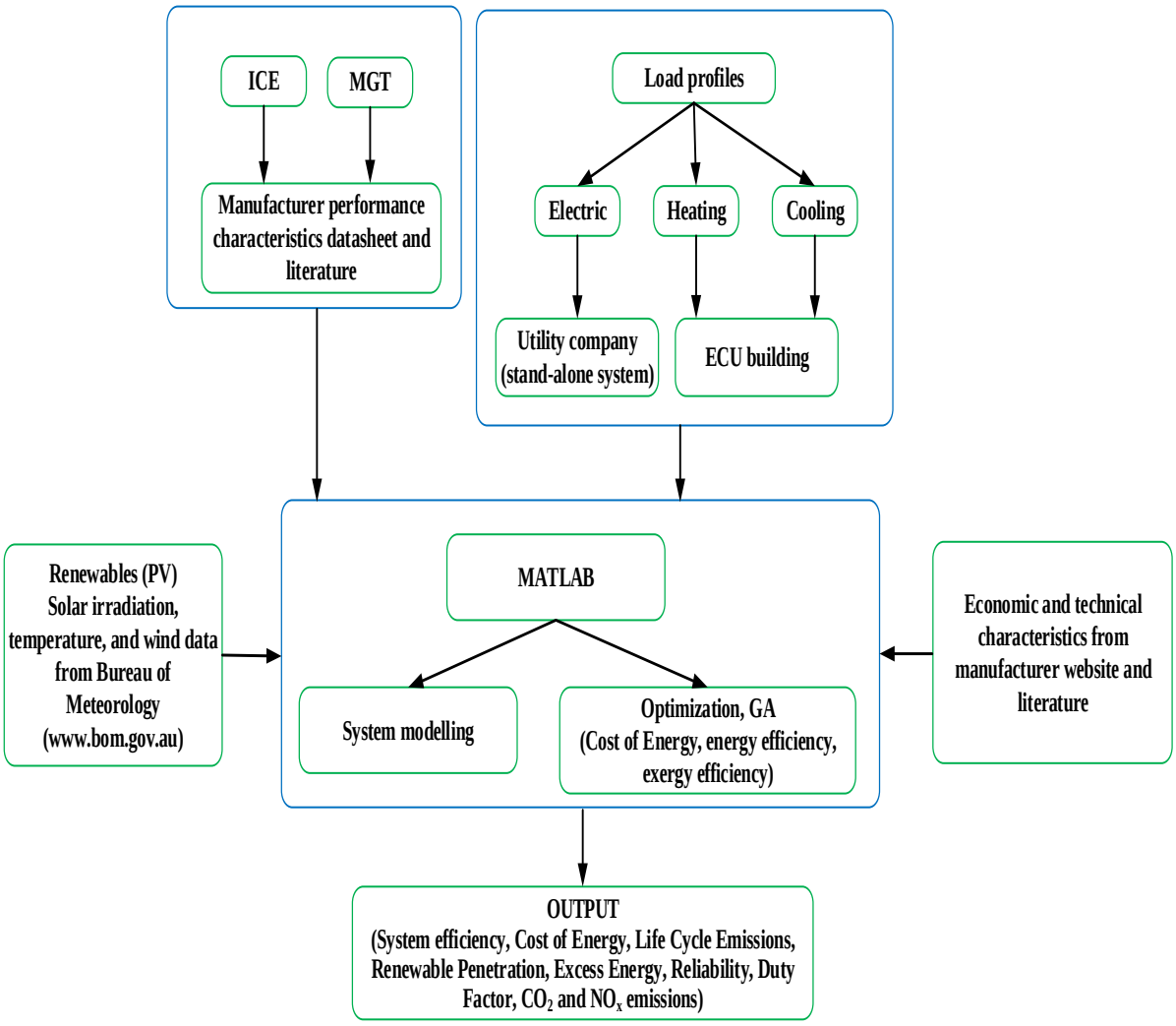

Fig. 1.6: Work flow of data collection, modelling, and analysis

1.8 Project deliverables and thesis format

This PhD project is structured as shown in Figure 1.7. The optimisation focuses on stand-alone systems which meet highly dynamic electric, heating, and cooling loads. The project is conceptualised so as to

incrementally increase the complexity of systems and load following strategies (i.e. Power Management Strategies). Throughout, the outcomes are reported with respect to the Cost of Energy, energy and exergy efficiency, Life Cycle Emissions, and other acceptable consequential performance indicators. This research has the following project deliverables:

- A stand-alone system of power generation (satisfying electric demand only) is investigated using a MATLAB-based Genetic Algorithm (GA) for a single objective (Cost of Energy, $/kWh) function while sizing the system components and quantifying the waste heat generation.
- Different battery technologies and scalability of electric load demand are investigated using HOMER to satisfy dynamic loads.
- A stand-alone hybridised CHP system is sized, taking into account both single- and double-objective functions while meeting dynamic electric and heating loads.
- Following this, a stand-alone hybridised CCHP system is optimised using a multi-objective GA to satisfy highly dynamic electric, heating, and cooling loads. This study considers Cost of Energy and overall energy efficiency as objective functions.
- Finally, the system is sized considering the three objective functions (COE, overall energy efficiency, and overall exergy efficiency) when meeting dynamic electric, heating and/or cooling.

The research in this thesis will contribute to the management of electric, heating, and cooling load demands in remote areas that are not connected to the national grid. The research highlights that using intelligent technique can achieve this in a cost effective way, with higher overall efficiency, and with fewer polluting emissions than combustion-based and PV-only systems.

This PhD follows the "Thesis with Publication" format[1]. The remaining five chapters of the thesis consist of published or under review in peer-reviewed journals followed by general discussions, conclusions, and future recommendations. The structure of the thesis is as follows:

[1] "Thesis with Publication" is thesis format for postgraduate research at ECU. The present thesis has been written based on the guidelines provided at http://www.ecu.edu.au/GPPS/policies_db/policies_view.php?rec_id=0000000434.
In this format, the submitted thesis can consist of publications that have already been published, are in the process of being published, or a combination of these.

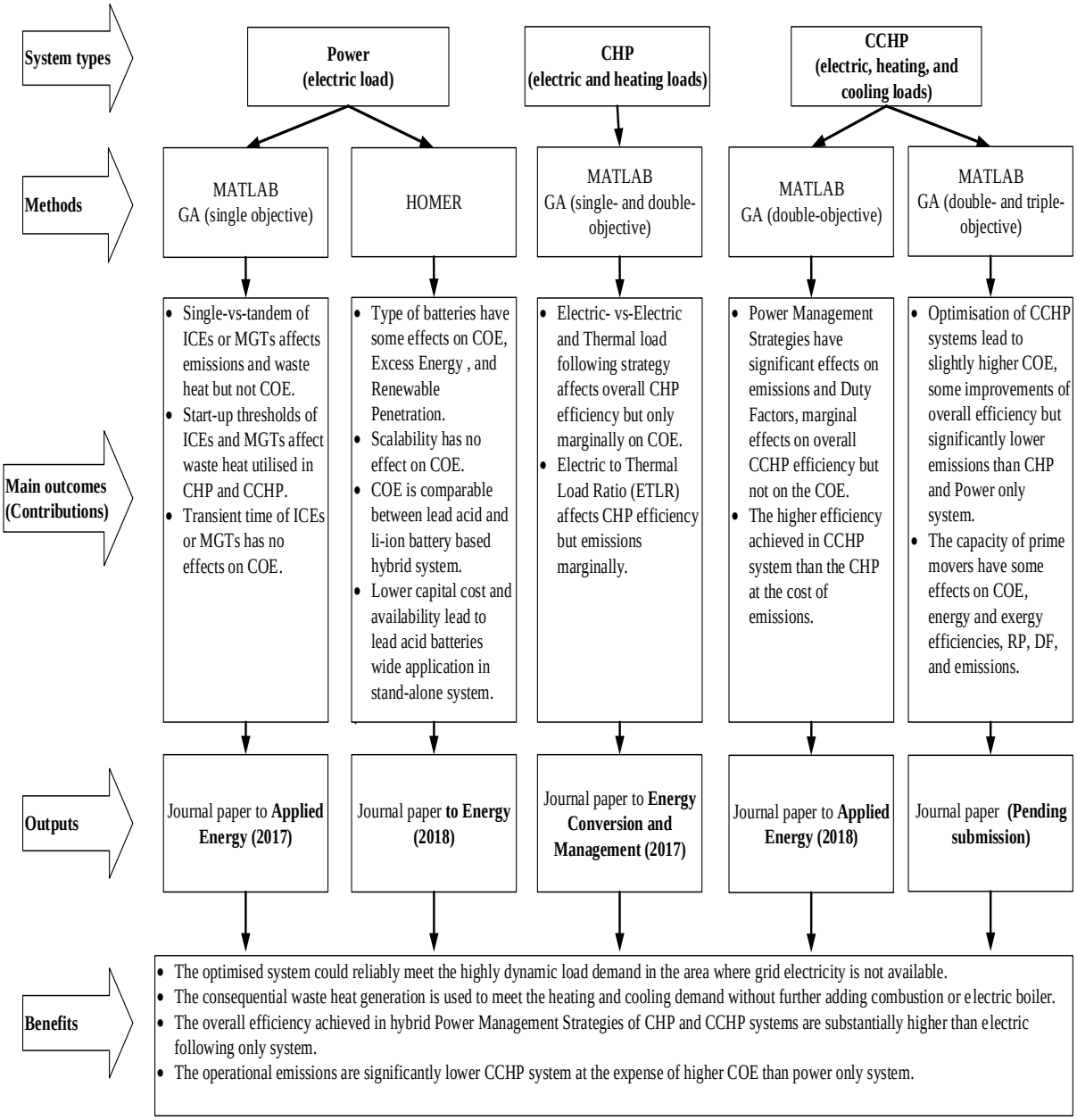

Fig. 1.7: Project research impact pathway

Chapter 1 gives a brief overview of energy systems along with some practical applications of stand-alone power, CHP, and CCHP systems. Chapter 1 also explains the need to integrate renewable energy sources with supplementary prime movers for energy generation (electric, heating, and cooling), in particular in areas where grid electricity is not readily available. This chapter concludes by outlining project motivations, research questions, and research methodologies.

Chapter 2 presents a stand-alone hybrid system meeting a highly dynamic electric load only. This study investigates the effects of different types of supplementary prime movers and their start-up thresholds,

temporal resolution, and sensitivity analysis on the Cost of Energy and the consequential performance indicators such as Life Cycle Emissions and quantification of waste heat generation.

Chapter 3 discusses the sizing optimisation of a stand-alone CHP system while satisfying both highly dynamic electric and heating loads with a specified load-meeting reliability. This research uses single objective (Cost of Energy) and multi-objective (Cost of Energy and Overall energy efficiency) functions. The detailed of Power Management Strategies for hybridised CHP system is reported.

Chapter 4 covers the effects of load-following strategies, system hardware components, and thermal load distribution on the stand-alone CCHP system sizing using Multi-objective GA meeting highly dynamic load profiles (i.e. electric, heating, and cooling) and meteorological conditions (i.e. solar irradiation, wind velocity, and ambient temperature).

Chapter 5 demonstrates the Multi-objective (Cost of Energy, energy efficiency, and exergy efficiency) optimisation of a stand-alone CCHP system. In this chapter, a comparative analysis of Power only, power and heat (CHP), and power, heating, and cooling (CCHP) is carried out. The effects of hardware parameters, multi-objective functions (double vs triple objectives), and scalability of load demands on Cost of Energy, overall energy efficiency, and exergy efficiency are investigated.

Chapter 6 describes the stand-alone power generation systems using HOMER in the context of three different battery storage technologies, scalability of load demand, and sensitivity analysis of input cost parameters.

Chapter 7 presents a general discussion of results presented in each chapter and addresses the research questions for the overall PhD project.

Chapter 8 incorporates the concluding remarks of all chapters and offers suggestions for future research directions.

Chapter references

[1] Agency, I.E., *Key world energy statistics*. 2014: International Energy Agency.

[2] Hiremath, R., S. Shikha, and N. Ravindranath, *Decentralized energy planning; modeling and application—a review.* Renewable and Sustainable Energy Reviews, 2007. **11**(5): p. 729-752.

[3] Nehrir, M., et al., *A review of hybrid renewable/alternative energy systems for electric power generation: configurations, control, and applications.* Sustainable Energy, IEEE Transactions on, 2011. **2**(4): p. 392-403.

[4] Darrow, K., et al., *Catalog of CHP technologies.* 2014.

[5] *Technology Roadmap: Solar Thermal Electricity*. 2014 [cited 2015 12/05/2015]; 2014:[Available from: https://www.iea.org/publications/freepublications/publication/technology-roadmap-solar-thermal-electricity---2014-edition.html.

[6] Elhadidy, M. and S. Shaahid, *Parametric study of hybrid (wind+ solar+ diesel) power generating systems.* Renewable Energy, 2000. **21**(2): p. 129-139.

[7] Bernal-Agustín, J.L. and R. Dufo-López, *Simulation and optimization of stand-alone hybrid renewable energy systems.* Renewable and Sustainable Energy Reviews, 2009. **13**(8): p. 2111-2118.
[8] Afzal, A., M. Mohibullah, and V. Kumar Sharma, *Optimal hybrid renewable energy systems for energy security: a comparative study.* International Journal of Sustainable Energy, 2010. **29**(1): p. 48-58.
[9] Courtecuisse, V., et al., *A methodology to design a fuzzy logic based supervision of Hybrid Renewable Energy Systems.* Mathematics and Computers in Simulation, 2010. **81**(2): p. 208-224.
[10] Wu, D.W. and R.Z. Wang, *Combined cooling, heating and power: a review.* Progress in Energy and Combustion Science, 2006. **32**(5–6): p. 459-495.
[11] Wu, D. and R. Wang, *Combined cooling, heating and power: a review.* progress in energy and combustion science, 2006. **32**(5): p. 459-495.
[12] *Combine Heat and Power Partnership. Catalog of CHP Technologies. U.S. Environmental Protection Agency. 2015. p.1-6,5.1-5.18.*
[13] Arun, P., R. Banerjee, and S. Bandyopadhyay, *Optimum sizing of battery-integrated diesel generator for remote electrification through design-space approach.* Energy, 2008. **33**(7): p. 1155-1168.
[14] Cho, H., A.D. Smith, and P. Mago, *Combined cooling, heating and power: A review of performance improvement and optimization.* Applied Energy, 2014. **136**: p. 168-185.
[15] Hong, Y.-Y. and R.-C. Lian, *Optimal sizing of hybrid wind/PV/diesel generation in a stand-alone power system using Markov-based genetic algorithm.* Power Delivery, IEEE Transactions on, 2012. **27**(2): p. 640-647.
[16] Wang, C. and M.H. Nehrir, *Power management of a stand-alone wind/photovoltaic/fuel cell energy system.* Energy Conversion, IEEE Transactions on, 2008. **23**(3): p. 957-967.
[17] Fthenakis, V., J.E. Mason, and K. Zweibel, *The technical, geographical, and economic feasibility for solar energy to supply the energy needs of the US.* Energy Policy, 2009. **37**(2): p. 387-399.
[18] Abusoglu, A. and M. Kanoglu, *Exergetic and thermoeconomic analyses of diesel engine powered cogeneration: Part 1–Formulations.* Applied Thermal Engineering, 2009. **29**(2): p. 234-241.
[19] Chesse, P., et al., *Performance simulation of sequentially turbocharged marine diesel engines with applications to compressor surge.* Journal of engineering for gas turbines and power, 2000. **122**(4): p. 562-569.
[20] Hountalas, D. and A. Kouremenos, *Development and application of a fully automatic troubleshooting method for large marine diesel engines.* Applied Thermal Engineering, 1999. **19**(3): p. 299-324.
[21] Lin, C.-Y., *Reduction of particulate matter and gaseous emission from marine diesel engines using a catalyzed particulate filter.* Ocean Engineering, 2002. **29**(11): p. 1327-1341.
[22] Onar, O.C., O.H.A. Shirazi, and A. Khaligh, *Grid Interaction Operation of a Telecommunications Power System With a Novel Topology for Multiple-Input Buck-Boost Converter.* Power Delivery, IEEE Transactions on, 2010. **25**(4): p. 2633-2645.
[23] Galanti, L. and A.F. Massardo, *Micro gas turbine thermodynamic and economic analysis up to 500 kWe size.* Applied Energy, 2011. **88**(12): p. 4795-4802.
[24] Ehyaei, M. and M. Bahadori, *Selection of micro turbines to meet electrical and thermal energy needs of residential buildings in Iran.* Energy and Buildings, 2007. **39**(12): p. 1227-1234.
[25] Mone, C., D. Chau, and P. Phelan, *Economic feasibility of combined heat and power and absorption refrigeration with commercially available gas turbines.* Energy Conversion and Management, 2001. **42**(13): p. 1559-1573.
[26] Pearce, J., B. Al Zahawi, and R. Shuttleworth. *Electricity generation in the home: modelling of single-house domestic combined heat and power*. in *Science, Measurement and Technology, IEE Proceedings-*. 2001. IET.
[27] Tanaka, K., C. Wen, and K. Yamada, *Design and evaluation of combined cycle system with solid oxide fuel cell and gas turbine.* Fuel, 2000. **79**(12): p. 1493-1507.

[28] Moya, M., et al., *Performance analysis of a trigeneration system based on a micro gas turbine and an air-cooled, indirect fired, ammonia–water absorption chiller.* Applied Energy, 2011. **88**(12): p. 4424-4440.
[29] Rosen, M.A., M.N. Le, and I. Dincer, *Efficiency analysis of a cogeneration and district energy system.* Applied Thermal Engineering, 2005. **25**(1): p. 147-159.
[30] Arteconi, A., C. Brandoni, and F. Polonara, *Distributed generation and trigeneration: Energy saving opportunities in Italian supermarket sector.* Applied Thermal Engineering, 2009. **29**(8–9): p. 1735-1743.
[31] Caresana, F., et al., *Use of a test-bed to study the performance of micro gas turbines for cogeneration applications.* Applied Thermal Engineering, 2011. **31**(16): p. 3552-3558.
[32] Dong, L., H. Liu, and S. Riffat, *Development of small-scale and micro-scale biomass-fuelled CHP systems–A literature review.* Applied thermal engineering, 2009. **29**(11): p. 2119-2126.
[33] Hur, K.-b., S.-k. Rhim, and J.-k. Park, *Mechanical characteristics evaluation of biogas micro turbine power systems.* Journal of Loss Prevention in the Process Industries, 2009. **22**(6): p. 1003-1009.
[34] Ehyaei, M. and A. Mozafari, *Energy, economic and environmental (3E) analysis of a micro gas turbine employed for on-site combined heat and power production.* Energy and Buildings, 2010. **42**(2): p. 259-264.
[35] Rocha, M., R. Andreos, and J. Simões-Moreira, *Performance tests of two small trigeneration pilot plants.* Applied Thermal Engineering, 2012. **41**: p. 84-91.
[36] Khatri, K.K., et al., *Experimental investigation of CI engine operated micro-trigeneration system.* Applied Thermal Engineering, 2010. **30**(11): p. 1505-1509.
[37] Lin, L., et al., *An experimental investigation of a household size trigeneration.* Applied Thermal Engineering, 2007. **27**(2–3): p. 576-585.
[38] Huang, J., C. Yue, and Z. Feng. *Multi-objective optimization and performance analysis of bchp systems using genetic algorithms*. in *ASME Turbo Expo 2006: Power for Land, Sea, and Air*. 2006. American Society of Mechanical Engineers.
[39] Mago, P. and L. Chamra, *Analysis and optimization of CCHP systems based on energy, economical, and environmental considerations.* Energy and Buildings, 2009. **41**(10): p. 1099-1106.
[40] Cardona, E. and A. Piacentino, *A methodology for sizing a trigeneration plant in mediterranean areas.* Applied Thermal Engineering, 2003. **23**(13): p. 1665-1680.
[41] Ramesh, V., et al., *A novel selective particle swarm optimization approach for combined heat and power economic dispatch.* Electric Power Components and Systems, 2009. **37**(11): p. 1231-1240.
[42] Vasebi, A., M. Fesanghary, and S. Bathaee, *Combined heat and power economic dispatch by harmony search algorithm.* International Journal of Electrical Power & Energy Systems, 2007. **29**(10): p. 713-719.
[43] Wang, L. and C. Singh, *Stochastic combined heat and power dispatch based on multi-objective particle swarm optimization.* International Journal of Electrical Power & Energy Systems, 2008. **30**(3): p. 226-234.
[44] Cho, H., et al., *Evaluation of CCHP systems performance based on operational cost, primary energy consumption, and carbon dioxide emission by utilizing an optimal operation scheme.* Applied Energy, 2009. **86**(12): p. 2540-2549.
[45] Erdinc, O. and M. Uzunoglu, *Optimum design of hybrid renewable energy systems: overview of different approaches.* Renewable and Sustainable Energy Reviews, 2012. **16**(3): p. 1412-1425.
[46] Banos, R., et al., *Optimization methods applied to renewable and sustainable energy: A review.* Renewable and Sustainable Energy Reviews, 2011. **15**(4): p. 1753-1766.
[47] Abdollahi, G. and H. Sayyaadi, *Application of the multi-objective optimization and risk analysis for the sizing of a residential small-scale CCHP system.* Energy and Buildings, 2013. **60**: p. 330-344.
[48] Bilal, B.O., et al., *Optimal design of a hybrid solar–wind-battery system using the minimization of the annualized cost system and the minimization of the loss of power supply probability (LPSP).* Renewable Energy, 2010. **35**(10): p. 2388-2390.

[49] Lagorse, J., D. Paire, and A. Miraoui. *Hybrid stand-alone power supply using PEMFC, PV and battery - Modelling and optimization*. in *Clean Electrical Power, 2009 International Conference on*. 2009.
[50] Ghaebi, H., M. Saidi, and P. Ahmadi, *Exergoeconomic optimization of a trigeneration system for heating, cooling and power production purpose based on TRR method and using evolutionary algorithm.* Applied Thermal Engineering, 2012. **36**: p. 113-125.
[51] Kavvadias, K. and Z. Maroulis, *Multi-objective optimization of a trigeneration plant.* Energy Policy, 2010. **38**(2): p. 945-954.
[52] Wang, J.-J., Y.-Y. Jing, and C.-F. Zhang, *Optimization of capacity and operation for CCHP system by genetic algorithm.* Applied Energy, 2010. **87**(4): p. 1325-1335.
[53] Li, Z., Z. Huo, and H. Yin. *Optimization and analysis of operation strategies for combined cooling, heating and power system*. in *Power and Energy Engineering Conference (APPEEC), 2011 Asia-Pacific*. 2011. IEEE.
[54] Wang, J., et al., *Particle swarm optimization for redundant building cooling heating and power system.* Applied Energy, 2010. **87**(12): p. 3668-3679.
[55] Kashefi Kaviani, A., G.H. Riahy, and S.M. Kouhsari, *Optimal design of a reliable hydrogen-based stand-alone wind/PV generating system, considering component outages.* Renewable Energy, 2009. **34**(11): p. 2380-2390.
[56] Hakimi, S.M. and S.M. Moghaddas-Tafreshi, *Optimal sizing of a stand-alone hybrid power system via particle swarm optimization for Kahnouj area in south-east of Iran.* Renewable Energy, 2009. **34**(7): p. 1855-1862.
[57] Ekren, O. and B.Y. Ekren, *Size optimization of a PV/wind hybrid energy conversion system with battery storage using simulated annealing.* Applied Energy, 2010. **87**(2): p. 592-598.
[58] Mellit, A., et al., *An adaptive artificial neural network model for sizing stand-alone photovoltaic systems: application for isolated sites in Algeria.* Renewable Energy, 2005. **30**(10): p. 1501-1524.
[59] Agency, I.E. *Energy Acess Database*. Available from: 15.09.2016. http://www.worldenergyoutlook.org/resources/energydevelopment/energyaccessdatabase.
[60] Brka, A., Y.M. Al-Abdeli, and G. Kothapalli, *The interplay between renewables penetration, costing and emissions in the sizing of stand-alone hydrogen systems.* International Journal of Hydrogen Energy, 2015. **40**(1): p. 125-135.
[61] Prasad, A.A., R.A. Taylor, and M. Kay, *Assessment of solar and wind resource synergy in Australia.* Applied Energy, 2017. **190**: p. 354-367.
[62] Das, B.K., et al., *A techno-economic feasibility of a stand-alone hybrid power generation for remote area application in Bangladesh.* Energy, 2017. **134**: p. 775-788.
[63] Ma, T., H. Yang, and L. Lu, *Study on stand-alone power supply options for an isolated community.* International Journal of Electrical Power & Energy Systems, 2015. **65**: p. 1-11.
[64] Ramli, M.A., A. Hiendro, and S. Twaha, *Economic analysis of PV/diesel hybrid system with flywheel energy storage.* Renewable Energy, 2015. **78**: p. 398-405.
[65] Tsuanyo, D., et al., *Modeling and optimization of batteryless hybrid PV (photovoltaic)/Diesel systems for off-grid applications.* Energy, 2015. **86**: p. 152-163.
[66] Hossain, M., S. Mekhilef, and L. Olatomiwa, *Performance evaluation of a stand-alone PV-wind-diesel-battery hybrid system feasible for a large resort center in South China Sea, Malaysia.* Sustainable Cities and Society, 2017. **28**: p. 358-366.
[67] Zhao, J. and X. Yuan, *Multi-objective optimization of stand-alone hybrid PV-wind-diesel-battery system using improved fruit fly optimization algorithm.* Soft Computing, 2015: p. 1-13.
[68] Maleki, A. and F. Pourfayaz, *Sizing of stand-alone photovoltaic/wind/diesel system with battery and fuel cell storage devices by harmony search algorithm.* Journal of Energy Storage, 2015. **2**: p. 30-42.
[69] Bortolini, M., et al., *Economic and environmental bi-objective design of an off-grid photovoltaic–battery–diesel generator hybrid energy system.* Energy Conversion and Management, 2015. **106**: p. 1024-1038.
[70] Rohani, G. and M. Nour, *Techno-economical analysis of stand-alone hybrid renewable power system for Ras Musherib in United Arab Emirates.* Energy, 2014. **64**: p. 828-841.

[71] Kaabeche, A. and R. Ibtiouen, *Techno-economic optimization of hybrid photovoltaic/wind/diesel/battery generation in a stand-alone power system.* Solar Energy, 2014. **103**: p. 171-182.
[72] Ismail, M., M. Moghavvemi, and T. Mahlia, *Techno-economic analysis of an optimized photovoltaic and diesel generator hybrid power system for remote houses in a tropical climate.* Energy Conversion and Management, 2013. **69**: p. 163-173.
[73] Rehman, S., et al., *Feasibility study of a wind–pv–diesel hybrid power system for a village.* Renewable Energy, 2012. **38**(1): p. 258-268.
[74] Lacko, R., et al., *Stand-alone renewable combined heat and power system with hydrogen technologies for household application.* Energy, 2014. **77**: p. 164-170.
[75] Ismail, M.S., M. Moghavvemi, and T.M.I. Mahlia, *Design of an optimized photovoltaic and microturbine hybrid power system for a remote small community: Case study of Palestine.* Energy Conversion and Management, 2013. **75**: p. 271-281.
[76] Rey, G., et al., *Performance analysis, model development and validation with experimental data of an ICE-based micro-CCHP system.* Applied Thermal Engineering, 2015. **76**: p. 233-244.
[77] Homayouni, F., R. Roshandel, and A.A. Hamidi, *Techno-economic and environmental analysis of an integrated standalone hybrid solar hydrogen system to supply CCHP loads of a greenhouse in Iran.* International Journal of Green Energy, 2017. **14**(3): p. 295-309.
[78] Ahmadi, P., M.A. Rosen, and I. Dincer, *Greenhouse gas emission and exergo-environmental analyses of a trigeneration energy system.* International Journal of Greenhouse Gas Control, 2011. **5**(6): p. 1540-1549.
[79] Nafeh, A.E.-S.A., *Optimal economical sizing of a PV-wind hybrid energy system using genetic algorithm.* International Journal of Green Energy, 2011. **8**(1): p. 25-43.
[80] Yang, H., et al., *Optimal sizing method for stand-alone hybrid solar–wind system with LPSP technology by using genetic algorithm.* Solar Energy, 2008. **82**(4): p. 354-367.
[81] Ipsakis, D., et al., *Power management strategies for a stand-alone power system using renewable energy sources and hydrogen storage.* international journal of hydrogen energy, 2009. **34**(16): p. 7081-7095.
[82] Moradi, M.H., et al., *An energy management system (EMS) strategy for combined heat and power (CHP) systems based on a hybrid optimization method employing fuzzy programming.* Energy, 2013. **49**: p. 86-101.
[83] Li, M., et al., *Optimal design and operation strategy for integrated evaluation of CCHP (combined cooling heating and power) system.* Energy, 2016. **99**: p. 202-220.
[84] Sanaye, S. and A. Sarrafi, *Optimization of combined cooling, heating and power generation by a solar system.* Renewable Energy, 2015. **80**: p. 699-712.
[85] Yousefi, H., M.H. Ghodusinejad, and A. Kasaeian, *Multi-objective optimal component sizing of a hybrid ICE + PV/T driven CCHP microgrid.* Applied Thermal Engineering, 2017. **122**: p. 126-138.
[86] Brandoni, C. and M. Renzi, *Optimal sizing of hybrid solar micro-CHP systems for the household sector.* Applied Thermal Engineering, 2015. **75**: p. 896-907.

Chapter 2: Optimisation of Stand-alone Hybrid Energy Systems Supplemented by Combustion-based Prime Movers[2]

This chapter discusses a comparative analysis undertaken between a baseline PV/Batt system, meeting a dynamic load profile, and systems hybridised with supplementary combustion-based prime movers such as Internal Combustion Engines or Micro Gas Turbines of 30-65 kW rating. This study sheds light for the first time on a number of research questions not addressed in earlier studies. The main contributions of the work are namely to: (i) analyse the effects of the start-up threshold and the type of supplementary prime mover on the Cost of Energy (COE, $/kWh), lifetime CO_2 emissions, and (unrecovered) waste heat for a specified reliability (Loss of Power Supply Probability-LPSP); (ii) investigate the effects of including the transient start-up periods of prime movers on systems sizing; and (iii) look into the effects of using two smaller sized (tandem) supplementary prime movers versus a single larger one on the operational characteristics. The research also analyses (iv) the effects of the methods used (e.g. temporal resolution of simulations, Genetic Algorithm (GA) population size) on the COE, lifetime CO_2 emissions, and (unrecovered) waste heat. In this chapter, Research Question 1(RQ1) is addressed where the effects of hardware components, load characteristics, and optimisation methods on the Cost of Energy and the consequential performance indicators are investigated.

2.1 Introduction

Global energy demand is rising steadily as a consequence of population growth and higher living standards. Around 1.2 billion people (17 % of the global population) live without electricity: of those, 22 % are in developing countries where a grid connection is not readily available [1]. The continuous depletion of fossil fuel reserves, growing awareness of the environmental impact of power generation solely reliant on combustion [2, 3], and the remoteness of many communities [4-7] are driving the development of more sustainable energy supply options. Photovoltaic (PV), solar thermal power plants, wind energy, as well as generators driven by combustion engines in hybridised power installations can be cost-effective choices in remote areas compared to grid connections [8-10]. However, amongst all the renewable energy systems, PV is the dominant configuration [11-15]. Wind energy may not be technically feasible at low wind speeds [16] and is more intermittent than PV [17], thus requiring the use of intelligent methods in many instances to predict availability [18] . PV systems are common in many stand-alone energy applications due to their lower maintenance requirements ($20/kW/year [19]) and more straightforward applications [13]. However, with solar irradiance also being seasonal and intermittent [20-23], PV systems need supplementation to increase the reliability of meeting electric

[2] This chapter has been published as a full research paper:

Das, B.K., Y.M. Al-Abdeli, and G. Kothapalli, **Applied Energy**, 2017. **196**: p. 18-33.

Whilst efforts were made to retain original content of the article, minor changes such as number formats and font size style were implemented in order to maintain the consistency in the formatting style of the thesis.

loads. Whilst storing surplus generated power in batteries over periods of low (electric) demand remains widespread [24], the environmental impact of such methods also needs to be considered [25, 26]. Even so, energy storage media are routinely used alongside renewables to stabilize power output [27-29]. An alternative approach to solely relying on (long-term) energy storage via batteries in energy systems based on renewables only involves deploying hybridisation featuring other (backup) prime movers [17]. With the exception of distributed energy systems, which can also be supplemented by grid connections [30, 31], the data presented in Table 2.1 clearly shows the lack of work done in integrating waste heat recovery into hybridised stand-alone systems. This has occurred even enough there are numerous hybrid systems in practice [32] and has led to these systems involving combustion processes which suffer from low thermal efficiency. Improving the sustainability of such hybridised systems can be achieved through increasing renewable energy penetration [33] and overall fuel utilisation efficiencies so as to reduce fossil fuel consumption [34]. In combustion-driven (supplemental) prime movers like Internal

Table 2.1: PV energy systems with different hybridisations.

	Prime Movers	Power (kW)	Storage	CHP/CCHP	Modelling Parameters	Methodology
Stand-alone	PV+WG+MGT [35]	510	Lead acid	No	ACS	GA
	PV+WG+ICE [36]	240	Lead acid	No	NPC, COE, EE, CO_2 emissions	HOMER
	PV+ICE [37]	160	Lead acid	No	COE, Fuel savings, CO_2 emissions	HOMER
	PV+ WG [38]	155.4	Lead acid	No	NPC, COE	HOMER
	PV+MGT [39]	64.6	Lead acid	Yes	COE	Iterative
	PV+MGT/ICE [40]	51.6	Lead acid	Yes	COE, Emissions	GA
	PV+ICE [41]	32-50	Lead acid, Pump storage	No	ACS	PSO
	PV+ICE+WG [42]	7.8-52.71	Lead acid	No	LCOE, ICC, Emissions	MOGA
	PV+WG [43]	18.46	Lead acid	No	LPSP, System cost	GA
	PV+ WG [44]	5.12-17.75	Lead acid	No	System cost, Autonomy level, Waste energy rate	MOGA
	PV+ICE [45]	4-17.6	Lead acid	No	System cost	HOGA
	PV+PEMFC [19]	1.5-3.5 kWh	Lead acid	No	NPC, CO2 emissions	PSO, HOMER
	PV+ WG [46]	1.5	Lead acid	No	LPSP, ACS	GA
	PV+WG+PEMFC [20]	--	Lead acid	No	LCE, EE, NPC	MOGA
Distributed	PV+ICE [31]	48	Lead acid	Yes	LCOE, Emissions	FORTRAN
	PV+ICE [30]	6.4-9.1	Lead acid	Yes	Capacity factor	HOMER

Key: **ACS:** Annualise Cost of System; **COE:** Cost of Energy; **CHP:** Combine Heating and Power; **CCHP:** Combine Cooling Heating and Power; **EE:** Excess Energy; **GA:** Genetic Algorithm; **HOMER:** Hybrid Optimization of Multiple Energy Resources; **HOGA:** Hybrid Optimisation by Genetic Algorithm; **ICE:** Internal Combustion Engine; **ICC:** Initial Capital Cost; **LCOE:** Levelized Cost of Energy; **LCE:** Life Cycle Emissions; **LPSP:** Loss of Power Supply Probability; **MGT:** Micro Gas Turbine; **MOGA:** Multiobjective Genetic Algorithm; **NPC:** Net Present Cost; **PV:** Photo-voltaic; **PSO:** Particle Swarm Optimisation; **WG:** Wind Generator.

Combustion Engines (ICEs) or Micro Gas Turbines (MGTs), the recovery of waste heat to meet local heating and cooling loads can achieve higher overall power plant efficiency [47] and fewer environmental pollutants [48, 49]. This results in stand-alone and distributed energy systems based on

Combined Heat and Power (CHP) or Combined Cooling, Heating, and Power (CCHP), commonly known as cogeneration and trigeneration [50].

Table 2.2 presents the typical technical characteristics of different prime movers used in CHP and CCHP applications. In this context, Khatri et al. [47] conducted an experimental investigation on a laboratory scale ICE-based CCHP system. Their results showed that thermal efficiency increases from 33.7 % to 86.2 % when the engine is operated in CCHP mode, with a similar reduction in CO_2 emissions from 0.308kg CO_2/kWh (power mode only) to 0.1211 kg CO_2/kWh (CCHP mode). Lin et al. [51] also carried out a similar type of experiment, but for a slightly larger residential size CCHP system featuring an ICE. They reported a significant increase in overall energy efficiency and a reduction in CO_2 emissions. In this regard, the higher temperature range typically associated with exhaust gas outlets for an MGT (200–650 ºC) may make them more suited for CHP applications compared to an ICE. However, the major concern for an MGT is its low electrical efficiency (~30 %), which reduces significantly at part load or when using fuels with lower heating values. However, from an environmental perspective, an MGT produces 100 times less NOx emissions than a diesel engine [52]. Studies on a 100 kW MGT (with CHP) have found electrical efficiencies up to 29 % in the 80-100 kW range, with primary energy savings and overall efficiency of about 23 % and 74 % (CHP), respectively, with substantially lower pollutants [53]. With this in mind, more research is warranted into the analysis of waste heat and its recovery when sizing hybridised energy systems (Table 2.1). This becomes more relevant when thermal (cooling or heating) loads can be met through waste heat recovery, rather than diverting the same (total) electric load for this purpose in power-only modes of operation. This study analyses the (secondary) waste heat potential incidentally generated in a hybridised stand-alone system meeting an electric load only.

Table 2.2: Typical characteristics of prime movers used in CHP and CCHP systems

Parameters	**Internal Combustion Engine (ICE)**	**Micro Gas Turbine (MGT)**
Capacity (kW) [52]	5-20,000	15-300
Fuels [52, 54]	Diesel, natural gas, propane	Diesel, natural gas, propane, biogas, kerosene
Electrical efficiency (%) [52, 54]	27-45	15-30
Overall efficiency with CHP/CCHP (%) [52, 54]	65-90	60-85
Part load performance [52]	High	Moderate
Exhaust gas temperature (º C) [52]	80-540	200-650
Thermal output (kJ/kWh) [52]	3,376-5,908	3,376-7,174
Start-up time (transient) [52, 54, 55]	10 s	60 s
CO_2 emissions (kg/MWh) [52]	650	720
NO_x emissions (kg/MWh) [52]	10	0.1
Life time (year) [52, 56]	10	10

The ability to optimise the Power Management Strategy (PMS), which governs device switching in energy systems, also impacts techno-economic feasibility [57-59]. Whilst there is excellent industry-based simulation software for systems sizing [60], these applications are not self-adaptive [19], nor do they readily account for device start-up transients [20]. These limitations, as well as the ability to integrate the effects of different Power Management Strategies (PMS) in simulations, have led to a number of intelligent techniques being used to size or optimise hybrid energy systems. These methods include Genetic Algorithms (GAs) [20, 42, 46, 61-66], Particle Swarm Optimization (PSO) [41, 67], Simulated Annealing (SA) [68, 69], Tabu Search (TS) [68], Artificial Bee Swarm Optimization (ABSO) [70], Harmony Search (HS) [68], Monte Carlo Simulation [71, 72], and Artificial Neural Networks (ANN) [73]. Most energy system simulations then target optimising a single and multiple objective function(s), including Net Present Cost (NPC, $/lifetime), the Cost of Energy (COE, $/kWh), or reducing environmental impact (kg CO_2 eq/kWh or kg CO_2 eq/lifetime), whilst meeting a specific load reliability [74]. The Loss of Power Supply Probability (LPSP) is widely considered to be a reliability index when sizing PV/wind [46, 75-77] or PV/wind/hydrogen [20] systems when meeting an electrical load only. However, it has not been considered while using an ICE or MGT to supplement electrical power supply or in the context of also meeting a thermal load [39, 41, 78]. In this regard, the effectiveness of GA is considered higher than other types of optimisation tools like PSO for finding the global optimum of an objective function, in addition to being able to handle larger numbers of parameters [79]. Although Dufo-Lopez and Bernal-Agustin [78] used GA and a multi-objective optimisation (levelised cost of energy and life cycle emissions) in a hybrid system (consisting of PV, wind turbines, diesel engines, and battery storage), they did not study the effects of transient start up for supplementary prime movers or waste heat generation, which would obviously show overall system potential in CHP and CCHP applications. In another study, Cristóbal-Monreal and Dufo-López [80] studied both single- and multi-objective optimisation (minimisation of system cost or its weight in PV/Batt/ICE stand-alone systems) using GA and reported the COE at 0.26 €/kWh. However, they only considered monthly averaged solar irradiation and ambient temperature profiles. Ismail et al. [40] also investigated GA optimisation of a PV/MGT system; however, they did not simulate the system using a dynamic load spanning an entire year, but only considered up to one week. This limits consideration of seasonal effects (e.g. temperatures, solar irradiation) which affects both the amount of PV power generated and the operational efficiency of PV modules as well as combustion-based prime movers. With the efficiency of ICEs and MGTs being temperature dependent [54], the use of coarser (larger) time steps may affect their derived analyses. They also did not discuss the effects of various modelling methodologies such as the effects of temporal resolution, the minimum starting threshold of supplementary prime movers, or the effects of single versus tandem ICE/MGT (i.e. using 60 kW versus two 30 kW engines) on the optimised systems. Details of their PMS (switching algorithm) were also not reported.

Some of the aforementioned gaps are overcome by the present paper, which not only compares the optimisation of stand-alone PV/Diesel and PV/MGT systems, but also these two types of system compared to solely renewable systems (PV only). The original contributions of this study include integrating the effects of the transient start-up time for prime movers (i.e. ICE, MGT), considering the waste heat produced as a consequence of systems sized when meeting an electric load, examining the effects of prime mover scalability and their minimum cut-in threshold, as well as the particulars of the GA methodologies used. The study utilises MATLAB R2015b for system modelling and its GA Optimisation Toolbox. The study also integrates typical power (efficiency) profiles for an ICE (30 kW, 60 kW), MGT (30 kW, 65 kW) and meteorological data for solar irradiation, temperature, and wind speed (which both affect PV panel efficiency) as well as dynamic electrical demand profiles to the conceptual stand-alone energy system studied. These outcomes are achieved in the context of using battery storage to cover (only) the start-up threshold of each combustion-based prime mover. Batteries are not used in the present research for long-term (seasonal) energy storage, as reported in other studies into hybridised systems [24, 37, 81] or for systems based on PV alone [82].

2.2 Methodology

A block diagram of a conceptual hybrid energy system is shown in Figure 2.1. PV arrays are used to provide the base load with combustion type supplementary prime movers: Internal Combustion Engine (ICE) or Micro Gas Turbine (MGT). The system is stand-alone with no access to grid power and is subject to dynamically varying renewables and load. In the simulations which follow, this system has been modelled to operate in one of three modes: PV/Batt (mode-I); PV/Batt/ICE and PV/Batt/MGT based on multiple units of supplementary prime movers (mode-II); and PV/Batt/ICE and PV/Batt/MGT using a single (larger) unit of a supplementary prime mover (mode-III). Batteries in mode-I function as

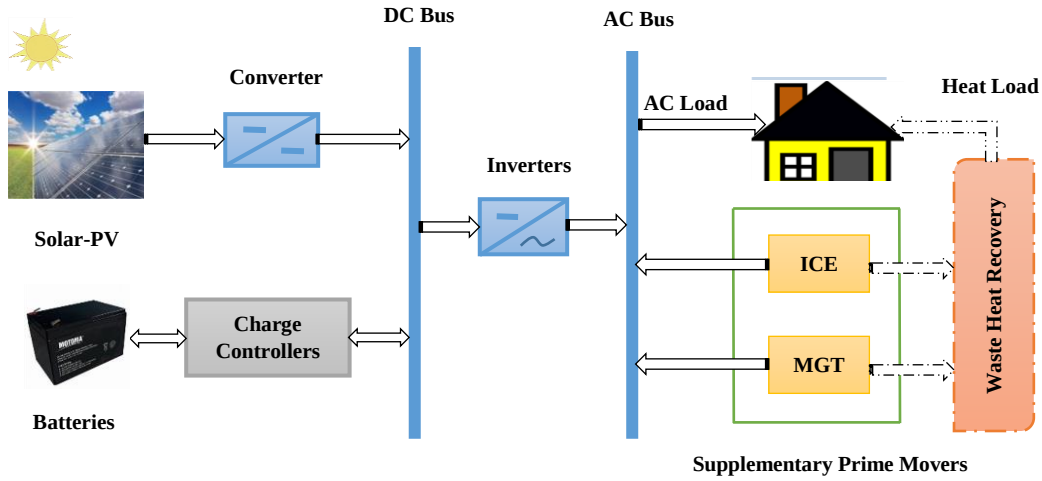

Fig. 2.1: A conceptual PV energy system supplemented by combustion engines which can operate in three modes (Mode-I: PV/Batt; Mode-II: PV/Batt with 2x30 kW ICE or MGT; Mode-III: PV/Batt with 1x60-65 kW ICE or MGT).

seasonal (long-term) storage and this forms the baseline case for comparison. In hybridised systems operating mode-II and mode-III, batteries supplement PV until the load deficits meet the minimum starting power of the supplementary ICE or MGT ($P_{sup,min}$).

2.2.1 Renewable profile and PV model

The performance characteristics of a commercially available PV module are used (Make: Heckert Solar, Model: HS-PL 135) [83]. Based on a single diode equivalent circuit for PV cells, saturation current is defined by Equation 2.1 [84, 85]:

$$I_{PV}(t) = I_L(t) - I_o\left[exp\left(\frac{V+I_{PV}(t)R_s(t)}{a(t)}\right) - 1\right] - \frac{V+I_{PV}(t)R_s(t)}{R_{sh}} \quad (2.1)$$

In this context, the light current $I_L(t)$, diode reverse saturation current I_o, series resistance $R_s(t)$, shunt resistance R_{sh} , and the parameter *a(t)* (modified ideality factor) are calculated to determine the solar current. These parameters can be obtained using measurements of the *I-V* characteristics of a module provided by the manufacturer under reference conditions and other known hardware-specific characteristics [83]. The bracketed terms (*t*) denote time varying quantities included in the simulations over each time interval. Based on the temporal resolution used, the light current, which depends on solar irradiance *G(t)* and cell temperature $T_{PV}(t)$, is calculated from Equation 2.2, where G_{ref} is the reference solar irradiation (1000 W/m^2), $I_{L,ref}$ is the short circuit current at the reference temperature (8.33A), κ_t is the temperature coefficient of short circuit current (0.0005 /ºC), and T_{ref} is the reference temperature (25º C) [83, 86]. As such, variations in meteorological data which occur at time scales finer than the temporal resolution used in the present paper, are not represented.

$$I_L(t) = \left(\frac{G(t)}{G_{ref}}\right)\left(I_{L,ref} + \kappa_t\left(T_{PV}(t) - T_{ref}\right)\right) \quad (2.2)$$

On the other hand, shunt resistance R_{sh} , can be calculated by Equation 2.3. Here V_{mp}, I_{mp}, V_{oc}, and I_{sc} are the maximum power point voltage (18 V), maximum power point current (7.48 A), nominal open circuit voltage (22.3 V) and short circuit current (7.95 A), respectively [83].

$$R_{sh} = \frac{V_{mp}}{I_{sc}-I_{mp}} - \frac{V_{oc}-V_{mp}}{I_{mp}} \quad (2.3)$$

It should also be noted here, that whilst PV has been integrated into energy system studies, many published works do not identify whether PV module performance accommodated meteorological data other than solar irradiance. In the present research, the performance of the PV modules at any time interval is dependent on the cell temperature, which is itself a function of solar irradiation, ambient temperature, and wind speed. The cell temperature is determined by Equation 2.4 [87], where $T_{amb}(t)$ is the ambient temperature (ºC), and $W_s(t)$ is the wind speed (m/s):

$$T_{PV}(t) = 0.943 \times T_{amb}(t) + 0.028 \times G(t) - 1.528 \times W_s(t) + 4.3 \quad (2.4)$$

Figure 2.2 shows the time-resolved meteorological data (solar irradiation, wind speed, ambient temperature) for the remote location in Western Australia that was used in relation to the conceptual system analysed (Broome: at latitude:17º56'S, and longitude:122º14'E) [88]. In the simulations, the effects of two temporal resolutions for this data (15 min and 60 min) were also studied. The total annual availability of solar irradiance is 2290 kW/m^2, with peak of 1.14 kW/m^2. In this study, the Renewable Penetration (RP) is defined as (useful) PV energy generated by the PV which is directed to meet the load demand. This is applied across modes I-III and excludes PV power generated but dumped due to lack of demand or batteries being fully charged.

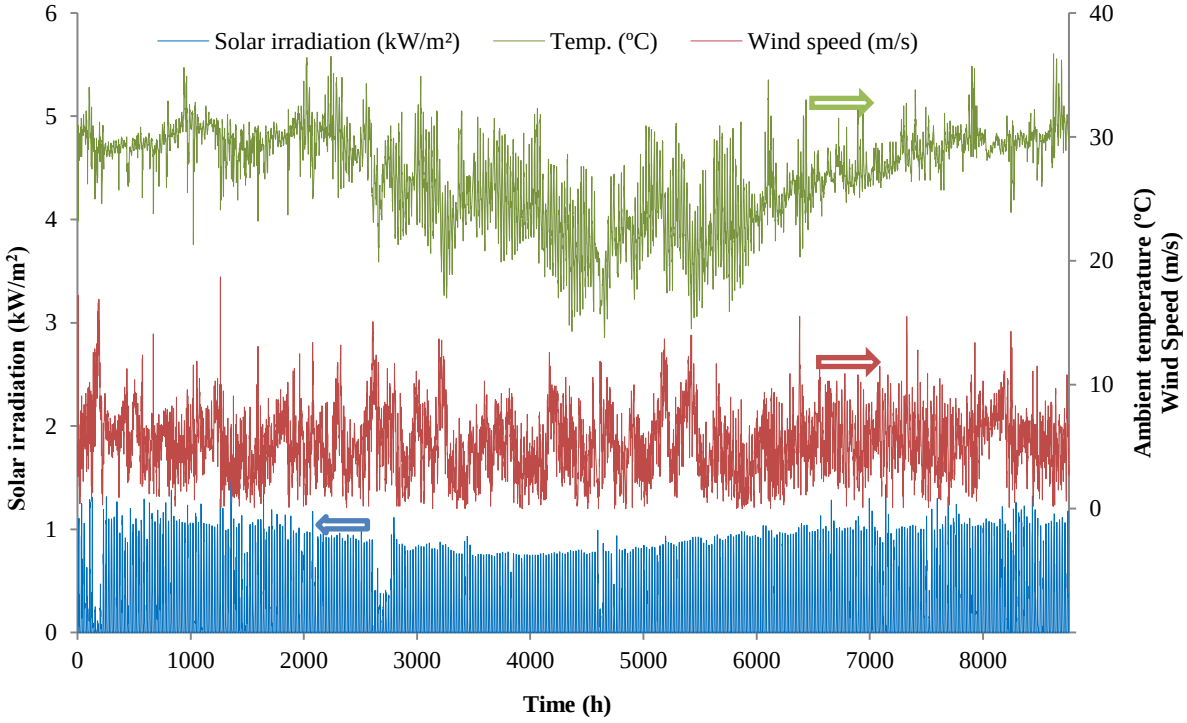

Fig. 2.2: Time resolved solar irradiation, ambient temperature and wind speed of selected area over the period (01/07/2014 to 30/06/2015).

2.2.2 Supplementary prime movers

The first type of supplemental prime movers considered are 30 kW and 60 kW Internal Combustion Engines (ICEs), fuelled by diesel (net heating value: 35.86 MJ/l, density: 0.832 kg/l). The performance of a diesel generator set is determined by its Specific Fuel Consumption (SFC) (l/kWh) or hourly fuel consumption (l/h). The simulations will also consider the effects of varying minimum engine starting threshold. In this regard, Ashari et al.[89] reported a diesel generator having maximum efficiency (3 kWh/l) when running at 80 % of its rated capacity, with efficiency becoming low at loads below 30 % of its rated capacity. Additionally, El-Hefnawi [90] reported optimised diesel generator sets at 70-89 % of the rated capacity. In the present simulations, the effects of the different (minimum) starting thresholds for the ICE are considered (15, 20, 25 and 30 % of rated power). Figures 2.3 and 2.4 show

typical (normalised) performance characteristics curves for both a 30 kW and 60 kW ICE [91, 92]. The hourly fuel consumption rate (l/h) for a diesel ICE can also be determined using polynomial fits of engine operating characteristics (Equations 2.5 and 2.6 for ICE 30 kW and ICE 60 kW, respectively).

$$C_{fuel_{ICE_{30}}}(t) = -0.0015 \times P^2{}_{ICE}(t) + 0.3055 \times P_{ICE}(\mathrm{t}) - 0.0138 \quad (2.5)$$

$$C_{fuel_{ICE_{60}}}(t) = 0.0021 \times P^2{}_{ICE}(t) + 0.0888 \times P_{ICE}(\mathrm{t}) + 3.0351 \quad (2.6)$$

In this regards, $P_{ICE}(t)$ refers to power generation from the diesel engine over any time interval. The heat energy produced from an ICE can also be calculated from the basic first law of thermodynamics applied to a steady system as follows:

$$\dot{W}H_{sup}(t) = \dot{m}_g(t)C_{pg}\big(T_2(t) - T_1(t)\big) \quad (2.7)$$

where $\dot{m}_g(t)$ is the exhaust gas flow rate, C_{pg} is the specific heat of exhaust gas (1 kJ/kg-K) and $T_1(t)$, $T_2(t)$ are inlet temperature of air into the ICE and exhaust gas temperature, respectively. The exhaust gas flow rate and temperature can also be determined using the technical data sheets related to the ICE modelled.

The second type of supplemental prime movers considered are comparably sized 30 kW and 65 kW Micro Gas Turbines (MGTs) fuelled by natural gas (net heating value: 34.60 MJ/m^3, density: 0.8 kg/m^3). Fuel consumption at any time interval depends on the operating power but is strongly affected by ambient temperature. At higher temperatures, power output decreases due to lower air density and decreases in mass flow rate. At the same time, efficiency also decreases as the compressor needs more power to compress the less dense (warmer) air. As such, up to an ambient temperature of 21 ºC, the MGT gives its rated power, but at 40 ºC its output power decreases to almost 20 % of its rated power. Although the average temperature of the selected area is 25 ºC, its maximum temperature reaches around 37 ºC (see Figure 2.2). Therefore, in this simulation the effects of ambient temperature on MGT output power have also been included in each time interval based on meteorological data. Normalised performance characteristic curves for the MGTs simulated are shown in Figures 2.3 and 2.4.

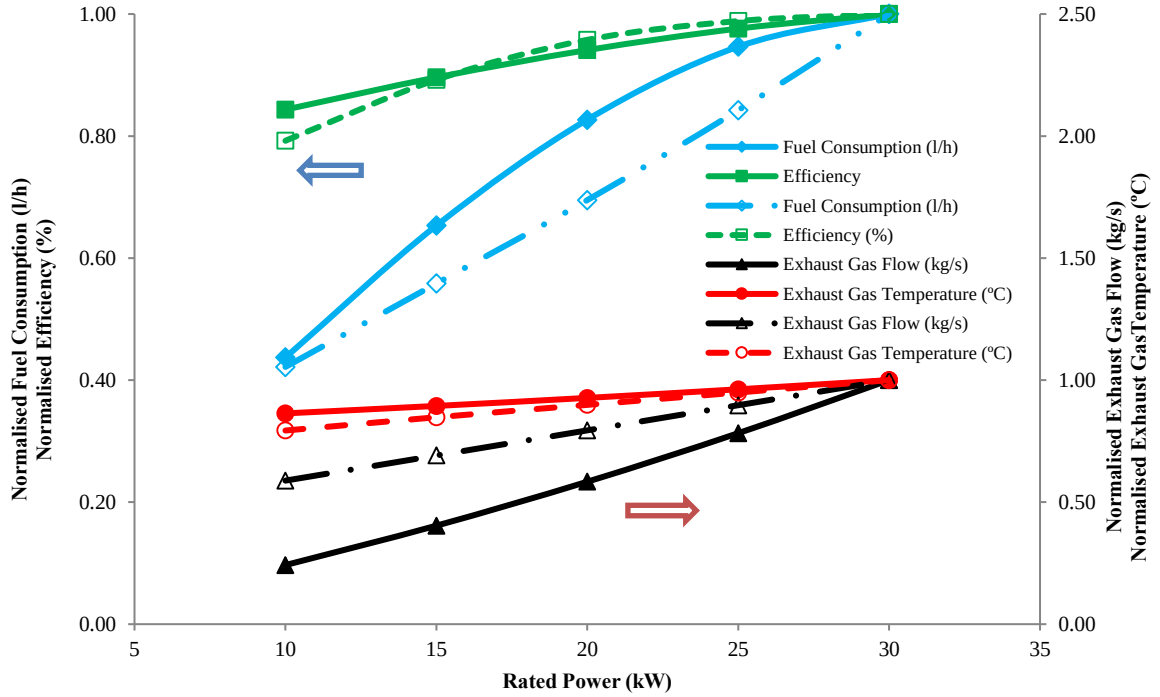

Fig. 2.3: Normalised fuel consumption, efficiency, exhaust gas flow and exhaust gas temperature of a typical 30 kW ICE (solid) and MGT (dashed).

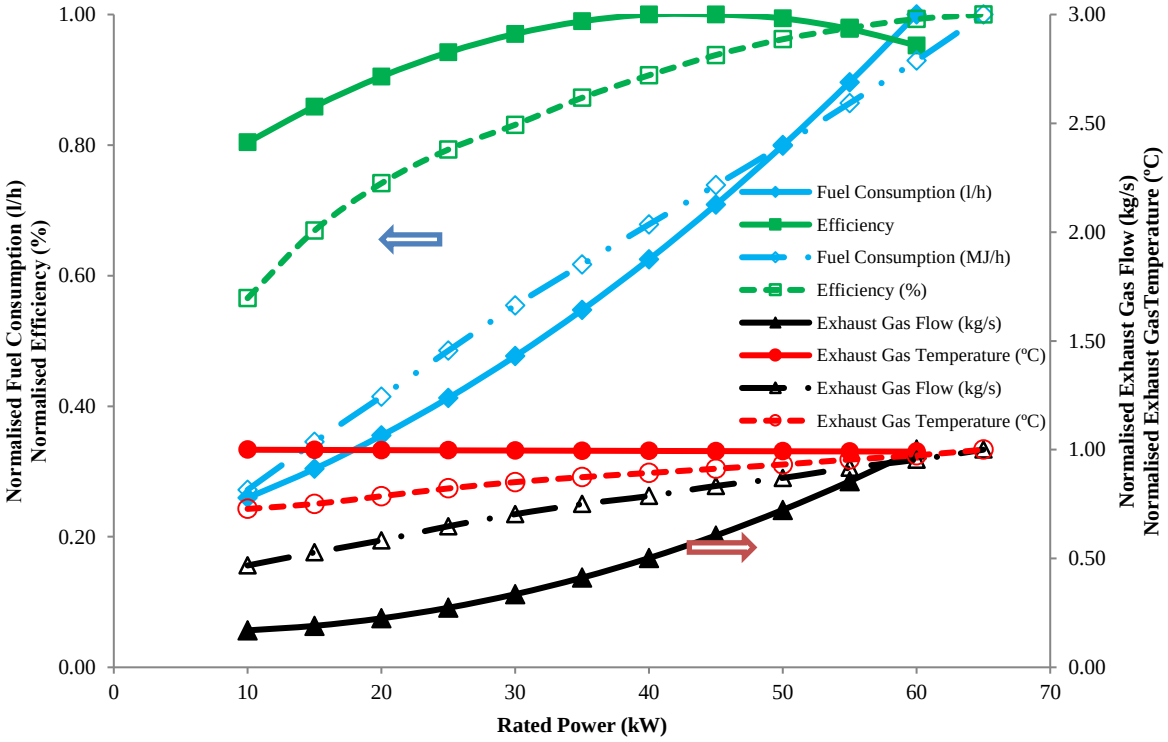

Fig. 2.4: Normalised fuel consumption, efficiency, exhaust gas flow and exhaust gas temperature of a typical 60 kW ICE (solid) and 65 kW MGT (dashed).

The fuel consumption (MJ/h) can be derived using polynomial fits of manufacturer specifications.

$$C_{fuel_{MGT_{30}}}(t) = 0.0422 \times P^2{}_{MGT}(t) + 10.352 \times P_{MGT}(t) + 66.26 \quad (2.8)$$

$$C_{fuel_{MGT_{65}}}(t) = -0.0127 \times P^2{}_{MGT}(t) + 11.457 \times P_{MGT}(t) + 109.85 \quad (2.9)$$

Taking into consideration the temperature effect, the power output can be calculated by following Equations [93]:

$$P_{MGT_{30}}(t) = -0.0046 \times T^2{}_{amb}(t) - 0.0006 \times T_{amb}(t) + 30.427 \quad (2.10)$$

$$P_{MGT_{65}}(t) = -0.0113 \times T^2{}_{amb}(t) + 0.1503 \times T_{amb}(t) + 64.96 \quad (2.11)$$

where $T_{amb}(t)$ (ºC) is the ambient temperature. The waste heat from the MGT during power generation can be calculated using Equation 2.7. The exhaust gas flow rate (m^3/h) and its temperature are determined from the technical data sheet [54, 93].

In the analyses which follow, the Waste Heat to Supply Power (WHSP) is the ratio of waste heat by the supplementary prime mover ($\dot{W}H_{sup}(t)$) relative to the supply power generated ($P_{sup}(t)$), and can be calculated from Equation 2.12:

$$WHSP = \frac{\sum_{t=1}^{T} \dot{W}H_{sup}(t)}{\sum_{t=1}^{T} P_{sup}(t)} \quad (2.12)$$

The Duty Factor (DF) is defined as the energy generation from the supplementary sources per start-stop and can also be formulated mathematically as follows:

$$DF = \frac{\sum_{t=1}^{T} E_{sup}(t)}{\sum_{t=1}^{T} N_{S/S}} \quad (2.13)$$

where E_{sup} (t) is the energy generation by the supplementary prime movers over the period T (year in this study resolved into either 15min or 60min intervals) and $N_{S/S}$ refers to the number of start of combustion engines during that period. The characteristics of both the ICE and MGT modelled (Figures 2.3 and 2.4) are typical of others cited in the literature [54, 93].

2.2.3 Battery modelling

In all simulations undertaken, a battery bank is utilised if PV (renewables) do not satisfy the load or if the supplementary prime movers are unavailable. In the latter case, this occurs if all (or part) of the base load to be satisfied exceeds available renewables, but this load also exceeds the (minimum) start-up threshold of supplementary prime movers. The consequence is that in non-hybridised PV (only) systems, batteries are sized for long-term (seasonal) energy storage. Alternatively, in hybridised systems batteries cover only limited storage when the ICE and MGT are used. Battery state of charge at any time step (t) is computed based on the state of charge at the previous time interval (t-1) and the additional charge over the current time step (t) and is defined by Equation 2.14 [43, 86]:

$$B_{SOC}(t) = B_{SOC}(t-1) + \frac{P_B(t) \times \Delta t}{1000 \times C_b} \quad (2.14)$$

where C_b is the nominal capacity of the battery and Δt is the simulation time step (15min and 60min in this study) whilst $P_B(t)$ is the power flow toward the battery, which can be calculated for a charging process as follows:

$$P_B(t) = \left(P_{PV}(t) - \frac{P_L(t)}{\eta_{inv}}\right) \times \eta_b \quad (2.15)$$

where $P_{PV}(t)$ is the power generated from PV modules, $P_L(t)$ is the load demand, η_{inv} is the inverter efficiency and η_b is the battery efficiency. However, during a discharging process Equation 2.15 can be written as:

$$P_B(t) = \left(\frac{P_L(t)}{\eta_{inv}} - P_{PV}(t)\right) \times \eta_b \quad (2.16)$$

Yang et al. [46] reported that the measurement of separate efficiency during the charging and discharging process is difficult and hence, the battery charging efficiency is taken to be equal to the round trip efficiency of the battery and discharging efficiency is set to 1.

At any time step (Δt), the state of charge of the battery bank is subjected to the following constraints:

$$B_{SOC,min} \leq B_{SOC}(t) \leq B_{SOC,max} \quad (2.17)$$

Whilst Equation 2.14 relates to the state of charge during charging, during discharging processes power flows ($P_B(t)$) out of the battery, and so the battery state of charge at time *t* can be determined by:

$$B_{SOC}(t) = B_{SOC}(t-1) - \frac{P_B(t) \times \Delta t}{1000 \times C_b} \quad (2.18)$$

The battery's lifetime depends on a number of parameters such as battery's state of charge, rate of charging/discharging, operating temperature, self-discharge rate, gassing, heating loss and diffusion [46, 94, 95]. For the longevity of the battery bank, the batteries should not be overcharged or over discharged during the process. The maximum charge ($B_{SOC,max}$) is set to nominal capacity of the battery bank and the minimum state of charge ($B_{SOC,min}$) should not be less than 20 % ($B_{SOC,\ min} = 0.2B_{SOC,max}$) for longer battery life [46]. In this paper, the designed lifetime of battery (float life) is 10 years [96]. The battery bank is connected to the PV module through a charge controller. A charge controller is a protective device whose main function is to protect the PV module from reversals of power and to protect the battery bank from overcharged or over discharged states. The DC bus and AC bus are connected by the inverter which converts DC voltage from the PV and battery sources to the AC voltage to supply AC loads. The conversion efficiency of the inverter is considered as 95 % [59]. In the present study, limits on the rate of battery charging [59] or the Peukert Effect [97] have not been considered.

2.2.4 Load profile and reliability index

The simulations consider the electric load profile when deriving the optimum sizing and target a reliability based on the LPSP. The LPSP which is widely adopted [20, 43, 46, 75, 77, 98] is the ratio of all Loss of Power Supply ($LPS(t)$) for given period of time *T* (kWh missed) to the sum of the load demand $E_L(t)$ and can be expressed as [77]:

$$LPSP = \frac{\sum_{t=1}^{T} LPS(t)}{\sum_{t=1}^{T} E_L(t)} \tag{2.19}$$

In this study, missed electric loads during the transient start-up time of the supplemental prime movers are also considered. In this regard, the present study also analyses the effect of neglecting start-up transients ($\Delta T_s = \emptyset$), or setting them to $\Delta T_s = 10s$ [52] for the ICE and $\Delta T_s = 60s$ [99] for the MGT, both of which are usually ignored while sizing system components. The load losses due to the transient start-ups (ΔT_s) depend on the load demand and can be calculated by dividing hourly resolved load demand into 10 s for the ICE and 60 s for the MGT and summing up the load demand over the transient time. It is assumed that the (originally) hourly resolved load demand shown in Figure 2.5 and electricity generation from PV and the ICE or MGT remain constant during each time interval (15 min or 60 min) in simulations.

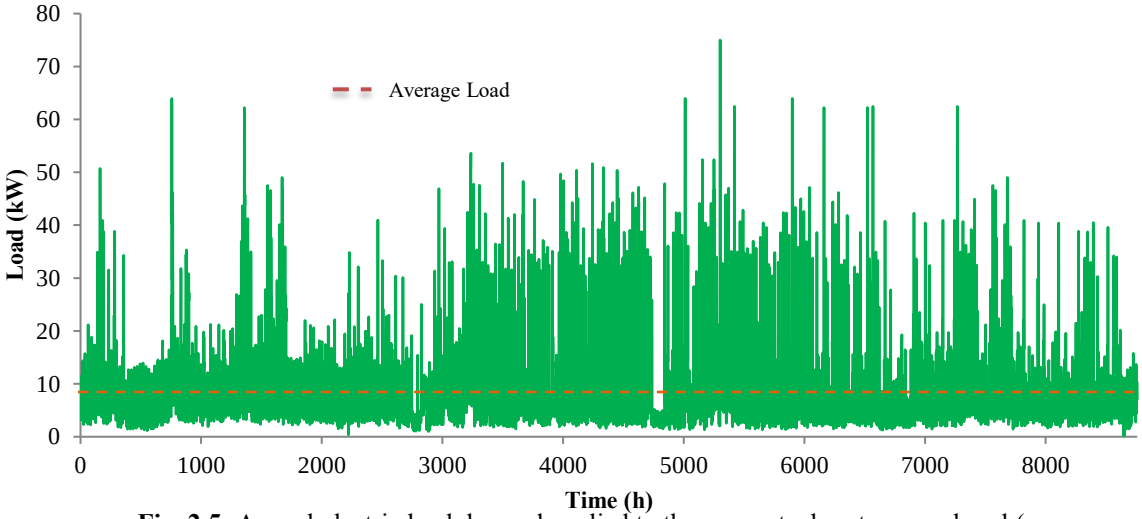

Fig. 2.5: Annual electric load demand applied to the conceptual systems analysed (see Acknowledgements section for source)

To facilitate the modelling the original (anonymous users) load data has been scaled-up in every time interval so that the average annual demand is 8.73 kW with a 75 kW maximum load. The standard deviation in the 15 min and 60 min data is 7.87 kW and 8.02 kW respectively, with standard deviation defined by Equation 2.20, whereby $\bar{x}$ is the mean of load x_i and N is the number of values.

$$S_{N-1} = \sqrt{\frac{\sum_{i=1}^{N}(x_i - \bar{x})^2}{N-1}} \tag{2.20}$$

In this study, an annual demand of 76,487 kWh which corresponds to 209.55 kWh per day with a nominal total of annual unmet load 765 kWh (1 %) have been chosen. The value of the $LPSP_{max}$ constraint is taken as 0.01±0.005.

2.2.5 Power management strategy

Figure 2.6 depicts the Power Management Strategy (PMS) which controls the switching of various components. The algorithm for the baseline PV system is extended to include the decision tree bound by the blue box when supplementary prime movers (such as an ICE or MGT) are included.

2.2.5.1 Baseline algorithm (PV/Batt)

Power generated from the PV ($P_{PV}(t)$) routed by a DC/AC inverter (smooth functioning) and compared with the load demand ($P_L(t)$) to determine the switching of devices and energy flows. The frequency of this switching depends on the time interval (t) chosen. In this study, two different time intervals have been tested (Δt=15 min and Δt=60 min). For each time interval, the deficit between the renewable power generations is compared to the load demand.

$$P_{Net}(t) = P_{PV}(t) - P_L(t) \quad (2.21)$$

where renewables equal the load ($P_{Net}(t) = 0$), the load is met in that time interval (Meet $P_L(t)$). However, where this is not the case, load demand must be satisfied through (long-term) battery storage in the baseline PMS which does not feature supplementary prime movers. This can only occur if sufficient storage capacity exists over that time interval ($B_{SOC}(t) > B_{SOC,min}$), otherwise the load is missed (Unmet $P_L(t)$) and the simulations move to the next time interval (PMS restarts).

If $P_{Net}(t)>0$ and batteries are not fully charged ($B_{SOC}(t) = B_{SOC,max}$), the rest of the power is used to charge the battery until it reaches the maximum state of charge ($B_{SOC,max}$). Additional available power is then dumped and considered as excess energy in this time interval (EE (t)), particularly if the batteries are at their maximum state of charge ($B_{SOC}(t) = B_{SOC,max}$).

2.2.5.1 Extended PMS (PV/Batt/ICE, PV/Batt/MGT)

In the baseline algorithm, batteries provide long-term storage as they are the only source to meet $P_L(t)$ when renewables $P_{PV}(t)$ are insufficient ($P_{Net}(t)>0$). In the case of the extended PMS (the area bounded by the blue box in Figure 2.6), one type of supplementary prime mover (either ICE or MGT) is instead used to meet $P_L(t)$ when $P_{PV}(t)$ is insufficient, provided the P_{Net} exceeds the lower start-up threshold for the ICE or MGT ($P_{sup,min} \leq |P_{Net}(t)|$). This condition is stipulated because the specific fuel consumption (l/kWh) at low power in an ICE is markedly inferior to that at higher power operation (Figures 2.3 and 2.4). Additionally, the part load efficiency of an MGT is also considerably lower [54].

Thus, meeting a minimum power delivery requirement ($P_{sup,min}$) is recommended by manufacturers before start-up is initiated as a function of rated power [56, 78]. When this power requirement is not met relative to the load ($P_{sup,min} > |P_{Net}(t)|$), the supplementary prime movers do not start. In the present study, the effects of different $P_{sup,min}$ have also been considered, particularly as these affect not

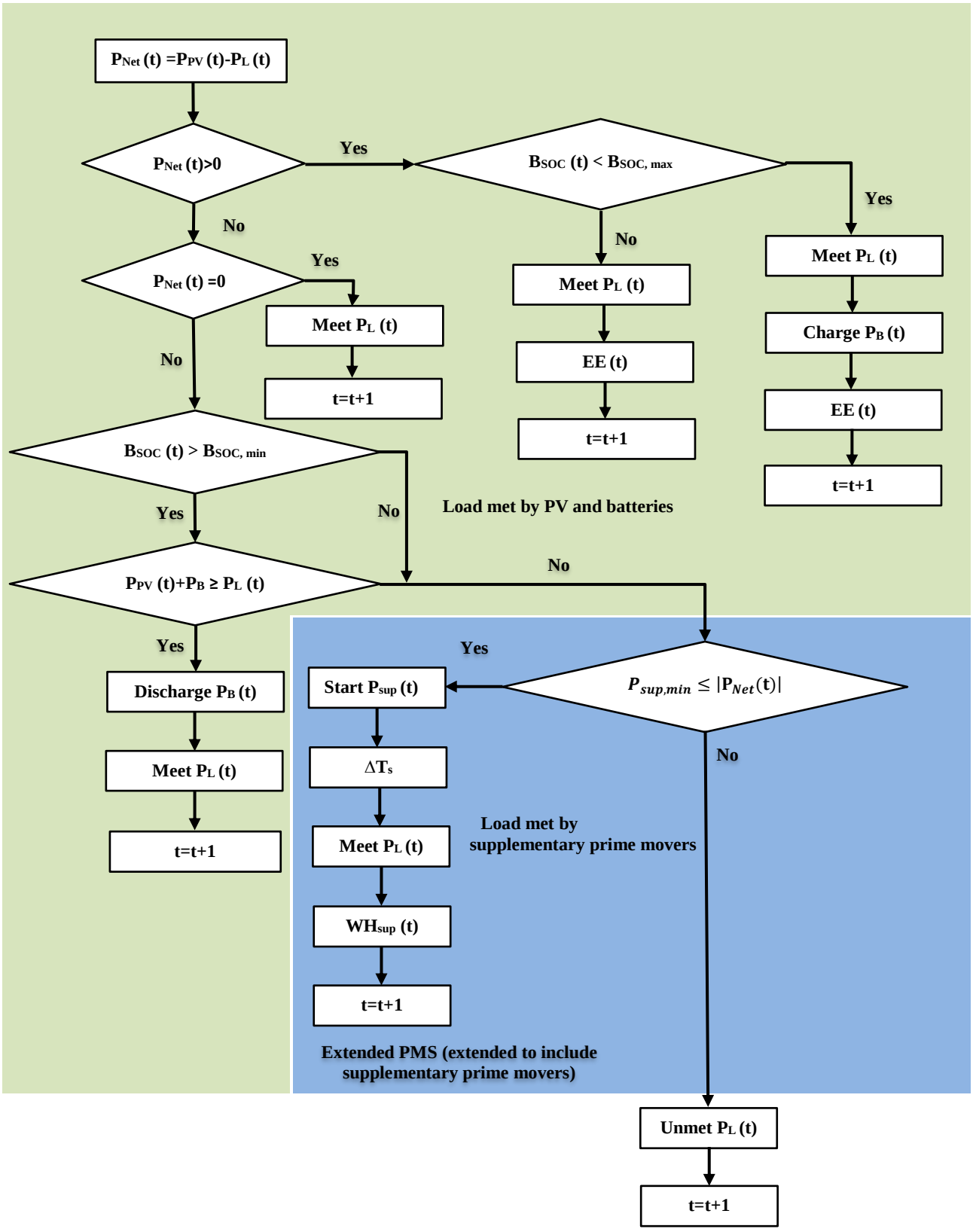

Fig. 2.6: Power Management Strategy (PMS) for the energy system. The area bound by the blue box is active only in the presence of supplementary prime movers (ICE or MGT).

only the COE to meet a specific load demand, but also the waste heat generated and the total operational time of supplementary prime movers. In the extended PMS, when there is insufficient solar power,

batteries are used to deliver the necessary power up to the minimum starting power of supplementary devices ($P_{sup,min}$), otherwise the demand is considered as unmet load if $P_{sup,min} > |P_{Net}(t)|$. At every start-up of the ICE or MGT, the transient start-up time is applied and this contributes to the load loss during that time interval. For every time interval while operating the supplementary device, waste heat generated ($\dot{W}H_{sup}(t)$) is calculated using Equation 2.7.

2.2.6 Optimisation parameters and constraints

The proposed system configuration is optimised by employing a genetic algorithm which dynamically searches for the optimum configuration (mix) of energy system components so as to meet a specific LPSP whilst being operated by the PMS (Figure 6) for each time interval. The objective function in this study is to minimise the annualised COE. During this iterative process, the system's LPSP is examined to establish whether it meets the targeted load reliability requirements. At the minimum COE, the simulations then derive the annual life cycle GHG emissions (kg CO_2-eq/yr), waste heat, excess/dumped energy (kWh/yr) and duty factor of supplementary prime movers (kWh/yr/start-stop) by summing up these values over all time intervals (Δt). Determining the optimal system configuration takes roughly 7-72hrs when running on a desktop PC (processor: Intel Core i5-4570 CPU@ 3.20Ghz, 32-bit operating system) based on the system architecture. The decision variables in this optimisation process include the number of PV modules N_{PV} and number of lead acid batteries N_{bat}. These are subject to the following constraints, whereby $N_{PV,min}$=10, $N_{PV,max}$=500, $N_{bat,\ min}$=1, and $N_{bat,max}$=50:

$$N_{PV,min} \leq N_{PV} \leq N_{PV,max} \quad (2.22)$$

$$N_{bat,min} \leq N_{bat} \leq N_{bat,max} \quad (2.23)$$

$$B_{SOC,min} \leq B_{SOC}(t) \leq B_{SOC,max} \quad (2.24)$$

$$P_{Sup,min} \leq P_{sup}(t) \leq P_{sup,max} \quad (2.25)$$

$$LPSP \leq LPSP_{max} \quad (2.26)$$

The lower bound $N_{bat,\ min}$=1 ensures that the baseline (Mode-I) system based on using PV included some battery capacity in its optimal solution. Whilst choosing the $N_{bat,max}$=50 should not affect the optimal solutions, all of which have far lesser battery numbers, imposing an upper bound does help reduce processing time as it limits the solution space and was determined at an early stage using trial and error. The bounds selected for the PV numbers ($N_{PV,min}$=10, $N_{PV,max}$=500) were also subject to such reasoning. The COE ($/kWh) is an appropriate economic parameter to determine the optimal sizing of energy system configurations and is calculated using Equation 2.27, where ACC is the annualised capital cost obtained via Equations 2.28 and 2.29, *d* refers to discount rate (10 % in the present study) and *n* is the component lifetime [56]. It is also worth noting that the International Energy Agency (IEA) has similarly applied two values for the discount (d) rate when estimating the cost of power generation projects: 5% and 10% [100].

$$COE = \frac{ACC + AOM + AFC}{E_S} \quad (2.27)$$

$$ACC = \sum_i C_{0i} \times CRF_i \quad (2.28)$$

CRF_i is known as capital recovery factor for the *i*th component, can be found from Equation 2.29:

$$CRF = \frac{d(1+d)^n}{(1+d)^n - 1} \quad (2.29)$$

Arun et al. [56] suggest the Annual Operating and Maintenance cost (AOM) can be taken as 2.5 % of capital. The Annual Fuel Cost (AFC*)* of the ICE or MGT is determined by its fuel consumption in the simulations over the year and E_S is the total annual useful energy production from the system (excluding excess energy).

The environmental impact of the energy system can be assessed by calculating the CO_2 equivalent emissions for system components per the energy converted in each component (kg CO_2-eq/kWh). The equivalent CO_2 LCE (kg CO_2-eq/kWh) includes equivalent CO_2 emissions from the energy used to manufacture, transport, and recycle the system components as well as the combustion of fuel in each ICE or MGT. Table 2.3 presents the values used in this simulation for each of these parameters.

Table 2.3: Stand-alone hybridised energy system components cost, lifetime and emissions aspects.

Components Type	**Description**	**Capital Cost ($)**	**Replacement Cost ($)**	**O&M Cost ($/yr)**	**Life time (yr)**	**LCE (kg CO_2-eq/kWh)**
PV module [20]	HS-PL135 (135 W)	310	310	0	25	0.045 [101]
ICE [102]	30 kW	10,500	10,500	260	10	0.880 [101]
	60 kW	12,175	12,700	320		
MGT [54]	30 kW	61,800	61,800	1,540	10	1.16 [103]
	65 kW	129,300	129,300	3,230		
Battery [96]	12 V, 200 Ah	419	419	11	10	0.028 [101]
Inverter [20]	1 kW	800	750	20	15	0 [101]
Charge controller [5]	1 kW	450	450	11	15	
Discount rate		10%				
Fuel cost	Diesel fuel	$0.91/L				
	Natural gas	$3.30/GJ				

The total life cycle emissions are calculated as the sum of the emissions by the system components over their lifetime and can be expressed by Equation 2.30 [20], where, β_i (kg CO_2-eq/kWh) is the lifetime equivalent CO_2 emissions of each hardware component (i) and E_L (kWh) is the amount of energy converted (or stored in batteries). The operational CO_2 emissions attributed to fuel usage for power generated from the ICE and the MGT are considered as 650 kg/MWh and 720 kg/MWh respectively based on the literature [52]. This method is also adopted elsewhere [40].

$$LCE = \sum_{i=1}^{N} \beta_i E_L \quad (2.30)$$

To implement the simulations, a MATLAB code representing the calculation of LPSP for the proposed hybrid system is written as an M-file. The fitness function (using the PMS and COE Equations 2.27-2.29) which calculates the values of objective function is written in another M-file. The constraints related to the bounds (number of components given in Equations 2.22 and 2.23, upper bound on LPSP in Equation 2.26) are entered directly into the optimisation toolbox. Other constraints (Equations 2.24-2.26) are formulated into the PMS. In the process of optimisation, it has been found that the GA population size has a significant effect on the time to solution convergence but only negligible on the accuracy variation (COE only changes by <0.5 % for a population size varying from 10 to 50). In this study, a GA population size of 10 (for two decision variables, N_{PV} and N_{bat}) is sufficient to find the desired solutions. To solve the single objective function, the GA optimisation toolbox uses the following settings: 10 individuals for population size, constraint dependent mutation, elite count 2, crossover fraction 0.8 with scattered crossover function, and 100 generations.

2.3 Results and discussion

In this paper, mode-I, -II, and –III configurations have been analysed when meeting the dynamic load at a specified LPSP (0.01±0.005). Table 2.4 shows various scenarios of optimised (single objective) hybrid energy systems in mode-II and –III configurations when compared to the baseline mode-I (PV/Batt) system. For the baseline scenario, PV along with battery storage is used to supply the necessary load demand. Systems sizing is based on the single objective COE ($/kWh), with the consequential system characteristics such as LCE (kg CO_2-eq/yr), renewable penetration (%), excess energy (kWh/yr), and duty factor (kWh/yr/start-stop) also reported.

2.3.1 Type of supplementary prime mover

2.3.1.1 Mode-I (PV/Batt)

The COE for the PV/Batt is 0.35 $/kWh. Renewable penetration in this case is 115 % of total energy demand, in which after meeting load, the surplus is diverted to battery storage. Though there are no operational emissions for the PV/Batt system, this mode has an LCE footprint of 7,117 kg CO_2-eq/yr through emissions from component production, transportation and decommissioning (cradle to grave). Furthermore, for this system to meet the annual reliability (LPSP), the excess energy generated is almost 10 % (7,547 kWh/yr) of total demand. This is attributed to the relatively excessive size of PV (387 panels) coupled with a large energy (seasonal) storage required to meet the specified LPSP (when irradiance is intermittent) over the year.

2.3.1.2 Mode-II (ICE, MGT 2x30kW)

In a hybridised system with multiple (alike) supplementary prime movers always operating in tandem, the PV/Batt/ICE system yields a COE at 0.34 $/kWh which is slightly lower than the PV/Batt system at 0.35 $/kWh COE. However, the PV/Batt/MGT is more costly at 0.50 $/kWh in contrast to the comparable power of an ICE based hybrid system. This is due to the higher capital and operational costs of MGT units (Table 2.3) and lower electrical efficiency (Table 2.2). On the other hand, the life cycle GHG emissions (LCE) for the PV/Batt/ICE are much greater (33,839 kg CO_2-eq/yr) than the PV/Batt system (7,117 kg CO_2-eq/yr), but lower than the PV/Batt/MGT system (41,160 kg CO_2-eq/yr). Although the energy generation from the MGT (32,259 kWh/yr) is slightly lower than the ICE (34,178 kWh/yr) because of larger battery storage and lesser excess energy, both systems are likely to meet the same demand with the specified LPSP. As the LCE factors (β_i) for the MGT (1.16 kg CO_2-eq/kWh) are much higher than the ICE (0.88 kg CO_2-eq/kWh), the former system produces greater LCE. Furthermore, this difference in LCE occurs whilst the renewable energy penetration for the PV/Batt/ICE is 65 %, which is comparable to the PV/Batt/MGT system (69 %).

Table 2.4: Summary results of hybrid systems for LPSP, 0.01±0.005 (temporal resolution of load profile, t=60min).

System Characteristics	Mode-I	Mode-II		Mode-III	
	PV/Batt	PV/Batt/ICE (ICE=2x30 kW)	PV/Batt/MGT (MGT=2x30 kW)	PV/Batt/ICE (60 kW)	PV/Batt/MGT (65 kW)
COE ($/kWh)	0.35	0.34	0.50	0.34	0.56
Number of solar panels, N_{pv}	387	227	222	296	298
Number of lead acid batteries, N_{batt}	44	4	6	18	17
PV energy generated (kWh/yr)	95,097	55,781	54,552	72,736	73,227
Renewable penetration (%)	115	65	69	92	93
ICE or MGT energy (kWh/yr)	-	34,178	32,259	18,493	17,346
Excess energy (kWh/yr)	7,547	6,288	1,916	2,410	2,309
Excess energy /total energy (%)	10	8	3	3	3
Unmet energy (kWh/yr)	726	721	725	758	733
$LPSP_{comp}$ (%)	0.95	0.94	0.95	0.99	0.96
ICE or MGT running time (h)	-	1,794	1,601	606	505
ICE or MGT start-stop	-	732	685	306	278
Duty factor (kWh/yr/start-stop)	-	47	47	60	62
Waste heat (kWh/yr)	-	43,961	101,820	25,020	48,999
Waste heat/ energy demand (%)	-	57	133	33	65
Waste heat/ supply power (%)	-	129	316	135	282
Diesel/Natural gas consumption (MJ/yr)	-	354,666	476,500	188,916	246,030
Operational (fuel) emissions (CO_2 kg/yr)	-	22,216	23,226	12,020	12,489
LCE (kg CO_2-eq/yr)	7,117	33,839	41,160	21,540	25,451

In the case of the system without supplementary prime movers, the renewable energy penetration is however much higher for the PV/Batt system (115 %) and the difference is attributed to higher excess energy (10 % of total demand) when normalised by the running time. Among the three systems, a PV/Batt/MGT system generates less excess energy (2.5 % of total demand) because of relatively fewer number of PV panels compared to the PV/Batt (excess is 10 % of total demand) and the PV/Batt/ICE (excess is 8 % of total demand). The results also show that if the transient start-up time (ΔT_s) for supplementary prime movers is considered non-zero in the PMS (Figure 2.6), the missed load during this period is aggregated to 35 kWh for the ICE and 210 kWh for the MGT over the year. This has an insignificant effect on the system sizing and the COE when meeting an overall load of 76,487 kWh/yr. The duty factor, which represents the overall energy provided (kWh) per total starts of the supplementary device, is similar (47 %) for both the MGT and the ICE when meeting a comparable LPSP.

In some other energy systems, the waste heat generation from supplementary devices could be an important feature in the supply a heating load. Although the COE for the MGT based hybrid system is much higher than the hybrid ICE system, the MGT produces 316 % waste heat to the electric power supplied by it. This figure is considerably lower for the ICE (129 % waste heat to supplied electric power) and could possibly make the MGT system a more favourable supplementary device for cogeneration applications. Further research into this is warranted.

2.3.1.3 Mode-III (ICE, MGT 1x60–65 kW)

Whilst the earlier characteristics in mode-II were reported for two relatively smaller supplementary prime movers (2x30 kW) operating in tandem, the ensuing analysis considers the effects of using much larger capacity (single) supplementary prime movers in the form of a 60 kW ICE or 65 kW MGT. Results show that the COE is similar (0.34 $/kWh) for the PV/Batt/ICE with the 2x30 kW alternative (mode-II) when compared to the 1x60 kW (mode-III). Although there is a 73 % difference in the capital costs of two ICEs at 30 kW each when compared to a single ICE at 60 kW (Table 2.3), the larger number of PV panels and battery storage devices in mode-III (Table 2.4) make the COE comparable for both modes. This variation in N_{PV} and N_{batt} arises because a larger capacity ICE (or MGT) also means its start-up power ($P_{sup,min}$) is greater which implies that more PV panels and batteries are required to meet the LPSP (Table 2.4) if the minimum start-up power is not reached in some intervals over the year. On the other hand, the COE for the two 30 kW MGT based hybrid system is appreciably lower (0.50 $/kWh) than the single 65 kW MGT (0.56 $/kWh). Again, this is due to the fact that whilst the capital costs for two 30 kW MGT units is almost similar to that of single 65 kW MGT (Table 2.3), a larger number of PV panels and batteries make the COE higher for mode-III compared to mode-II. The LCE for the hybrid system with single (larger) unit produces 36~38 % less than the two unit scenarios whether based on ICE or MGT. The underlying reason for this is the greater minimum start-up threshold

(for larger capacity ICE's and MGT's in mode-III) which then causes fewer running hours for the prime movers, higher renewable penetration, and leads to lower fuel consumption and reduced CO_2 emissions (Table 2.4). In relation to operational CO_2 emissions, a single (larger) unit ICE and MGT systems (mode-III) produce 54 % less compared to two (smaller) unit ICE and MGT's (mode-II). This is because the smaller capacity prime movers have lower minimum starting thresholds, and so operate more of the time and this leads to higher running hours (more fuel consumption). The end result is also much lower LCE in mode-II as compared to mode-III. Renewable penetration for the PV/Batt/ICE (1x60 kW) and the PV/Batt/MGT (1x65 kW) are 92 % and 93 % of total energy supply, respectively, in contrast to 65 % and 69 % of total energy, respectively, for the PV/Batt/ICE (2x30 kW) and the PV/Batt/MGT (2x30 kW). This is because of the higher minimum starting threshold of larger capacity engines, which forces the PMS with greater PV penetration in the systems as compared to lower rating supplementary units. The PV/Batt/ICE (1x60 kW) produces less excess energy (3 % of the total energy at 2,410 kWh/yr) as compared to the PV/Batt/ICE (2x30 kW) (8 % of the total energy at 6,288 kWh/yr), whereas the PV/Batt/MGT (1x65 kW) and the PV/Batt/MGT (2x30 kW) produces almost the same amount of excess energy (3 % of total energy). Nevertheless, the waste heat generation in relation to the total demand, the 60 kW ICE generates 33 % compared to 57 % for the ICE (2x30 kW), whereas, the 65 kW MGT produces 65 % compared to 133 % for the MGT (2x30 kW). Additionally, waste heat generation (relative to supplied power) by the supplementary prime movers for both cases is comparable (ICE: 135 % and 129 % for single unit and two units respectively; MGT: 282 % for a single unit and 316 % for two units). This implies that in relation to waste heat generation (relative to total energy demand), two (smaller) units produce almost twice the waste heat produced by single (larger) capacity prime mover. The effects of system sizing and configuration (mode) on waste heat generation have significant impacts on decision making when it comes to stand-alone CHP and CCHP applications and this warrants further research.

As far as duty factor is concerned, PV/Batt/ICE (1x60 kW) has over 60 kWh/yr/start-stop, while the PV/Batt/ICE (2x30 kW) has 47 kWh/yr/start-stop. A similar trend is observed in relation to the use of a single larger MGT or two smaller ones. A higher duty factor leads to less power loss due to transient start-up and also affects operational emissions adversely due to cold starting of supplementary prime movers [104].

From the above discussion, it is evident that both mode-II and mode-III hybrid PV/Batt/ICE systems offer the least COE (0.34 $/kWh) among all scenarios, closely followed by the baseline PV/Batt (0.35 $/kWh) only. As mentioned earlier, because of the peak load requirements over the year to meet specified LPSP, hybridised systems (mode-III) require a larger number of PV panels and greater capacity of the ICE or MGT which contributes to a higher COE. Hossain et al. [105] optimised a PV/Batt/ICE system using HOMER where the COE was at 0.31 $/kWh. In another study, Salehin et al.

[106] used both HOMER and RETScreen and reported a COE of 0.35 $/kWh for PV/Batt/ICE systems. As such, the COE derived in the present study is comparable to those from other studies, albeit this paper has examined the effects of several factors on the COE. Additionally, neither of the systems in [105] and [106] considered dynamic electric load profiles or hourly resolved meteorological data for their sizing which could affect the outcomes and load meeting reliability. The annual operational time (h) for two (smaller) units (2x30 kW) is almost three times greater than the single (larger) unit (60~65 kW). The higher number of operational hours also contributed to higher energy generation, waste heat generation, LCE, and fuel consumption and also to lower duty factor.

2.3.2 Start-up thresholds

With the above results in mind, more analysis is now undertaken into the effects of different start-up thresholds ($P_{sup,min}$) for the 60 kW ICE and 65 kW MGT based systems. Figure 2.7 represents the effects of different starting thresholds on the COE, operational CO_2 emissions, LCE, and waste heat to supply power. The starting thresholds considered are at 15, 20, 25, and 30 % of rated power. Results indicate that varying the $P_{sup,min}$ to these thresholds causes the COE to change by only 4 % for the 60 kW ICE and 7 % for the 65 kW MGT. So, this parameter is unlikely to affect system selection when single objective optimisation is used. However, if multiple objective optimisations are done and CO_2 (operational emissions) are considered or LCE, the effects of $P_{sup,min}$ should be analysed. A more notable effect of minimum starting thresholds for supplementary (combustion based) prime movers appears in relation to the waste heat generated (relative to supplied power) in systems involving waste heat recovery (for cogeneration or trigeneration). The data indicates that whilst the choice of $P_{sup,min}$ should also be considered with MGTs, its effects on systems involving ICEs is less appreciable. This is because MGT systems have lower power to useful heat output ratios (typically 0.46 to 0.73 for MGT as compared to 0.51 to 1.19 for ICE) and this implies comparatively more heat generation [107].

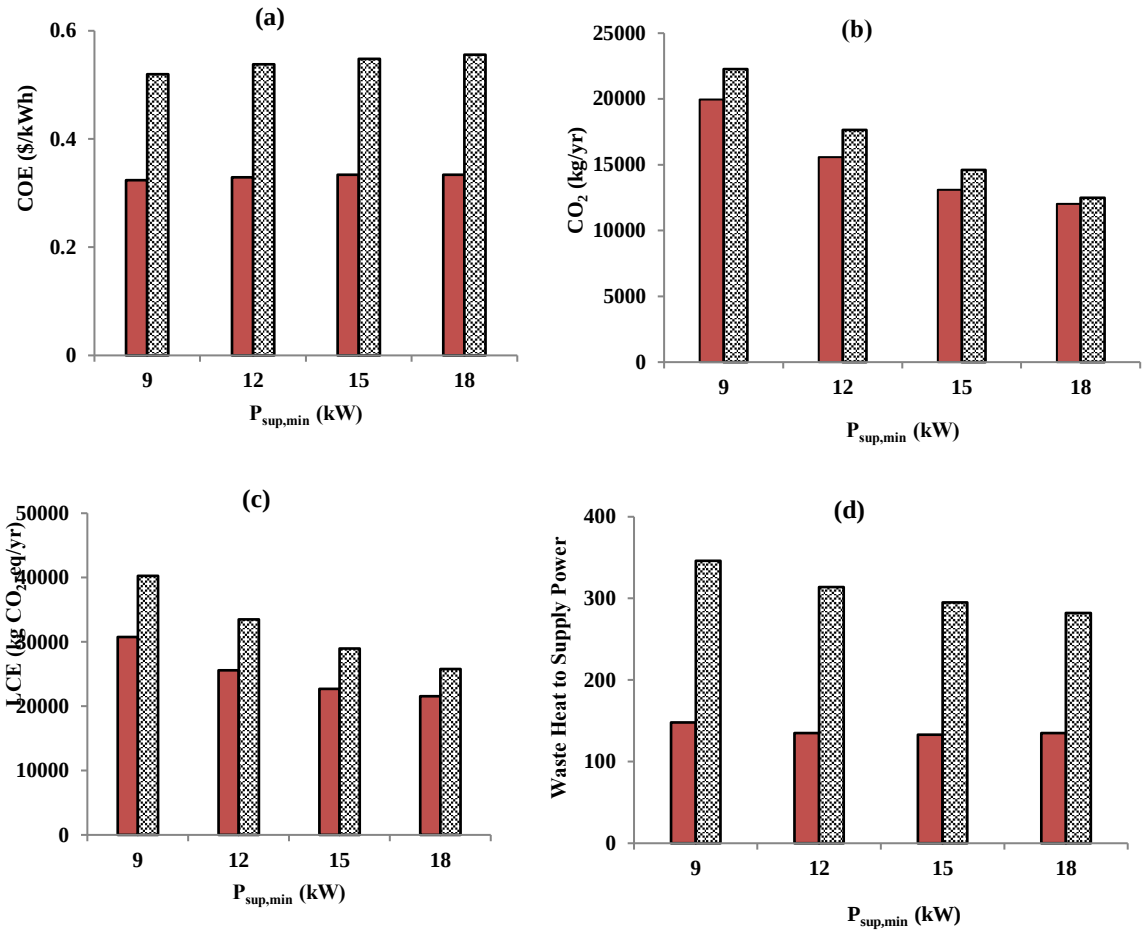

Fig.2.7: Comparisons between COE, CO_2 emissions, LCE, and Waste heat to supply power (a, b, c and d respectively) for minimum starting threshold of prime movers: ICE 60 kW (solid) and MGT 65 kW (dashed).

2.3.3 Temporal resolution

The earlier results were obtained for 60min resolution data. System sizing and operational characteristics are further analysed in this section for the effects of either using 15min or 60min temporal resolution of the dynamic load profiles, solar irradiation, ambient temperature, and wind speed (for the same LPSP). Figure 2.8 shows the variation of the COE in the 15min data is only 2~5 % as compared to the 60min resolved profiles. Reducing the temporal resolution even further (from 15min to 5min) shows the COE is only affected by <1 %. Resolutions below 5min are not used as they are of the same order as the transient start-up of some of the prime movers modelled (MGT). As such, in simulations based on a single objective (COE) optimisation minimal effects occur when using 15 min vs 60 min temporal resolution.

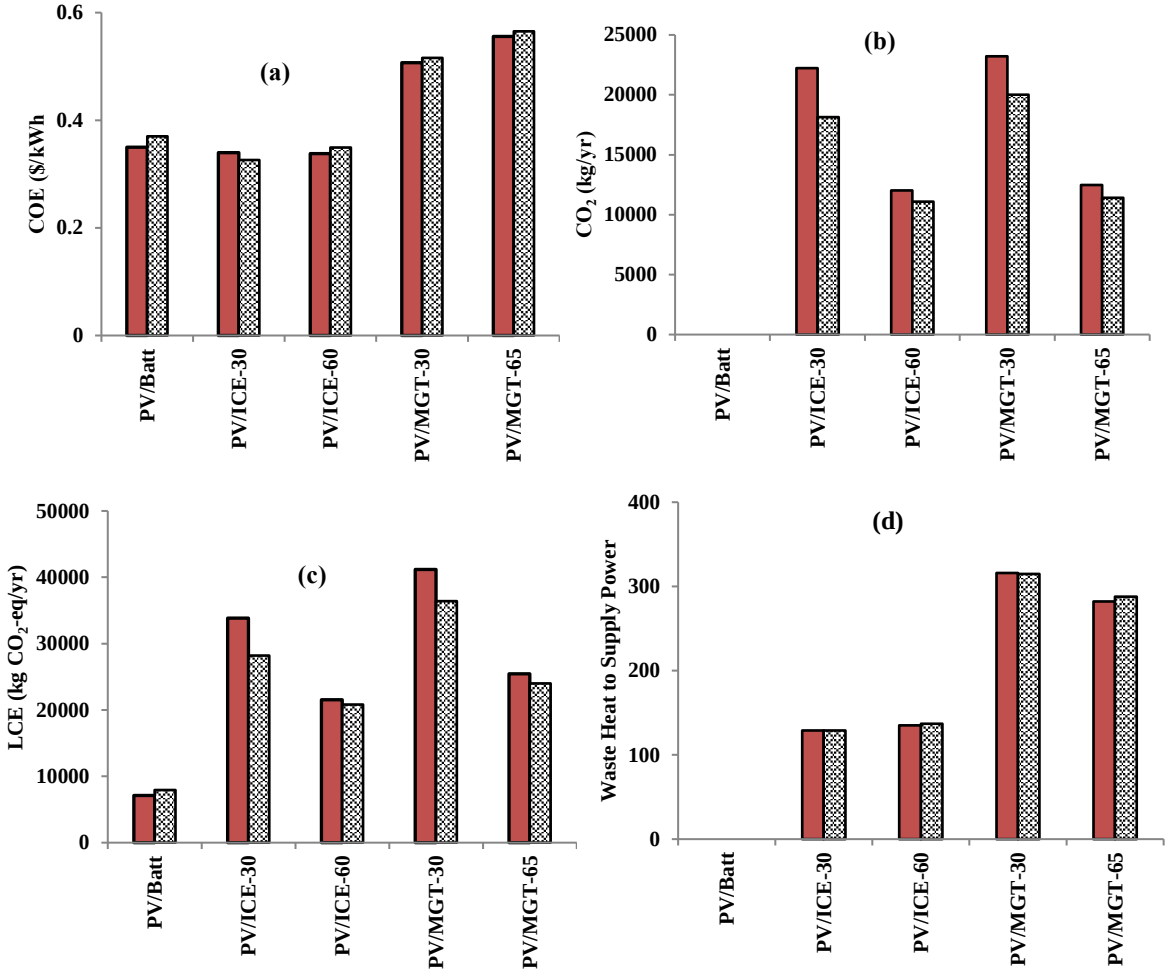

Fig.2.8: Comparisons between COE, CO_2 emissions, LCE, and Waste Heat to Supply Power (a, b, c and d respectively) for 60 min (solid) and 15 min (dashed) resolution of different scenarios.

The waste heat (in relation to supply power) for supplementary prime movers is also comparable for both data profiles. The running time of supplementary prime movers based on 15min resolution is 4 %-20 % lower as compared to the 60min resolved profiles that also affect waste heat generation. However, more appreciable effects on the generation of CO_2 and the LCE appear with the different temporal resolution. This is because of the higher renewable energy penetration for the 60min temporal resolution that leads to greater excess energy. The most significant outcomes found in relation to duty factors where this case, duty factors decreases more than 178 % to 247 % in contrast to 60min resolved data profiles. This is due to the higher number of start-stops and a smaller contribution from supplementary power sources.

2.3.4 Sensitivity analysis

The final part of this research is a sensitivity analysis of the effects which arise from the variation of input parameters on the optimal results achieved in the optimal solutions across the four hybrid systems listed in Table 4. In this regard, the effects of interest rate, fuel price, and cost of PV panels, overall

capital, and ICE or MGT unit capital costs are analysed. The data presented in Figure 2.9 shows the effects of varying the above parameters on the COE in an ICE (1x60 kW, COE=0.34 $/kWh) and MGT (2x30 kW, COE=0.50 $/kWh) system**.** From this analysis, it is evident that changes in fuel price have insignificant effects on the COE. However, a 40 % decrease in PV capital costs would cut the COE by 18 % for the PV/Batt/ICE (1x60 kW), by 20 % for the PV/Batt system, and by 6 % for the PV/Batt/MGT (2x30 kW).

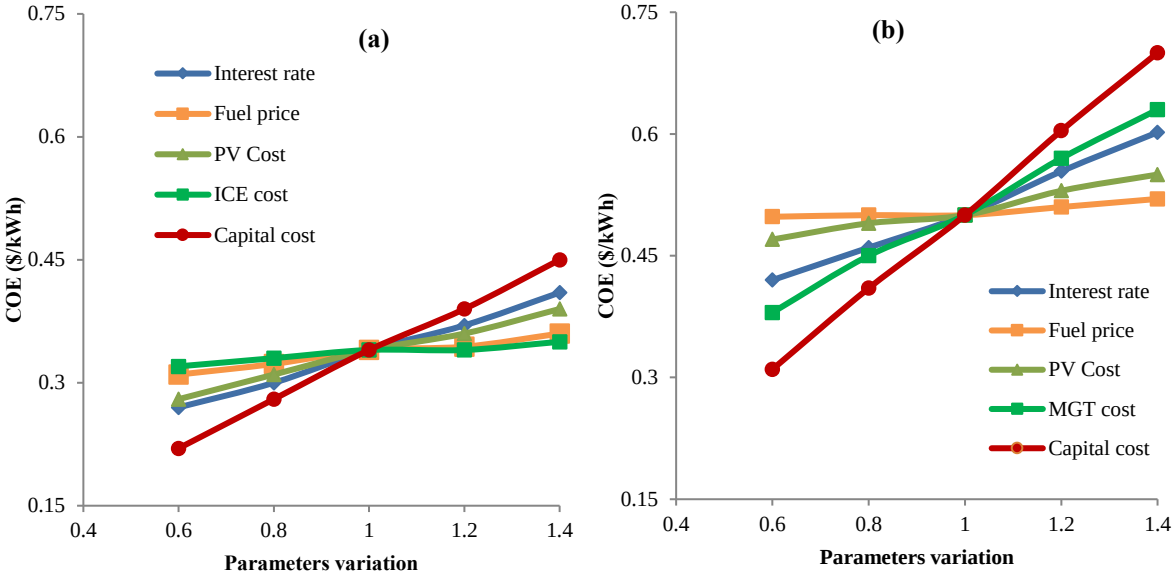

Fig.2.9: Sensitivity analysis of (a) PV/Batt/ICE (1x60kW) and (b) PV/Batt/MGT (2x30kW).

This difference is due to the lesser number of PV panels for two (smaller) capacity prime movers. The variation of the ICE capital costs also has an insignificant effect on the COE, whereas a 40 % reduction in the MGT capital costs would reduce the COE by 24 %. The result indicates that the variation in overall capital costs may have considerable effects on the COE for the both ICE and MGT based hybrid systems but this depends on the type of system and hardware components considered. In PV/Batt/MGT (2x30 kW), a 40 % decrease in capital cost reduces the COE almost 38 % compared to the base case.

Additionally, a further 40 % drop in interest rate would decline the COE 16 ~20 % from the base case, whereas a 40 % rise would increase the COE by12 %. Bortolini et al. [81] optimised a hybrid PV/Batt/ICE system both economically and environmentally and found the COE to be 0.26 $/kWh. In another study, Ismail et al. [108] optimised PV/Batt/ICE using GA for a typical Malaysian household and reported a Cost of Energy of 0.24 $/kWh based on an interest rate of 8 % and a diesel price of 0.60 $/l. This is comparable to the Cost of Energy (0.28 $/kWh) derived in the present study under similar conditions. From the above discussion, it can be said that the changes of interest rate and overall capital costs of components have noticeable effect on the COE for both scenarios while the other parameters (fuel cost, PV costs, and capital costs of ICE) have a less significant effect.

2.4 Conclusions

This paper has analysed the impact of different types of prime movers when used to hybridise PV/Batt systems (PV/Batt/MGT and PV/Batt/ICE). It presents an insight into the effects of simulation methodology and different hardware parameters on the optimisation of hybridised energy systems. Whilst the outcomes are based on a set of assumptions and methods and are not meant to identify the general merits or drawbacks of specific models of prime movers (or energy system hardware), the outcomes of this study are summarised as follows:

- The Cost of Energy in a (combustion-based) hybridised PV/Batt/ICE system (featuring either a single or tandem configuration of ICE's) can be comparable to a (purely renewable-based) PV/Batt system. However, in a PV/Batt system an excessive number of PV arrays maybe needed (to reliably cover the load) which then leads the generation of more excess power (and the dumping of more excess power) over periods of low demand. Combustion-based hybridised systems however also produce significant amounts of waste heat as well as CO_2 (operational) and life cycle emissions, even though the Cost of Energy may be similar to PV/Batt systems. As such, single objective optimisations (which feature only Cost of Energy) may not be effective in identifying the best/optimal choice. This is likely to be exacerbated if a thermal load (through cogeneration or trigeneration) also needs to be met, which then impacts overall efficiency and not just Cost of Energy.
- The use of single versus tandem (multiple) combustion-based prime movers appears not to significantly affect the Cost of Energy in PV/Batt/ICE hybridised systems. The same is true for PV/Batt/MGT systems. However, the use of single versus tandem supplementary prime movers does significantly affect the emissions (CO_2, life cycle emissions) and waste heat generated. As such, the type of configuration used (single vs tandem) needs more attention in research using multi-objective optimisations that considers performance measures other than just Cost of Energy.
- The Waste Heat to Supply Power in PV/Batt/MGT systems is 2.5 to 3 times higher than PV/Batt/ICE. However, this is also dependent on the start-up threshold ($P_{sup,min}$) of the Micro Gas Turbine. These factors are likely to become more significant in cogeneration applications. The analyses however reveal that transient start-up time and minimum start-up power of the supplementary prime movers have a negligible effect on the Cost of Energy in single objective optimisations.
- Sensitivity analysis shows that the Cost of Energy is less sensitive to variations of fuel price, while the effects of capital cost dominate the variation in Cost of Energy. However, variations in capital cost depend on the type of energy system component.

The present paper has successfully identified the effects of both hardware and simulation parameters in the (single objective function) optimisation of the Cost of Energy in hybridised stand-alone energy systems meeting a single dynamic (electric) load profile. However, further research is warranted bearing in mind the relatively large waste heat incidentally generated as applicable in Combined Heating and Power and Combined Cooling, Heating, and Power stand-alone systems. The lifetime of batteries and other energy system components is also affected by the number of charging/discharging (start-up) cycles.

Chapter references

[1] Agency, I.E. *Energy Acess Database*. Available from: 15.09.2016. http://www.worldenergyoutlook.org/resources/energydevelopment/energyaccessdatabase.

[2] Rohani, G. and M. Nour, *Techno-economical analysis of stand-alone hybrid renewable power system for Ras Musherib in United Arab Emirates.* Energy, 2014. **64**: p. 828-841.

[3] Adefarati, T. and R.C. Bansal, *Reliability assessment of distribution system with the integration of renewable distributed generation.* Applied Energy, 2017. **185, Part 1**: p. 158-171.

[4] Kaldellis, J.K., et al., *Cost benefit analysis of a photovoltaic-energy storage electrification solution for remote islands.* Renewable Energy, 2009. **34**(5): p. 1299-1311.

[5] Ismail, M.S., M. Moghavvemi, and T.M.I. Mahlia, *Design of an optimized photovoltaic and microturbine hybrid power system for a remote small community: Case study of Palestine.* Energy Conversion and Management, 2013. **75**: p. 271-281.

[6] Hoque, S.N. and B.K. Das, *Present status of solar home and photovoltaic micro utility systems in Bangladesh and recommendation for further expansion and upgrading for rural electrification.* Journal of Renewable and Sustainable Energy, 2013. **5**(4): p. 042301.

[7] Bekele, G. and B. Palm, *Feasibility study for a standalone solar–wind-based hybrid energy system for application in Ethiopia.* Applied Energy, 2010. **87**(2): p. 487-495.

[8] Bala, B.K. and S.A. Siddique, *Optimal design of a PV-diesel hybrid system for electrification of an isolated island—Sandwip in Bangladesh using genetic algorithm.* Energy for Sustainable Development, 2009. **13**(3): p. 137-142.

[9] Qoaider, L. and D. Steinbrecht, *Photovoltaic systems: A cost competitive option to supply energy to off-grid agricultural communities in arid regions.* Applied Energy, 2010. **87**(2): p. 427-435.

[10] Kanase-Patil, A.B., R.P. Saini, and M.P. Sharma, *Sizing of integrated renewable energy system based on load profiles and reliability index for the state of Uttarakhand in India.* Renewable Energy, 2011. **36**(11): p. 2809-2821.

[11] Dresselhaus, M. and I. Thomas, *Alternative energy technologies.* Nature, 2001. **414**(6861): p. 332-337.

[12] Tyagi, V., et al., *Progress in solar PV technology: research and achievement.* Renewable and Sustainable Energy Reviews, 2013. **20**: p. 443-461.

[13] Parida, B., S. Iniyan, and R. Goic, *A review of solar photovoltaic technologies.* Renewable and Sustainable Energy Reviews, 2011. **15**(3): p. 1625-1636.

[14] Muneer, T., M. Asif, and J. Kubie, *Generation and transmission prospects for solar electricity: UK and global markets.* Energy Conversion and Management, 2003. **44**(1): p. 35-52.

[15] Hoque, S.N. and B.K. Das, *Analysis of Cost, Energy and Emission of Solar Home Systems in Bangladesh.* International Journal of Renewable Energy Research 2013. **3**(2): p. 347-352.

[16] Marciukaitis, M., V. Katinas, and A. Kavaliauskas, *Wind power usage and prediction prospects in Lithuania.* Renewable and Sustainable Energy Reviews, 2008. **12**(1): p. 265-277.

[17] Nema, P., R.K. Nema, and S. Rangnekar, *A current and future state of art development of hybrid energy system using wind and PV-solar: A review.* Renewable and Sustainable Energy Reviews, 2009. **13**(8): p. 2096-2103.

[18] Brka, A., Y.M. Al-Abdeli, and G. Kothapalli, *Influence of neural network training parameters on short-term wind forecasting.* International Journal of Sustainable Energy, 2016. **35**(2): p. 115-131.
[19] Clarke, D.P., Y.M. Al-Abdeli, and G. Kothapalli, *Multi-objective optimisation of renewable hybrid energy systems with desalination.* Energy, 2015. **88**: p. 457-468.
[20] Brka, A., Y.M. Al-Abdeli, and G. Kothapalli, *The interplay between renewables penetration, costing and emissions in the sizing of stand-alone hydrogen systems.* International Journal of Hydrogen Energy, 2015. **40**(1): p. 125-135.
[21] Courtecuisse, V., et al., *A methodology to design a fuzzy logic based supervision of Hybrid Renewable Energy Systems.* Mathematics and Computers in Simulation, 2010. **81**(2): p. 208-224.
[22] Celik, A., *Optimisation and techno-economic analysis of autonomous photovoltaic–wind hybrid energy systems in comparison to single photovoltaic and wind systems.* Energy Conversion and Management, 2002. **43**(18): p. 2453-2468.
[23] Prasad, A.A., R.A. Taylor, and M. Kay, *Assessment of solar and wind resource synergy in Australia.* Applied Energy, 2017. **190**: p. 354-367.
[24] Hrayshat, E.S., *Techno-economic analysis of autonomous hybrid photovoltaic-diesel-battery system.* Energy for Sustainable Development, 2009. **13**(3): p. 143-150.
[25] Nelson, D.B., M.H. Nehrir, and C. Wang, *Unit sizing and cost analysis of stand-alone hybrid wind/PV/fuel cell power generation systems.* Renewable Energy, 2006. **31**(10): p. 1641-1656.
[26] Agbossou, K., et al., *Performance of a stand-alone renewable energy system based on energy storage as hydrogen.* Energy Conversion, IEEE Transactions on, 2004. **19**(3): p. 633-640.
[27] Vazquez, S., et al., *Energy storage systems for transport and grid applications.* Industrial Electronics, IEEE Transactions on, 2010. **57**(12): p. 3881-3895.
[28] Kim, M. and S. Bae, *Decentralized control of a scalable photovoltaic (PV)-battery hybrid power system.* Applied Energy, 2017. **188**: p. 444-455.
[29] Wen, S., et al., *Allocation of ESS by interval optimization method considering impact of ship swinging on hybrid PV/diesel ship power system.* Applied Energy, 2016. **175**: p. 158-167.
[30] Shah, K.K., A.S. Mundada, and J. Pearce, *Performance of US hybrid distributed energy systems: Solar photovoltaic, battery and combined heat and power.* Energy Conversion and Management, 2015. **105**: p. 71-80.
[31] Askari, I.B., M.O. Sadegh, and M. Ameri, *Effect of heat storage and fuel price on energy management and economics of micro CCHP cogeneration systems.* Journal of Mechanical Science and Technology, 2014. **28**(5): p. 2003-2014.
[32] *Rural Electrification with PV Hybrid Systems.* [cited 2017 02/01]; Available from: 02.01.2017. https://www.iea.org/media/openbulletin/Rural_Electrification_with_PV_Hybrid_systems.pdf.
[33] Zhou, W., et al., *Current status of research on optimum sizing of stand-alone hybrid solar–wind power generation systems.* Applied Energy, 2010. **87**(2): p. 380-389.
[34] Banos, R., et al., *Optimization methods applied to renewable and sustainable energy: A review.* Renewable and Sustainable Energy Reviews, 2011. **15**(4): p. 1753-1766.
[35] Kalantar, M., *Dynamic behavior of a stand-alone hybrid power generation system of wind turbine, microturbine, solar array and battery storage.* Applied Energy, 2010. **87**(10): p. 3051-3064.
[36] Ngan, M.S. and C.W. Tan, *Assessment of economic viability for PV/wind/diesel hybrid energy system in southern Peninsular Malaysia.* Renewable and Sustainable Energy Reviews, 2012. **16**(1): p. 634-647.
[37] Lau, K.Y., et al., *Performance analysis of hybrid photovoltaic/diesel energy system under Malaysian conditions.* Energy, 2010. **35**(8): p. 3245-3255.
[38] Ma, T., H. Yang, and L. Lu, *A feasibility study of a stand-alone hybrid solar–wind–battery system for a remote island.* Applied Energy, 2014. **121**: p. 149-158.
[39] Ismail, M., M. Moghavvemi, and T. Mahlia, *Design of an optimized photovoltaic and microturbine hybrid power system for a remote small community: case study of Palestine.* Energy Conversion and Management, 2013. **75**: p. 271-281.

[40] Ismail, M., M. Moghavvemi, and T. Mahlia, *Genetic algorithm based optimization on modeling and design of hybrid renewable energy systems.* Energy Conversion and Management, 2014. **85**: p. 120-130.
[41] Stoppato, A., et al., *A PSO (particle swarm optimization)-based model for the optimal management of a small PV (Photovoltaic)-pump hydro energy storage in a rural dry area.* Energy, 2014. **76**: p. 168-174.
[42] Perera, A., et al., *Designing standalone hybrid energy systems minimizing initial investment, life cycle cost and pollutant emission.* Energy, 2013. **54**: p. 220-230.
[43] Nafeh, A.E.-S.A., *Optimal economical sizing of a PV-wind hybrid energy system using genetic algorithm.* International Journal of Green Energy, 2011. **8**(1): p. 25-43.
[44] Shi, J.H., X.J. Zhu, and G.Y. Cao, *Design and techno-economical optimization for stand-alone hybrid power systems with multi-objective evolutionary algorithms.* International Journal of Energy Research, 2007. **31**(3): p. 315-328.
[45] Dufo-Lopez, R. and J.L. Bernal-Agustín, *Design and control strategies of PV-Diesel systems using genetic algorithms.* Solar Energy, 2005. **79**(1): p. 33-46.
[46] Yang, H., et al., *Optimal sizing method for stand-alone hybrid solar–wind system with LPSP technology by using genetic algorithm.* Solar Energy, 2008. **82**(4): p. 354-367.
[47] Khatri, K.K., et al., *Experimental investigation of CI engine operated micro-trigeneration system.* Applied Thermal Engineering, 2010. **30**(11): p. 1505-1509.
[48] Ahmadi, P., M.A. Rosen, and I. Dincer, *Greenhouse gas emission and exergo-environmental analyses of a trigeneration energy system.* International Journal of Greenhouse Gas Control, 2011. **5**(6): p. 1540-1549.
[49] Ghaebi, H., M. Saidi, and P. Ahmadi, *Exergoeconomic optimization of a trigeneration system for heating, cooling and power production purpose based on TRR method and using evolutionary algorithm.* Applied Thermal Engineering, 2012. **36**: p. 113-125.
[50] Jradi, M. and S. Riffat, *Tri-generation systems: Energy policies, prime movers, cooling technologies, configurations and operation strategies.* Renewable and Sustainable Energy Reviews, 2014. **32**: p. 396-415.
[51] Lin, L., et al., *An experimental investigation of a household size trigeneration.* Applied Thermal Engineering, 2007. **27**(2–3): p. 576-585.
[52] Wu, D.W. and R.Z. Wang, *Combined cooling, heating and power: a review.* Progress in Energy and Combustion Science, 2006. **32**(5–6): p. 459-495.
[53] Caresana, F., et al., *Use of a test-bed to study the performance of micro gas turbines for cogeneration applications.* Applied Thermal Engineering, 2011. **31**(16): p. 3552-3558.
[54] *Combine Heat and Power Partnership. Catalog of CHP Technologies. U.S. Environmental Protection Agency. 2015. p.1-6,5.1-5.18*.
[55] Ismail, M., M. Moghavvemi, and T. Mahlia, *Current utilization of microturbines as a part of a hybrid system in distributed generation technology.* Renewable and Sustainable Energy Reviews, 2013. **21**: p. 142-152.
[56] Arun, P., R. Banerjee, and S. Bandyopadhyay, *Optimum sizing of battery-integrated diesel generator for remote electrification through design-space approach.* Energy, 2008. **33**(7): p. 1155-1168.
[57] Dufo-Lopez, R., J.L. Bernal-Agustín, and J. Contreras, *Optimization of control strategies for stand-alone renewable energy systems with hydrogen storage.* Renewable Energy, 2007. **32**(7): p. 1102-1126.
[58] Clarke, D.P., Y.M. Al-Abdeli, and G. Kothapalli, *The impact of renewable energy intermittency on the operational characteristics of a stand-alone hydrogen generation system with on-site water production.* International Journal of Hydrogen Energy, 2013. **38**(28): p. 12253-12265.
[59] Brka, A., Y.M. Al-Abdeli, and G. Kothapalli, *Predictive power management strategies for stand-alone hydrogen systems: Operational impact.* International Journal of Hydrogen Energy, 2016. **41**(16): p. 6685-6698.
[60] *National Renewable Energy Laboratory (NREL). The hybrid optimisation model for electric renewables (HOMER)*. Available from: 15.02.2016. www.nrel.gov/homer; .
[61] Koutroulis, E., et al., *Methodology for optimal sizing of stand-alone photovoltaic/wind-generator systems using genetic algorithms.* Solar Energy, 2006. **80**(9): p. 1072-1088.

[62] Ismail, M., M. Moghavvemi, and T. Mahlia, *Techno-economic analysis of an optimized photovoltaic and diesel generator hybrid power system for remote houses in a tropical climate.* Energy Conversion and Management, 2013. **69**: p. 163-173.
[63] Yang, H., Z. Wei, and L. Chengzhi, *Optimal design and techno-economic analysis of a hybrid solar–wind power generation system.* Applied Energy, 2009. **86**(2): p. 163-169.
[64] Ogunjuyigbe, A.S.O., T.R. Ayodele, and O.A. Akinola, *Optimal allocation and sizing of PV/Wind/Split-diesel/Battery hybrid energy system for minimizing life cycle cost, carbon emission and dump energy of remote residential building.* Applied Energy, 2016. **171**: p. 153-171.
[65] Fan, Y. and X. Xia, *A multi-objective optimization model for energy-efficiency building envelope retrofitting plan with rooftop PV system installation and maintenance.* Applied Energy, 2017. **189**: p. 327-335.
[66] Sardi, J., et al., *Multiple community energy storage planning in distribution networks using a cost-benefit analysis.* Applied Energy, 2017. **190**: p. 453-463.
[67] Hakimi, S. and S. Moghaddas-Tafreshi, *Optimal sizing of a stand-alone hybrid power system via particle swarm optimization for Kahnouj area in south-east of Iran.* Renewable Energy, 2009. **34**(7): p. 1855-1862.
[68] Maleki, A. and A. Askarzadeh, *Comparative study of artificial intelligence techniques for sizing of a hydrogen-based stand-alone photovoltaic/wind hybrid system.* International Journal of Hydrogen Energy, 2014. **39**(19): p. 9973-9984.
[69] Ekren, O. and B.Y. Ekren, *Size optimization of a PV/wind hybrid energy conversion system with battery storage using simulated annealing.* Applied Energy, 2010. **87**(2): p. 592-598.
[70] Maleki, A. and A. Askarzadeh, *Artificial bee swarm optimization for optimum sizing of a stand-alone PV/WT/FC hybrid system considering LPSP concept.* Solar Energy, 2014. **107**: p. 227-235.
[71] Lu, Y., et al., *Robust optimal design of renewable energy system in nearly/net zero energy buildings under uncertainties.* Applied Energy, 2017. **187**: p. 62-71.
[72] Garshasbi, S., J. Kurnitski, and Y. Mohammadi, *A hybrid Genetic Algorithm and Monte Carlo simulation approach to predict hourly energy consumption and generation by a cluster of Net Zero Energy Buildings.* Applied Energy, 2016. **179**: p. 626-637.
[73] Mellit, A., et al., *An adaptive artificial neural network model for sizing stand-alone photovoltaic systems: application for isolated sites in Algeria.* Renewable Energy, 2005. **30**(10): p. 1501-1524.
[74] Secanell, M., J. Wishart, and P. Dobson, *Computational design and optimization of fuel cells and fuel cell systems: A review.* Journal of Power Sources, 2011. **196**(8): p. 3690-3704.
[75] Mokheimer, E.M., et al., *A new study for hybrid PV/wind off-grid power generation systems with the comparison of results from homer.* International Journal of Green Energy, 2015. **12**(5): p. 526-542.
[76] Diaf, S., et al., *A methodology for optimal sizing of autonomous hybrid PV/wind system.* Energy Policy, 2007. **35**(11): p. 5708-5718.
[77] Borowy, B.S. and Z.M. Salameh, *Methodology for optimally sizing the combination of a battery bank and PV array in a wind/PV hybrid system.* Energy Conversion, IEEE Transactions on, 1996. **11**(2): p. 367-375.
[78] Dufo-López, R., et al., *Multi-objective optimization minimizing cost and life cycle emissions of stand-alone PV–wind–diesel systems with batteries storage.* Applied Energy, 2011. **88**(11): p. 4033-4041.
[79] Erdinc, O. and M. Uzunoglu, *Optimum design of hybrid renewable energy systems: overview of different approaches.* Renewable and Sustainable Energy Reviews, 2012. **16**(3): p. 1412-1425.
[80] Cristóbal-Monreal, I.R. and R. Dufo-López, *Optimisation of photovoltaic–diesel–battery stand-alone systems minimising system weight.* Energy Conversion and Management, 2016. **119**: p. 279-288.
[81] Bortolini, M., et al., *Economic and environmental bi-objective design of an off-grid photovoltaic–battery–diesel generator hybrid energy system.* Energy Conversion and Management, 2015. **106**: p. 1024-1038.

[82] Lai, C.S. and M.D. McCulloch, *Levelized cost of electricity for solar photovoltaic and electrical energy storage.* Applied Energy, 2017. **190**: p. 191-203.
[83] *Solarshopnet. Technical data heckert HS-PL 135.*; Available from: 05.11.2016. http://www.solarshop-erope.net/solar-components/solarmodules/heckert_hs_pl-135_m_634.html.
[84] Duffie, J.A. and W.A. Beckman, *Solar engineering of thermal processes*. Vol. 3. 1980: Wiley New York. p.750-760.
[85] Deshmukh, S.S. and R.F. Boehm, *Review of modeling details related to renewably powered hydrogen systems.* Renewable and Sustainable Energy Reviews, 2008. **12**(9): p. 2301-2330.
[86] Clarke, D.P., Y.M. Al-Abdeli, and G. Kothapalli, *The effects of including intricacies in the modelling of a small-scale solar-PV reverse osmosis desalination system.* Desalination, 2013. **311**: p. 127-136.
[87] Tamizh Mani, G., et al. *Photovoltaic module thermal/wind performance: long-term monitoring and model development for energy rating*. in *Proc.NCPV and solar program review meeting, 2003. p. 936-939.*
[88] *BOM.South Australia weather and warnings* Available from: 12.12.2018. http://reg.bom.gov.au/climate/reg/oneminsolar/.
[89] Ashari, M. and C. Nayar, *An optimum dispatch strategy using set points for a photovoltaic (PV)–diesel–battery hybrid power system.* Solar Energy, 1999. **66**(1): p. 1-9.
[90] El-Hefnawi, S.H., *Photovoltaic diesel-generator hybrid power system sizing.* Renewable Energy, 1998. **13**(1): p. 33-40.
[91] *Cummins South Pacific (12.10.2015). B3.3 Engine Data Sheet & Performance Curve (60kW FR 30004). Source: Personal Communication.*
[92] *Cummins South Pacific (12.10.2015). B3.3 Engine Data Sheet & Performance Curve (30kW FR 30002). Source: Personal Communication.*
[93] *Technical Reference : Capstone Model C30 Performance*. Available from: 15.11.2015. http://www.wmrc.edu/projects/bar-energy/manuals/c-30-manuals/410004_Model_C30_Performance.pdf.
[94] Bajpai, P. and V. Dash, *Hybrid renewable energy systems for power generation in stand-alone applications: a review.* Renewable and Sustainable Energy Reviews, 2012. **16**(5): p. 2926-2939.
[95] Lujano-Rojas, J.M., et al., *Operating conditions of lead-acid batteries in the optimization of hybrid energy systems and microgrids.* Applied Energy, 2016. **179**: p. 590-600.
[96] *Lead-acid battery*. Available from: 20.11.2015. http://www.sunstonepower.com/upload/userfiles/files/ML12-200.pdf.
[97] Hausmann, A. and C. Depcik, *Expanding the Peukert equation for battery capacity modeling through inclusion of a temperature dependency.* Journal of Power Sources, 2013. **235**: p. 148-158.
[98] Belmili, H., et al., *Sizing stand-alone photovoltaic–wind hybrid system: Techno-economic analysis and optimization.* Renewable and Sustainable Energy Reviews, 2014. **30**: p. 821-832.
[99] Ismail, M.S., M. Moghavvemi, and T.M.I. Mahlia, *Current utilization of microturbines as a part of a hybrid system in distributed generation technology.* Renewable and Sustainable Energy Reviews, 2013. **21**: p. 142-152.
[100] Agency, I.E. *Projected costs of generating electricity, 2010*. Available from: 12.09.2016. http://www.worldenergyoutlook.org/media/weowebsite/energymodel/ProjectedCostsofGeneratingElectricity2010.pdf.
[101] Katsigiannis, Y., P. Georgilakis, and E. Karapidakis, *Multiobjective genetic algorithm solution to the optimum economic and environmental performance problem of small autonomous hybrid power systems with renewables.* Renewable Power Generation, IET, 2010. **4**(5): p. 404-419.
[102] *Central Maine Diesel*. Available from: 03.02.2016. http://www.centralmainediesel.com/cummins-generators.asp.
[103] Brown Jr, E.G., *Life Cycle Assessment Of Existing and Emerging Distributed Generation Technologies in California.* 2011.
[104] Gumus, M., *Reducing cold-start emission from internal combustion engines by means of thermal energy storage system.* Applied Thermal Engineering, 2009. **29**(4): p. 652-660.

[105] Hossain, M., S. Mekhilef, and L. Olatomiwa, *Performance evaluation of a stand-alone PV-wind-diesel-battery hybrid system feasible for a large resort center in South China Sea, Malaysia.* Sustainable Cities and Society, 2017. **28**: p. 358-366.
[106] Salehin, S., et al., *Assessment of renewable energy systems combining techno-economic optimization with energy scenario analysis.* Energy, 2016. **112**: p. 729-741.
[107] Darrow, K., et al., *Catalog of CHP technologies.* 2014.
[108] Ismail, M.S., M. Moghavvemi, and T.M.I. Mahlia, *Techno-economic analysis of an optimized photovoltaic and diesel generator hybrid power system for remote houses in a tropical climate.* Energy Conversion and Management, 2013. **69**: p. 163-173.

Chapter 3: Optimisation of Stand-alone Hybrid CHP Systems Meeting Electric and Heating Loads[3]

This chapter investigates the role of both electric and heating loads on the optimisation of hybridised stand-alone Combined Heating and Power (CHP) systems. Research Question (RQ) 2 is addressed by this chapter. In this chapter load following strategy in these systems (electric only FEL, versus electric and thermal FEL/FTL) and the relative magnitude of the heating load are analysed on system cost and performance. The conceptual CHP systems modelled also consider waste system derived from either multiple Internal Combustion Engines (ICEs) or Micro Gas Turbines (MGTs). The research uses MATLAB-based Genetic Algorithm (GA) optimisation throughout and features detailed hardware characteristics as well as temporally fluctuating meteorological (solar irradiance, temperature) and load (electric, heating) data. The outcomes are also tested in relation to CHP systems sized whilst optimising either single (Cost of Energy-COE, $/kWh) or multiple functions (COE and overall system efficiency, η_{CHP} %).

3.1 Introduction

Energy usage is a key indicator of national development with the major sources being conventional fossil fuels such as coal, petroleum oil, and natural gas. However, limited reserves of fossil fuels and the environmental emissions from burning them have forced policy makers to deploy more alternative energy sources. Unlike conventional sources, renewables produce negligible operational GHG emissions and can theoretically be generated worldwide. Even though the application of renewable energy in electricity generation has increased significantly [1-3], due to its seasonal and temporal variations neither PV nor wind can reliably satisfy the load demand [4, 5]. Therefore, many stand-alone systems integrate combustion based prime movers such as Internal Combustion Engines (ICEs) or Micro Gas Turbines (MGTs) alongside renewables. These hybridised energy systems also include energy storage media (batteries, hydrogen, capacitors) since renewable energy resources are inherently intermittent [6-13]. Thus, much reliance remains on conventional fossil fuel based power generation units. However, in relation to stand-alone hybrid systems, very few research studies are available in literature which examine their optimisation when waste heat recovery exists in the context of cogeneration or trigeneration [14-18].

A combustion powered stand-alone (completely off-grid) or distributed (occasional access to grid) cogeneration system, commonly known as Combined Heat and Power (CHP), involves the

[3] This chapter has been published as a full research paper.
Das, B.K., Y.M. Al-Abdeli, **Energy Conversion and Management**, 2017. 153: p. 391-408.
Whilst efforts were made to retain original content of the article, minor changes such as number formats and font size style were implemented in order to maintain consistency in the formatting style of the thesis.

simultaneous production of heat and power from a single fuel source to meet an electric and heating load. In contrast, trigeneration additionally meets a cooling load along with the CHP application for a similar fuel usage. These systems which are commonly termed Combined Cooling, Heating, and Power (CCHP) provide improved power quality and reliability, save energy, reduce net emissions [19-24]. However, the vast majority of these systems do not integrate renewables [25-28]. As such, a conventional power plant transforms around 35–55 % of the fuel's energy into electric power and the rest is released to the environment as waste heat. By introducing CHP, efficiency can exceed 90 % [29, 30] with 20–30 % lesser fuel consumption. Additionally, approximately 50 % fuel savings can be achieved for CCHP applications [31]. CHP systems can be operated on a topping cycle (electric energy first and recovered waste heat can then be used for thermal applications), bottoming cycle (thermal load is satisfied first and electric energy is then generated from surplus thermal energy), and combined cycle (produce additional electricity using recovered waste heat to run a steam turbine) [32]. Several different types of prime movers can be used in stand-alone CHP applications including ICEs, MGTs, and high temperature Fuel Cells (FCs). Incorporating a waste heat recovery system with these prime movers to meet local heating and cooling loads, can help achieve higher overall efficiency [33], with fewer environmental pollutants [34, 35]. Caresana et al. [36] studied a 100 kW MGT system and found electrical efficiencies up to 29 % when operating in power only made in the 80-100 kW range, but these could increase to an overall efficiency of about 74 % when operating in CHP with substantially lower pollutants. Onovwiona et al. [37] used parametric modelling in a techno-economic analysis of an ICE based residential cogeneration system. Their investigation with three different ICE capacities (2 kW, 3.5 kW, and 6 kW), simulated these systems in 15min time steps and revealed that electrical efficiency of 23.3 % can be raised to almost 80 % overall efficiency using CHP technology. However, any deficit in meeting electric and thermal demand had to be satisfied by resorting to the utility grid and an auxiliary burner. As such, their system was not stand-alone as with the current study.

Identifying the optimum sizing of stand-alone hybrid systems is a major challenge as several parameters must be concurrently considered, such as the choice of renewables, hardware/device characteristics, variations in load profiles, and the modelling methods used as well as their constraints and parameters. Because of the complexity and nonlinearity involved in optimal sizing, artificial intelligence has been applied instead of conventional analytical methods [38]. Specifically, Genetic Algorithms (GAs) [39-44], Particle Swarm Optimization (PSO) [45-48], Artificial Neural Networks (ANN) [49], and Fuzzy Logic [46, 50], have been extensively used for CHP and CCHP system optimisation. The Power Management Strategy (PMS) is another important parameter that can affect the optimal sizing. The most commonly used PMS's are: Following Electric Load (FEL), and Following Thermal Load (FTL) [51]. In the former, prime movers are operated to satisfy all electricity demand, with the waste heat meeting part or all of the thermal demand and the rest being met by an auxiliary boiler. In the latter, the system is operated to meet all the thermal demand but the electrical power produced by the generating

unit can satisfy part (or all) of the electrical load, deficits likely to be imported from the grid [52]. Integration of PV with CHP systems potentially reduces emissions and increase reliability [53-55]. In this context, Brandoni et al. [54] evaluated a residential hybrid (PV) micro-CHP system but used non-adaptive linear programming. However, unlike the present paper which considers a stand-alone system, their system was dependant on grid electricity for additional power requirement as well as using additional hardware such as a boiler and vapour compression chiller to meet additional heating and cooling not satisfied by the CHP. Their detailed PMS, a consideration which can strongly impact the outcomes of any system optimisation was not reported. Ebrahimi et al. [50] alternatively used a multi-criteria sizing function to optimise the size of prime movers for a another residential micro-CCHP system and investigated thermodynamical parameters (fuel energy saving ratio, exergetic efficiency), economic criteria (net present value, internal rate of return, and payback period), and environmental parameters (CO_2, CO and NO_x reduction). They did not consider a dynamic load profile. In another study, Abdollahi et al. [40] performed multi-objective Genetic Algorithm (GA) optimisation for a residential CCHP system with exergetic efficiency, total levelized cost rate, and environmental cost rate as objective functions. The study considered a Micro Gas Turbine, Heat Recovery Steam Generator (HRSG), and an absorption chiller to meet cooling, heating, and electrical power. Their system was not stand-alone as it had an additional electric boiler and auxiliary chiller, both powered by a grid connection, for meeting peak demands. Moreover, their study only used a (coarse) monthly averaged load profile which also affects the operational characteristics and system efficiencies. Ahmadi et al. [42] reported a multi-objective optimisation of exergy efficiency, total cost, and CO_2 emission when modelling a 50 MW gas turbine supplying electric power and thermal energy in a CHP system in a paper mill. From the above it is evident that optimisation of stand-alone hybrid CHP systems based on ICE or MGT has not been received attention in the recent literature.

The main objectives of this paper are to (i) analyse the effects of various parameters on the optimal sizing of stand-alone hybridized CHP energy system meeting reliability constraints (both electric and thermal loads); (ii) highlight the impact of FEL or FEL/FTL Power Management Strategies on system sizing and operation; and (iii) compare between systems sized using single– vs multi–objective GA optimisation (minimising cost and maximising efficiency). To achieve this, the present study extends work done on CHP energy systems through simultaneously considering four aspects. Firstly, the system studied does not include auxiliary boilers to meet heating demand but solely relies on renewables and multiple units of supplementary prime movers (either ICE or MGT) to satisfy both P_{elec} (t) (electric) and P_{ther} (t) (thermal) loads. Whilst energy systems meeting an electric load (only) have been optimised when achieving a target load reliability constraint such as LPSP [56-59], considering LPSP into CHP systems which also meet a thermal demand has not been widely reported in the literature [51, 60-65]. Additionally, this paper differs to others [37, 54, 66, 67] in that the CHP systems analysed are stand-alone and not connected to a grid. Secondly, this research presents the intricate details of the Power

Management Strategy used, which is not always done in earlier works. Moreover, the PMS deployed herein features varying relative magnitudes of P_{elec} (t) and P_{ther} (t) even when operating under FEL/FTL and FEL. In this context, it should be noted that despite PMS architectures affecting the performance of stand-alone energy systems [68], other CHP system studies [69, 70] have not presented their PMS architectures (algorithms) to the same level of detail done in the present work. Thirdly, in this paper the outcomes of Genetic Algorithm system optimisation are compared between using single- (COE, \$/kWh) or dual-objective functions (COE, \$/kWh; and $\eta_{CHP,}$ %), whilst other studies using GA to analyse CHP systems [23, 42-44] neither contrast between single- and multi-objectives (for the same hardware) nor do they feature Cost of Energy (COE) and overall efficiency (η_{CHP}). Fourthly, the simulations undertaken are applied to systems which are highly dynamic as they are based on 15min temporal resolution, compared to other studies of CHP systems which have considered hourly [23, 70], weekly or monthly temporal resolutions [40, 50].The GA Optimisation Toolbox within MATLAB R2015b is used throughout along with meteorological data and time series of both electrical and heating load profiles spanning a winter season (three months). This paper is organised as follows: Section 2 illustrates the methodology; Section 3 covers the results and discussion followed by the conclusions in Section 4 along with some recommendations for future research.

3.2 Methodology

The conceptual design architecture of the stand-alone hybrid cogeneration system that is considered is shown in Figure 3.1. The key hardware components are PV modules, supplementary prime movers in the form of multiple similar units of Internal Combustion Engines (ICEs) or Micro Gas Turbines (MGTs), batteries (Batt), Heat exchangers (Hex) and inverters. The system considered meets three relative magnitudes of highly dynamic load profiles which have been processed so as to vary their relative magnitudes but retain their time fluctuating nature. The first is designated as 60:40 shown in Figure 3.2(a). The mean for the electric load demand is 28.88 kW and the standard deviation is 29.53 kW; the mean for the thermal load is 17.95 kW and the standard deviation is 49.44 kW. The second load profile is designated as 40:60 shown in Figure 3.2(b), where the thermal demand exceeds the electric. In this regard, the mean for the electric load demand is 17.95 kW and the standard deviation is 18.35 kW; the mean for the thermal load is 28.88 kW and the standard deviation is 56.26 kW. This research also considers a third load profile as 30:70 shown in Figure 3.2(c). The mean for the electric load demand is 13.46 kW and the standard deviation is 13.76 kW; the mean for the thermal load is 33.69 kW and the standard deviation is 65.64 kW. Our earlier work [65] has featured a similar electric load profile but of a lower overall magnitude and modelled in the context of stand-alone systems that have no waste heat recovery or the need to meet a thermal demand as in the present study.

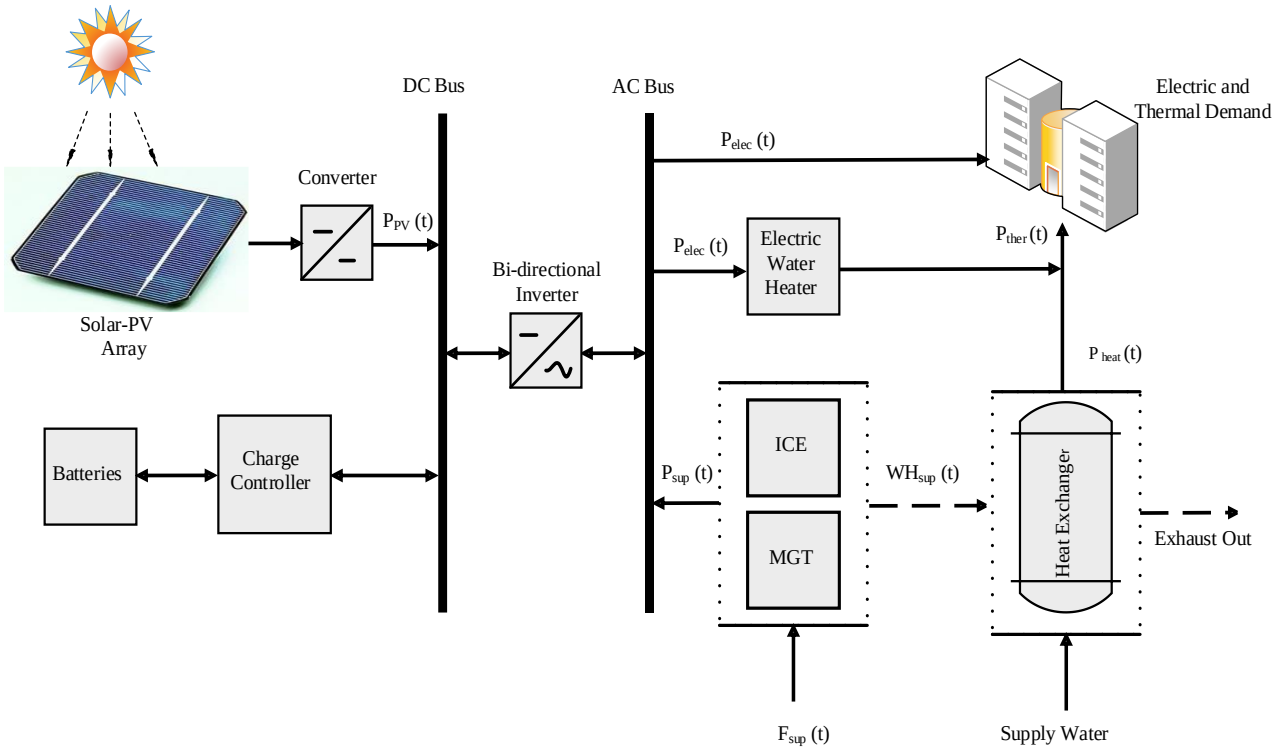

Fig. 3.1: Schematic diagram of stand-alone hybrid CHP system.

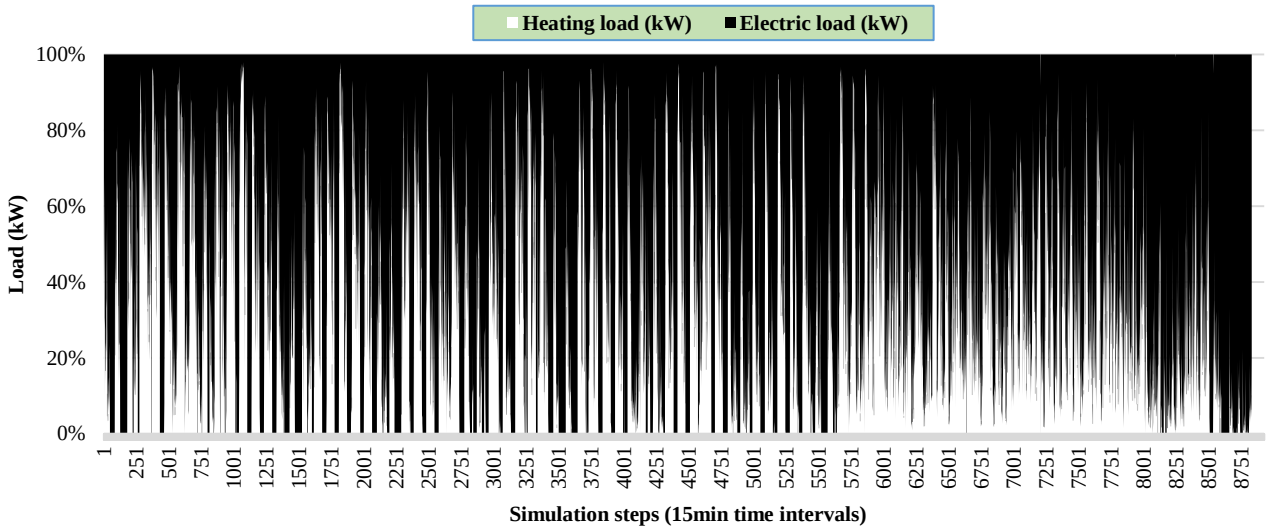

Fig. 3.2(a): Electricity (64,462 kWh) and heating (40,058 kWh) load demand (60:40) of the selected area.

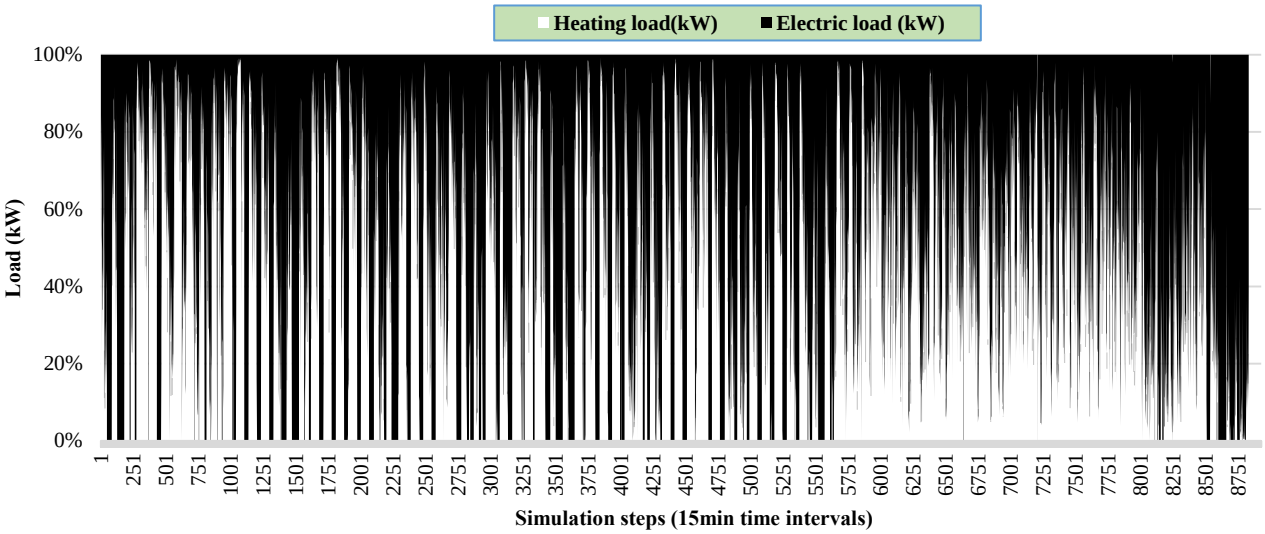

Fig. 3.2(b): Electricity (40,058 kWh) and heating (64,462 kWh) load demand (40:60) of the selected area.

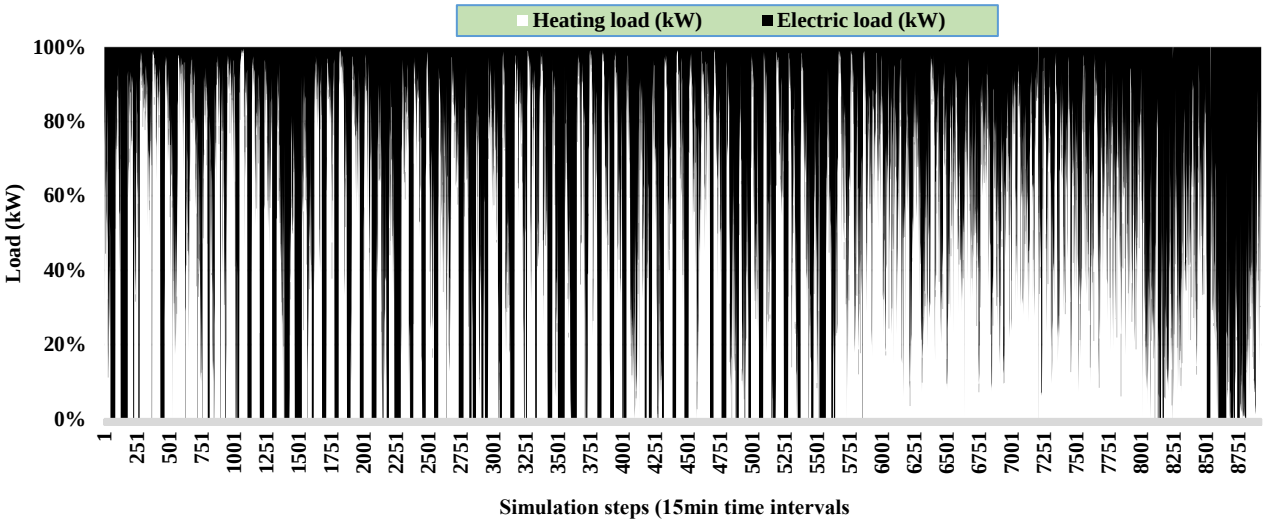

Fig. 3.2(c): Electricity (30,050 kWh) and heating (74,470 kWh) load demand (30:70) of the selected area.

3.2.1 PV model and meteorological data

In order to determine the time resolved solar power generation, the performance characteristics curve of commercially available PV modules is used (Make: Heckert Solar, Model: HS-PL 135) [71]. These are mono-crystalline silicon PV modules of 0.8 m^2 and 135 W each, maximum power point voltage of 18 V, maximum power point current of 7.48 A, nominal open circuit voltage of 22.3 V, and a short circuit current of 7.95 A [71, 72]. Dynamic profiles of solar irradiation data and ambient temperature, both shown in Figure 3.3, are used in the simulations. These are for a remote location in Western Australia and obtained from the Australian Bureau of Meteorology (Broome: latitude:17º56'S, longitude:122º14'E) [73]. The total annual availability of solar irradiance is 2,290 kW/m^2, with a peak of 1.14 kW/m^2. The performance of the PV modules at any time interval is dependent on the cell temperature, which itself a function of solar irradiation, ambient temperature, and wind speed, all of

which have not been commonly integrated in many previous studies when deriving PV power [59, 74, 75]. In this study, a mathematical model based on a single diode equivalent circuit for PV modules, wherein the effects of ambient temperature and wind speed on the power output have been used [76, 77]. The PV module parameters such as the light current, diode reverse saturation current, series resistance, shunt resistance, and the modified ideality factor are calculated to determine the solar current. These parameters can be obtained using the *I-V* characteristics provided by the manufacturer at reference conditions and other known hardware specific characteristics [71].

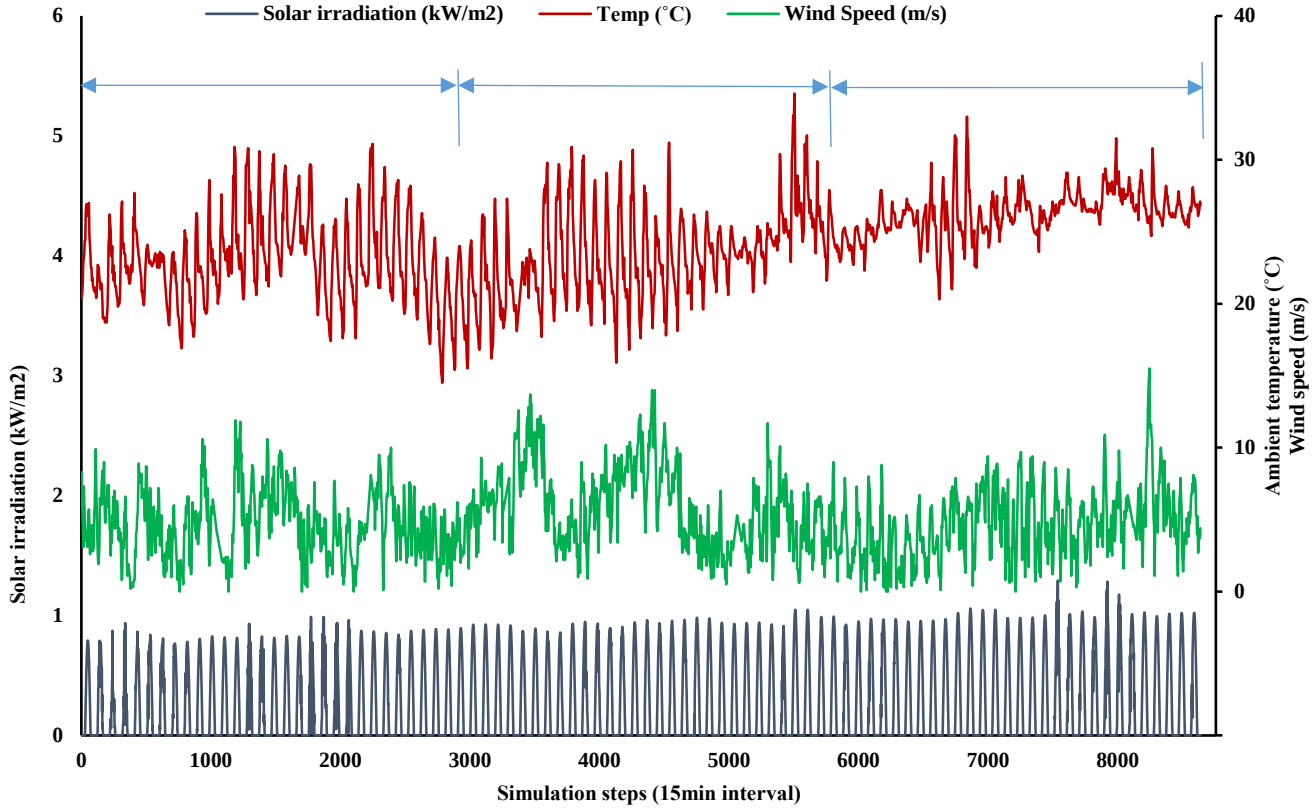

Fig.3. 3: Time resolved solar irradiation, ambient temperature, and wind speed over three months (July to September 2016).

As such, this study also includes a detailed modelling of the renewable power generated using methods found in the Appendix D. In this study, Renewable Penetration (RP) is percentile which expresses usable PV energy converted to meet load but excludes dumped/excess energy relative to the load demand, made of electric P_{elec} (t) and thermal P_{ther} (t)) at any time step.

3.2.2 Battery modelling

In this study, the primary role of the battery bank is to supply the necessary energy if PV is unable to satisfy part of the load demand (electric and thermal) or if the minimum starting threshold ($P_{sup,min}$) of supplementary prime movers is not reached to warrant their operation. As such, batteries are not used for seasonal (bulk) energy storage. Surplus energy generated by the PV modules is stored in the batteries

and redrawn from the battery when required. After meeting the thermal demand P_{ther} (t) in any time interval, excess energy from supplementary prime movers is also used to charge the battery bank. Lead acid batteries of 200 Ah nominal capacity, 12 V nominal voltage, and round-trip efficiency of 85 % have been considered [78]. For the longevity of the battery bank, the battery should not be overcharged or over discharged. The maximum charge ($B_{SOC,max}$) is set to the nominal capacity of each battery and the minimum state of charge is represented by $B_{SOC,min} = 0.2B_{SOC,max}$ for longer battery life [57]. In the simulations, the battery charge efficiency is taken equal to the round trip efficiency, whereas the discharge efficiency is 100 % [57]. The battery charging and discharging equations are adopted from Appendix E. The battery bank is connected to the PV modules through a charge controller. The DC and AC buses are connected by the bi-directional inverter which converts DC voltage (from PV and battery sources) to AC voltage to supply AC loads, and alternatively AC voltage (from prime movers) to DC voltage to charge the battery bank. The conversion efficiency of the bio-directional inverter is considered as 95 % [79].

3.2.3 Supplementary prime movers

The conceptual CHP systems considered in this study integrate one or more units of similar combustion-based prime movers to supplement the PV/Batt and meet the electric demand. These supplementary prime movers are either Internal Combustion Engines (30 kW ICE) or comparable rating Micro Gas Turbines (30 kW MGT). An exhaust heat recovery system is coupled with the ICE or MGT units so as to meet thermal demand. The performance characteristics of commercially available ICEs and MGTs are chosen for system modelling [80, 81]. The fuel energy (F_{sup} (t)) supplied to each supplementary prime mover corresponds to the output power (P_{sup}) of these prime movers in every time step based on their instantaneous thermal efficiency (ICE: 33–37 % over 10 kW– 30 kW; MGT: 20.6–26 % over 10 kW–30 kW). It is assumed that all simulation parameters remain constant during each time interval. A minimum time step of 15 min has been considered in this study. The relatively small temporal resolution used allows for sensitivity to any higher frequency of prime mover start/stops as well as partial load operation, both of which can cause significant amounts of fuel consumption and long term maintenance problems [82, 83]. In any time steps, the fuel consumption rate (kg/h) for the 30 kW ICE and the MGT are derived using the polynomial fits of engine operating characteristics (Equation 3.1 and Equation 3.2, respectively) [80, 81, 84], where $P_{ICE}(t)$ and $P_{MGT}(t)$ is the power generation from the ICE and MGT, respectively. The ambient temperature is also used to model MGT to calculate the output power. Figure 3.4 represents the normalised performance characteristics curves for the 30 kW ICE and the MGT.

$$C_{fuel\_ICE\_30}(t) = 0.0001 \times P_{ICE}^2(t) + 0.2108 \times P_{ICE}(t) + 0.3551 \quad (3.1)$$

$$C_{fuel\_MGT\_30}(t) = 0.00005 \times P_{MGT}^2(t) + 0.3132 \times P_{MGT}(t) + 0.7054 \quad (3.2)$$

In this regard, consumed fuel energy (kW) can be determined using Equation 3.3, where LHV is the lower heating value of the fuel (43,100 kJ/kg for diesel in the ICE and 43,250 kJ/kg for natural gas in the MGT).

$$F_{sup}(t) = \frac{C_{fuel\_sup}(t) \times LHV}{3600} \tag{3.3}$$

In this study, a Thermal to Electric Ratio (TER) is determined from Equation 3.4, where Q_{th} is the recoverable heating energy. Systems have higher TER for MGT (typically 1.37 to 2.17 as compared to ICE (0.84 to 1.96)that implies comparatively more heat generation [84].

$$TER = \frac{Q_{th}(t)}{P_{sup}(t)} \tag{3.4}$$

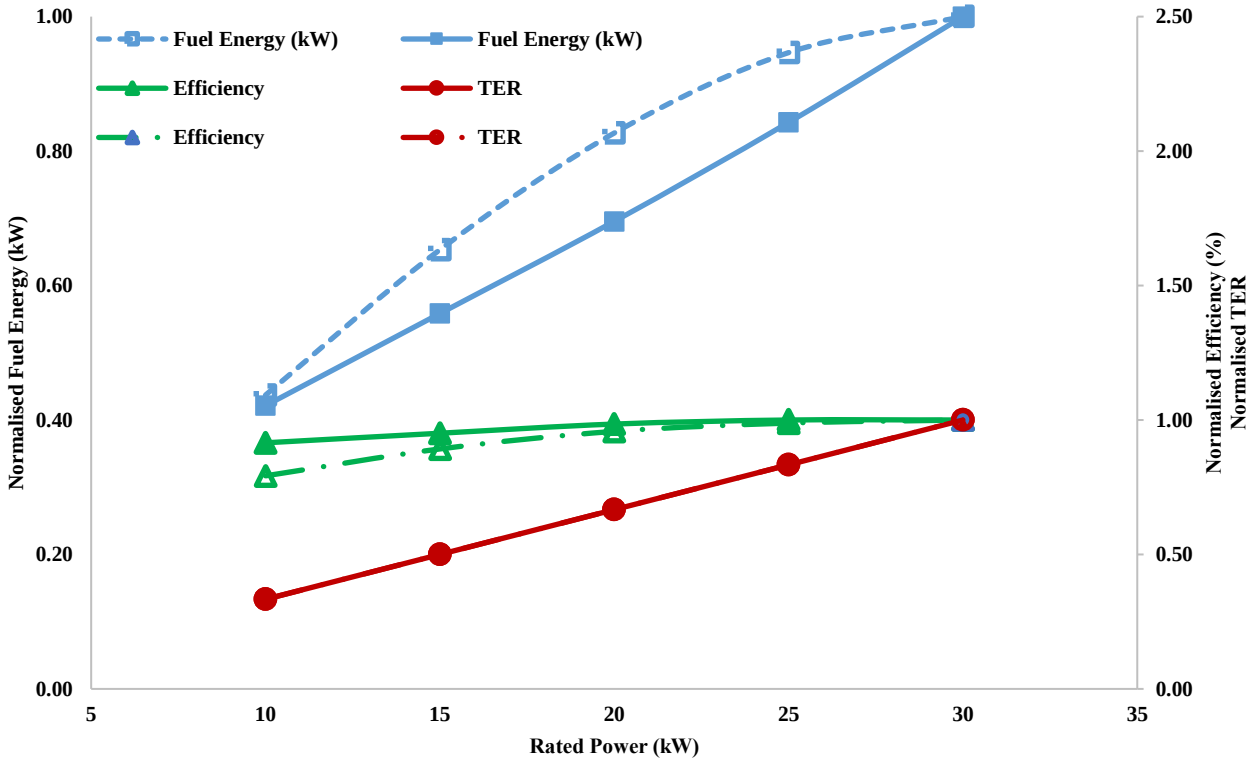

Fig. 3.4: Normalised fuel energy, efficiency, and Thermal to Electric Ratio (TER) of a typical 30 kW ICE (solid) and MGT (dashed).

The recoverable heating energy ($Q_{th}(t)$) includes the combined waste heat of exhaust gas and jacket water for the ICE, but only waste heat of exhaust gas for MGT which is air cooled. In this paper, a TER value of 2.17 for the MGT and 1.96 for the ICE has been considered for calculating the potential to meet a thermal load in each time interval. Additionally, the Recovered Waste Heat to Power Generation (RWHP) is defined by the Equation 3.5, where $P_{heat}(t)$ is the thermal load met by the recoverable heating energy ($Q_{th}(t)$) relative to the total (electric) power output (P_{sup} (t)) of the ICE or MGT over each time step.

$$RWHP = \frac{P_{heat}(t)}{P_{sup}(t)} \quad (3.5)$$

The consequential total life cycle emissions (LCE) are the sum of the emissions by the system components over their lifetime (cradle to grave) and includes that from fuel consumption. This is expressed by Equation 3.6 [4], where, β_i (kg CO_2-eq/kWh) is the lifetime equivalent CO_2 emissions of each hardware component (i) and E_L (kWh) is the amount of energy converted (or stored in batteries).

$$LCE = \sum_{i=1}^{N} \beta_i E_L \quad (3.6)$$

3.2.4 Electric water heater

In this study, when the load deficit (P_{Net}) is below the minimum starting threshold of supplementary prime movers, process heating using electric resistance heaters (powered by renewables and batteries) is used to supply the necessary heating load. The electric energy (kWh) requirements can be measured from the overall process heater efficiency ($\eta_{wh,sys}$) which is calculated by the Equation 3.7 [85], where E_{elec} is the electrical energy input to the heater and E_{ther} is the total thermal energy. In this study, an efficiency, $\eta_{wh,sys} = 97\ \%$ has been considered for system modelling [86]. In the present study, the thermal load is composed purely of heating (no cooling as with CCHP).

$$\eta_{wh,sys} = \frac{E_{ther}(t)}{E_{elec}\ (t)} \quad (3.7)$$

3.2.5 Load profile and reliability index

The Loss of Power Supply Probability (LPSP) is extensively used as a reliability index for sizing hybrid power generation when meeting electric loads [56-59]. However, the LPSP has not been considered while meeting thermal demand [51, 60-65]. In this regard, the simulations within this paper consider a combined electric and thermal load when deriving the optimum system. The target reliability is based on the LPSP (combined electrical and thermal) and is calculated using Equation 3.8, whereby $LPS_{elec}(t)$ and $LPS_{ther}\ (t)$ are the missed (kWh) electric and thermal in any time interval and $E_{elec}(t)$ and $E_{ther}\ (t)$ are the total electric and thermal load demands, respectively, over the period (T). It should be noted here that in order to modify the expression for LPSP from that applied to electric loads [59], two terms (for thermal load) have been introduced into the numerator and denominator of Equation 3.8. In the present paper, t=15min and T=132,480 min (8,832 time steps, 3 months).

$$LPSP = \frac{\sum_{t=1}^{T}(LPS_{elec}\ (t) + LPS_{ther}(t))}{\sum_{t=1}^{T}(E_{elec}\ (t) + E_{ther}(t))} \quad (3.8)$$

where, $LPS\ (t) = \left(LPS_{elec}(t) + LPS_{ther}(t)\right)$ (3.9)

In this case, the LPS (t) can be calculated using the following Equation (modified from the electric loads [59]):

$$LPS\ (t) = \left(P_L(t) - P_{sup}(t) - P_{heat}(t)\right)\Delta t - \left(P_{PV}(t)\Delta t + \frac{C_b}{\Delta t}\left(B_{SOC}(t-1) - B_{SOC,min}\right)\right)\eta_{inv} \quad (3.10)$$

Any time interval, the total load P_L (t) is designated to be the sum of the electrical load P_{elec} (t) and the thermal load P_{ther} (t). Figure 3.2 represents the electric load and heating load demand for both 60:40, 40:60, and 30:70 load profiles. The maximum value of the LPSP constraint is taken as 0.01±0.005, which is equivalent to a missed load of 1045 kWh combined electric and heating.

3.2.6 Power management strategy

In this study, the hybrid cogeneration system is assumed to meet a time varying domestic hot water supply and electric load as represented by a specific (combined) LPSP. A Power Management Strategy (PMS) is the switching algorithm which controls various components and is given in Figure A3.9 (Appendix). This study includes a comparison between two types of PMS. The first is a strategy which sets operating decisions based on meeting the electric load and then using the consequential waste heat from supplementary prime movers to satisfy part/all the heating load (termed FEL). The second strategy is hybrid (termed FEL/FTL) and necessarily meets both the electric and heating loads.

Power generated from the PV module P_{PV} (t) is compared with P_L (t) to determine the net deficit P_{Net} (t) = P_{PV} (t) - P_L (t) in each time interval. The deficit P_{Net} (t) can either be met solely by renewables, requires augmentation through discharging battery storage at P_B (t), or operating supplementary prime movers at P_{sup} (t). Below the minimum starting threshold ($P_{sup,min}$) of supplementary prime movers which is set at 30 % of nominal rated power [87, 88], PV along with the battery bank would supply necessary energy requirements. Where renewables are greater than the load demand (P_{Net} (t)>0) but batteries are not fully charged (B_{SOC} (t) < $B_{SOC,max}$), surplus PV power is delivered to charge the battery bank at P_B (t). Once the battery state of charge reaches its maximum value ($B_{SOC,\ max}$), additional surplus power in this time interval is considered as excess energy EE (t) and dumped. Alternatively, when power generation from PV is equal the load demand P_{Net} (t) =0, the load is met in that time interval (Meet P_L (t)). However, when the load demand is greater than renewables P_{Net} (t) <0, but sufficient storage capacity exists (B_{SOC} (t) > $B_{SOC,min}$) and total energy (PV+Batt) is equal or greater than the demand, the battery would supply the necessary load demand alongside the PV. As soon as battery state of charge reaches its minimum level (B_{SOC} (t) = $B_{SOC,min}$) , the deficit load requirement is considered as unmet (Unmet P_L (t)).

If P_{Net} (t) exceeds the minimum starting threshold for the prime movers ($P_{sup,min} \leq |P_{Net}(t)|$), the ICE or MGT are used to meet the demand (P_L (t)) when renewable energy along with battery bank is insufficient. At this stage, the prime movers are operated to meet all the electricity demand (P_{elec} (t)) and the thermal demand (P_{ther} (t)) using the waste heat recovery system. However, for a hybridised system such as that described in this study, when the heating load is much higher compared to the electrical demand, prime movers can meet only part of the thermal demand. In such time intervals, the

PMS shifts from FEL to FEL/FTL where prime movers supplement power to first meet the relatively higher heating load requirements. In Figure A3.9 (Appendix), this strategy is shown using a dashed box, where the supplementary prime mover switches priority so as to meet the thermal demand P_{ther} (t) instead of P_{elec} (t). The PMS then checks whether it also meets the electric demand in that same time interval. In this regard, the deficit (combined) electric and heating load requirements are considered as Unmet P_L (t). On the other hand, the additional electric energy generated by the ICE or MGT, after meeting the demand, is used to charge batteries until they reach their maximum state of charge ($B_{SOC, max}$), with the excess being dumped. In an FEL strategy, after first meeting electricity demand (P_{elec} (t)), the recovered waste is used to meet the thermal demand (full P_{ther} (t) or part of it). The rest of the heating demand is met by the electric (resistance) water heater if there is enough state of charge ($>B_{SOC, min}$) or it is considered as (Unmet P_L (t)). In this study, for both cases (i.e FEL/FTL and FEL) if the P_{elec} (t) load is below the minimum starting threshold of the supplementary prime mover, the electric demand (P_{elec} (t)) is then met by the PV and battery bank, whereas the thermal demand (P_{ther} (t)) is met by the electric resistance heating operated using PV along with a battery bank.

3.2.7 GA Optimisation, modelling parameters, and constraints

In this work, at first the system is optimised based on single objective function (COE, $/kWh) using a MATLAB-based Genetic Algorithm (GA). The results obtained from single objective optimisation are then compared with the multi-objective optimisation technique using the same modelling parameters and constraints. The solution of a multi-objective optimisation problem, such as that in the present paper, may yield a set of non-dominant solutions known as Pareto optimal solutions. In arriving at these solutions, the simulations solve for a number of objective functions subjected to inequality constraints (LPSP in this study). The optimisation process search's for optimum values that are to be maximised (or minimised) for the objective functions subject to bounds (limits). System sizing can be formulated as follows [89, 90]:

$$\left.\begin{array}{lll} Min/Max & F(x) = [f_1(x), f_2(x), f_3(x), \dots\dots\dots, f_n(x)] & \\ Subject\ to & G_j(x) \leq 0 & j = 1,2, \dots\dots\dots, J \\ & H_k(x) \leq 0 & k = 1,2, \dots\dots\dots, K \end{array}\right\} \quad (3.11)$$

In this context, *F* is the expression for the objective function (either singular or multiple), *x* are the decision variables, *G* are the inequality constraints (e.g. LPSP), and *H* are the equality constraints (e.g. B_{SOC}, P_{sup}). In this study, multi-objective Genetic Algorithm optimisation problems have two objectives over the span of the period modelled (three months): the COE is to be minimised while the energy efficiency η_{CHP} of combustion based supplementary prime movers is maximised. Alternatively, single objective optimisations are solely based on the COE, albeit with the resulting (consequential) η_{CHP} also reported in the results given. The sizing optimisation using multi-objective Genetic Algorithm is summarised in Figure 3.5. A summary of other studies and parameters used in other single- and multi-

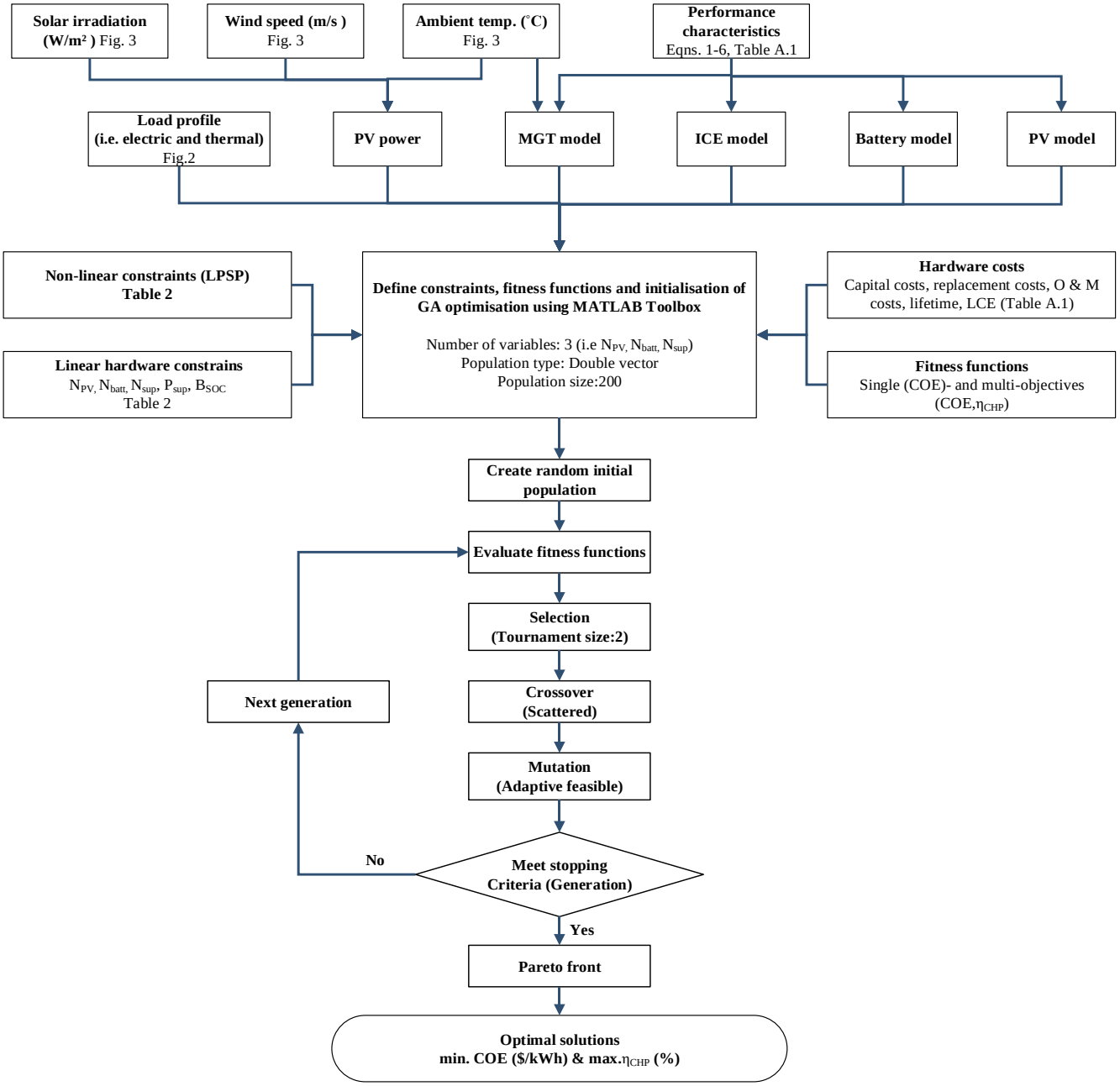

Fig. 3.5: Multi-objective GA procedure.

objective optimisation of CHP and CCHP systems is shown in Table 3.1. The technical and economical details of the hybridised system components are incorporated to the fitness function and the constraints (i.e linear and non-linear constraints). These are defined as an input to the optimisation toolbox. Additionally, a set of parameters need to be specified before the optimisation process running such as population type and size, selection function, crossover function, mutation function, and stopping criteria. In this regard, the selection function is chosen as tournament with size 2, crossover function is the scattered, and mutation is the adaptive feasible as there is both linear and non-linear constraints. The stopping criteria is selected based on the specified number of generations (100 in this study) and the function tolerance is $1e^{-6}$. Using the given input parameters, multi-objective GA optimisation offers an iterative process until the predefined stopping criteria is met. In the process of optimisation, each

generation calculates the LPSP for each population member. For those cannot satisfy the load requirements of a certain value of LPSP is excluded from the population for next generation to progress crossover, migration, and mutation processes. The process continues until all generations are finished. Finally, the Pareto front is selected which gives the values of all non-inferior solutions. More details about the methodologies of multi-objective Genetic Algorithms can be found in literature [89, 91] and from the Help menu in the MATLAB optimisation Toolbox.

Table 3.1: GA application for optimisation of CHP systems.

System components	No of objectives	Modelling parameters	Optimisation parameters
PV+MGT/ICE [39]	Single	COE, Emissions	Population size 50, number of generation 80, crossover probability 0.8, mutation factor 0.2, selection function Roulette, crossover function arithmetic.
Gas turbine+Solar thermal plant [92]	Multi	Exergy analysis, product cost	Population size 350, number of generation 3500, crossover probability 0.4, selection process tournament, mutation function constraint dependant
ORC+HRSG [93]	Multi	Exergy efficiency, overall capital cost	Population size 30, number of generation 150, crossover probability 0.7, selection process tournament
Gas turbine+ORC +HRSG+Absorption chiller+PEM [94]	Multi	Exergy efficiency, total cost rate	Population size 100, number of generation 250, crossover probability 0.9
Gas turbine+ORC+HRSG [95]	Multi	Thermal efficiency, total volume of the system, and net present value	Population size 1,000, number of generation 200, crossover probability 0.8, selection process tournament

The overall efficiency of supplementary prime mover-based cogeneration systems is determined from Equation 3.12, where P_{heat} (t) is the heating load demand met using the waste heat recovered from the ICE or MGT:

$$\eta_{CHP}(t) = \frac{P_{sup}(t)+P_{heat}(t)}{F_{sup}(t)} \tag{3.12}$$

In this study, the COE can be calculated using Equation 3.13, where C_A is the total annualised energy system cost which includes: capital costs, Operation and Maintenance (O&M) costs, discount rate and fuel costs of system components. The discount rate for energy generation projects differs from 5 % to 10 % [96]. In this paper, a value of 10% is considered with a project lifetime of 25 years in accordance with maximum lifetime of PV module. Additionally, E_s (kWh) is the annual load to be met (electrical and thermal). Further details in this regard are given in [87].

$$COE = \frac{C_A}{E_s} \tag{3.13}$$

The annualised cost is sum of annualised capital cost (C_{A_cap}), annualised Operation and Maintenance cost ($C_{A\_O\&M}$), and annualised fuel cost ($C_{A_{fuel}}$) of the system components and can be calculated by the Equation 3.14,

$$C_A = C_{A\_cap} + C_{A\_O\&M} + C_{A\_fuel} \quad (3.14)$$

The data for cost and equivalent CO_2 emissions attributed to the system components are presented in the Appendix (Table A3.5). Costs presented represent only hardware and do not include civil works, mechanical, and electrical fabrication works as well as installation and labour costs. However, the cost associated with the heat recovery system does include with the capital cost of a 30 kW MGT. The cost for circulation pumps, interconnection piping, and control instrumentation are not considered in this study.

The study utilises MATLAB optimisation toolbox to implement the single- and multi-objective genetic algorithm. In this regard, the non-linear constrains (representing the calculation of LPSP) are written in one M-file, whilst another M-file representing the fitness function (using the PMS, and Equations 12 and 13) calculates the all objective functions. The decision variables considered in this optimisation are the number of PV modules N_{PV}, the number of lead acid batteries N_{batt}, and the number of supplementary prime movers $N_{sup.}$ The simulations are also subjected to some constrains presented in Table 3.2 which are initially determined using trial and error to ensure the target LPSP (0.01±0.005) is satisfied. Constraints B_{SOC}, P_{sup}, and LPSP are formulated in the PMS, and other constrains related to bounds (number of components, N_{PV}, N_{batt}, N_{sup}) are directly entered into the optimisation toolbox.

Table 3.2: Optimisation constraints.

Decision variables	Lower bound	Upper bound
N_{PV}	100	1000
N_{batt}	10	50
N_{sup}	1	10
B_{SOC}	20	100
P_{sup}	0	30
LPSP	0.005	0.015

In achieving these simulations, a sensitivity analysis is also done into the effects of population size on the solutions in both single- (COE) and multi-objective (COE, η_{CHP}) optimisations. Figure A3.10 (Appendix) shows that with single objective optimisation, a population size of 10 is chosen as no appreciable improvement in the COE is achieved with further increases in the population size (up to 50), albeit it at the expense of computational time. In the case of multi-objective optimisations, although a larger population size is needed, both the COE and the η_{CHP} stabilise for a population size of 200. Additionally, in single objective optimisations, constraint dependent mutations, a crossover fraction of 0.8 with scattered function, elite count 2, and 50 generations are used. On the other hand, a crossover fraction of 0.8 with 100 generations are used in the MATLAB multi-objective optimisation toolbox.

3.3 Results and discussion

The data which follows examines the effects of two types of PMS, the more commonly used type governing device switching based only on electric load demand (FEL), and a hybrid PMS which accommodates following both electric and thermal loads which are made up completely of heating in this study (FEL/FTL). The results will also discuss how changes to the relative proportions of electric to thermal load affect the optimisation of a hybrid CHP system over one season (3months). Most of the analyses presented are based on single objective optimisation (COE, $/kWh) but the sensitivity of the outcomes to alternatively using a multi-objective function optimisation (COE, $/kWh; $\eta_{CHP,}$ %) is also given.

3.3.1 Type of load following strategy

The first set of results presented considers prime movers having $P_{sup,min}$=30 % whereby the Electric to Thermal Load Ratio (ETLR) is 60:40. Summary data are presented in Table 3.3, with the first three rows giving the optimised size (i.e., the solution to the system's sizing problem) and the remaining rows identifying the consequential performance.

Table 3.3: Summary results of single (COE) and multi-objective (COE and η_{CHP}) optimisations of hybrid CHP systems (load profile 60:40, LPSP=0.01±0.005).

Characteristics	PV/Batt/ICE				PV/Batt/MGT			
	Single objective		Multi-objective		Single objective		Multi-objective	
	FEL/FTL	FEL	FEL/FTL	FEL	FEL/FTL	FEL	FEL/FTL	FEL
Number of solar panels, N_{PV}	976	922	968	974	967	959	780	973
Number of lead acid batteries, N_{batt}	42	50	25	44	32	43	15	37
Number of prime movers, N_{sup}	2	2	2	1	1	1	1	1
$LPSP_{comp}$	0	0.0111	0	0.0077	0.0009	0.0085	0.0096	0.0079
PV energy generated (kWh)	62,573	59,111	62,060	62,444	61,355	61,483	50,007	62,380
Renewable penetration, RP (%)	60	57	59	60	59	59	48	60
ICE/MGT energy, P_{sup} (kWh)	25,724	33,453	27,602	32,265	27,398	33,105	35,318	33,393
RWHP (%)	76	35	77	35	78	37	72	37
Unmet energy (kWh)	0	1,165	0	802	99	885	1008	826
Fuel energy, F_{sup} (kWh)	69,139	90,824	74,203	87,588	110,090	132,130	142,630	133,280
Recovered waste heat to thermal demand (P_{heat} /P_{ther}, %)	49	29	53	28	53	30	63	31

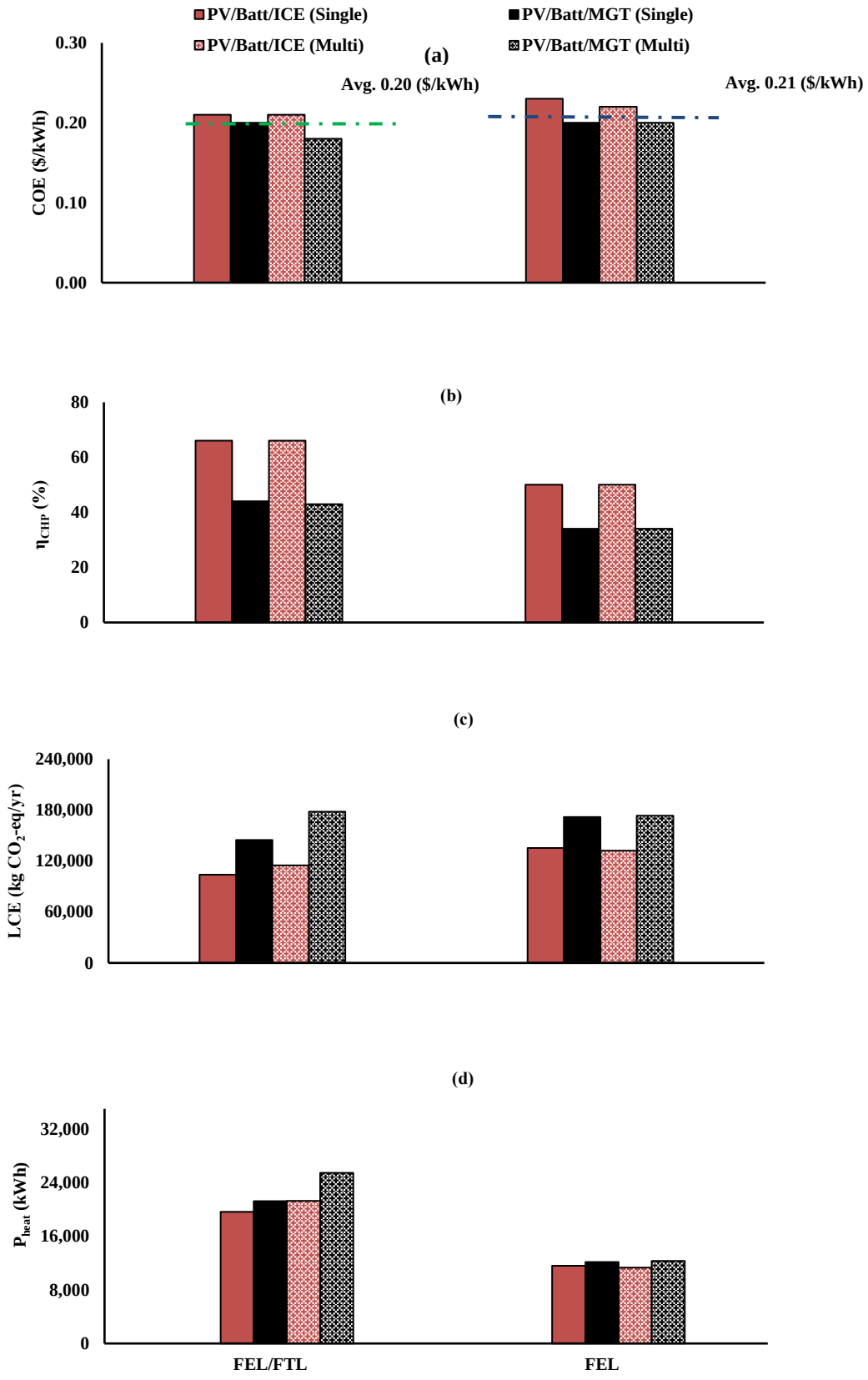

Fig. 3.6: The effects of load following strategy (FEL/FTL, FEL) on hybrid CHP systems operating to meet load profiles with an ETLR=60:40. A comparison between single- (COE) and multi-objective optimisations (COE, η_{CHP}) are shown for both PV/Batt/ICE and PV/Batt/MGT.

From Figure 3.6 (a) it is evident that a PMS based on FEL/FTL or FEL has comparable COE whether optimised using single- or multi-objectives. For PV/Batt/MGT-based systems, PMS hybridisation (FEL/FTL) has an insignificant effect on the COE (avg. 0.19 $/kWh) compared to FEL (avg. 0.20 $/kWh). Similarly, for PV/Batt/ICE-based systems, PMS hybridisation only marginally gives better COE (avg. 0.21 $/kWh) compared to FEL (avg. 0.23 $/kWh). It is also evident from the results that the COE for the PV/Batt/MGT is generally (slightly) lower in contrast to PV/Batt/ICE systems. The COE for the PV/Batt/MGT is optimised as 0.27 $/kWh in the literature [39]. This is attributed to the higher RWHP with PV/Batt/MGT systems, the lower price of natural gas used to run MGT's (3.3 $/GJ) compared to diesel (0.91 $/l). However, the higher capital cost of each MGT unit (Appendix, Table A3.5) also means optimisations always select fewer MGT units than ICE units as shown in Tables 3.3 and 3.4.

In relation to the Overall CHP Efficiency (η_{CHP}, %), the FEL/FTL PMS in both single- and multi-objective optimisations is better than the FEL PMS. Optimisations when applied to size the ICE-based systems on FEL/FTL give η_{CHP} =66 % for both single- and multi-objective optimisations as shown in Figure 3.6 (b). However, in the case of ICE-based systems using an FEL, the overall efficiencies are much lower at η_{CHP} =50 % for both single- and multi-objective optimisation. In MGT-based systems running on a FEL/FTL PMS, η_{CHP} =44 % and η_{CHP} =43 % with single- and multi-objective optimisations. These also fall when alternatively operating on an FEL PMS for single- and multi-objective optimisations with η_{CHP} =34 %. From the above discussion, it is also evident that the η_{CHP} (%) for the ICE in the PV/Batt/ICE systems have higher η_{CHP} (%) than the PV/Batt/MGT system under the same operating conditions. The reason behind this is that the ICE has higher thermal efficiency (33–37 % over 10 kW– 30 kW) as compared to the MGT (20.6–26 % over 10 kW–30 kW).The output power for an MGT is also more susceptible to ambient temperature changes (rated power is up to 18 ˚C but decreases by a further 20 % at 35 ˚C) which imposes an additional change across seasons.

Although in the FEL/FTL PMS there are no significant gains in COE or η_{CHP} between using single- and multi-objective optimisations, the latter produce slightly higher LCE ($kgCO_2$-eq/yr) in both ICE and MGT-based systems. This is because in multi-objective optimisation achieving a higher η_{CHP} the Genetic Algorithm attempts to maximise utilisation of the recovered waste heat so as to meet the thermal demand, which attributed to relatively higher contributions from supplementary prime movers. Therefore, the number of PV modules and batteries are less in multi-objective solutions compared to the single objective optimisation as see in Table 3.3. However, hybridisation of the PMS using FEL/FTL in CHP systems not only to marginally improve the COE but more cleanly the η_{CHP}, it also carries some benefits in terms of LCE in both ICE and MGT systems. For example, the data in Figure 3.6 (c) shows that in ICE based CHP systems sized using single objectives, LCE= 135,340 $kgCO_2$-eq/yr with FEL but is smaller by around 30 % at 104,010 $kgCO_2$-eq/yr with FEL/FTL. From Figure 3.6 (c) it is also obvious

that the PV/Batt/ICE-based system produces lower LCE ($kgCO_2$-eq/yr) as compared to the PV/Batt/MGT-based system for similar following load and optimisation techniques. This is because of the higher lifetime equivalent CO_2 emissions (1.16 $kgCO_2$-eq/kWh) for MGT than the ICE (0.88 $kgCO_2$-eq/kWh).

In regard to the meeting thermal load demand using the recovered waste heat (P_{heat}), the multi-objective optimisation in the FEL/FTL mode is far higher than any other operating conditions as shown in Figure 3.6 (d). Table 3.3 shows that almost 50 % of the thermal load demand is met by recovering waste heat from the supplementary prime movers while operating in the FEL/FTL mode for systems sized using single objective optimisation. This is even more (PV/Batt/ICE=53 %, and PV/Batt/MGT= 63 %) while on the multi-objective optimisation for the same operating condition. On the other hand, only around 30 % of the thermal demand is met by using the recovered heat when the system operating in the FEL mode regardless of optimisation technique (Table 3.3).

Despite this, the data also indicates the Renewable Penetration (RP) is comparable (57–60 %) in both single- and multi-objective optimisations for the both FEL/FTL and FEL operating strategy except for PV/Batt/MGT system (48 %) in multi-objective FEL/FTL mode. The reason behind this in multi-objective optimisation, the recovered waste heat to meet the thermal demand is higher (63 %) than the other mode of operation and hence the optimisation select the fewer number of PV modules and battery bank to meet the load demand. However, in the FEL mode the PMS allows only to meet the thermal demand which is produced as a consequence of meeting electric demand first by the supplementary prime movers and the rest is met by the electric (resistance) water heater powered by the renewably charged battery bank. For this reason the number of battery is higher in FEL strategy than the FEL/FTL mode for all optimisation techniques.

From the above discussion, it is obvious that although the PV/Batt/ICE and PV/Batt/MGT hybridised CHP systems meeting a P_{elec} (t) and P_{ther} (t) have comparable COE, the overall CHP efficiency (η_{CHP}, %) of the ICE is greater than that of the MGT regardless of optimisation technique under all operating conditions. The results also show that the FEL/FTL operating mode for both systems have higher share of meeting thermal demand using recovered waste and better environmental benefits than the FEL mode. This is true for both single- and multi-objective optimisation techniques. The renewable penetration is comparable for both systems in single-and multi-objective optimisation. Figure 3.7 also shows that supplementary prime movers are responsible for meeting heating loads where these are relatively significant. The hybrid PMS therefore does not oversize the PV and battery capacities but relies on combustion engines.

3.3.2 Changes of Electric to Thermal Load Ratio (ETLR)

To analyse the effects of Electric to Thermal Load Ratio (ETLR) on the hybrid FEL/FTL strategy, Figure 8 shows single objective optimisation data for ETLR=60:40, 40:60, and 30:70. Results indicate that for PV/Batt/ICE systems, the effect of ETLR is very subtle on the COE (avg. 0.22 $/kWh) in the case of ICE-based CHP systems. However, with MGT-based CHP systems, increases to the relative significance of the thermal load (i.e. a smaller ETLR) generally lead to higher COE (0.20 $/kWh for ETLR=60:40, and ~0.30 $/kWh for both ETLR=40:60 and ETLR=30:70). This is attributed to the fact that at lower electric load demand (P_{elec} (t)), as occurs with smaller ETLR, there is more likelihood of electric load falling below the minimum starting threshold ($P_{sup,min}$=9 kW) of supplementary prime movers at any time step. The PMS then forces the optimisation algorithm to select more PV modules and a larger battery bank irrespective of thermal demand in that time step. This also has the potential to cause a higher number of supplementary prime movers once the PV modules and battery units reach their upper bound in Table 3.2 to meet the specified LPSP (0.01±0.005). The sizing data in Table 3.4 supports this. For the above reasons, at the greater thermal demand (e.g. ETLR=30:70) the COE is higher. However, this is more apparent in PV/Batt/MGT systems as the capital unit cost of an MGT is higher than the ICE for the same power rating.

Table 3.4: Summary results of single objective (COE, $/kWh) optimisations of hybrid CHP systems operating at different ETLR (P_{elec}:P_{ther}) for hybrid CHP systems (LPSP=0.01±0.005, $P_{sup,min}$=9 kW).

System characteristics	PV/Batt/ICE (FEL/FTL)			PV/Batt/MGT (FEL/FTL)		
	(60:40)	(40:60)	(30:70)	(60:40)	(40:60)	(30:70)
Number of solar panels, N_{PV}	976	864	989	967	979	994
Number of lead acid batteries, N_{batt}	42	48	50	32	50	50
Number of prime movers, N_{sup}	2	7	7	1	4	4
$LPSP_{comp}$	0	0.0530	0.0957	0.0009	0.0414	0.0993
PV energy generated (kWh)	62,573	55,392	63,406	61,355	62,765	63,727
Renewable penetration, RP (%)	60	53	60	59	60	61
ICE/MGT energy, P_{sup} (kWh)	25,724	24,981	18,694	27,398	22,670	18,956
RWHP (%)	76	97	115	78	99	115
Unmet energy (kWh)	0	5,542	10,070	99	4,327	10,453
Fuel energy, F_{sup} (kWh)	69,139	67,612	50,707	110,090	90,277	75,932
Recovered waste heat to thermal demand (P_{heat} /P_{ther}, %)	49	37	29	53	35	29

However, a more significant effect of ETLR appears in relation to the η_{CHP} (%) which increases significantly in the PV/Batt/ICE (from 66 % at ETLR=60:40 to 79 % at ETLR=30:70) when working on the FEL/FTL mode. This is because RWHP grows where there is greater thermal load than the electrical load. This change whilst still appreciable is less significant in the PV/Batt/MGT system (η_{CHP} = 44 % at ETLR=60:40 but 54 % at ETLR=30:70) which is attributed to the lower thermal efficiency of the MGT as compared to the ICE.

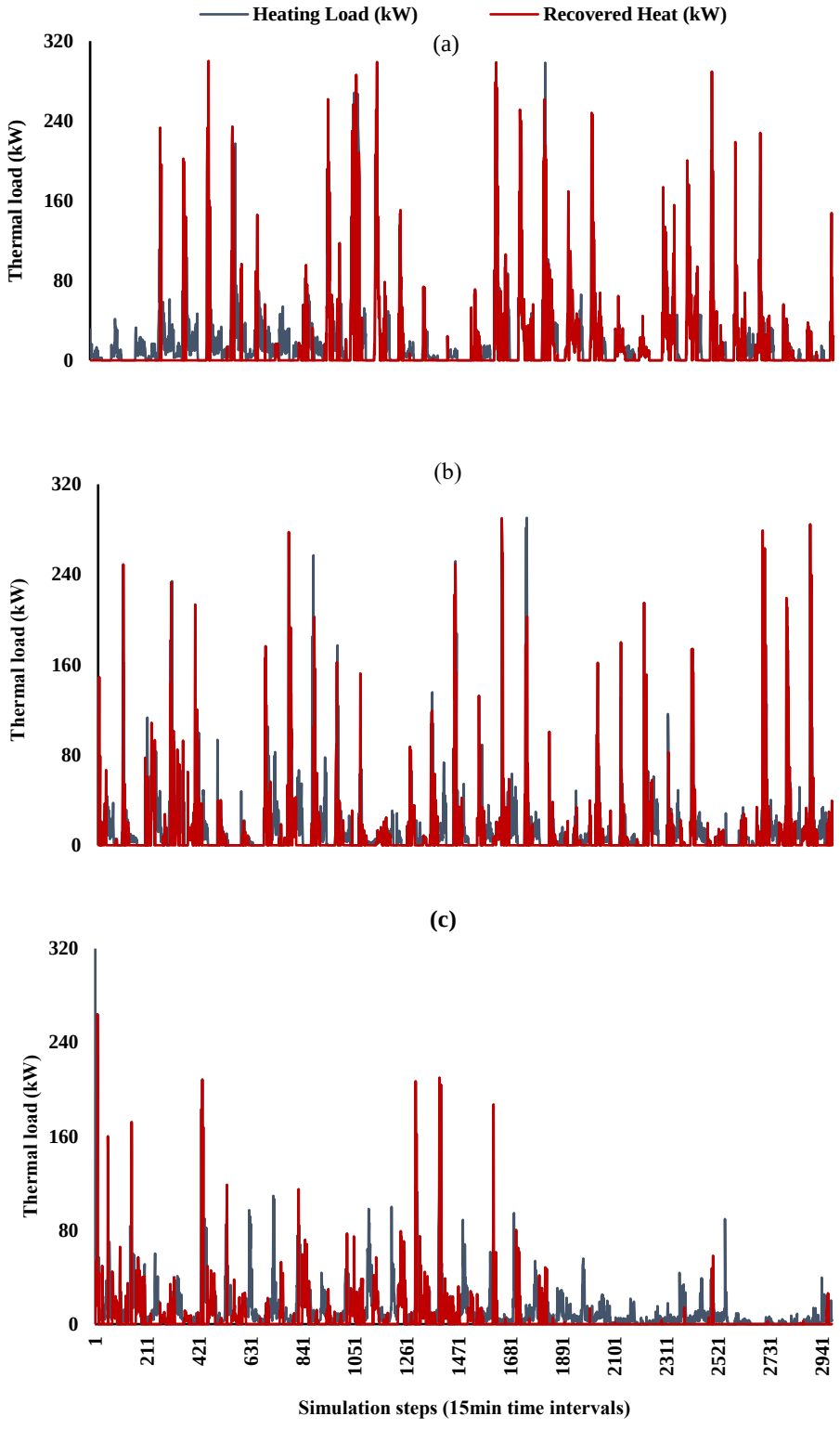

Fig. 3.7: Heating demand and recovered waste heat in (a) July, (b) August, and (c) September for PV/Batt/ICE in FEL/FTL PMS using multi-objective optimisation.

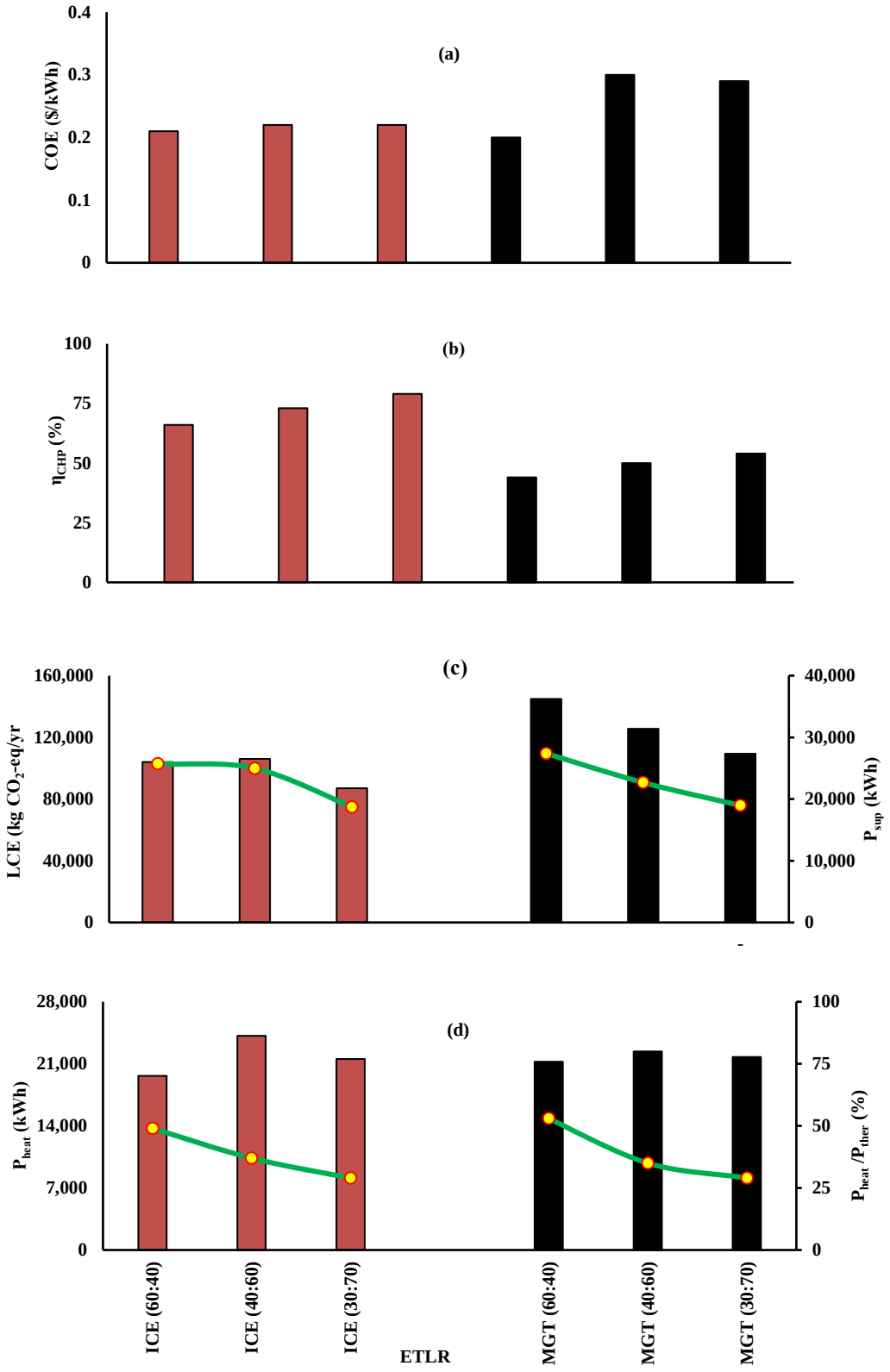

Fig. 3.8: The effects of Electric to Thermal Load Ratio (60:40, 40:60, and 30:70) on hybrid CHP systems sized using single objective optimisation in a PMS of the FEL/FTL type. Trend lines shown (Fig. 9c, Fig. 9d) should be read against the right vertical axis.

For hybrid systems operating with $P_{sup,min}$=9 kW in the FEL/FTL mode and meeting the same (combined) electrical and thermal demand, Figure 3.8 (c) shows that greater relative contributions of

thermal load (from ETLR=60:40 to ETLR=30:70) lead to lower level of LCE. The LCE for the PV/Batt/ICE systems vary from 104,010 $kgCO_2$-eq/yr to 87,005 $kgCO_2$-eq/yr when the ETLR changes from 60:40 to 30:70. For the PV/Batt/MGT systems, these vary from 144,900 $kgCO_2$-eq/yr to 109,380 $kgCO_2$-eq/yr when the ETLR changes from 60:40 to 30:70. This is because of the lower contribution of electric energy (P_{sup}) from the supplementary prime movers with bigger relative thermal contribution as shown in Figure 3.8 (c). The results also indicate that the PV/Batt/MGT produces more LCE ($kgCO_2$-eq/yr) than the PV/Batt/ICE for all operating conditions because of the MGT has the higher lifetime equivalent CO_2 emissions (Appendix, Table A3.5). Although both the PV/Batt/ICE and the PV/Batt/MGT operating on the FEL/FTL mode have comparable recovered waste heat from the supplementary prime movers, the ratio of this recovered waste heat (P_{heat}) to the total thermal demand (P_{ther}) decreases significantly where there is larger thermal load as shown in Figure 3.8 (d).

In relation to renewable penetration, there are insignificant effects of changing the relative load profiles. From Table 3.4 it is evident that the reliability of meeting load demand (LPSP) decreases as ETLR changes from 60:40 to 30:70. This is due to more likelihood at smaller ETLR of electric loads falling below $P_{sup,min}$ in any time interval. This can lead to lower reliability (LPSP) since the GA optimisation algorithm cannot increase (PV, battery) units beyond the constraints set in Table 3.2.

3.4 Conclusions

Most research published to date on hybrid energy systems only considers following (meeting) an electric load. The present study has examined hybrid CHP systems and the effects of load following strategies (electric only versus electric and heating demand). Additionally, the relative magnitude of the thermal load has also been varied when determining the sizing optimisations so as to analyse the impact on COE, η_{CHP}, LCE, and other performance indicators. Genetic Algorithms based on single objective optimisations are used for system sizing with Loss of Power Supply Probability (LPSP) as the reliability index. The results are also analysed and compared to that of sizing CHP systems using multi-objective optimisations under the same constraints. Although the techno-economic feasibility and optimisation techniques presented in this study are based on a set of data and constraints and not intend to highlight the merits or limitations of certain types of prime movers (energy system components), the outcomes can be summarised as:

- **COE:** In CHP systems, the use of (solely) electric load following (PMS based on FEL) or both electric and thermal load following (FEL/FTL) has only marginal effects on the Cost of Energy (COE). Greater thermal loads relative to the total load to be met (i.e. a smaller ETLR) appear to have a stronger effect on the COE in MGT-based CHP systems.
- **η_{CHP}:** The more notable effect of PMS type in CHP systems appears in relation to the Overall CHP Efficiency (η_{CHP}). PMS hybridisation (FEL/FTL) results in better performance in both

PV/Batt/ICE and PV/Batt/MGT systems, but particularly for ICE-based systems. A PMS based on FEL/FTL also allows for more thermal load to be satisfied using recovered waste heat (P_{heat}) when meeting the same load as a PMS based on FEL. In single objective optimisations, greater relative magnitudes of heating load demand also appear to lead to increased Overall CHP Efficiencies, with the degree of influence varying between ICE- and MGT-based CHP systems.

- **LCE:** Although using a PMS which follows both electric and thermal loads (FEL/FTL) in CHP systems does not carry with it significant financial incentives based on COE, it does however improve system Life Cycle Emissions (LCE) compared to an electric (only) load following strategy (FEL). The use of hybrid PMS in CHP systems (FEL/FTL) also leads to fewer LCE in system sized using single objective optimisations when the relative contributions of the thermal load increases (ETLR reduced).
- **Single- versus multi-objective optimisations:** One of the biggest merits from sizing CHP systems using multi-objectives (COE, η_{CHP}), compared to only using single objective (COE) optimisation, is to increase the fraction of total thermal demand which can be satisfied by recovered waste heat (P_{heat}/P_{ther}).

Whilst this research has focused on a hybrid stand-alone Combined Power and Heating (CHP) system, further research is warranted into systems taking into consideration a cooling load as well as heating (CCHP systems) and the impact of variations in their hardware components on overall costs and performance indicators.

3.5 Chapter appendices

3.5.1 Data used for system design and optimisation

Table A3.5: Stand-alone hybridised CHP system components cost, lifetime and emissions aspects.

Components	**Description**	**Capital Cost ($)**	**Replacement Cost ($)**	**O&M Cost ($/yr)**	**Life time (yr)**	**LCE (kg CO_2-eq/kWh)**
PV module [4]	HS-PL135 (135 W)	310	310	0	25	0.05 [96]
ICE [97]	30 kW	10,500	10,500	260	10	0.88 [96]
MGT [98]	30 kW	75,300	75,300	1,880	10	1.16 [99]
Battery [78]	12 V, 200 Ah	419	419	11	10	0.03 [96]
Inverter [4]	1 kW	800	750	20	15	0 [96]
Charge controller [100]	1 kW	450	450	11	15	
Electric heater [101]	14.4 kW	1,160	1,160	28	5	
Heat exchanger [102]	Shell and Tube, 8 m^2	9,800	9,800	245	10	
Discount rate		10%				
Fuel cost	Diesel fuel	0.91 $/l				
	Natural gas	3.30 $/GJ				

3.5.2 Power management strategy

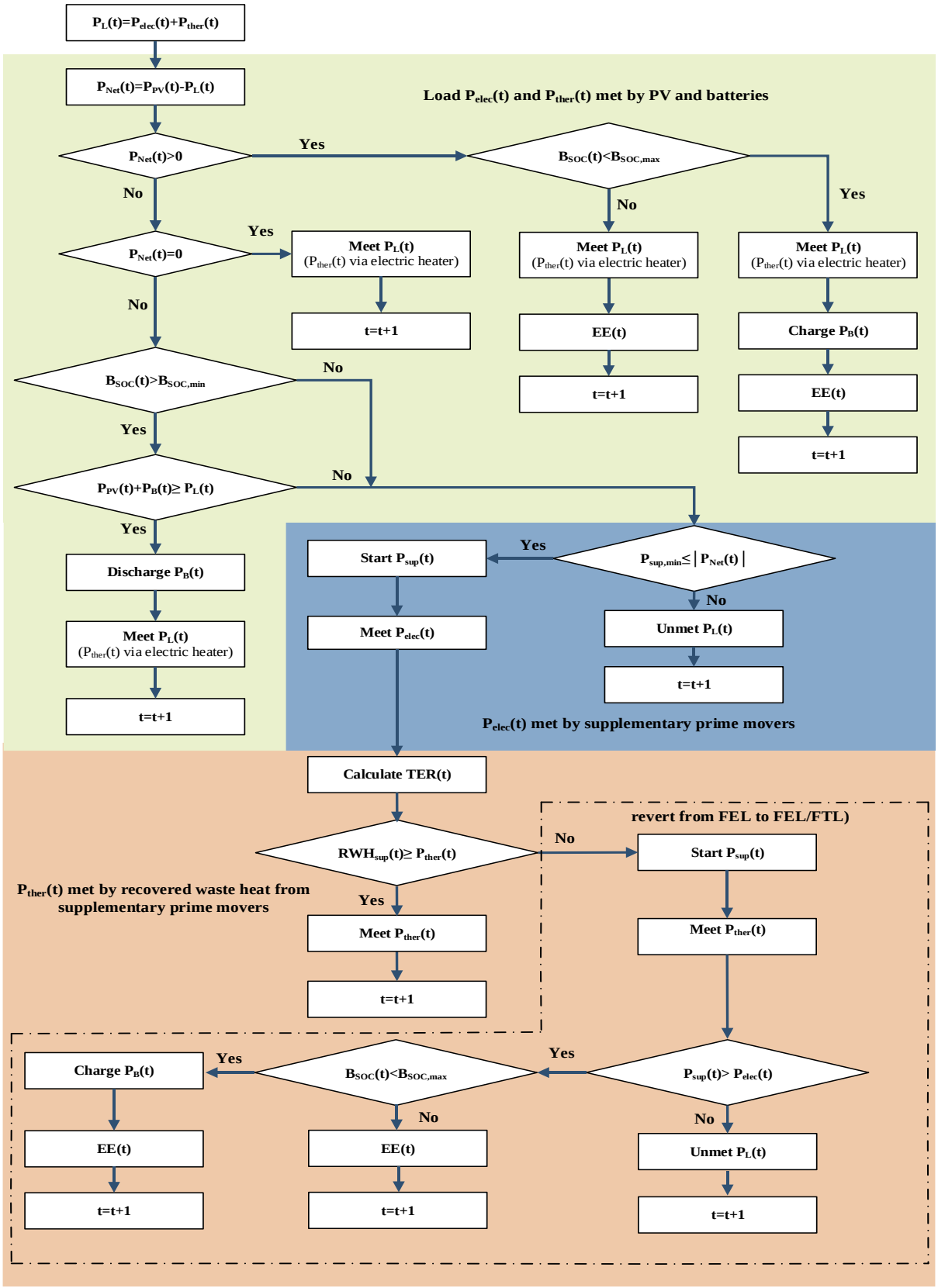

Fig. A3.9: Power Management Strategy (PMS) for meeting electricity (P_{elec} (t)) and heating demand (P_{ther} (t)).

3.5.3 Sensitivity analysis of GA population size

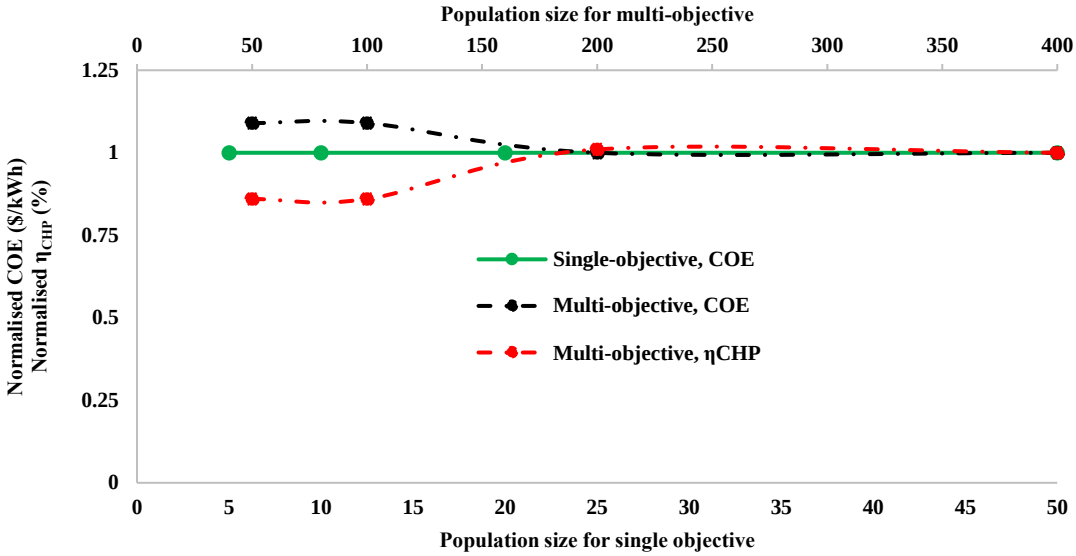

Fig. A3.10: Effect of population size on system optimisation for PV/Batt/ICE on FEL/FTL opearting strategy at ETLR=60:40.

3.5.4 PV modelling

The PV module's current based on the single diode equivalent circuit is defined by the following Equation [76, 77], whereby $I_L(t)$ is the light current, I_o is the diode reverse saturation current, $R_s(t)$ is the series resistance, R_{sh} is the shunt resistance, and *a(t)* is the modified ideality factor.

$$I_{PV}(t) = I_L(t) - I_o\left[exp\left(\frac{V + I_{PV}(t)R_s(t)}{a(t)}\right) - 1\right] - \frac{V + I_{PV}(t)R_s(t)}{R_{sh}} \quad (3.15)$$

The light current $I_L(t)$ of PV module can be calculated using the Equation 3.16, where *S(t)* is the solar irradiance, $T_{PV}(t)$ is the cell temperature, S_{ref} is the reference solar irradiation (1000 W/m^2), $I_{L,ref}$ is the short circuit current at the reference temperature (8.33 A), κ_t is the temperature coefficient of short circuit current (0.0005 /ºC), and T_{ref} is the reference temperature (25 º C) [71, 72].

$$I_L(t) = \left(\frac{S(t)}{S_{ref}}\right)\left(I_{L,ref} + \kappa_t\left(T_{PV}(t) - T_{ref}\right)\right) \quad (3.16)$$

Additionally shunt resistance R_{sh} is calculated by the Equation 3.17, where V_{mp} is the maximum power point voltage, I_{mp} is the maximum power point current, V_{oc} is the nominal open circuit voltage, and I_{sc} is the short circuit current.

$$R_{sh} = \frac{V_{mp}}{I_{sc} - I_{mp}} - \frac{V_{oc} - V_{mp}}{I_{mp}} \quad (3.17)$$

On the other hand, the cell temperature is determined by Equation 3.18 [103], where $T_{amb}(t)$ is the ambient temperature (ºC), and $W_s(t)$ is the wind speed (m/s):

$$T_{PV}(t) = 0.943 \times T_{amb}(t) + 0.028 \times S(t) - 1.528 \times W_s(t) + 4.3 \quad (3.18)$$

3.5.5 Battery modelling

The state of charge of lead acid battery at any time step (t) is the summation of state of charge at the previous time interval (t-1) and the additional charge over the current time step (t) and is calculated by the Equation 3.19, whereas the battery state of charge during discharging can be calculated by Equation 3.20 [59, 72], where C_b is the nominal capacity of the battery, $P_{PV}(t)$ is the power generation from PV module, $P_{sup}(t)$ is the power generation by supplementary prime movers, η_{inv} is the inverter efficiency, and Δt is the simulation time step (15min).

$$B_{SOC}(t) = B_{SOC}(t-1) + \frac{\left((P_{PV}(t)+P_{sup}(t)) - \frac{P_L(t)}{\eta_{inv}}\right) \times \eta_b \times \Delta t}{C_b} \quad (3.19)$$

$$B_{SOC}(t) = B_{SOC}(t-1) - \frac{\left(\frac{P_L(t)}{\eta_{inv}} - \left(P_{PV}(t)+P_{sup}(t)\right)\right) \times \eta_b \times \Delta t}{C_b} \quad (3.20)$$

In this study, the battery charging efficiency (η_b) is taken to be equal to the round trip efficiency of the battery and discharging efficiency (η_b) is set to 1 [57], and the battery state of charge is subjected to the following constraints at any time step (Δt):

$$B_{SOC,min} \leq B_{SOC}(t) \leq B_{SOC,max} \quad (3.21)$$

Chapter references

[1] Kabalci, E., *Design and analysis of a hybrid renewable energy plant with solar and wind power.* Energy Conversion and Management, 2013. **72**: p. 51-59.

[2] Baghdadi, F., et al., *Feasibility study and energy conversion analysis of stand-alone hybrid renewable energy system.* Energy Conversion and Management, 2015. **105**: p. 471-479.

[3] Hoque, S.N. and B.K. Das, *Analysis of Cost, Energy and Emission of Solar Home Systems in Bangladesh.* International Journal of Renewable Energy Research 2013. **3**(2): p. 347-352.

[4] Brka, A., Y.M. Al-Abdeli, and G. Kothapalli, *The interplay between renewables penetration, costing and emissions in the sizing of stand-alone hydrogen systems.* International Journal of Hydrogen Energy, 2015. **40**(1): p. 125-135.

[5] Clarke, D.P., Y.M. Al-Abdeli, and G. Kothapalli, *The impact of renewable energy intermittency on the operational characteristics of a stand-alone hydrogen generation system with on-site water production.* International Journal of Hydrogen Energy, 2013. **38**(28): p. 12253-12265.

[6] Courtecuisse, V., et al., *A methodology to design a fuzzy logic based supervision of Hybrid Renewable Energy Systems.* Mathematics and Computers in Simulation, 2010. **81**(2): p. 208-224.

[7] Brka, A., Y.M. Al-Abdeli, and G. Kothapalli, *Predictive power management strategies for stand-alone hydrogen systems: Operational impact.* International Journal of Hydrogen Energy, 2016. **41**(16): p. 6685-6698.

[8] Zubi, G., et al., *Concept development and techno-economic assessment for a solar home system using lithium-ion battery for developing regions to provide electricity for lighting and electronic devices.* Energy Conversion and Management, 2016. **122**: p. 439-448.

[9] Najmul Hoque, S. and B. Kumar Das, *Present status of solar home and photovoltaic micro utility systems in Bangladesh and recommendation for further expansion and upgrading for rural electrification.* Journal of Renewable and Sustainable Energy, 2013. **5**(4): p. 042301.

[10] Devrim, Y. and L. Bilir, *Performance investigation of a wind turbine–solar photovoltaic panels–fuel cell hybrid system installed at İncek region – Ankara, Turkey.* Energy Conversion and Management, 2016. **126**: p. 759-766.
[11] Bortolini, M., M. Gamberi, and A. Graziani, *Technical and economic design of photovoltaic and battery energy storage system.* Energy Conversion and Management, 2014. **86**: p. 81-92.
[12] Das, B.K., et al., *A techno-economic feasibility of a stand-alone hybrid power generation for remote area application in Bangladesh.* Energy, 2017. **134**: p. 775-788.
[13] Clarke, D.P., Y.M. Al-Abdeli, and G. Kothapalli, *The impact of using Particle Swarm Optimisation on the operational characteristics of a stand-alone hydrogen system with on-site water production.* International Journal of Hydrogen Energy, 2014. **39**(28): p. 15307-15319.
[14] Homayouni, F., R. Roshandel, and A.A. Hamidi, *Techno-economic and environmental analysis of an integrated standalone hybrid solar hydrogen system to supply CCHP loads of a greenhouse in Iran.* International Journal of Green Energy, 2017. **14**(3): p. 295-309.
[15] Fux, S.F., M.J. Benz, and L. Guzzella, *Economic and environmental aspects of the component sizing for a stand-alone building energy system: A case study.* Renewable Energy, 2013. **55**: p. 438-447.
[16] Lacko, R., et al., *Stand-alone renewable combined heat and power system with hydrogen technologies for household application.* Energy, 2014. **77**: p. 164-170.
[17] Angrisani, G., et al., *Performance assessment of cogeneration and trigeneration systems for small scale applications.* Energy Conversion and Management, 2016. **125**: p. 194-208.
[18] Akikur, R., et al., *Performance analysis of a co-generation system using solar energy and SOFC technology.* Energy Conversion and Management, 2014. **79**: p. 415-430.
[19] Çakir, U., K. Çomakli, and F. Yüksel, *The role of cogeneration systems in sustainability of energy.* Energy Conversion and Management, 2012. **63**: p. 196-202.
[20] Dorer, V. and A. Weber, *Energy and CO_2 emissions performance assessment of residential micro-cogeneration systems with dynamic whole-building simulation programs.* Energy Conversion and Management, 2009. **50**(3): p. 648-657.
[21] Liu, M., Y. Shi, and F. Fang, *Combined cooling, heating and power systems: A survey.* Renewable and Sustainable Energy Reviews, 2014. **35**: p. 1-22.
[22] Yao, E., et al., *Multi-objective optimization and exergoeconomic analysis of a combined cooling, heating and power based compressed air energy storage system.* Energy Conversion and Management, 2017. **138**: p. 199-209.
[23] Franco, A. and M. Versace, *Multi-objective optimization for the maximization of the operating share of cogeneration system in District Heating Network.* Energy Conversion and Management, 2017. **139**: p. 33-44.
[24] Zhang, X., et al., *Analysis of a feasible trigeneration system taking solar energy and biomass as co-feeds.* Energy Conversion and Management, 2016. **122**: p. 74-84.
[25] Yao, E., et al., *Thermo-economic optimization of a combined cooling, heating and power system based on small-scale compressed air energy storage.* Energy Conversion and Management, 2016. **118**: p. 377-386.
[26] Mojica, J.L., et al., *Optimal combined long-term facility design and short-term operational strategy for CHP capacity investments.* Energy, 2017. **118**: p. 97-115.
[27] Kaviri, A.G., et al., *Exergoenvironmental optimization of heat recovery steam generators in combined cycle power plant through energy and exergy analysis.* Energy conversion and management, 2013. **67**: p. 27-33.
[28] Khaljani, M., R.K. Saray, and K. Bahlouli, *Comprehensive analysis of energy, exergy and exergo-economic of cogeneration of heat and power in a combined gas turbine and organic Rankine cycle.* Energy Conversion and Management, 2015. **97**: p. 154-165.
[29] Abusoglu, A. and M. Kanoglu, *Exergetic and thermoeconomic analyses of diesel engine powered cogeneration: Part 1–Formulations.* Applied Thermal Engineering, 2009. **29**(2): p. 234-241.
[30] Rosen, M.A., M.N. Le, and I. Dincer, *Efficiency analysis of a cogeneration and district energy system.* Applied Thermal Engineering, 2005. **25**(1): p. 147-159.

[31] Balli, O., H. Aras, and A. Hepbasli, *Thermodynamic and thermoeconomic analyses of a trigeneration (TRIGEN) system with a gas–diesel engine: Part II–An application.* Energy Conversion and Management, 2010. **51**(11): p. 2260-2271.
[32] ASHRAE, P., *Heating and Cooling, ASHRAE Handbook-HVAC Systems and Equipment, SI ed.* American Society of Heating Refrigerating and Air-Conditioning Engineers (ASHRAE) Atlanta, GA, US, 2008.
[33] Khatri, K.K., et al., *Experimental investigation of CI engine operated micro-trigeneration system.* Applied Thermal Engineering, 2010. **30**(11): p. 1505-1509.
[34] Ahmadi, P., M.A. Rosen, and I. Dincer, *Greenhouse gas emission and exergo-environmental analyses of a trigeneration energy system.* International Journal of Greenhouse Gas Control, 2011. **5**(6): p. 1540-1549.
[35] Ghaebi, H., M. Saidi, and P. Ahmadi, *Exergoeconomic optimization of a trigeneration system for heating, cooling and power production purpose based on TRR method and using evolutionary algorithm.* Applied Thermal Engineering, 2012. **36**: p. 113-125.
[36] Caresana, F., et al., *Use of a test-bed to study the performance of micro gas turbines for cogeneration applications.* Applied Thermal Engineering, 2011. **31**(16): p. 3552-3558.
[37] Onovwiona, H.I., V.I. Ugursal, and A.S. Fung, *Modeling of internal combustion engine based cogeneration systems for residential applications.* Applied Thermal Engineering, 2007. **27**(5): p. 848-861.
[38] Kusakana, K. and H.J. Vermaak, *Hybrid diesel generator/renewable energy system performance modeling.* Renewable Energy, 2014. **67**: p. 97-102.
[39] Ismail, M., M. Moghavvemi, and T. Mahlia, *Genetic algorithm based optimization on modeling and design of hybrid renewable energy systems.* Energy Conversion and Management, 2014. **85**: p. 120-130.
[40] Abdollahi, G. and H. Sayyaadi, *Application of the multi-objective optimization and risk analysis for the sizing of a residential small-scale CCHP system.* Energy and Buildings, 2013. **60**: p. 330-344.
[41] Wang, J.-J., Y.-Y. Jing, and C.-F. Zhang, *Optimization of capacity and operation for CCHP system by genetic algorithm.* Applied Energy, 2010. **87**(4): p. 1325-1335.
[42] Ahmadi, P., et al., *Multi-objective optimization of a combined heat and power (CHP) system for heating purpose in a paper mill using evolutionary algorithm.* International Journal of Energy Research, 2012. **36**(1): p. 46-63.
[43] Borji, M., et al., *Parametric analysis and Pareto optimization of an integrated autothermal biomass gasification, solid oxide fuel cell and micro gas turbine CHP system.* International Journal of Hydrogen Energy, 2015. **40**(41): p. 14202-14223.
[44] Pirkandi, J., et al., *Simulation and multi-objective optimization of a combined heat and power (CHP) system integrated with low-energy buildings.* Journal of Building Engineering, 2016. **5**: p. 13-23.
[45] Mohammadi-Ivatloo, B., M. Moradi-Dalvand, and A. Rabiee, *Combined heat and power economic dispatch problem solution using particle swarm optimization with time varying acceleration coefficients.* Electric Power Systems Research, 2013. **95**: p. 9-18.
[46] Moradi, M.H., et al., *An energy management system (EMS) strategy for combined heat and power (CHP) systems based on a hybrid optimization method employing fuzzy programming.* Energy, 2013. **49**: p. 86-101.
[47] Wang, J., et al., *Particle swarm optimization for redundant building cooling heating and power system.* Applied Energy, 2010. **87**(12): p. 3668-3679.
[48] Clarke, D.P., Y.M. Al-Abdeli, and G. Kothapalli, *Multi-objective optimisation of renewable hybrid energy systems with desalination.* Energy, 2015. **88**: p. 457-468.
[49] Seijo, S., et al., *Modeling and multi-objective optimization of a complex CHP process.* Applied Energy, 2016. **161**: p. 309-319.
[50] Ebrahimi, M. and A. Keshavarz, *Sizing the prime mover of a residential micro-combined cooling heating and power (CCHP) system by multi-criteria sizing method for different climates.* Energy, 2013. **54**: p. 291-301.

[51] Hajabdollahi, H., A. Ganjehkaviri, and M.N.M. Jaafar, *Assessment of new operational strategy in optimization of CCHP plant for different climates using evolutionary algorithms.* Applied Thermal Engineering, 2015. **75**: p. 468-480.
[52] Mago, P.J. and A.K. Hueffed, *Evaluation of a turbine driven CCHP system for large office buildings under different operating strategies.* Energy and Buildings, 2010. **42**(10): p. 1628-1636.
[53] Mostofi, M., A. Nosrat, and J.M. Pearce, *Institutional scale operational symbiosis of photovoltaic and cogeneration energy systems.* International Journal of Environmental Science & Technology, 2011. **8**(1): p. 31-44.
[54] Brandoni, C. and M. Renzi, *Optimal sizing of hybrid solar micro-CHP systems for the household sector.* Applied Thermal Engineering, 2015. **75**: p. 896-907.
[55] Basrawi, F., T. Yamada, and S.y. Obara, *Economic and environmental based operation strategies of a hybrid photovoltaic–microgas turbine trigeneration system.* Applied Energy, 2014. **121**: p. 174-183.
[56] Borowy, B.S. and Z.M. Salameh, *Methodology for optimally sizing the combination of a battery bank and PV array in a wind/PV hybrid system.* Energy Conversion, IEEE Transactions on, 1996. **11**(2): p. 367-375.
[57] Yang, H., et al., *Optimal sizing method for stand-alone hybrid solar–wind system with LPSP technology by using genetic algorithm.* Solar Energy, 2008. **82**(4): p. 354-367.
[58] Belmili, H., et al., *Sizing stand-alone photovoltaic–wind hybrid system: Techno-economic analysis and optimization.* Renewable and Sustainable Energy Reviews, 2014. **30**: p. 821-832.
[59] Nafeh, A.E.-S.A., *Optimal economical sizing of a PV-wind hybrid energy system using genetic algorithm.* International Journal of Green Energy, 2011. **8**(1): p. 25-43.
[60] Cho, H., et al., *Evaluation of CCHP systems performance based on operational cost, primary energy consumption, and carbon dioxide emission by utilizing an optimal operation scheme.* Applied Energy, 2009. **86**(12): p. 2540-2549.
[61] Pfeifer, A., et al., *Economic feasibility of CHP facilities fueled by biomass from unused agriculture land: Case of Croatia.* Energy Conversion and Management, 2016. **125**: p. 222-229.
[62] Daghigh, R. and A. Shafieian, *An investigation of heat recovery of submarine diesel engines for combined cooling, heating and power systems.* Energy Conversion and Management, 2016. **108**: p. 50-59.
[63] Karellas, S. and K. Braimakis, *Energy–exergy analysis and economic investigation of a cogeneration and trigeneration ORC–VCC hybrid system utilizing biomass fuel and solar power.* Energy Conversion and Management, 2016. **107**: p. 103-113.
[64] Calise, F., et al., *Exergetic and exergoeconomic analysis of a novel hybrid solar–geothermal polygeneration system producing energy and water.* Energy Conversion and Management, 2016. **115**: p. 200-220.
[65] Das, B.K., Y.M. Al-Abdeli, and G. Kothapalli, *Optimisation of stand-alone hybrid energy systems supplemented by combustion-based prime movers.* Applied Energy, 2017. **196**: p. 18-33.
[66] Costa, A. and A. Fichera, *A mixed-integer linear programming (MILP) model for the evaluation of CHP system in the context of hospital structures.* Applied Thermal Engineering, 2014. **71**(2): p. 921-929.
[67] Ghadimi, P., S. Kara, and B. Kornfeld, *The optimal selection of on-site CHP systems through integrated sizing and operational strategy.* Applied Energy, 2014. **126**(Supplement C): p. 38-46.
[68] Ipsakis, D., et al., *Power management strategies for a stand-alone power system using renewable energy sources and hydrogen storage.* international journal of hydrogen energy, 2009. **34**(16): p. 7081-7095.
[69] Long, W.C., R. Luck, and P.J. Mago, *Uncertainty based operating strategy selection in combined heat and power systems.* Applied Thermal Engineering, 2016. **98**: p. 1013-1024.
[70] Smith, A.D. and P.J. Mago, *Effects of load-following operational methods on combined heat and power system efficiency.* Applied Energy, 2014. **115**(Supplement C): p. 337-351.

[71] *Solarshopnet. Technical data heckert HS-PL 135.*; Available from: 05.11.2016. http://www.solarshop-erope.net/solar-components/solarmodules/heckert_hs_pl-135_m_634.html.
[72] Clarke, D.P., Y.M. Al-Abdeli, and G. Kothapalli, *The effects of including intricacies in the modelling of a small-scale solar-PV reverse osmosis desalination system.* Desalination, 2013. **311**: p. 127-136.
[73] *BOM.South Australia weather and warnings* Available from: 12.12.2018. http://reg.bom.gov.au/climate/reg/oneminsolar/.
[74] Kashefi Kaviani, A., G.H. Riahy, and S.M. Kouhsari, *Optimal design of a reliable hydrogen-based stand-alone wind/PV generating system, considering component outages.* Renewable Energy, 2009. **34**(11): p. 2380-2390.
[75] Shabani, B., J. Andrews, and S. Watkins, *Energy and cost analysis of a solar-hydrogen combined heat and power system for remote power supply using a computer simulation.* Solar Energy, 2010. **84**(1): p. 144-155.
[76] Deshmukh, S.S. and R.F. Boehm, *Review of modeling details related to renewably powered hydrogen systems.* Renewable and Sustainable Energy Reviews, 2008. **12**(9): p. 2301-2330.
[77] Duffie, J.A. and W.A. Beckman, *Solar engineering of thermal processes*. Vol. 3. 1980: Wiley New York. p.750-760.
[78] *Lead-acid battery*. Available from: 20.11.2015. http://www.sunstonepower.com/upload/userfiles/files/ML12-200.pdf.
[79] Kim, H.-S., et al., *High-efficiency isolated bidirectional AC–DC converter for a DC distribution system.* IEEE Transactions on Power Electronics, 2013. **28**(4): p. 1642-1654.
[80] *Cummins South Pacific (12.10.2015). B3.3 Engine Data Sheet & Performance Curve (30kW FR 30002). Source: Personal Communication.*
[81] *Technical Reference : Capstone Model C30 Performance*. Available from: 15.11.2015. http://www.wmrc.edu/projects/bar-energy/manuals/c-30-manuals/410004_Model_C30_Performance.pdf.
[82] Infield, D., et al., *Review of wind/diesel strategies.* IEE Proceedings A (Physical Science, Measurement and Instrumentation, Management and Education, Reviews), 1983. **130**(9): p. 613-619.
[83] Hoevenaars, E.J. and C.A. Crawford, *Implications of temporal resolution for modeling renewables-based power systems.* Renewable Energy, 2012. **41**: p. 285-293.
[84] Darrow, K., et al., *Catalog of CHP technologies.* 2014.
[85] Wiehagen, J. and J. Sikora, *Performance comparison of residential hot water systems*, in *NAHB Research Center, Upper Marlboro, Maryland, NREL*. 2003.
[86] Aguilar, C., D. White, and D.L. Ryan, *Domestic water heating and water heater energy consumption in Canada.* Canadian Building Energy End-Use Data and Analysis Centre, 2005.
[87] Arun, P., R. Banerjee, and S. Bandyopadhyay, *Optimum sizing of battery-integrated diesel generator for remote electrification through design-space approach.* Energy, 2008. **33**(7): p. 1155-1168.
[88] Dufo-López, R., et al., *Multi-objective optimization minimizing cost and life cycle emissions of stand-alone PV–wind–diesel systems with batteries storage.* Applied Energy, 2011. **88**(11): p. 4033-4041.
[89] Srinivas, N. and K. Deb, *Muiltiobjective optimization using nondominated sorting in genetic algorithms.* Evolutionary Computation, 1994. **2**(3): p. 221-248.
[90] Wang, J., et al., *Multi-objective optimization of an organic Rankine cycle (ORC) for low grade waste heat recovery using evolutionary algorithm.* Energy Conversion and Management, 2013. **71**(Supplement C): p. 146-158.
[91] Tezer, T., R. Yaman, and G. Yaman, *Evaluation of approaches used for optimization of stand-alone hybrid renewable energy systems.* Renewable and Sustainable Energy Reviews, 2017. **73**: p. 840-853.
[92] Soltani, R., et al., *Multi-objective optimization of a solar-hybrid cogeneration cycle: application to CGAM problem.* Energy Conversion and Management, 2014. **81**: p. 60-71.

[93] Wang, J., et al., *Multi-objective optimization of an organic Rankine cycle (ORC) for low grade waste heat recovery using evolutionary algorithm.* Energy Conversion and Management, 2013. **71**: p. 146-158.
[94] Ahmadi, P., I. Dincer, and M.A. Rosen, *Thermodynamic modeling and multi-objective evolutionary-based optimization of a new multigeneration energy system.* Energy Conversion and Management, 2013. **76**: p. 282-300.
[95] Pierobon, L., et al., *Multi-objective optimization of organic Rankine cycles for waste heat recovery: Application in an offshore platform.* Energy, 2013. **58**: p. 538-549.
[96] Katsigiannis, Y., P. Georgilakis, and E. Karapidakis, *Multiobjective genetic algorithm solution to the optimum economic and environmental performance problem of small autonomous hybrid power systems with renewables.* Renewable Power Generation, IET, 2010. **4**(5): p. 404-419.
[97] *Central Maine Diesel*. Available from: 03.02.2016. http://www.centralmainediesel.com/cummins-generators.asp.
[98] *Combine Heat and Power Partnership. Catalog of CHP Technologies. U.S. Environmental Protection Agency. 2015. p.1-6,5.1-5.18*.
[99] Brown Jr, E.G., *Life Cycle Assessment Of Existing and Emerging Distributed Generation Technologies in California.* 2011.
[100] Ismail, M.S., M. Moghavvemi, and T.M.I. Mahlia, *Design of an optimized photovoltaic and microturbine hybrid power system for a remote small community: Case study of Palestine.* Energy Conversion and Management, 2013. **75**: p. 271-281.
[101] *Electric Water Heater*. Available from: 10.06.2017 https://1stchoicehotwater.com.au/product/rheem-heavy-duty-electric-613050g7-50l/.
[102] Lin, C.-S. *Capture of heat energy from diesel engine exhaust*. 2008; Available from: 10.02.2017 https://www.osti.gov/scitech/servlets/purl/963351.
[103] Tamizh Mani, G., et al. *Photovoltaic module thermal/wind performance: long-term monitoring and model development for energy rating*. in *Proc.NCPV and solar program review meeting, 2003. p. 936-939*.

Chapter 4: Effect of Load Following Strategies, Hardware, and Thermal Load Distribution on Stand-alone Hybrid CCHP Systems[4]

This chapter investigates the effects of two types of supplementary prime movers (internal combustion engines and micro gas turbines) when integrated with photovoltaic modules into hybrid energy systems (PV/Batt/ICE, PV/Batt/MGT). All systems analysed meet highly dynamic electric, heating, and cooling demands to a specified reliability (Loss of Power Supply Probability). The effects of adding an absorption chiller, thereby fundamentally transforming the systems from Combined Heat and Power to Combined Cooling, Heating, and Power is studied. This is done in the context of two different load following strategies (Following Electric to Thermal Load–FEL/FTL vs Following Electric Load–FEL). A Multi-objective Genetic Algorithm (GA) is implemented to optimise these systems based on both Cost of Energy and overall efficiency, the consequential outcomes of the simulations are also reported in terms of several key operational indicators. In this chapter, RQ 3 is addressed where optimised stand-alone CCHP system is investigated the effects of hardware, load characteristics, and power management strategies on the COE and energy efficiency.

4.1 Introduction

Combined Cooling, Heating, and Power (CCHP) systems utilise the waste heat from prime movers to satisfy cooling loads whilst also meeting heating and power demands. The merits of trigeneration include potentially improving overall system efficiency and reducing environmental emissions, and hence these systems have attracted attention globally [1]. Although CCHP systems are featured in large scale commercial and industrial applications (>1 MW), small–medium scale CCHP systems (<1 MW) are considered for remote communities, hospitals, and households especially where grid electricity is not readily available. In CCHP technologies, which integrate combustion–based prime movers, a proportion of the waste heat in the flue gases, 30 % of fuel input energy in Internal Combustion Engines (ICEs) or 66–73 % of fuel input energy in Micro Gas Turbines (MGTs), is recovered. Alternatively up to 30 % of the fuel energy input may be recovered from the water jacket in ICEs [2]. When larger scale trigeneration systems are connected to a national grid [3], any deficit of heating and cooling load can be met by a boiler (either electric or combustion driven) as well as electric chiller, respectively. On the other hand, in relation to small scale stand-alone hybridised CCHP systems, limited research is available in the literature [4, 5], particularly if these systems are hybridized by the addition of renewables. Hybridisation of CCHP applications is beneficial in three ways. Firstly, integrating renewable sources

[4] This chapter has been published as a full research paper.
Das, B.K., Y.M. Al-Abdeli, Kothapalli, G., **Applied Energy**, 2018. 220: p. 735-753.
Whilst efforts were made to retain original content of the article, minor changes such as number formats and font size style were implemented in order to maintain consistency in the formatting style of the thesis.

reduces reliance on fossil fuels; secondly, capturing the waste heat from supplementary prime movers substantially improves the overall efficiency; and thirdly, the availability of supplementary prime movers (i.e. ICE, MGT) helps increase system reliability when insufficient renewable power exists. In this regard, integrating renewable energy (e.g. PV, wind, biomass etc.) with conventional sources (e.g. ICE, MGT etc) also reduces dependency on fossil fuels and has the potential to improve the overall system efficiency up to 90 % [6] by using waste heat from supplementary prime movers to meet heating and cooling load.

Prime movers such as Internal Combustion Engines, Micro Gas Turbines, gas turbines, steam turbines, Stirling engines, and high temperature fuel cells (FCs) are used extensively in CCHP applications [7-9]. However, where stand–alone hybrid energy systems are concerned, most of the research to date focuses on meeting electric (utility) the power demand only [10-13]. Although some studies use biomass [14], integrated solar collectors [15, 16] for meeting the heating and cooling demand, very little research has studied CCHP systems where PV with the supplementary prime movers is considered [17, 18]. In this context, Basrawi et al. [17] analysed a hybrid PV/MGT-based CCHP system with the economic (Net Present Value-NPV) and the environmental (CO_2, NOx, and CO) consideration. They used life cycle cost analysis to assess the economic performance and environmental impact from operational emissions for MGT. However, the system was not optimised using intelligent techniques and only considered an hourly averaged (single) day load profile (not a dynamic load profile). Their study also did not have any details of the power management strategy. In a recent study, Yousefi et al. [18] carried out multi-objective optimisation of a hybrid ICE/PV-T driven CCHP system using dynamic load profiles and hourly resolved solar irradiation data, but did not present their load meeting reliability or the PMS. Additionally, their research was not based on stand-alone systems which gives merit for the present study.

The choice of Power Management Strategies strongly affects the system performance in particular stand-alone hybridised system to meet the reliably energy demand [19]. For this reason, providing details of the PMS used is significant to help interpret energy system research. In this regard, Wang and Yang [20] proposed a solar energy (evacuated tube collector) and ICE based grid connected CCHP system to meet electricity, hot water, and space heating/cooling using a hybrid PMS. Kang et al. [21] also compared the four types of PMS in a CCHP system, namely Following Electric Load (FEL), Following Thermal Load (FTL), their hybridisation (FEL/FTL or FHL) and Maximum efficiency. They found following a PMS focussed on maximum electrical efficiency is more beneficial under certain considerations. Zheng et al. [22] introduced a novel operational strategy based on Minimum Distance (MD) and found this to be more flexible and adaptable compared to FEL, FTL, and FEL/FTL. Liu et al. [23] optimised the operational strategy for the CCHP system using Matrix modelling approach. However, these strategies other than FEL, FTL, and FEL/FTL have benefits for some specific criterion.

Table 4.1: Summary of studies on the optimisation of CCHP systems

System components	Stand-alone/ Grid-connected	Optimisation methods	No of objectives	Modelling parameters	Optimisation parameters
ICE+ PV/Solar collector+Fuel Cell+ HE+ Absorption chiller [4]	Stand-alone	PSO	Single	Minimization Net Present Cost (NPC)	-
ICE+HE+Heat Pump [24]	Stand-alone	TRNSYS	-	Overall efficiencies, potential for integration in buildings	-
PV+CPVT+ET [25]	Stand-alone /Grid-connected	GA	Multi	Relative Net Annual Benefit (RNAB) and exergy efficiency	Population size 100, number of generation 100, crossover probability 0.65, mutation probability 0.2
ICE+HE+ Absorption chiller [1]	Grid-connected	GA	Multi	Minimising energy cost, maximising energy-saving ratio	Population size 150, number of generation 400, crossover probability 0.9, mutation rate 0.1
MGT+HRSG+ Absorption chiller [26]	Grid-connected	GA	Multi	Exergy efficiency, levelised cost, environmental cost	Population size 500, number of generation 300, crossover probability 0.9, selection process tournament
ICE + PV/T [18]	Grid-connected	GA	Multi	Minimize Net Present Cost (NPC), maximize Primary Energy Saving (PES)	Population size 50, number of generation 100, crossover probability 0.7, mutation probability 0.30, selection process Roulette wheel
ICE+HRSG+ Absorption chiller [27]	Grid-connected	Multi-objective Linear Programming (MOLP)	Multi	Total energy costs, CO_2 emissions	-
ICE+PV/Solar collector+ HE+ Absorption chiller [28]	Grid-connected	GA	Single	Lifecycle environmental assessment	Population size 20, number of generation 100
ICE+Solar collectors+ HE+Absorption chiller [29]	Grid-connected	GA and PSO	Single	Actual Annual Benefit (AAB)	GA: Population size 50-150, number of generation 300, crossover probability 0.8-0.9, Mutation probability 0.025-0.045 PSO: Number of particles 50-150, Inertia weight factor 0.5-0.75, self-confidence factor 1.5-1.75, Swarm confidence factor 1.6-1.8
ICE+HE+ Absorption chiller [30]	Grid-connected	GA and PSO	Single	Relative Annual Benefit (NAB)	GA: Population size 50-150, crossover probability 0.8-0.9, Mutation probability 0.025-0.045 PSO: Number of particles 50-150, Inertia weight factor 0.5-0.75, self-confidence factor 1.5-1.75, Swarm confidence factor 1.6-1.8

In CCHP systems, energy efficiency as well as considerations of economic and environmental sustainability are major optimisation objectives. The system sizing and optimisation process becomes more complicated if it involves many design parameters. As a consequence, the number of simulations (iterations) and thus optimisation process requires more time to reach the most viable solution. In this regard, evolutionary algorithms such as Genetic Algorithm (GA) [31, 32], Particle Swarm Optimisation (PSO) [33, 34] are effective. In this regard, Wang et al. [35] using GA optimised the capacity and operation of a CCHP system based on economic and environmental (CO_2 emission) indicators. Yao et

al. [36] studied a CCHP system with a gas engine, heat exchangers, and ammonia-water absorption refrigeration systems coupled with a compressor air storage system. Their system was optimised by an evolutionary multi-objective algorithm based on the thermodynamic (i.e. maximised exergy efficiency) and economic objectives (i.e. minimise total specific cost). The optimised solutions found from their study had an overall exergy efficiency of 53.04 % at a cost of 0.20 $/kWh. However, their system was not hybridised CCHP nor were details of the PMS used to derive their analyses reported. Wang et al. [37] investigated multi-objective optimisation of CCHP system based on flat-plate solar collectors with thermal storage (for heating) and an organic Rankine cycle with an ejector refrigeration system (for power and cooling). However, the study did not provide the details of load demands as well as the PMS. In summary, from Table 4.1, it is evident that there is a lack of research in relation to the optimisation of stand-alone hybrid CCHP systems using multi–objectives. In this study not only sufficient details are given in relation to the power management strategies used but also highly resolved load data or basing the load meeting reliability on the three loads (electric, heating and cooling) are incorporated, rather than electric only.

Utilising waste heat and integrating renewable energy with prime movers can significantly reduce the Cost of Energy (COE, $/kWh) and Life Cycle Emissions (LCE, kg-eq CO_2/yr) compared to meeting power only. However, in relation to studying CCHP systems designed to meet specific electric and thermal loads (i.e. cooling, heating), Soheyli et al. [38] optimised a system which included PV modules, wind turbines, and Solid Oxide Fuel Cells (SOFCs) as prime movers. They used a co-constrained multi–objective particle swarm optimization (CC-MOPSO) algorithm considering annual total cost and CCHP system area as objective functions using both Following Electric Load (FEL) and Following Thermal Load (FTL) strategies. They found that a CCHP system is more effective in terms of fuel consumption and emissions reduction compared to separatly by using grid electricity for power and cooling as well as boiler for heating. Nevertheless, their system did not include any supplementary combustion–based prime movers for back–up and nor did they analyse the effects of different power management strategies to compare the system optimisations. Sanaye and Sarrafi [25] studied a grid connected CCHP system optimisation using NSGA-II (objective functions: relative annual benefit and exergy efficiency) equipped with PV, solar thermal, and evacuated tube to meet the power, heating, and cooling demand. Although the system used hourly load profiles, this was not stand-alone hybridised CCHP system as well as Power Management Strategies were not studied.

Justification for the present research is based on the fact that the aforementioned studies are mostly grid connected and used coarse time series (load profiles) for electrical power, heating, and cooling loads their optimisations. Although some of the earlier research works featured systems that were hybridised with renewable sources, none of them studied the load meeting reliability using well established indicators such as Loss of Power Supply Probability (LPSP). Additionally, details of the Power

Management Strategies (PMS) used were not available in many of these works. This makes it extremely challenging to contextualise the outcomes in relation to other conditions. In this context, the present study goes further keeping in mind the limitations discussed above and includes the following contributions:

- The CCHP system considered is not only entirely stand-alone and hybridised, but also supplemented by two types of prime movers (i.e. PV/Batt/ICE or PV/Batt/MGT) by using hardware performance characteristics. It does not consider auxiliary boilers to meet the heating (P_{heat} (t)) demand but uses waste heat and electrical plant equipment to meet heating (P_{heat} (t)), and cooling (P_{cool} (t)) load demands within a specific load reliability (LPSP, 0.01±0.005).
- Two types of PMS are tested to see the effects of using a Following Electric Load (FEL) versus both Following Electrical and Thermal Load (FEL/FTL). The intricate details of these are given.
- A multi-objective GA is used to simultaneously minimise the Cost of Energy (COE, $/kWh) and maximise the overall system efficiency (η_{CCHP}, %) and the Technique for Order Preference by Similarity to Ideal Solution (TOPSIS) [39] is applied to determine the final solution.
- The analyses are based on highly dynamic electric, heating, and cooling load profiles and meteorological data (15min temporal resolution) and the relative contributions of heating loads to cooling loads are varied for the same electric demand.
- The study also compares a CCHP system designed to meet an electric and heating load, with cooling met using electric and absorption chillers, with a CHP system meeting the same electric and heating load, but with cooling satisfied using electric chillers. This comparison therefore examines the impact of absorption chillers on the overall sizing and operational performance.

The analyses of both CHP and CCHP systems are reported using a magnitude of accepted indicators namely: CO_2, NO_x and LCE (kg-eq CO_2/yr), Duty Factor (DF), Recovered Waste Heat to Power (RWHP) generation, ratio of recovered waste to thermal demand, and Renewable Penetration (RP). As such, the simulations undertaken are based on comprehensive energy and cost analysis of stand–alone CCHP systems. The proposed small-scale hybridised CCHP system can be applied in the remote areas such as community hospitals, supermarkets, schools, offices, and small industry where grid connection is infeasible. However, the system needs to be experimentally validated and needs sufficient policy support for real world application in the remote community.

The present study is structured as follows: Section 2 describes the simulation methodology of different sub-systems and the optimisation; Section 3 analyses the effects of load following strategies and relative significance of heating to cooling load. The final section discusses the conclusions along with the future recommendations.

4.2 Methodology

Figure 4.1 shows a block diagram of the conceptual stand-alone hybrid CCHP system modelled in this paper. The renewably powered components within the design architecture consist of PV modules and a battery bank which are connected to a DC bus. Combustion–based supplementary prime movers in the form of multiple units of ICE or MGT along with the load demand (electric, heating, and cooling) are connected to the AC bus. The AC and DC bus exchange power through bi–directional converters. In this manner, the battery bank can be charged from both renewable sources (i.e. PV modules) as well as supplementary prime movers when power generation exceeds the load demand. One type of supplementary prime mover is considered in each simulated CCHP system, but with one or multiple units of ICEs (rated capacity 30 kW each) or similar capacity MGTs to supplement the base–line CCHP PV/Batt system. An exhaust heat recovery unit and absorption chiller are coupled with the prime movers to meet the heating (P_{heat} (t)) and cooling (P_{cool}(t)) demand, respectively. The simulations are undertaken using the performance characteristics of commercially available ICEs and MGTs [40, 41] with $P_{sup,min}$=30 % of rated power as used elsewhere [42, 43]. It should be noted that data for these polynomial fits appear as continuous trend lines and presented in an earlier work [44].

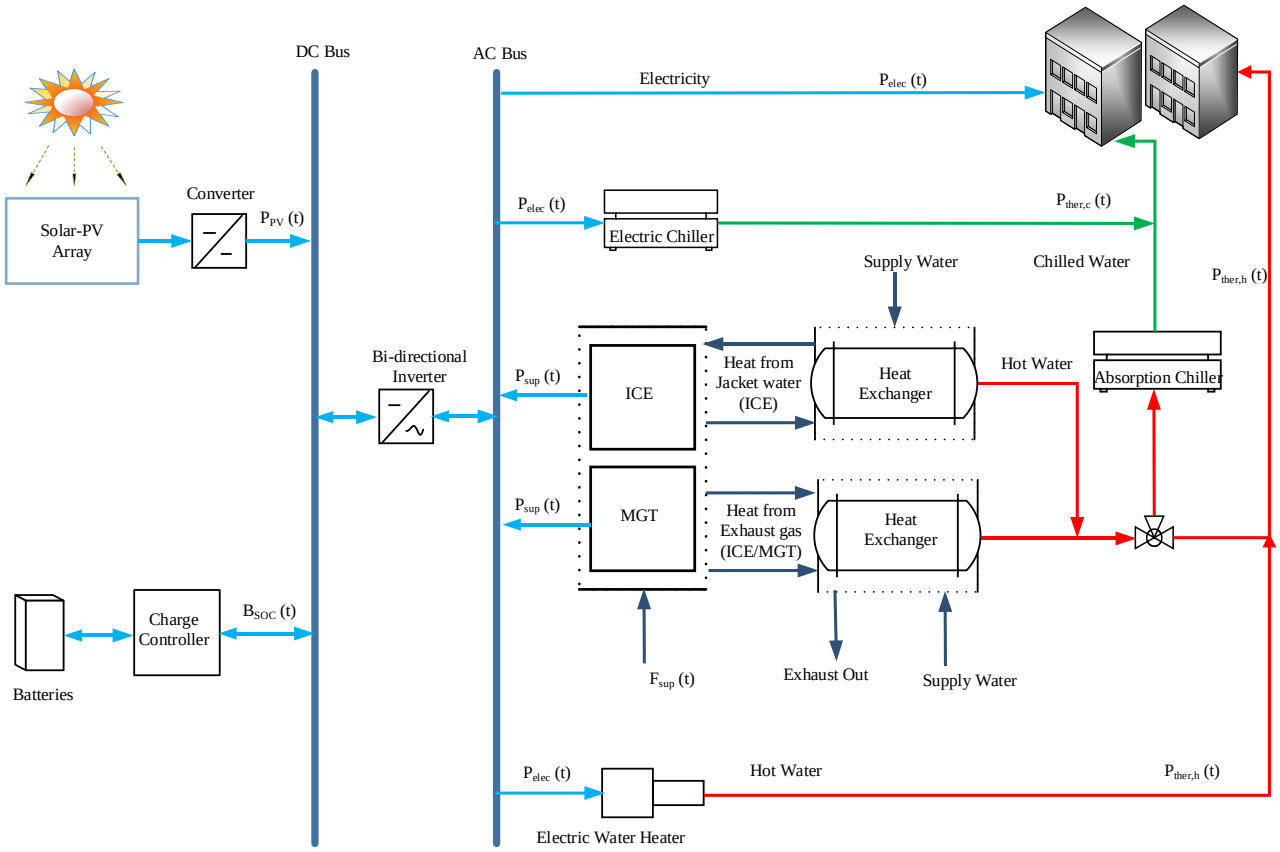

Fig.4.1: Schematic diagram of PV/Batt/ICE and PV/Batt/MGT-based hybrid CCHP system.

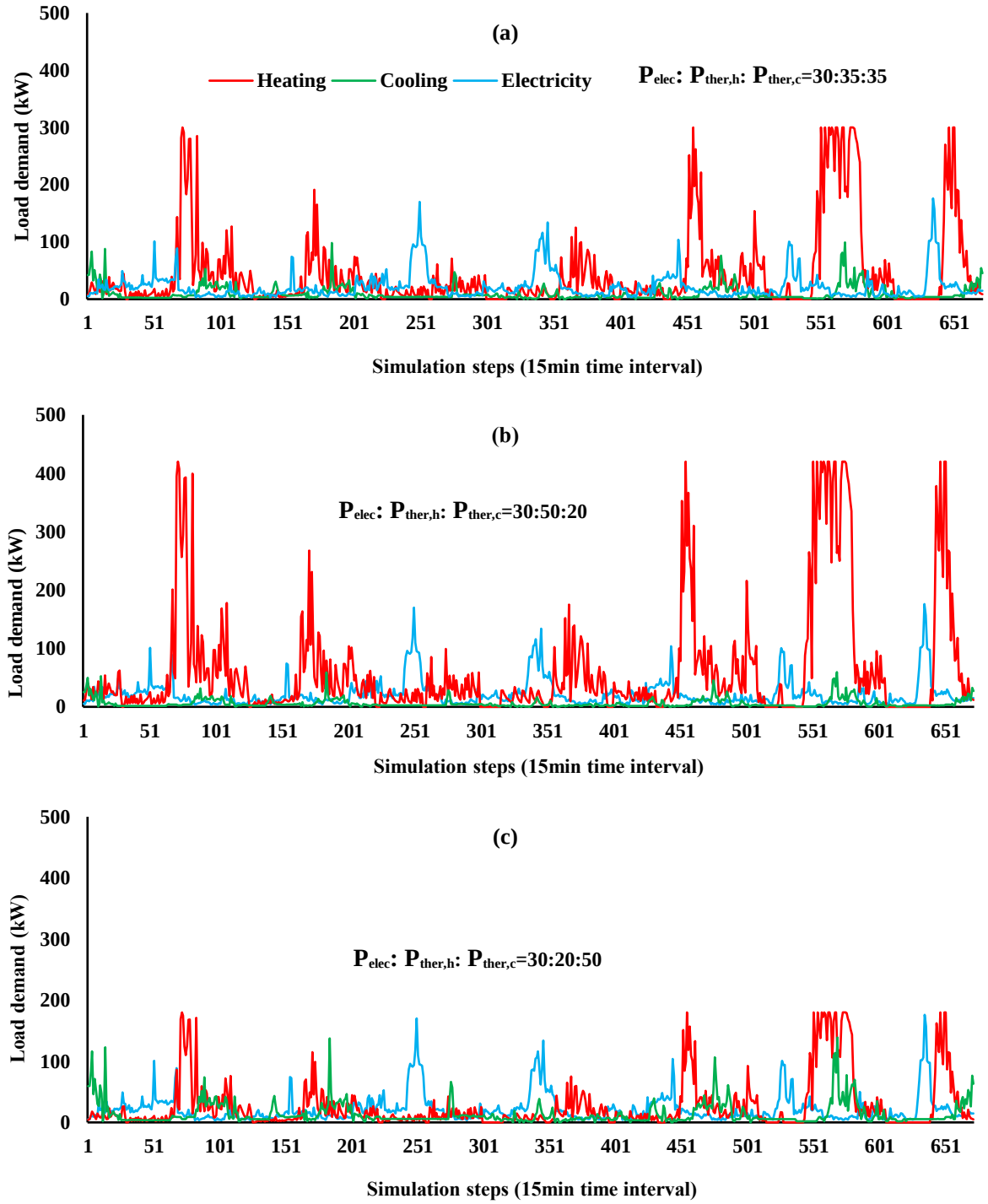

Fig. 4.2: Relative contributions of electric (P_{elec}), heating ($P_{ther,h}$), and cooling ($P_{ther,c}$) load towards total demand over one week in July. Profiles relate to three monthly (July to September) averages of P_{elec}, $P_{ther,h,}$ and $P_{ther,c.}$

Figure 4.2 (a) demonstrates the dynamically varying electric, heating, and cooling load demands which are kept in the ratio 30:35:35 when averaged over the three months (July to September). Additionally, Figures 4.2 (b-c) also depict the two scenarios of varying the relative contributions of electric, heating, and cooling (30:50:20; and 30:20:50) where heating and cooling are varied twice (70:30 and 30:70) within the thermal load. In this study, load profiles and meteorological data are assumed constant within the 15min time interval. In Figure 4.1 hardware components related to meeting the thermal demand

include two types of heat exchangers to recover waste heat from either the water jacket (ICE) or exhaust gases (ICE and MGT). Absorption chillers are also used to meet the cooling demand (using the waste heat).Where waste heat from supplementary prime movers is not sufficient to meet the heating or cooling load, an electric (resistance) water heater and electric chiller are used as back–up sources, respectively. Their power is then combined within the electric load.

4.2.1 PV model and meteorological data

In this work, mono crystalline silicon PV modules, each of 0.8 m^2 area and 135 W capacity are considered (Make: Heckert Solar, Model: HS-PL 135). The power generation from the array made up of multiple of these PV modules is determined using the performance characteristics curve [45]. A single diode equivalent circuit for developing the mathematical model of the PV module is considered [46, 47]. The performance characteristics of the PV modules are as follows: nominal open circuit voltage of 22.3 V; short circuit current of 7.95 A; maximum power point voltage of 18 V; maximum power point current of 7.48 A; reference solar irradiation of 1000 W/m^2; reference temperature of 25 ˚C; short circuit current at reference temperature of 8.33 V; and temperature coefficient of short circuit current of 0.0005/ ˚C [45, 48]. The effects of ambient temperature and the wind speed have also been integrated into the model, which is not commonly done in some previous studies [49, 50]. To facilitate using real meteorological data, a remote area of Western Australia (Broome: latitude of 17˚56'S, longitude of 122 ˚14'E) is selected.

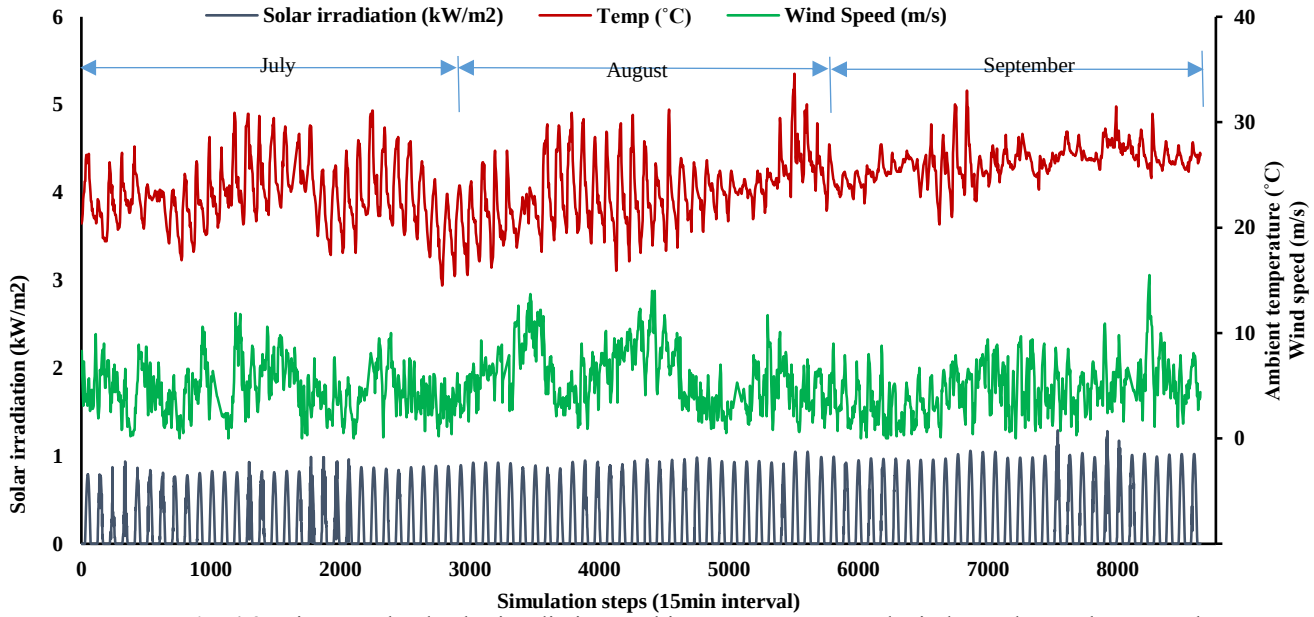

Fig. 4.3: Time resolved solar irradiation, ambient temperature, and wind speed over three months (July to September 2016).

Meteorological data (i.e. solar irradiation, wind speed, and ambient temperature) from the Australian Bureau of Meteorology [51] is used for a three month period as shown in Figure 4.3. The annual solar irradiation of the region is 2,290 kW/m^2 with a peak of 1.14 kW/m^2.

4.2.2 Battery modelling

Surplus energy generated by the PV modules and supplementary prime movers is stored into a lead acid battery bank. Each battery has a 2.4 kWh (200 Ah, 12 V) capacity with 85% round-trip efficiency [52]. The battery charge efficiency of 85 % (as round-trip efficiency) and battery discharge efficiency of 100 % have been taken while calculating the battery state of charge [53]. The role of the battery bank is to supply the required energy in the absence of any operational supplementary prime movers (not feasible due to their operating loads falling below the minimum starting threshold ($P_{sup,min}$) of the ICE or MGT). In this study, a minimum state of charge of 20 % ($B_{SOC,min}$=0.2$B_{SOC,max}$) is considered for the longevity of the battery bank [53]. A bi–directional inverter with 95 % efficiency [54] is connected between AC and DC buses. This acts both ways to convert DC voltage (to AC) from PV modules and AC voltage (to DC) from prime movers to charge the batteries. In the process of optimisation, battery charging and discharging models are adopted from the research [48, 49]. Battery lifetime can be expressed based on number of years or charge/discharge cycles. In the present study, the former method is used in agreement with other research [13].

4.2.3 Waste heat recovery and heat exchangers

In this study, shell and tube heat exchangers are considered for waste heat recovery from ICEs and MGTs. In the absence of published models for the ICE exhaust gas temperature or jacket water temperatures (and their flow rates) for similarly sized ICEs at part load condition, the approach taken in this study to calculate waste heat recovered relies on reported fuel consumption (at partial load) for naturally aspirated diesel engines [2]. In this manner the recovered waste from jacket water and exhaust gas can be determined by Equation 4.1 and Equation 4.2, respectively and the fuel energy consumed over each time step (Equation 4.1).

$$\dot{WH}_{JW\_ICE}(t) = 0.000008 \times P_{ICE}^2(t) + 0.7503 \times P_{ICE}(t) + 2.4757 \quad (4.1)$$

$$\dot{WH}_{Exh\_ICE}(t) = 0.000001 \times P_{ICE}^2(t) + 0.6573 \times P_{ICE}(t) - 0.314 \quad (4.2)$$

In Following Hybrid Load (FEL/FTL) demand where a Power Management Strategy (PMS) needs to operate based on both the FEL and the FTL. In this regard, FTL strategy to run based on the thermal demand. The relationship between the total recovered waste ($\dot{WH}_{ICE}(t)$) and at partial loads can then be determined by Equation 4.3.

$$P_{ICE}(t) = -0.000002 \times \dot{WH}_{ICE}^2(t) + 0.7104 \times \dot{WH}_{ICE}(t) - 1.5246 \quad (4.3)$$

However, the heat recovered system is integrated for the MGT system with the engine. A simple schematic diagram for exhaust heat exchanger and jacket water heat exchanger are shown in Figures 4.4 (a) and 4.4 (b), respectively. The exhaust gas heat exchanger outlet temperature ($T_{HE,out}$) is considered as 423K to avoid corrosive effects of condensation in exhaust piping [41].

As for the MGT, exhaust gas mass flow rates (kg/h) and exhaust gas temperature (K) are used from operational data [41, 55]. These are dependent on the power supplied by the supplementary prime movers at any time interval and calculated for a single 30 kW MGT unit as follows:

$$\dot{M}_{Exh\_MGT}(t) = 1 \times 10^{-14} \times P_{MGT}^2(t) + 22.982 \times P_{MGT}(t) + 426.82 \quad (4.4)$$

$$T_{Exh\_MGT}(t) = -0.0048 \times P_{MGT}^2(t) + 3.0235 \times P_{MGT}(t) + 462.43 \quad (4.5)$$

The available heat energy recovered from the supplementary prime movers can be calculated from Equation 4.6, whereby $\dot{M}_{Exh\_MGT}(t)$ is the exhaust gas flow rate for the MGT. Additionally, $C_{pg}(t)$ is the specific heat of exhaust gas and is calculated using Equation 4.7 [56], where $T_{Exh\_MGT}(t)$, $T_{HE,out}$ are exhaust outlet temperature of MGT and heat exchanger outlet temperature, respectively.

$$\dot{WH}_{Exh\_MGT}(t) = \dot{M}_{Exh_{MGT}}(t) \times C_{pg}(t) \times \left(T_{Exh\_MGT}(t) - T_{HE,out}\right) \quad (4.6)$$

$$C_{pg}(t) = 0.991615 + \frac{6.99703 T_{Exh\_MGT}}{10^5} + \frac{2.71298 T^2{}_{Exh\_MGT}}{10^7} - \frac{1.22442 T^3{}_{Exh_{MGT}}}{10^{10}} \quad (4.7)$$

Using Equation 6, the recoverable waste heat based on partial load of MGT can be modelled by the following Equation:

$$\dot{WH}_{MGT}(t) = -0.000003 \times P_{MGT}^2(t) + 1.3056 \times P_{MGT}(t) - 1.0554 \quad (4.8)$$

However, in a PMS based on an FEL/FTL strategy in some instances, the supplementary prime movers need to operate based on the thermal demand requirements and hence the power generation in such cases can be calculated using the following Equation:

$$P_{MGT}(t) = 0.000002 \times \dot{WH}_{MGT}^2(t) + 0.7659 \times \dot{WH}_{MGT}(t) + 0.8122 \quad (4.9)$$

For both ICEs and MGTs, and by taking into account heat loss due to piping, the available exhaust heat energy is then calculated using Equation 4.10, whereby ζ is the pipe loss co-efficient (0.95) [17].

$$Q_{heat,avl}\,(t) = \zeta\, \dot{WH}_{sup}(t) \quad (4.10)$$

The actual available useful heat energy can be obtained from Equation 4.11, where ε is the effectiveness (0.8) of heat exchanger.

$$Q_{heat}\,(t) = \varepsilon Q_{heat,avl}\,(t) \quad (4.11)$$

4.2.4 Absorption chiller

The heat energy from a heat exchanger is first fed into the absorption chiller to meet the cooling load (chilled water in this study). LiBr-water and NH_3-water are two of the most commonly used working fluids as refrigerants; however, the COP for LiBr-water is higher than NH_3-water shown in Table 4.2. In this study, a single-effect hot water (inlet temperature to generator section at 358 K shown in Figure 4.4 (c)) driven absorption chiller with LiBr-water as the working fluid is integrated into the simulation. Chilled water from the evaporator section is then supplied as a cooling load to the demand site. The system is however considered to operate as steady-state and so the transient behaviour of absorption chillers is not taken into account. In this context, there is no conclusive evidence in the literature to help

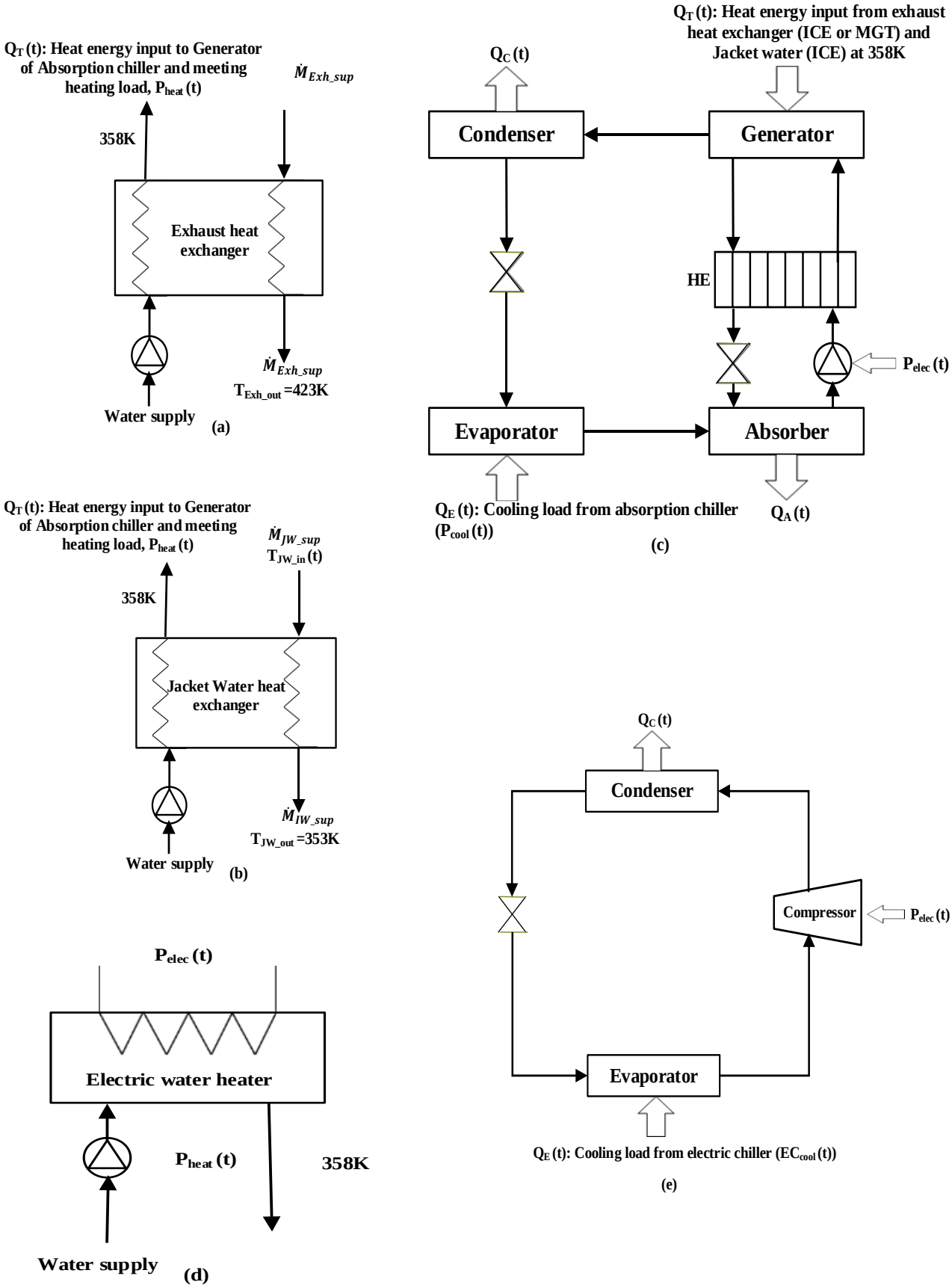

Fig. 4.4: Functional block diagram of (a) Exhaust heat exchanger, (b) Jacket water heat exchanger, (c) single effect H_2O-LiBr absorption chiller, (d) electric water heater, and (e) electric chiller.

establish the time required to reach steady-state in these devices [57]. Moreover, none of the studies reported in Table 4.1 included the transient behaviour of absorption chillers. The cooling load $P_{cool}(t)$ satisfied by the absorption chiller is calculated by Equation 4.12 [58], where $Q_T(t)$ is the heat energy input to the absorption chiller and COP_{AC} is the co-efficient of performance of the absorption chiller.

$$P_{cool}(t) = Q_T(t) \times COP_{AC} \tag{4.12}$$

4.2.5 Electric water heater

In both CHP and CCHP systems, electric (resistance) heaters are used to supply the necessary thermal load demand when this cannot be satisfied using ICEs or MGTs as shown in Figure 4.4(d). However, in this study, a combustion based boiler has not been considered to limit the operational emissions as the electric water heater is powered by the PV modules and battery bank. The electrical energy requirements can be measured from the overall process heater efficiency ($\eta_{wh,sys}$) which is calculated by the Equation 4.13, where $EWH_{elec}\ (t)$ is the electrical energy input to the heater and $EWH_{heat}(t)$ is the total outlet energy [59]. An efficiency, $\eta_{wh,sys} = 97\%$ has been considered for system modelling [60].

$$EWH_{elec}\ (t) = \frac{EWH_{heat}(t)}{\eta_{wh,sys}} \tag{4.13}$$

Table 4.2: Characteristics of absorption chillers [61].

	Single effect (LiBr-Water)	**Single effect (NH_3-Water)**	**Double effect (LiBr-Water)**	**Double effect (NH_3-Water)**	**Triple effect (LiBr-Water)**
Operating temperature (˚C)					
-Heating	80–110	120–150	120–150	120–150	200–230
-Cooling	5–10	<0	5–10	<0	5–10
Cooling capacity, kW (ton)	35 (10)–5,250 (1500)	10.5 (3)–3,500+ (1000+)	700 (200)–5,250 (1500)	Up to 3,500 (1000)	N/A
COP	>0.7	0.5	>1.2	0.8–1.2	1.4–1.5
Applications	Large water chiller	Commercial	Large water chiller	Experimental unit	Computer model and experimental unit

4.2.6 Electric chiller

The deficit of cooling load requirement for CCHP system can be met using electric chillers. A centrifugal type water chiller is considered in this study. Figure 4.4 (e) shows the simple schematic diagram of an electric chiller. The power requirement for chiller is obtained from the following Equation [1]:

$$EC_{elec}(t) = \frac{EC_{cool}(t)}{COP_{EC}} \tag{4.14}$$

where, COP_{EC} is the Coefficient of Performance of the electric chiller ($COP_{EC} = 3.50$ in this study) and $EC_{cool}(t)$ is the cooling load (heat removed by the chiller in kW).

4.2.7 Reliability index

In this study, Loss of Power Supply Probability (LPSP) a feasible measure of hybridised system performance, is considered as it is widely used with hybridised power systems meeting electric demand [10, 53, 62]. An LPSP of zero (0) means the total load demand is always satisfied, whereas an LPSP of unity (1) means the load is never satisfied. However, the concept of LPSP has not been considered in the context of CCHP systems [1, 17]. In this regard, LPSP is defined as the ratio of missed load (electric, thermal, and cooling, kWh) over a given period of time T, to the load demand over that time as calculated by Equation 4.15. Here $LPS(t)$ is the sum of the loss of electric load $LPS_{elec}(t)$, thermal load $LPS_{heat}(t)$ to equivalent electric load and cooling load $LPS_{cool}(t)$ to equivalent electric load at any time interval and $E_L(t)$ is the sum of the equivalent electric load demand ($E_L(t) = E_{elec}(t) + \frac{E_{heat}(t)}{\eta_{wh,sys}} + \frac{E_{cool}(t)}{COP_{EC}}$),over the period T. This system is assumed to meet electric, hot water as heating load, and cold water as cooling load in a stand-alone (off-grid) areas with specified LPSP (0.01±0.005).

$$LPSP = \frac{\sum_{t=1}^{T} LPS(t)}{\sum_{t=1}^{T} E_L(t)} \tag{4.15}$$

4.2.8 Power management strategy

A Power Management Strategy (PMS) to control the switching algorithm among the different components of the hybrid CCHP system is shown in Figure 4.5. In this study, a hybrid (FEL/FTL) PMS incorporating both Following Electric Load (FEL) and Following Thermal Load (FTL) has been considered. Additionally, a comparison has been made between FEL/FTL and FEL.

The PMS starts by first calculating the total load demand $P_L(t)$ at any time step. This is represented by the sum of electric (P_{elec} (t), heating ($P_{ther,\,h}$ (t)), and cooling ($P_{ther,\,c}$ (t)) load demand, corrected for the efficiency of electric heating and cooling devices, as given in Equation 4.16. The time-dependant term $P_L(t)$ will also be used (later) to calculate the Cost of Energy (COE).

$$P_L(t) = P_{elec}(t) + \frac{P_{ther,h}(t)}{\eta_{wh,sys}} + \frac{P_{ther,c}(t)}{COP_{EC}} \tag{4.16}$$

The demand is then compared with the power generated in that time interval from the PV module P_{PV} (t) to determine the net deficit or surplus as per Equation 4.17.

$$P_{Net}(t) = P_{PV}(t) - P_L(t) \tag{4.17}$$

Where renewables generate greater power than the load demand ($P_{Net}(t) > 0$) and batteries are not fully charged (B_{SOC} (t)<$B_{SOC,max}$), surplus renewable energy is used to charge the batteries until they reach a maximum state of charge (B_{SOC} (t)=$B_{SOC,max}$). Any remaining (surplus) available power after battery state of charge touches to its maximum level is considered excess energy EE (t) in that time

interval. As such, this excess energy that cannot be stored anymore is referred as dump energy. However, when P_{PV} (t)= P_L(t), it follows that $P_{Net}(t) = 0$ and the load is met (Meet P_L(t)). On the other hand, when renewable power cannot meet instantaneous demand ($P_{Net}(t) < 0$) it can be met by one of two options. If the battery bank power P_B (t) is above its minimum state of charge ($B_{SOC,min}$=0.2 $B_{SOC,max}$) and $P_{PV}(t) + P_B(t) \geq P_L(t)$, then batteries are discharged so as to completely meet the demand. If $P_{PV}(t) + P_B(t) < 0$, the load demand is met by supplementary prime movers operating at P_{sup}(t) if the demand is above the minimum starting threshold ($P_{sup,min}$=30 % of rated power). In any time interval if either of the above options are not available, then the demand is considered as unmet load in that time interval (Unmet P_L(t)). The above described parts of the algorithm only relate to meeting electric and thermal loads using PV, stored energy and electric heaters or chillers, whereby the electric demand is lower than the $P_{sup,min}$, electric heaters and electric chillers are used to satisfy thermal loads.

At any stage, when the deficit power ($P_{Net}(t) > 0$) is above the minimum starting threshold of the supplementary prime movers (i.e. ICEs or MGTs), the load demand (P_L(t)) is then met by running the ICE or MGT. In this stage waste heat generated from the ICE (exhaust and jacket water heat) and MGT (exhaust heat) is calculated using Equations 2, 3, and 11. This emulates the Following Electric Load (FEL) where the thermal demand can fully or partially be met by recovered waste heat and the rest of the demand is met by using electric heaters and electric chillers.

In following a FEL/FTL strategy, prime movers are first dispatched to meet all the electric demand (P_{elec}(t)), with recovered waste to meet the heating demand ($P_{ther,\,h}$(t)) via heat exchangers and absorption chiller to meet cooling demand ($P_{ther,\,c}$(t)). In this process, the PMS checks whether thermal demand is met fully or partially by the recovered waste heat generated on the way to meeting the electric demand. However, when the thermal demand ($P_{ther}(t) = P_{ther,h}(t) + \frac{P_{ther,c}(t)}{COP_{AC}}$) is much greater than the electric demand, the prime movers then run to meet the thermal load requirements as shown in dashed frame box in Figure 4.5. In this time interval after meeting the electric demand the additional electrical energy from the supplementary prime movers is used to charge the battery until the maximum state of charge ($B_{SOC,max}$), and rest of energy is considered as excess energy which is dumped.

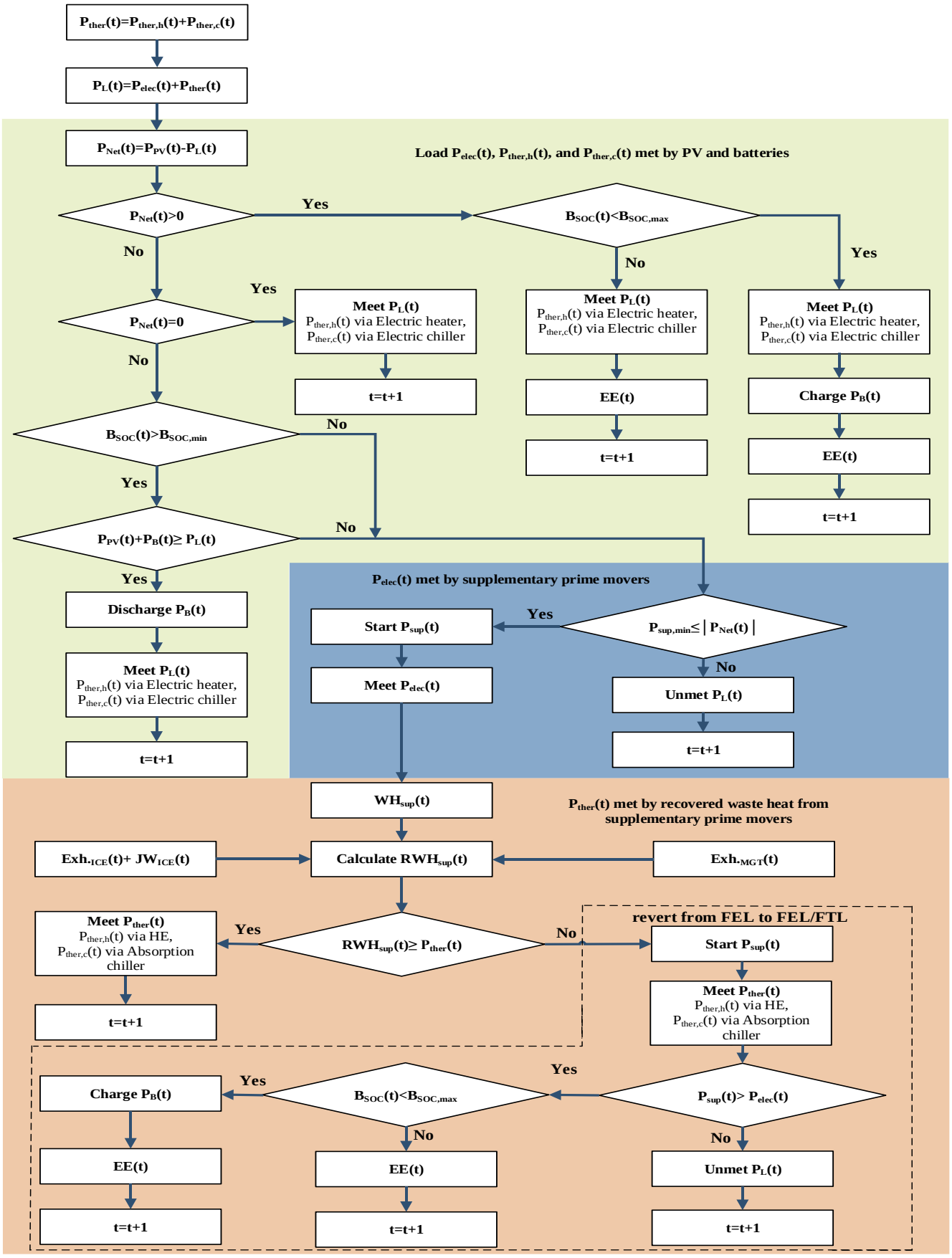

Fig. 4.5: Power Management Strategy (PMS) for meeting electricity (P_{elec} (t)), heating ($P_{ther,h}$(t)) and cooling demand ($P_{ther,c}$ (t)).

4.2.9 GA optimisation modelling

The hybridised CCHP system is optimised based on the multi-objective functions (COE, $/kWh and η_{CHP}, %) using MATLAB-based Genetic Algorithm (GA) technique. In this regard, the optimal sizing of hardware components is determined while meeting a specified LPSP (0.01±0.005). The decision variables in this study include the number of supplementary prime movers (N_{sup}), number of PV modules (N_{PV}), and the number of lead acid batteries (N_{batt}).

Objective functions: In this study, two objective functions: (i) Cost of Energy-COE ($/kWh) which is to be minimised and (ii) the overall CHP/CCHP efficiency, $\eta_{CHP/CCHP}$ (%) of supplementary prime movers is to be maximised in the process of optimisation.

Cost of Energy (COE): Cost of Energy is an important parameter for economic optimisation of hybridised system configurations which is calculated using Equation 4.18, where c_{A_cap} is the capital cost determined using Equation 4.19 and 4.20 [42].

$$Min\ COE = \frac{c_{A\_cap} + c_{A\_O\&M} + c_{A\_fuel}}{E_S} \tag{4.18}$$

$$c_{A\_cap} = \sum_i C_{cap,i} \times CRF_i \tag{4.19}$$

$$CRF = \frac{d(1+d)^n}{(1+d)^n - 1} \tag{4.20}$$

where $C_{cap,i}$ is the capital cost of *i*th system components, CRF_i is the capital recovery factor for *i*th components, *d* is the discount rate (10 % in this study), and *n* is the components life time. A project life time of 25 years in accordance with the maximum life time of PV module is considered. The $c_{A\_O\&M}$ is taken as 2.5 % of capital cost [42] and the c_{A_fuel} of the supplementary prime movers is determined using the fuel consumption over the years. In this regard, $E_S = (\sum P_L - \sum U_L) \times \Delta t$ is the annual equivalent electrical energy which is combined heating, cooling, and electric energy served and excludes the excess and the unmet load. Table A4.6 (Appendix) presents the relevant costs for the system components. However, the costs presented here do not include fabrication, installation, and labour costs. The cost for circulation pumps, piping, fabrication materials, and control instrumentations are also not included in this study. As the MGT has heat recovery module integrated with the power generating set, the cost associated with the heat exchanger has not been considered separately. The lifetime of heat exchanger is considered equal to the life span of supplementary prime movers.

Overall CHP/CCHP Efficiency ($\eta_{CHP/CCHP}$): The second objective function is considered as utilisation overall efficiency of supplementary prime movers which is to be maximised. In deriving this efficiency, the fuel consumption of prime movers needs to be considered.

For the ICEs used in the present simulations, the fuel energy (kW) can derived from engine operating characteristics [40]. Polynomial fits of these are described in Equation 4.21, whereby $P_{ICE}(t)$ is the ICE operating power of ICE in any time interval.

$$F_{ICE}(t) = -0.00001 \times P_{ICE}^2(t) + 2.7074 \times P_{ICE}(t) + 0.7194 \quad (4.21)$$

As for the MGTs, the fuel energy (kW) is similarly derived from polynomial fits based on operational characteristics [41, 55]. Equation 4.22 expresses this fuel usage whereby $P_{MGT}(t)$ is the MGT operating power at any time interval.

$$F_{MGT}(t) = 0.00003 \times P_{MGT}^2(t) + 3.8507 \times P_{MGT}(t) + 6.3341 \quad (4.22)$$

With the above in mind, Equation 4.23 can is used to find the overall CCHP system efficiency, with it also describing CHP efficiency if cooling load is not met via recovered waste heat.

$$Max\ \left(\eta_{CCHP}(t)\right) = \left((-)\frac{P_{sup}(t) + P_{heat}(t) + P_{cool}(t)}{F_{sup}(t)}\right) \quad (4.23)$$

where $P_{sup}(t)$ is the power generation from the supplementary prime movers (i.e. ICEs or MGTs), $P_{heat}(t)$ is the heating demand met using recovered waste heat via heat exchanger, $P_{cool}(t)$ is the cooling demand met using recovered waste heat via absorption chiller, and $F_{sup}(t)$ is the fuel energy input to the supplementary prime movers. The global optimisation toolbox using MATLAB minimises objective functions. In this regard, to maximise the objective function, minimise (-) $Max\ \eta_{CCHP}(t)$ as the point at which the minimisation of function occurs is the same point maximisation of $Max\ \eta_{CCHP}(t)$ takes place.

Constraints: The system sizing optimisation is subjected to the following constraints:

$$N_{sup,min} \leq N_{sup} \leq N_{sup,max} \quad (4.24)$$

$$N_{PV,min} \leq N_{PV} \leq N_{PV,max} \quad (4.25)$$

$$N_{bat,min} \leq N_{bat} \leq N_{bat,max} \quad (4.26)$$

$$B_{SOC,min} \leq B_{SOC} \leq B_{SOC,max} \quad (4.27)$$

$$P_{sup,min} \leq P_{sup} \leq P_{sup,max} \quad (4.28)$$

$$0.005 \leq LPSP \leq 0.015 \quad (4.29)$$

The lower and upper bounds in Equations 4.24 to 4.26 are directly entered into the optimisation toolbox. Lower bounds of $N_{sup,min} = 1$, $N_{PV,min} = 100$, $N_{bat,min} = 10$, and upper bounds of $N_{sup,max} = 10$, $N_{PV,max} = 1500$, $N_{bat,max} = 100$ are chosen for the optimisations. The constraints expressed by Equations 4.27-4.29 related are formulated in the PMS and reflected in the MATLAB M-file representing both objective functions and non-linear constraints

Consequential performance: The optimised system configurations are further simulated to analyse the consequential CO_2 and NO_x emissions over the period. In this study, the emissions factors for ICE are considered as 650 kgCO_2/MWh and 10 kgNO_x/MWh, whereas for the MGT these factors are 720

$kgCO_2$/MWh and 0.1 $kgNO_x$/MWh [61]. The study also estimates the Life Cycle Emissions (LCE, $kgCO_2$-eq/yr) which is calculated from Equation 4.30 and Table A4.6 (Appendix), where, β_i (kg CO_2-eq/kWh) is the lifetime equivalent CO_2 emissions of each hardware component (i) and E_L (kWh) is the amount of energy converted (or stored in batteries). It should be noted here that despite many works being undertaken into CCHP systems [1, 4, 18, 24, 26-29] as shown in Table 4.1, no details are presented in relation to the consequential LCE.

$$LCE = \sum_{i=1}^{N} \beta_i E_L \tag{4.30}$$

Additionally, the Recovered Waste Heat to Power Generation (RWHP) is defined in this study by Equation 4.31, where $P_{heat}(t)$ is the thermal load and $P_{cool}(t)$ is the cooling load met by the recoverable waste relative to the total (electric) power output (P_{sup} (t)) of the ICE or MGT over each time step.

$$RWHP = \frac{\sum P_{heat}(t) + \sum P_{cool}(t)}{\sum P_{sup}(t)} \tag{4.31}$$

The Duty Factor which is the amount of energy generation per start-stop of the supplementary prime movers calculated using Equation 4.32, where $E_{sup}(t)$ is the energy generation from the supplementary prime movers over the period of T and $N_{s/s}$ is the number of start-stop of prime movers over the same period.

$$DF = \frac{\sum_{t=1}^{T} E_{sup}(t)}{\sum_{t=1}^{T} N_{s/s}} \tag{4.32}$$

In this study, Renewable Penetration (RP) is also calculated which is the energy generated (useful, excludes dumped/excess PV energy) by the PV modules to meet the load demand (i.e. electric P_{elec} (t), thermal $P_{ther,h}$ (t), and cooling $P_{ther,c}$ (t).

Determination of final solution: In multi-objective optimisation, every solution in the Pareto front is an optimal solution, therefore a decision making process is necessary to find a single solution. There are several decision making methods to find the final single solution in multi-objective optimisation problems: Fuzzy membership function [63], LINMAP (Linear programming technique for Multidimensional Analysis of Preferences) [39], and TOPSIS (Technique for Order Preference by Similarity to Ideal Solution) [39]. Sayyaadi and Mehrabipour [39] used multi-objective optimisation and found the best results using the TOPSIS decision making process. In the present study, a TOPSIS decision making process is also applied to find the final optimal solution. As the dimension of various objective functions could be different (e.g. Overall Efficiency is non-dimensional, and COE is $/kWh); hence it is necessary to unify the dimensions and scales of all the objective functions. In this regard, an Euclidian non-dimensionalisation is used as shown in Equation 4.33, where the non-dimensionalised objective F_{ij}^{n} is used for both minimisation and maximisation problems [39].

$$F_{ij}^{n} = \frac{F_{ij}}{\sqrt{\sum_{i=1}^{m}(F_{ij})^2}} \quad (4.33)$$

In the TOPSIS method, the Euclidian distance of each solution on the Pareto front from the ideal solution, a solution which is optimised without satisfaction of other objectives is calculated as follows:

$$D_{i+} = \sqrt{\sum_{j=1}^{n}\left(F_{ij} - F_j^{ideal}\right)^2} \quad (4.34)$$

where *n* is the number of objective functions, *i* is the each solution on the Pareto front (i=1,2,3…….m), and F_j^{ideal} is the ideal solution for *j*th objective. The solution also needs to determine the distance from the non-ideal point (i.e. worst value of each objective in the solution space) using Equation 4.35.

$$D_{i-} = \sqrt{\sum_{j=1}^{n}\left(F_{ij} - F_j^{non-ideal}\right)^2} \quad (4.35)$$

In the process of achieving final solution a parameter Cl_i is defined as follows:

$$Cl_i = \frac{D_{i-}}{D_{i+} + D_{i-}} \quad (4.36)$$

In this method, one of the solutions on the Pareto frontier which maximises Cl_i is designated as the final solution as shown by Equation 4.37.

$$i_{Final} = i \in max(Cl_i) \quad (4.37)$$

In this context, Figures 4.6 (a) and (b) show the final solution of Pareto front for PV/Batt/ICE, and PV/Batt/MGT, respectively while operating on FEL/FTL type PMS. Although MATLAB toolbox gives the efficiency as negative values (so as to minimisation occurs at maximum negative value of the objective function), the data reported here 1-η_{CCHP} as shown in Figures 4.6 (a) and (b). The final solution is selected based on the shortest possible geometric distance from the ideal solution and the longest possible distance from the non–ideal solution. Table 4.3 shows the choice of GA parameters for the multi-objective optimisations. The detailed methodology and justification for selecting the GA population size, number of generation, and other parameters features in an earlier work [44]. The study uses a MATLAB optimisation toolbox to implement the multi-objective genetic algorithm. The decision variables include: number of PV modules, N_{PV}; number of lead acid batteries, N_{batt}; and number of supplementary prime movers, N_{sup}. A non-linear constraint function which is a representation of LPSP is written in one M-file. Another M-file of fitness functions (objective functions) is developed using the PMS and Equations 4.20, 4.23, and 4.27-4.29. Constraints related to bounds (upper and lower bound depicts in Equations 4.24 to 4.26) are directly entered into the toolbox.

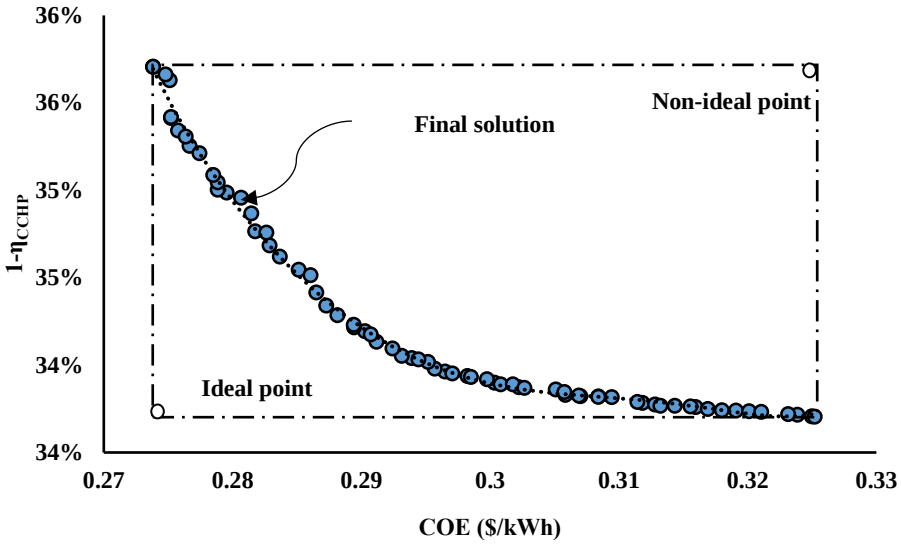

Fig. 4.6(a): Pareto Front for PV/Batt/ICE when operating FEL/FTL type PMS.

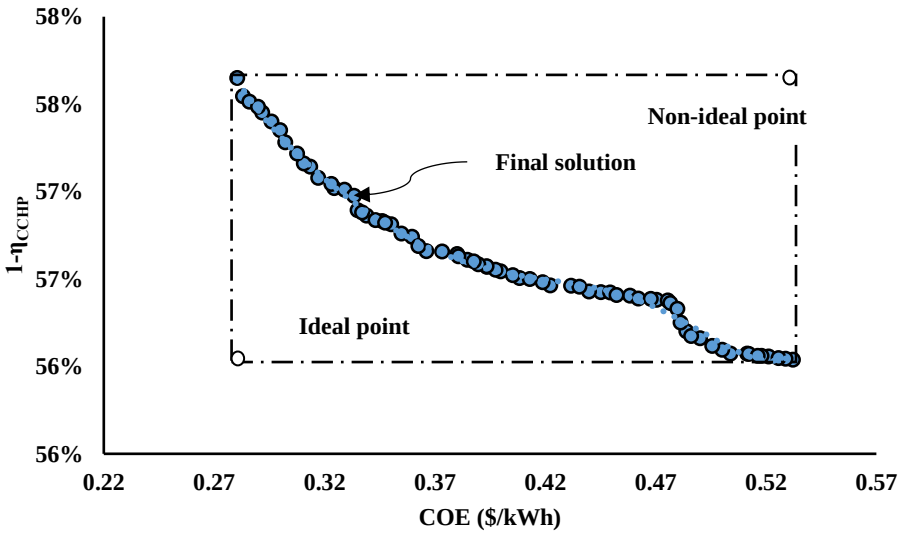

Fig. 4.6(b): Pareto Front for PV/Batt/MGT when operating FEL/FTL type PMS.

Table 4.3: Multi-objective genetic algorithm optimisation parameters.

Parameters	Value
Population size	200
Maximum number of generations	100
Crossover probability	0.8
Crossover function	Constraints dependant
Selection function	Tournament
Tournament size	2

4.3 Results and discussion

In this study, analyses are presented for the effects of different load following strategies (FEL/FTL vs FEL) while meeting an electric $P_{elec}(t)$, heating $P_{ther,h}(t)$, and cooling $P_{ther,c}(t)$ load. In the first part of this section, the effects of adding an absorption chiller to a CHP system, thus yielding CCHP, are compared to meeting the same cooling load (in CHP systems) via electric chillers. In the second part of this section, the sensitivity of the outcomes when using different ratios of heating and cooling demands against the same electric load, are examined. Throughout these analyses, results are reported not only in terms of the GA optimised functions (COE, \$/kWh; η_{CHP} or η_{CCHP}, %) but also consequential system performance expressed through operational CO_2, NO_x emissions (kg), Renewable Penetration (RP, %), and Duty Factor (DF, kWh/start-stop) are included. The effects of using different type supplementary prime movers (ICE or MGT) on these systems are also presented.

4.3.1 Effect of hardware and PMS (FEL vs FEL/FTL)

An Electric to Thermal Load Ratio (ETLR) of 30:70 is first considered, whereby almost equal heating (52,549 kWh) and cooling demands (53,781 kWh) apply alongside the need to meet an electric load (48,347 kWh). Systems compared operate on a FEL/FTL type PMS. In the CCHP configuration analysed, the cooling load is met by an absorption chiller (if supplementary prime movers operate) or by a back–up electric chiller (if prime movers do not run when loads are relatively low and do not meet the start-up criteria $P_{sup,min}$). With the CHP systems, cooling load is only met by an electric chiller. In both CHP and CCHP systems, the heat source is either recovered waste heat from the ICE (exhaust gas and water jacket) or MGT (exhaust gas). As such, the analysis which follows specifically addresses the question: how does adding absorption chillers affect stand–alone hybrid systems meeting three loads (P_{elec}, $P_{ther,\,h}$, $P_{ther,\,c}$)?

Cost of Energy (COE): In terms of the two objective functions which are optimised in each of the systems studied, the first (CCHP) and third column pairs (CHP mode which does not include an absorption chiller) in Figure 4.7 (a) shows that for both PV/Batt/ICE and PV/Batt/MGT systems all on the same PMS (FEL/FTL), the CHP mode has cost of energy reductions of around 11 % compared to the CCHP. This is because adding the absorption chiller to CCHP systems increases the annualised cost when meeting the same LPSP.

Efficiency ($\eta_{CHP/CCHP}$): Figure 4.7 (b) indicates that using an absorption chiller (FEL/FTL, CCHP) leads to some improvements in system efficiency over CHP in both PV/Batt/ICE and PV/Batt/MGT systems. However, these efficiency gains compared to CHP are negligible when CCHP systems operate on a simpler FEL type PMS (middle column pair). Therefore, adding absorption refrigeration systems under some Power Management Strategies (FEL) may not necessarily lead to the optimal efficiency

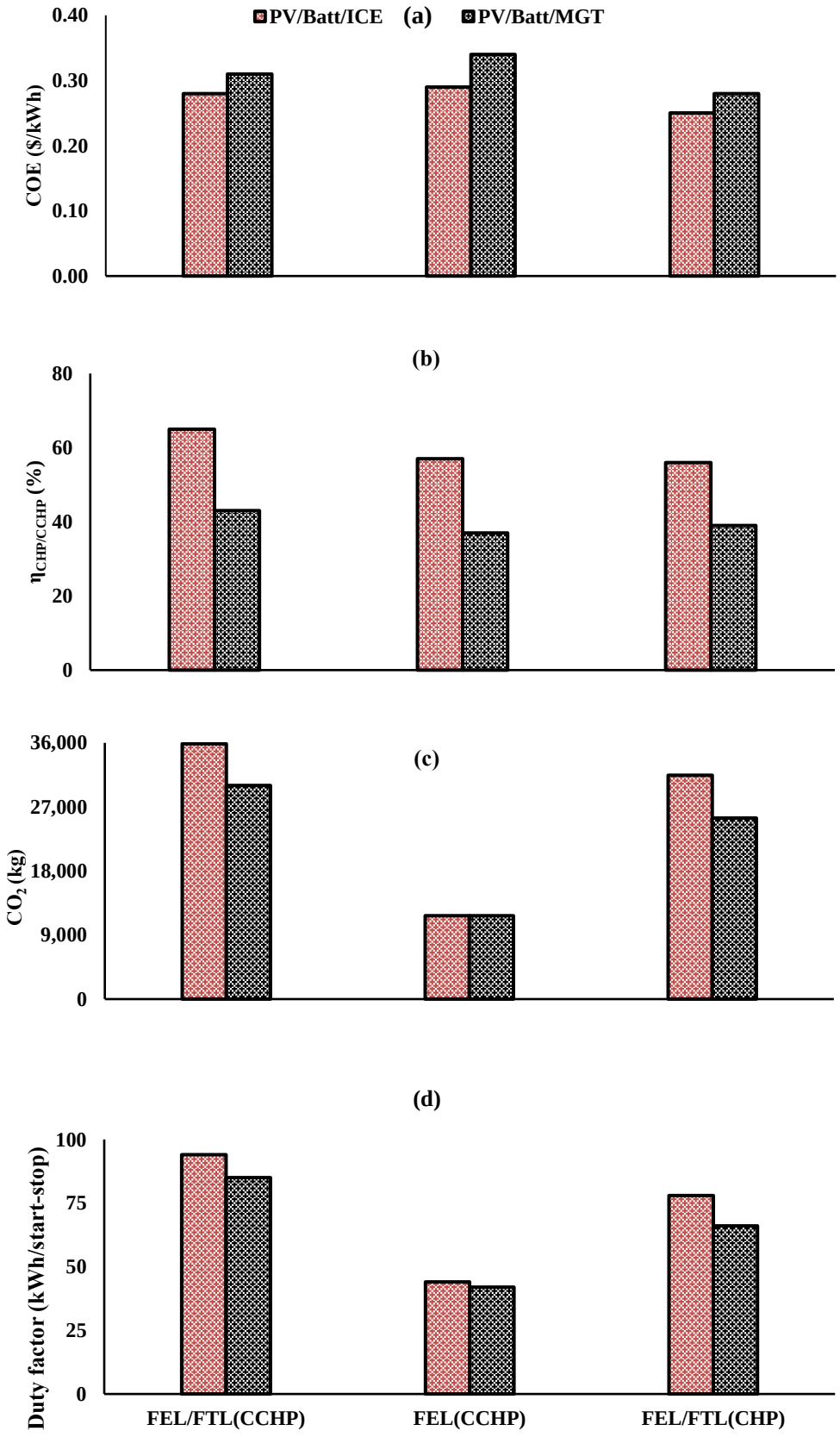

Fig. 4.7: The effects of load following strategy (FEL/FTL, FEL) on hybrid systems operating to meet load profiles with P_{elec}:P_{ther}=30:70. A comparison between CHP and CCHP configurations is shown for both PV/Batt/ICE and PV/Batt/MGT.

gains, whilst also potentially increasing COE in comparison to using other types of PMS (FEL/FTL) as shown from the data in Figure 4.7 (a).

Table 4.4: Summary results of multi-objective (COE, $/kWh and η_{CCHP}, %) optimisations for hybrid CHP/CCHP systems (load profile P_{elec}:P_{ther}=30:70, LPSP=0.01±0.005).

Characteristics	PV/Batt/ICE			PV/Batt/MGT		
	FEL/FTL (CCHP)	FEL (CCHP)	FEL/FTL (CHP)	FEL/FTL (CCHP)	FEL (CCHP)	FEL/FTL (CHP)
Number of solar panels, N_{PV}	501	1,390	737	952	1,485	1,195
Number of lead acid batteries, N_{batt}	62	82	23	76	78	22
Number of prime movers, N_{sup}	5	3	3	4	3	3
$LPSP_{comp}$	0.01	0.01	0.001	0.009	0.006	0
PV energy generated (kWh)	32,120	89,115	47,250	61,034	95,205	76,613
Renewable penetration, RP (%)	27	76	40	52	81	66
ICE/MGT energy, P_{sup} (kWh)	55,207	18,001	48,354	41,681	16,269	35,312
RWHP (%)	77	56	53	68	50	54
Unmet energy (kWh)	1,286	1,249	229	1,074	710	0
Fuel energy, F_{sup} (kWh)	149,960	49,064	131,550	164,280	65,332	139,740
Recovered waste heat to thermal demand (Q_T /P_{ther}, %)	57	19	50	38	15	33
Transient start-ups	590	410	621	491	391	534
LCE (kg CO_2-eq/yr)	208,210	91,358	184,700	213,020	105,420	186,330
NO_x emissions (kg)	552	180	484	4	2	4

Emissions: If the consequential system parameters that result from the above optimisations are considered, Figure 4.7(c) relates to the CO_2 fuel emissions in PV/Batt/ICE systems featuring absorption chillers (CCHP) and shows these are 14 % higher than for PV/Batt/ICE systems having electric chillers only (CHP). Figure 4.7 (c) also shows that in relation to the CO_2 emissions, PV/Batt/MGT–based systems operating with FEL/FTL have a somewhat smaller environmental footprint compared to the PV/Batt/ICE–based systems. Table 4.4 shows this is attributed to the higher renewable energy penetration for PV/Batt/MGT (RP=52 %) systems as compared to PV/Batt/ICE (RP=27 % only). The outcome is that fewer PV modules (501) exist in CCHP compared to CHP systems (737). When meeting similar overall loads, this results in a lower Renewable Penetration for CCHP systems (27 %) compared to CHP systems (40 %). Similar trends also appear for PV/Batt/MGT–based systems which is reflected in Table 4.4 by the fuel energy (F_{sup}). Alternatively, although CCHP system efficiency is lower in the FEL strategy, the CO_2 and NO_x emissions are also lower compared to the FEL/FTL type PMS irrespective of hybridised system configurations. This is due to the higher running hours for supplementary prime movers under FEL/FTL which causes greater fuel consumption compared to FEL. To exemplify, Table 4.4 shows that for PV/Batt/ICE, fuel (energy) conversion is 149,960 kWh (FEL/FTL) and 49,064 kWh (FEL). In comparison, for PV/Batt/MGT fuel conversion is 164,280 kWh (FEL/FTL) and 65,332 kWh (FEL). However, the PV/Batt/MGT configuration shows substantial improvements in NO_x emissions as compared to the PV/Batt/ICE–based system regardless of Power

Management Strategies. This is because the NO_x emissions factor for MGT is much lower (0.1 kg NO_x/MWh) compared to ICE (10 kg NO_x/MWh) [61]. Although the CO_2 and NO_x emissions are higher in PV/Batt/ICE–based CCHP systems, the LCE (kg CO_2-eq/yr) for PV/Batt/MGT is higher than the PV/Batt/ICE (Table 4.4) which again is because of the greater LCE factor for MGT's (1.16 kg CO_2-eq/kWh) compared to ICE's (0.88 kg CO_2-eq/kWh) as shown in Table A4.6 (Appendix).

Duty Factor (DF): The data in Figure 4.7 (d) points to the Duty Factor (DF), for both ICE and MGT–based CCHP systems (featuring absorption chillers) is also better (94, 85 kWh/start-stop, respectively) compared to CHP (78, 66 kWh/start-stop, respectively). The number of transient start-ups is also lower in CCHP systems (PV/Batt/ICE=590; PV/Batt/MGT=491) compared to CHP (PV/Batt/ICE=621; PV/Batt/MGT=534) as shown in Table 4.4. Both these data sets indicate supplementary prime movers are used over more prolonged periods in FEL/FTL once started up.

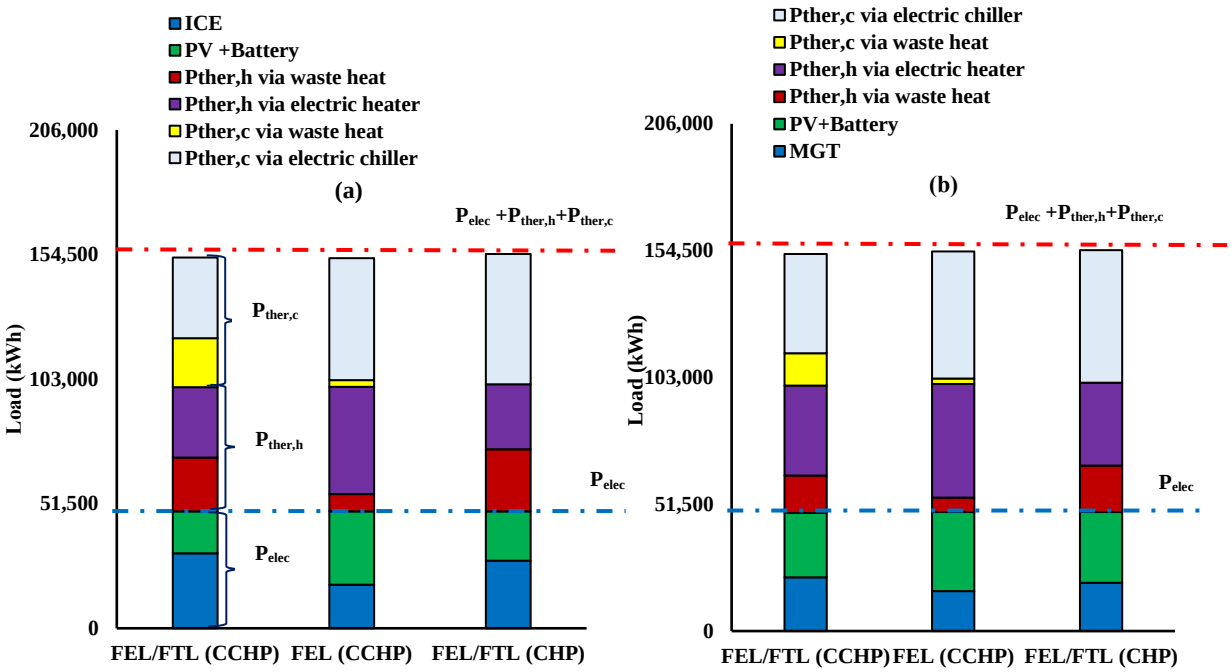

Fig. 4.8: Breakdown of operational modes used to meet electric, cooling, and heating demands at P_{elec}:P_{ther}=30:70. Data shows wheather thermal loads are met using waste heat or electric chillers and heaters. (a) PV/Batt/ICE and (b) (c) PV/Batt/MGT. The red (dashed) horizontal line represents the total load (i.e. electric, heating, and cooling), whereas the blue (dashed) line illustrates the electric load only.

Recovered waste heat to thermal demand: As for the effect of PMS on how the thermal (heating, cooling) demand is satisfied, Table 4.4 shows that in the case of CCHP systems based on PV/Batt/MGT and running on FEL/FTL, the recovered waste heat to thermal demand (Q_T/P_{ther}) is 38 %. In comparison, for PV/Batt/ICE it is 57 %. These fractions fall to 15 % and 19 % in the case of FEL for PV/Batt/MGT and PV/Batt/ICE CCHP systems, respectively. In both PV/Batt/ICE and PV/Batt/MGT systems operating in CCHP mode, the type of PMS affects the proportion of thermal demand (total of $P_{ther,\,h}$ and $P_{ther,\,c}$) that is met by recovered waste heat. Figure 4.8 (a) compares the FEL/FTL (first column) and FEL

(second column) and shows that by changing PMS the contribution of waste heat in CCHP system falls from 40 % to 10 %, respectively, in PV/Batt/ICE. Similar trends occur in Figure 4.8 (b) for PV/Batt/MGT with the contributions falling from 27 % to 8 % when changing from FEL/FTL.

Renewable Penetration (RP): The Renewable Penetration (RP) is marginally higher in the FEL for PV/Batt/ICE and PV/Batt/MGT systems (76, 81 %, respectively) compared to the FEL/FTL (27, 52 %, respectively). The reason behind this in FEL/FTL strategy is that share of energy generation and consequently the utilisation of recovered waste heat is higher than the FEL strategy shown in Figure 4.8, therefore requires less PV modules in FEL/FTL mode to meet the demand. Figure 4.8 (a) shows that for PV/Batt/ICE–based CHP systems (FEL/FTL) around 24 % of the thermal demand is met by recovered waste heat, whereas the share is greater at 40 % in CCHP systems. On the other hand Figure 4.8 (b) shows that for PV/Batt/MGT–based CHP systems (FEL/FTL), these fractions are much lower at 18 % of the thermal load satisfied by using recovered waste heat compared to the 27 % in CCHP systems. At rated power (30 kW), the overall waste heat for each ICE (water jacket and exhaust gas) is 42.36 kWh. In comparison, the overall waste heat from each MGT (exhaust gas only) is 39.10 kWh. The higher RP for PV/Batt/MGT–based systems (66 % for CHP systems, 52 % for CCHP systems, Table 4.4) leads to the lesser contribution of energy from MGTs, subsequently produce lower waste heat (Figure 4.8 (c)) compared to PV/Batt/ICE–based systems (40 % for CHP systems, 27 % for CCHP systems, Table 4.4). As such, it appears that if operating on FEL/FTL type PMS, the optimisation algorithm forces the supplementary prime movers to run more often to meet the higher thermal demand (combined heating and cooling demand). In comparison, CHP systems have a higher renewable penetration and lower fuel usage indicating that renewables (PV) are being used to meet thermal demand via electric chillers and heaters. Therefore, the generation from supplementary prime movers in CCHP systems is higher as opposed to the CHP.

4.3.2 Effect of relative magnitudes of heating and cooling loads

The earlier results have focussed on studying the effects of both hardware parameters (absorption chillers, type of supplementary prime mover) as well as Power Management Strategies (FEL/FTL, FEL). The ensuing analysis will now seek to answer the question: what effects arise from changing the relative proportions of heating and cooling ($P_{ther,h}$: $P_{ther,c}$) load while keeping the electric load demand same (P_{elec}=48, 347 kWh)? Once again, the results will be presented by first discussing the two optimised functions (COE, \$/kWh; η_{CHP} or η_{CCHP}, %) followed by consequential (post optimisation) data. The analyses consider an FEL/FTL type PMS while changing $P_{ther,h}$:$P_{ther,c}$ to 30:70; 50:50; and 70:30 as shown in Figure 4.2.

Figure 4.9 (a) indicates that changing the relative magnitude of $P_{ther,h}$: $P_{ther,c}$ in PV/Batt/ICE–based CCHP systems has insignificant effects on the COE. However, increasing $P_{ther,h}$ at the expense of $P_{ther,c}$

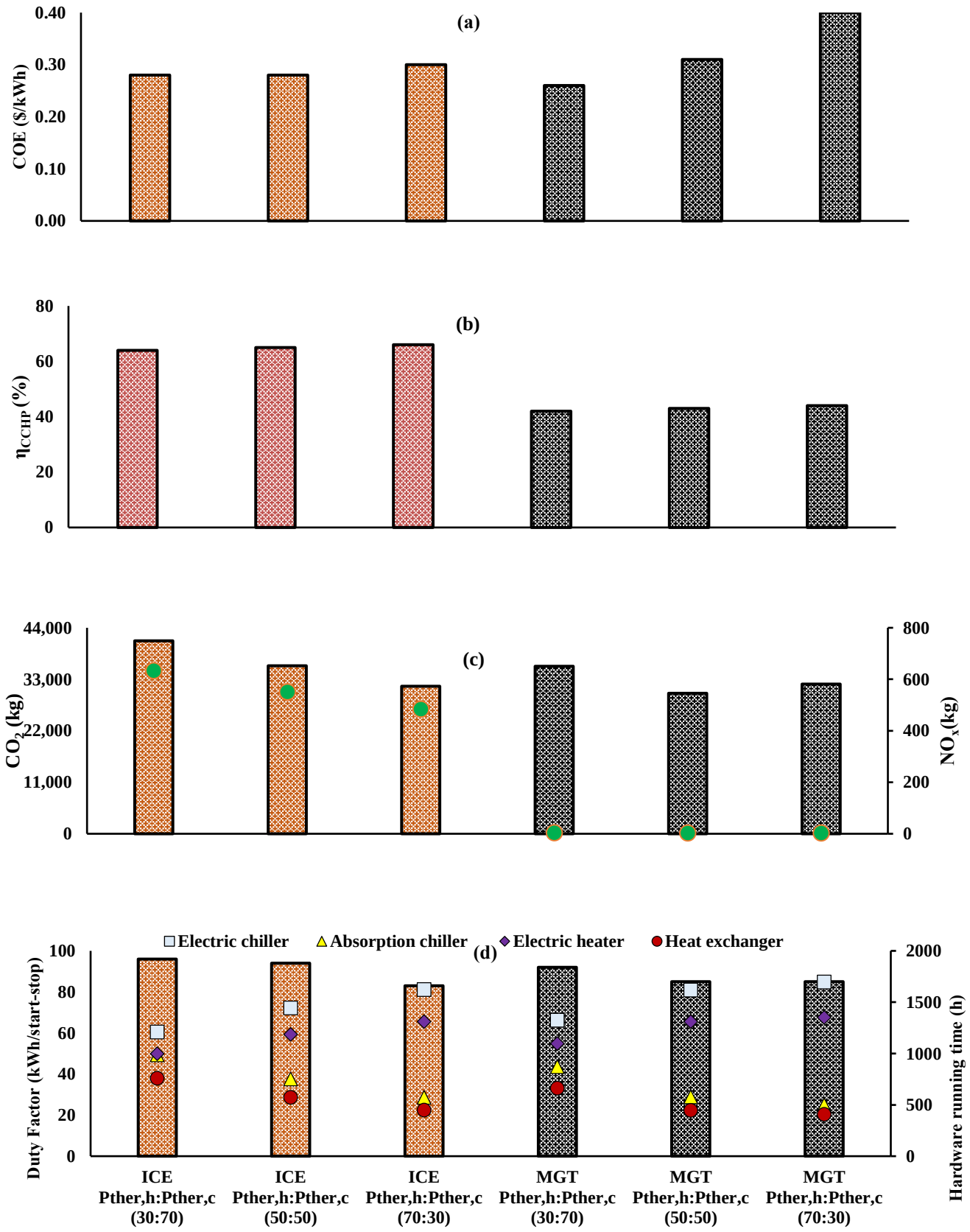

Fig. 4.9: The effects of different heating and cooling load ratio (30:70, 50 :50, and 70:30) on hybrid CCHP systems sized using Multi-objective optimisation in a PMS of the FEL/FTL type. In the plots shown, all the coloured markers are read against the secondary vertical axis.

for PV/Batt/MGT leads to higher costs, with it increasing gradually from 0.26 \$/kWh ($P_{ther,h}$: $P_{ther,c}$ =30:70) to 0.40 \$/kWh ($P_{ther,h}$: $P_{ther,c}$ =70:30). In this regard, the capital cost of MGT is much higher than the ICE and that factor along with the lower efficiency and greater temperature dependency for MGTs leads to lower supplementary power generation and more PV modules (Table 4.5).

In relation to the overall system efficiency (η_{CCHP}), changing the ratio $P_{ther,h}$: $P_{ther,c}$ does not appear to have any effect. Results also indicate that the PV/Batt/ICE–based hybridised CCHP systems while operating on FEL/FTL strategy have higher overall CCHP efficiency as compared to the PV/Batt/MGT–based systems for

Table 4.5: Summary results of multi-objective (COE, \$/kWh and η_{CCHP}, %) optimisations for hybrid CCHP systems of hybrid PMS (FEL/FTL) at different heating and cooling load with electric load at 48,347 kWh (LPSP=0.01±0.005).

Characteristics	**PV/Batt/ICE**			**PV/Batt/MGT**		
	$P_{ther,h}$:$P_{ther,c}$ (30:70)	**$P_{ther,h}$:$P_{ther,c}$ (50:50)**	**$P_{ther,h}$:$P_{ther,c}$ (70:30)**	**$P_{ther,h}$:$P_{ther,c}$ (30:70)**	**$P_{ther,h}$:$P_{ther,c}$ (50:50)**	**$P_{ther,h}$:$P_{ther,c}$ (70:30)**
Number of solar panels, N_{PV}	188	501	816	561	952	1,244
Number of lead acid batteries, N_{batt}	54	62	58	65	76	50
Number of prime movers, N_{sup}	4	5	8	3	4	7
$LPSP_{comp}$	0.001	0.01	0.01	0.01	0.01	0.01
PV energy generated (kWh)	12,053	32,120	52,315	35,966	61,034	79,755
Renewable penetration, RP (%)	12	27	40	35	52	60
ICE/MGT energy, P_{sup} (kWh)	63,407	55,207	48,478	49,691	41,681	44,407
Recovered waste heat, Q_T (kWh)	69,490	60,330	52,839	48,596	40,888	43,650
RWHP (%)	75	77	80	67	68	73
Unmet energy (kWh)	225	1,286	1,435	1,242	1,074	1,235
Fuel energy, F_{sup} (kWh)	172,330	149,960	131,610	197,020	164,280	174,340
Recovered waste heat to thermal demand (Q_T/P_{ther}, %)	64	57	50	45	38	41
Transient start-ups	661	590	585	538	491	521
LCE (kg CO_2-eq/yr)	231,950	208,210	190,110	242,820	213,020	230,670

the same reason as discussed above. Interestingly, the data in Table 4.5 and Figure 4.10 also shows that increases to $P_{ther,h}$: $P_{ther,c}$ generally lead to a smaller proportion of the thermal loads being met through waste heat. Thus as heating loads are increased from 30:70 to 70:30 and Q_T/P_{ther} falls, heavier reliance on electrically powered heaters and chillers becomes evident which is also reflected by the significant increases in the number of PV modules (N_{PV}).

Figure 4.9 (c) shows that some environmental benefits occur for systems running with higher heating demand (ratio of $P_{ther,h}$: $P_{ther,c}$). For the PV/Batt/ICE–based systems CO_2 emissions vary from 41,215 kg ($P_{ther,h}$:$P_{ther,c}$=30:70) to 31,511 kg ($P_{ther,h}$:$P_{ther,c}$=70:30). In PV/Batt/MGT–based systems, CO_2 emissions vary from 35,778 kg ($P_{ther,h}$:$P_{ther,c}$=30:70) to 31,973 kg ($P_{ther,h}$:$P_{ther,c}$=70:30). The reason behind this is

that the higher Renewable Penetration (RP) in systems with larger heating load (40–60 % for $P_{ther,h}$:$P_{ther,c}$=70:30) compared to the lesser heating load (12–35 % for $P_{ther,h}$:$P_{ther,c}$=30:70). In this context, lower RP leads to higher contribution of prime movers energy to the total energy demand that attributed to greater CO_2 emissions. In relation to NO_x emissions, similar trends appear for both ICE and MGT–based systems. However, the PV/Batt/MGT produces negligible amount of NO_x than the PV/Batt/ICE. From Table 4.5, it is also evident that the LCE for the systems with $P_{ther,h}$:$P_{ther,c}$=70:30 (for PV/Batt/ICE=190,110 kg CO_2-eq/yr; for PV/Batt/MGT=230,670 kg CO_2-eq/yr) generates lesser than the systems with $P_{ther,h}$:$P_{ther,c}$=30:70 (for PV/Batt/ICE=231,950 kg CO_2-eq/yr; for PV/Batt/MGT=242,820 kg CO_2-eq/yr). As far as DF is concerned, the lower heating demand has higher DF for both PV/Batt/ICE and PV/Batt/MGT systems shown in Figure 4.9 (d). This is due to the substantial contribution of prime movers to the total meeting load demand as shown in Figure 4.10. It is also evident from Figure 4.9 (d) that the running hour of relative hardware components varies with the relative changes of heating and cooling load profiles.

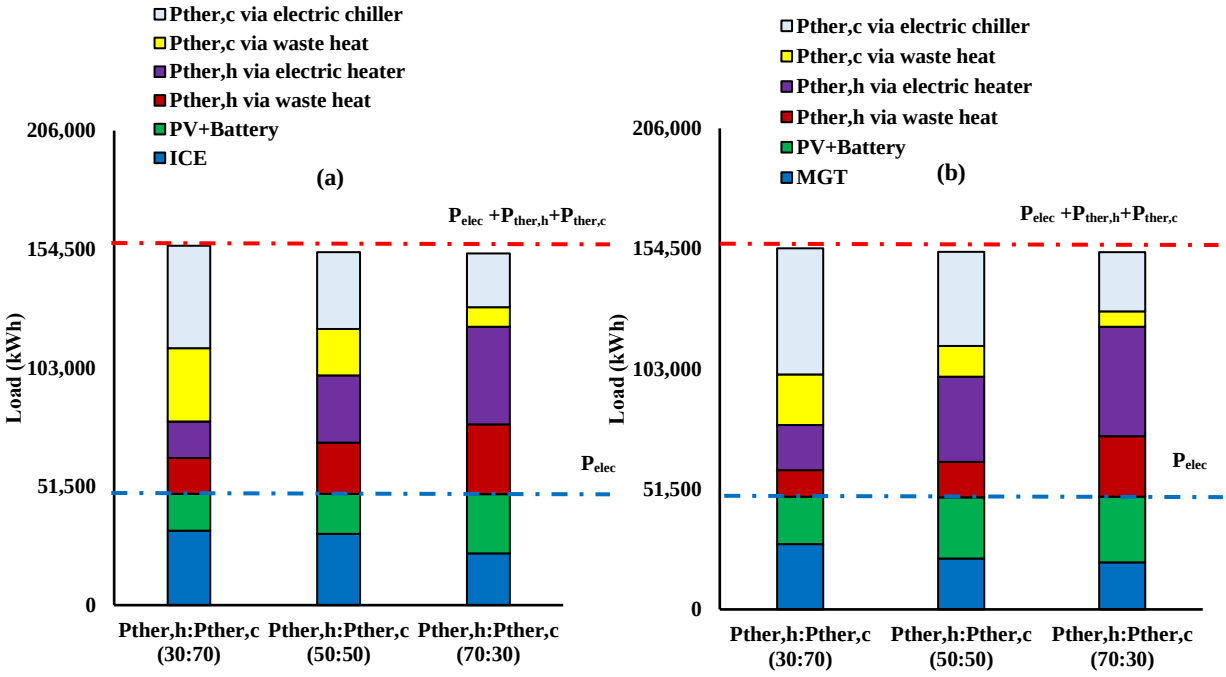

Fig. 4.10: Breakdown of operational modes used to meet electric, cooling, and heating demands with relative changes of load profile for (a) PV/Batt/ICE (b) PV/Batt/MGT–based CCHP systems using FEL/FTL type PMS. The red (dashed) horizontal line represents the total load (i.e. electric, heating, and cooling), whereas the blue (dashed) line illustrates the electric load only.

4.4 Conclusions

The present study investigates the effects of two types of supplementary prime movers when integrated into hybrid energy systems (i.e. PV/Batt/ICE or PV/Batt/MGT) satisfying both heating and cooling. The effects of meeting these loads using CHP systems or adding absorption chiller (CCHP) is also modelled in the context of two different load following strategies (FEL/FTL vs FEL). Multi-objective Genetic

Algorithm optimisation of these systems has also been done under varying contributions of heating ($P_{ther,h}$) and cooling ($P_{ther,c}$) loads alongside the need to meet an electric demand (P_{elec}). The outcomes of the simulations have been reported in terms of several key operational indicators subject to LPSP and other constraints. Under the specific set of constraints tested, the key findings can be summarised within three sub–headings:

- **Hardware parameters (absorption chiller, types of supplementary prime movers):** The Cost of Energy for PV/Batt/ICE systems is consistently, but only marginally, better compared to PV/Batt/MGT for the same loads or Power Management Strategy, whether in Combined Heat and Power or Combined Cooling Heating, and Power configurations. In terms of overall efficiency, PV/Batt/ICE systems are clearly more advantageous. However, when the type of configuration changes from CCHP to CHP, it is observed that a lower COE (in CHP) comes at the expense of a smaller overall efficiency. In Power Management Strategies designed to follow both electric and thermal loads (FEL/FTL), higher Renewable Penetration in CHP systems by virtue of them using electric chillers only to meet cooling loads, leads to a smaller environmental footprint (CO_2, NO_x, and LCE) than in CCHP systems. The PV/Batt/MGT systems have better environmental benefits in terms of CO_2 and NO_x emissions compared to PV/Batt/ICE. It is evident from this study that the fuel dependant emissions (CO_2 and NO_x) are actually higher in CCHP compared to CHP (even though CCHP system operate at a slightly better overall thermal efficiency). This behaviour is very interesting to note because whilst the literature for grid-connected CCHP systems indicates better overall efficiency compared to power only or CHP [38, 64], the results of this study which for the first time compares between CHP and CCHP systems that are hybridised with PV and operate (solely) off-grid, indicate that improved efficiency in CCHP comes at the expense of higher CO_2 and NO_x emissions compared to CHP. However, whether this is due to the range of constraints tested in the GA simulations or scale of thermal loads requires further study.
- **Power Management Strategies (FEL/FTL vs FEL):** In CCHP systems, differences in COE, overall efficiency, fuel emissions (CO_2, NO_x) as well as hardware specific and operational LCE are strongly dependant on the type of PMS. For CCHP systems subject to multi-objective optimisation using two functions (COE, η_{CCHP}), FEL/FTL leads to lower cost of energy and better overall efficiency compared to FEL in PV/Batt/ICE and PV/Batt/MGT configurations. However, under the same scenarios, the FEL strategy results in drastic reductions to fuel emissions (CO_2, NO_x) compared to the FEL/FTL. This happens at the expense of duty factors for the supplementary prime movers in PV/Batt/ICE and PV/Batt/MGT–based CCHP systems.
- **Relative changes of thermal load:** The relative magnitude of $P_{ther,h}$:$P_{ther,c}$ has insignificant effects on COE for PV/Batt/ICE–based CCHP systems. However in PV/Batt/MGT systems, a greater $P_{ther,h}$:$P_{ther,c}$ significantly increases the COE. Increases to the relative magnitude of

heating load at the expense of cooling (i.e. greater P_{ther}) is also accompanied with smaller reliance on using waste heat from ICEs and MGTs to feed absorption chillers (for $P_{ther,c}$) or heat exchangers (for $P_{ther,h}$). This also results in smaller total fuel usage, significantly more renewable penetration accompanied with lower levels of CO_2, NO_x and LCE. As such, increases in the ratio $P_{ther,h}$:$P_{ther,c}$ leads to better environment footprints, albeit the expense of slightly higher cost PV/Batt/ICE systems. These increases in costs are however higher with PV/Batt/MGT.

Despite simulations used in this study incorporating some hardware characteristics, the general outcomes reported are not intended to highlight the merits or limitations of specific models of energy system components. This is because a specific set of constraints are being assumed. Whilst the present study is a continuation of earlier works on CHP and CCHP stand-alone hybrid systems [10, 44], future research in this area may include exergy and emissions into the GA objective functions, place constraints on the total operating hours, or variations to the hardware (boilers, heat pumps).

4.5 Chapter appendices

Data used for system design and optimisation.

Table A4.6: Stand-alone hybridised CHP system components cost, lifetime and emissions aspects.

Components	**Description**	**Capital Cost ($)**	**Replacement Cost ($)**	**O&M Cost ($/yr)**	**Life time (yr)**	**LCE (kg CO_2-eq/kWh)**
PV module [63]	HS-PL135 (135 W)	310	310	0	25	0.05 [65]
ICE [66]	30 kW	10,500	10,500	260	10	0.88 [65]
MGT [67]	30 kW	75,300	75,300	1,880	10	1.16 [68]
Battery [52]	12 V, 200 Ah	419	419	11	10	0.03 [65]
Inverter [63]	1 kW	800	750	20	15	0 [65]
Charge controller [69]	1 kW	450	450	11	15	
Electric heater [70]	14.4 kW	1,160	1,160	28	5	
Heat exchanger [71]	Shell and Tube, 8m^2	9,800	9,800	245	10	
Absorption Chiller [17]	COP: 0.83	300/kW	300/kW	8/kW	20	
Electric chiller [72]	COP:3.5	700/kWe	700/kWe	18/kWe	20	
Discount rate		10%				
Fuel cost	Diesel fuel	0.91 $/l				
	Natural gas	3.30 $/GJ				
CO_2 emissions for ICE (kg/MWh) [61]		650				
CO_2 emissions for MGT (kg/MWh) [61]		720				
NO_x emissions for ICE (kg/MWh) [61]		10				
NO_x emissions for MGT (kg/MWh) [61]		0.1				

Chapter references

[1] Wei, D., et al., *Multi-objective optimal operation and energy coupling analysis of combined cooling and heating system.* Energy, 2016. **98**: p. 296-307.

[2] *ASHRAE Handbook - Heating, Ventilating, and Air-Conditioning Systems and Equipment (I-P Edition)*. 2016, American Society of Heating, Refrigerating and Air-Conditioning Engineers, Inc. p. 7.33.

[3] Cho, H., et al., *Evaluation of CCHP systems performance based on operational cost, primary energy consumption, and carbon dioxide emission by utilizing an optimal operation scheme.* Applied Energy, 2009. **86**(12): p. 2540-2549.

[4] Homayouni, F., R. Roshandel, and A.A. Hamidi, *Techno-economic and environmental analysis of an integrated standalone hybrid solar hydrogen system to supply CCHP loads of a greenhouse in Iran.* International Journal of Green Energy, 2017. **14**(3): p. 295-309.

[5] Maraver, D., et al., *Environmental assessment of CCHP (combined cooling heating and power) systems based on biomass combustion in comparison to conventional generation.* Energy, 2013. **57**: p. 17-23.

[6] Abusoglu, A. and M. Kanoglu, *Exergetic and thermoeconomic analyses of diesel engine powered cogeneration: Part 1–Formulations.* Applied Thermal Engineering, 2009. **29**(2): p. 234-241.

[7] Jradi, M. and S. Riffat, *Tri-generation systems: Energy policies, prime movers, cooling technologies, configurations and operation strategies.* Renewable and Sustainable Energy Reviews, 2014. **32**: p. 396-415.

[8] Liu, M., Y. Shi, and F. Fang, *Combined cooling, heating and power systems: A survey.* Renewable and Sustainable Energy Reviews, 2014. **35**: p. 1-22.

[9] Wang, L., et al., *Energy, environmental and economic evaluation of the CCHP systems for a remote island in south of China.* Applied Energy, 2016. **183**: p. 874-883.

[10] Das, B.K., Y.M. Al-Abdeli, and G. Kothapalli, *Optimisation of stand-alone hybrid energy systems supplemented by combustion-based prime movers.* Applied Energy, 2017. **196**: p. 18–33.

[11] Das, B.K., et al., *A techno-economic feasibility of a stand-alone hybrid power generation for remote area application in Bangladesh.* Energy, 2017. **134**: p. 775-788.

[12] Bortolini, M., et al., *Economic and environmental bi-objective design of an off-grid photovoltaic–battery–diesel generator hybrid energy system.* Energy Conversion and Management, 2015. **106**: p. 1024-1038.

[13] Ogunjuyigbe, A.S.O., T.R. Ayodele, and O.A. Akinola, *Optimal allocation and sizing of PV/Wind/Split-diesel/Battery hybrid energy system for minimizing life cycle cost, carbon emission and dump energy of remote residential building.* Applied Energy, 2016. **171**: p. 153-171.

[14] Wang, J. and Y. Yang, *Energy, exergy and environmental analysis of a hybrid combined cooling heating and power system utilizing biomass and solar energy.* Energy Conversion and Management, 2016. **124**: p. 566-577.

[15] Chen, H.-C., *Optimum capacity determination of stand-alone hybrid generation system considering cost and reliability.* Applied Energy, 2013. **103**: p. 155-164.

[16] Su, B., W. Han, and H. Jin, *Proposal and assessment of a novel integrated CCHP system with biogas steam reforming using solar energy.* Applied Energy, 2017. **206**: p. 1-11.

[17] Basrawi, F., T. Yamada, and S.y. Obara, *Economic and environmental based operation strategies of a hybrid photovoltaic–microgas turbine trigeneration system.* Applied Energy, 2014. **121**: p. 174-183.

[18] Yousefi, H., M.H. Ghodusinejad, and A. Kasaeian, *Multi-objective optimal component sizing of a hybrid ICE + PV/T driven CCHP microgrid.* Applied Thermal Engineering, 2017. **122**: p. 126-138.

[19] Ipsakis, D., et al., *Power management strategies for a stand-alone power system using renewable energy sources and hydrogen storage.* international journal of hydrogen energy, 2009. **34**(16): p. 7081-7095.

[20] Wang, J. and Y. Yang, *A hybrid operating strategy of combined cooling, heating and power system for multiple demands considering domestic hot water preferentially: A case study.* Energy, 2017. **122**: p. 444-457.
[21] Kang, L., et al., *Effects of load following operational strategy on CCHP system with an auxiliary ground source heat pump considering carbon tax and electricity feed in tariff.* Applied Energy, 2017. **194**: p. 454-466.
[22] Zheng, C., J. Wu, and X. Zhai, *A novel operation strategy for CCHP systems based on minimum distance.* Applied Energy, 2014. **128**: p. 325-335.
[23] Liu, M., Y. Shi, and F. Fang, *Optimal power flow and PGU capacity of CCHP systems using a matrix modeling approach.* Applied Energy, 2013. **102**: p. 794-802.
[24] Rey, G., et al., *Performance analysis, model development and validation with experimental data of an ICE-based micro-CCHP system.* Applied Thermal Engineering, 2015. **76**: p. 233-244.
[25] Sanaye, S. and A. Sarrafi, *Optimization of combined cooling, heating and power generation by a solar system.* Renewable Energy, 2015. **80**: p. 699-712.
[26] Abdollahi, G. and H. Sayyaadi, *Application of the multi-objective optimization and risk analysis for the sizing of a residential small-scale CCHP system.* Energy and Buildings, 2013. **60**: p. 330-344.
[27] Di Somma, M., et al., *Multi-objective operation optimization of a Distributed Energy System for a large-scale utility customer.* Applied Thermal Engineering, 2016. **101**: p. 752-761.
[28] Wang, J., et al., *Life cycle assessment (LCA) optimization of solar-assisted hybrid CCHP system.* Applied Energy, 2015. **146**: p. 38-52.
[29] Sanaye, S. and H. Hajabdollahi, *Thermo-economic optimization of solar CCHP using both genetic and particle swarm algorithms.* Journal of Solar Energy Engineering, 2015. **137**(1): p. 011001.
[30] Hajabdollahi, H., A. Ganjehkaviri, and M.N.M. Jaafar, *Assessment of new operational strategy in optimization of CCHP plant for different climates using evolutionary algorithms.* Applied Thermal Engineering, 2015. **75**: p. 468-480.
[31] Li, L., et al., *Optimization and analysis of CCHP system based on energy loads coupling of residential and office buildings.* Applied Energy, 2014. **136**: p. 206-216.
[32] Sadeghi, M., et al., *Thermodynamic analysis and optimization of a novel combined power and ejector refrigeration cycle – Desalination system.* Applied Energy, 2017. **208**: p. 239-251.
[33] Wang, J., et al., *Particle swarm optimization for redundant building cooling heating and power system.* Applied Energy, 2010. **87**(12): p. 3668-3679.
[34] Jayasekara, S., et al., *Optimum sizing and tracking of combined cooling heating and power systems for bulk energy consumers.* Applied Energy, 2014. **118**: p. 124-134.
[35] Wang, J.-J., Y.-Y. Jing, and C.-F. Zhang, *Optimization of capacity and operation for CCHP system by genetic algorithm.* Applied Energy, 2010. **87**(4): p. 1325-1335.
[36] Yao, E., et al., *Multi-objective optimization and exergoeconomic analysis of a combined cooling, heating and power based compressed air energy storage system.* Energy Conversion and Management, 2017. **138**: p. 199-209.
[37] Wang, M., et al., *Multi-objective optimization of a combined cooling, heating and power system driven by solar energy.* Energy Conversion and Management, 2015. **89**: p. 289-297.
[38] Soheyli, S., M.H.S. Mayam, and M. Mehrjoo, *Modeling a novel CCHP system including solar and wind renewable energy resources and sizing by a CC-MOPSO algorithm.* Applied Energy, 2016. **184**: p. 375-395.
[39] Sayyaadi, H. and R. Mehrabipour, *Efficiency enhancement of a gas turbine cycle using an optimized tubular recuperative heat exchanger.* Energy, 2012. **38**(1): p. 362-375.
[40] *Cummins South Pacific (12.10.2015). B3.3 Engine Data Sheet & Performance Curve (30kW FR 30002). Source: Personal Communication.*
[41] Darrow, K., et al., *Catalog of CHP technologies.* 2014.
[42] Arun, P., R. Banerjee, and S. Bandyopadhyay, *Optimum sizing of battery-integrated diesel generator for remote electrification through design-space approach.* Energy, 2008. **33**(7): p. 1155-1168.

[43] Dufo-López, R., et al., *Multi-objective optimization minimizing cost and life cycle emissions of stand-alone PV–wind–diesel systems with batteries storage.* Applied Energy, 2011. **88**(11): p. 4033-4041.
[44] Das, B.K. and Y.M. Al-Abdeli, *Optimisation of stand-alone hybrid CHP systems meeting electric and heating loads.* Energy Conversion and Management, 2017. **153**: p. 391-408.
[45] *Solarshopnet. Technical data heckert HS-PL 135.*; Available from: 05.11.2016. http://www.solarshop-erope.net/solar-components/solarmodules/heckert_hs_pl-135_m_634.html.
[46] Deshmukh, S.S. and R.F. Boehm, *Review of modeling details related to renewably powered hydrogen systems.* Renewable and Sustainable Energy Reviews, 2008. **12**(9): p. 2301-2330.
[47] Duffie, J.A., *William A. Beckman Solar Engineering of Thermal Processes*. 2006, John Wiley & Sons, Inc. NY.
[48] Clarke, D.P., Y.M. Al-Abdeli, and G. Kothapalli, *The effects of including intricacies in the modelling of a small-scale solar-PV reverse osmosis desalination system.* Desalination, 2013. **311**: p. 127-136.
[49] Nafeh, A.E.-S.A., *Optimal economical sizing of a PV-wind hybrid energy system using genetic algorithm.* International Journal of Green Energy, 2011. **8**(1): p. 25-43.
[50] Kashefi Kaviani, A., G.H. Riahy, and S.M. Kouhsari, *Optimal design of a reliable hydrogen-based stand-alone wind/PV generating system, considering component outages.* Renewable Energy, 2009. **34**(11): p. 2380-2390.
[51] *BOM.South Australia weather and warnings* Available from: 12.12.2018. http://reg.bom.gov.au/climate/reg/oneminsolar/.
[52] *Lead-acid battery*. Available from: 20.11.2015. http://www.sunstonepower.com/upload/userfiles/files/ML12-200.pdf.
[53] Yang, H., et al., *Optimal sizing method for stand-alone hybrid solar–wind system with LPSP technology by using genetic algorithm.* Solar Energy, 2008. **82**(4): p. 354-367.
[54] Kim, H.-S., et al., *High-efficiency isolated bidirectional AC–DC converter for a DC distribution system.* IEEE Transactions on Power Electronics, 2013. **28**(4): p. 1642-1654.
[55] *Technical Reference : Capstone Model C30 Performance*. Available from: 15.11.2015. http://www.wmrc.edu/projects/bar-energy/manuals/c-30-manuals/410004_Model_C30_Performance.pdf.
[56] Kurt, H., Z. Recebli, and E. Gedik, *Performance analysis of open cycle gas turbines.* International Journal of Energy Research, 2009. **33**(3): p. 285-294.
[57] Ochoa, A., et al., *Dynamic study of a single effect absorption chiller using the pair LiBr/H 2 O.* Energy Conversion and Management, 2016. **108**: p. 30-42.
[58] Salmi, W., et al., *Using waste heat of ship as energy source for an absorption refrigeration system.* Applied Thermal Engineering, 2017. **115**: p. 501-516.
[59] Wiehagen, J. and J. Sikora, *Performance comparison of residential hot water systems*, in *NAHB Research Center, Upper Marlboro, Maryland, NREL*. 2003.
[60] Aguilar, C., D. White, and D.L. Ryan, *Domestic water heating and water heater energy consumption in Canada.* Canadian Building Energy End-Use Data and Analysis Centre, 2005.
[61] Wu, D.W. and R.Z. Wang, *Combined cooling, heating and power: a review.* Progress in Energy and Combustion Science, 2006. **32**(5–6): p. 459-495.
[62] Belmili, H., et al., *Sizing stand-alone photovoltaic–wind hybrid system: Techno-economic analysis and optimization.* Renewable and Sustainable Energy Reviews, 2014. **30**: p. 821-832.
[63] Brka, A., Y.M. Al-Abdeli, and G. Kothapalli, *The interplay between renewables penetration, costing and emissions in the sizing of stand-alone hydrogen systems.* International Journal of Hydrogen Energy, 2015. **40**(1): p. 125-135.
[64] Wu, J.-y., J.-l. Wang, and S. Li, *Multi-objective optimal operation strategy study of micro-CCHP system.* Energy, 2012. **48**(1): p. 472-483.
[65] Katsigiannis, Y., P. Georgilakis, and E. Karapidakis, *Multiobjective genetic algorithm solution to the optimum economic and environmental performance problem of small autonomous hybrid power systems with renewables.* Renewable Power Generation, IET, 2010. **4**(5): p. 404-419.
[66] *Central Maine Diesel*. Available from: 03.02.2016. http://www.centralmainediesel.com/cummins-generators.asp.

[67] *Combine Heat and Power Partnership. Catalog of CHP Technologies. U.S. Environmental Protection Agency. 2015. p.1-6,5.1-5.18*.
[68] Brown Jr, E.G., *Life Cycle Assessment Of Existing and Emerging Distributed Generation Technologies in California.* 2011.
[69] Ismail, M.S., M. Moghavvemi, and T.M.I. Mahlia, *Design of an optimized photovoltaic and microturbine hybrid power system for a remote small community: Case study of Palestine.* Energy Conversion and Management, 2013. **75**: p. 271-281.
[70] *Electric Water Heater*. Available from: 10.06.2017 https://1stchoicehotwater.com.au/product/rheem-heavy-duty-electric-613050g7-50l/.
[71] Lin, C.-S. *Capture of heat energy from diesel engine exhaust*. 2008; Available from: 10.02.2017 https://www.osti.gov/scitech/servlets/purl/963351.
[72] Akbari, K., et al., *Optimal investment and unit sizing of distributed energy systems under uncertainty: A robust optimization approach.* Energy and Buildings, 2014. **85**: p. 275-286.

Chapter 5: Energy, Exergy, and Cost Optimisation
of Stand-alone Hybrid Power, CHP, and CCHP Systems
is not included in this version of the thesis

Chapter 6: Effects of Battery Technology and Load Scalability on Stand-alone PV/ICE Hybrid Micro-grid System Performance[6]

This chapter investigates the performance of hybridised micro-grids based on solar PV supplemented by Internal Combustion Engines (ICE). Three different battery technologies (lead acid, lithium-ion, and vanadium redox flow) as well as the effects of load demand scalability are considered. The optimisations are based on Cost of Energy (COE) but the analyses consider several performance indicators including Excess Energy (EE), Renewable Penetration (RP), and Duty Factors (DF). Optimisations are done using the software tool HOMER (Hybrid Optimisation Model for Electric Renewable). A sensitivity analysis of hardware and operational costs is also conducted to see the effects of various input parameters on the Cost of Energy. RQ 5 is addressed in this chapter.

6.1 Introduction

As modern societies grow, the demand for power increases at an accelerated rate. On the other hand, electricity production using conventional energy sources such as natural gas, coal and diesel is one of the highest contributors to Green House Gases (GHG). Fossil fuels used in power generation account for around 54 % of GHG emissions [1]. In this context, policy makers focus on the alternative sources of energy. Renewables reduce reliance on fossil fuels, mitigate overall GHG emissions, enable remote communities to access the power needed to operate services as well as household appliances [2, 3] and can reduce transmission losses associated with grids.

The increased uptake of solar-PV technology by Australian households appears to place upward pressure on grid connected electricity. Within Australia, the top three states with significant solar energy potential (including planned, under construction, and commissioned) are Queensland (Project: 11,099 MW solar/6,578 MWh storage), New South Wales (Project: 5,530 MW solar/3,816 MWh storage), and South Australia (Project: 2,784 MW solar/2,930-3,100 MWh storage) [4]. For example, under the approach of one state Government's "climate change strategy 2015–2050" and "a low carbon investment plan for South Australia", the goal is to achieve 50 % electric from renewables by 2025 and zero net CO_2 emissions by 2050 [5]. States such as South Australia have the highest energy costs (~0.05 $/kWh) of any state in Australia as well as being one of the highest in the world with grid electricity being not readily available in some remote or rural areas [6]. As seen in Figure 6.1, states such as South Australia already produce roughly a half of their electricity from renewable energy sources [7] and so

[6] This chapter has been published as a full research paper.
Das, B.K., Al-Abdeli, Y.M., Woolridge, M., **Energy**, 2019. 168: p. 57-69.

Whilst efforts were made to retain original content of the article, minor changes such as number formats and font size style were implemented in order to maintain consistency in the formatting style of the thesis.

there is also expected to be reliance on battery storage technology. In recent years South Australia also faced significant energy crises and, as a result, has integrated into its grid a 100 MW/129 MWh Li-ion battery amongst the largest in the world of this type (connected to the Hornsdale wind farm) [8].

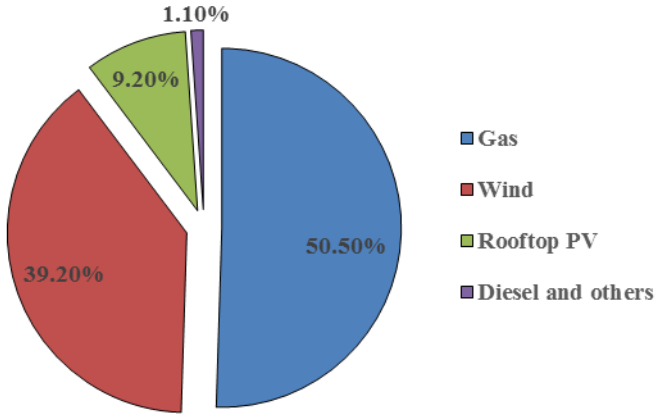

Fig. 6.1: Electricity generation from different sources in South Australia [7].

Reliability, cost effectiveness, and power quality are the main challenges associated with operating stand-alone renewable energy systems. This is because renewable resources (PV, wind, etc.) are seasonal and subject to strong intermittency [9-12]. It is the seasonal and short-term temporal variations to both solar and wind energy resources which means reliance cannot be placed on them to fully satisfy load demand. In this regard, very short-term, short-term, medium-term, and long-term prediction of energy sources is important for overall feasibility of a renewable energy-based project [13-15]. It is for these reasons that many stand-alone systems are hybridised by combining PV, other renewables, and Internal Combustion Engine (ICE) along with battery storage [2, 16]. Given that renewable sources are inherently intermittent in character, hybridised energy systems include some energy storage media to stabilise power output (batteries, hydrogen, capacitors) when operated in stand-alone mode [17, 18].Table 6.1 presents a comparison of the different types of storage media applicable to stand-alone energy systems.

Table 6.1: Comparison of different energy storage media [17, 19-23].

Parameters	Lead-acid battery	Li-ion battery	Ni-Cadmium	Flywheel	Pump-storage	Vanadium-redox
Storage mechanism	Electrochemical	Electrochemical	Electrochemical	Mechanical	Mechanical	Electrochemical
Life time (years)	3-12	15-20	15-20	>20	50	>20
Life cycle	1500	500-2000	3000	$<10^7$	-	10000
Self-discharging rate	Very low	Medium	Very low	Very high	Negligible	Negligible
Duration	Medium term	Medium term	Medium term	Short term	Long term	Medium term
Energy density	30 Wh/kg	100-200 Wh/kg	15-50 Wh/kg	5 Wh/kg steel, 100 Wh/kg composite	-	30-45 Wh/kg
Power density	180 W/kg	360 W/kg	50-1000 W/kg	1000 W/kg composite	-	166 W/kg
Technology	Proven	Proven	Proven	Promising (Proven)	Promising (Proven)	Promising
Energy efficiency (%)	70-80	70-85	60-90	95	65-80	75-80
Environmental issues	Chemical disposal issues	Chemical disposal issues	Chemical disposal issues	Slight	High	Chemical disposal issues

The hybridisation of energy systems helps realise benefits which include: higher load meeting reliability compared to one-source energy systems [9, 24], increased renewable penetration from ~33 % (wind only) to 90 % (PV/Wind) [25], improved techno-economic performance (PV/Wind/ICE compared to PV/Wind) [26], and reduced emissions footprints (30 %) compared to grid connected power using conventional fuels [27]. With the above in mind, PV panels, which are assembled into modules or arrays, provide an excellent solution for providing electricity to remote or rural areas in many parts of the world [25, 27-30] where a grid-connection is uneconomical [31]. Table 6.2 shows that the hybridisation and optimisation of such systems has relied on one of the three main storage technologies: lead acid [32-38], Li-ion [39, 40], and vanadium redox flow [41, 42] batteries (which are the basis of the present study). However, there are very few studies which have compared between different battery technologies when applied to stand-alone systems, particularly when these cover a range of operating scales. In the present paper this is achieved when the load profile of a single house is scaled up to cover multiple households as would exist in a stand-alone micro-grid. Exceptions to this include the work done by Testa et al. [39] who reported optimal design of hybrid PV/Wind systems with Lead Acid Battery-LAB, Li-ion, and Vanadium Redox Flow battery-VRF considering LPSP as a reliability index. The study showed that the cost of energy (COE) is lower for Li-ion batteries (0.45 €/kWh) than for the lead acid battery (0.99 €/kWh), but VRF (0.29 €/kWh) was the most economical of all three (LAB=17 kWh; Li-ion=5 kWh; VRF=13 kWh). However, they used a probabilistic approach for the optimal solution and did not consider the scalability of load demand or the sensitivity of the outcomes to cost parameters or optimisations technique as undertaken in the present paper.

In some stand-alone PV-based power generation units, it has been reported that a Li-ion system appeared to be the most expensive option (PV/Li-ion: 1.62 $/kWh; PV/LAB: 1.13 $/kWh), which may be because lead acid technology offered the lowest initial cost compared to the Li-ion [40]. Even so, the system analysed was not hybridised through the inclusion of combustion engines and indicators of environmental impact were not considered alongside cost as occurs in the present paper. Although Merei et al. [43] used Genetic Algorithms to optimise a stand-alone hybrid PV/Wind/ICE system with LAB, Li-ion, and VRF batteries and reported that VRF batteries (0.34 €/kWh) are the cheapest option, the scalability of load demand as well as other consequential performance indicators, such as dumped Excess Energy (EE), Renewable Penetration (RP), emissions, duty factors (kWh/start-stop/yr), or their sensitivity to cost parameters, were not reported. It would appear that although Li-ion batteries have better technical performance, the affordability and availability of these remain as two major factors which may contribute to the continued (wide) application of LAB technology in renewable energy systems [44].

This paper focuses on identifying the impact of using different battery technologies when powering a (conceptual) stand-alone energy system to serve differently sized micro-grids based on the total daily demand for one South Australian dwelling. The comparative analysis which includes three major battery

technologies (LAB, Li-ion, and VRF) is applied to systems featuring hybridisation through the addition of diesel generator sets (Internal Combustion Engines) with the solar-PV. The main contribution of this study based on a widely accepted analysis tool HOMER, is to compare between three different battery technologies (LAB, Li-ion, VRF) in the context of (stand-alone) hybridised PV/ICE/Batt micro-grids operated under various scales. This comparison is also subjected to a sensitivity analysis to explore how variations of cost elements impact on the COE in system configurations based on PV/ICE/LAB, PV/ICE/Li-ion, and PV/ICE/VRF.

Table 6.2: Hybrid energy systems with different storage technologies using HOMER/Genetic Algorithm.

Type of hybridisation	Storage	Stand-alone/grid connected	Performance criteria	COE ($/kWh)
PV/ICE/Batt [45]	LAB	Stand-alone	NPC, COE, O & M cost, EE, Load reliability, CO_2 emissions	0.26
PV/Wind/ICE/Batt [46]	LAB	Stand-alone	NPC, COE, initial capital cost	0.44
PV/Wind/ICE/Batt [47]	LAB	Stand-alone	NPC, COE, CO_2 emission reduction	1.88
PV/ICE/Batt [36]	LAB	Stand-alone	NPC, Fuel consumption, RP	-
PV/ICE/Batt [37]	LAB	Stand-alone	NPC, COE, RP, Fuel emissions	0.30
PV/Wind/Batt [48]	LAB	Stand-alone	COE, EE, Unmet load	0.37
PV/Wind/ICE/Batt [28]	LAB	Stand-alone	NPC, COE, Payback period, RP, Fuel emissions	0.28
PV/ICE/Batt [29]	LAB	Stand-alone	COE, Investment cost, RP, Fuel emissions	-
PV/ICE [49]	LAB/Flywheel	Stand-alone	NPC, COE, CO_2 emission reduction	0.37
PV/Wind/ICE/Micro-hydro/Batt [50]	LAB	Stand-alone	NPC, COE, Fuel savings, CO_2 emission reduction	0.14
PV/Wind [51]	Pump hydro	Stand-alone	Power production, efficiency, energy utilization, and CO_2 emission reduction.	-
PV/Wind/ICE/Batt [43]	LAB, Li-ion, VRF	Stand-alone		VRF:0.34 €/kWh; LAB: 0.68 €/kWh; Li-ion: 0.72 €/kWh;
PV/ICE/Batt [52]	LAB	Stand-alone/grid connected	NPC, COE, RP, Fuel emissions	0.28
PV/Wind/ICE/Batt [53]	VRF	Stand-alone/grid connected	NPV, COE, RP, CO_2 emissions	-
PV/Wind/Biomass/Batt [54]	LAB	Grid connected	COE, Reliability	0.18

Throughout this study, the electrical load demand based on the usage of a single (sample) household (7,665 kWh/yr) are used. This is then scaled up to span five differently sized hybrid (stand-alone) micro-grids covering a range of 10–50 houses. The results are reported in the form of indicators such as Cost of Energy (COE), Net Present Cost (NPC), annualised cost; supplementary prime mover (fuel)

emissions; and consequential performance such as Duty Factor (DF), Excess Energy (EE), and Renewable Penetration (RP). As such the study considers several factors which may be impacted under different battery options.

6.2 Methodology

Figure 6.2 shows the design architecture of the conceptual (stand-alone) hybrid micro-grid system modelled to satisfy a single community load of ten-to-fifty households. An AC load bus is connected with an ICE while the DC bus is connected with the PV modules and a battery bank in the form of lead acid, Li-ion, or vanadium redox flow batteries. These two buses are linked with the inverter where DC current is converted to AC. Surplus energy produced by the PV modules is used to charge the battery bank or dumped when the batteries reach their maximum state of charge.

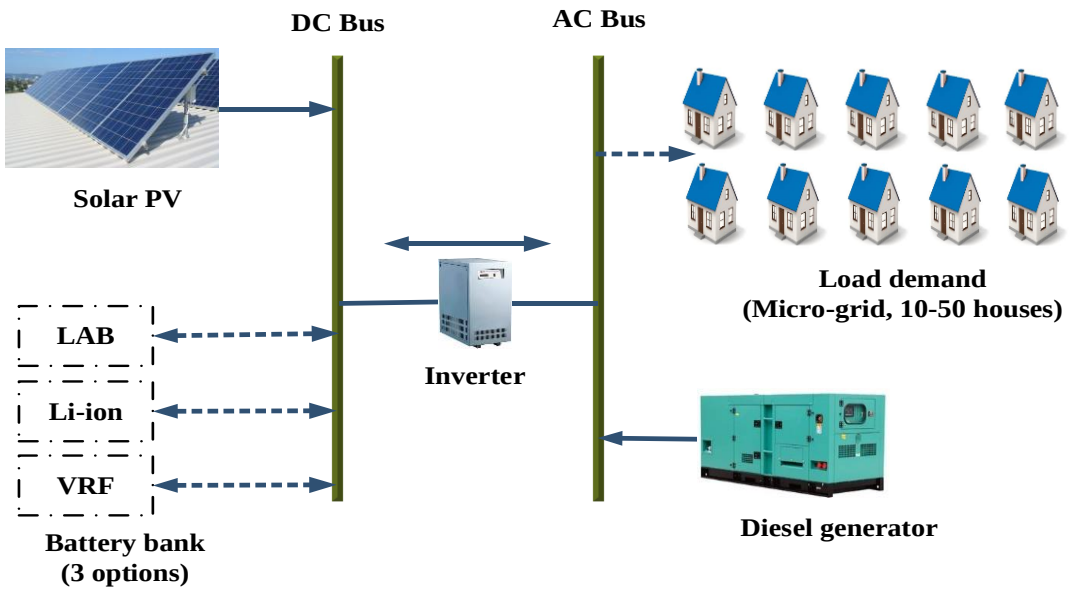

Fig. 6.2: Schematic diagram of the conceptual hybridised system which is also scaled up.

The analysis undertaken with the software tool HOMER compares between the three battery technologies (i.e. LAB, Li-ion, and VRF). The solution given for each case is based on a single set of input data which comprises hardware specifications, operational constraints, and meteorological data for the location analysed. Based on this data, HOMER gives optimised sizing configurations for the micro-grid on the basis of the (lower) Cost of Energy (COE) when using each of the three different battery technologies. As such, the outcomes are taken to be exact with no error (±) given for the optimised solutions. A Load Following (LF) strategy is used for HOMER which relies on the ICE to satisfy load demand when PV modules and batteries are unable to meet the required demand. This strategy helps reduce excess energy and gives lower Cost of Energy and Net Present Cost [37, 55]. The system optimisation constraints include project lifetime (25yr) and dispatch strategy (LF) as well as other and technical and economical constraints listed in the ensuing sections for system components.

6.2.1 Load profile of selected area

The assumed total daily electric load demand for a single household is 21 kWh/day for summer (January) [56]. In HOMER, a residential load is selected which produces the time resolved 24-hour profile meeting this overall demand as shown in Figure 6.3(a). This load is then multiplied by a factor of 10–50 to get the following loads for the differently sized micro-grids: (i) 10 households with 210 khW/day; (ii) 20 households with 420 kWh/day; (iii) 30 households with 630 kWh/day; (iv) 40 households with 840 kWh/day; and (v) 50 households with 1,050 kWh/day. Table 6.3 also presents a likely scenario for various appliance usage. HOMER calculates yearly time series (hourly) electric load profile based on the type of load (residential in this study), meteorological data of selected area (Streaky bay) and the peak season (January).

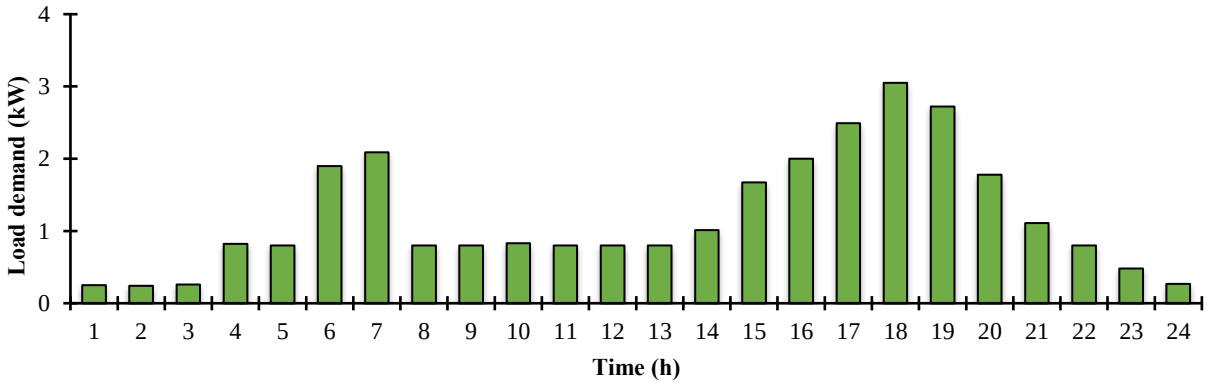

Fig 6.3(a): Daily hourly load demand for a single household (21 kWh) for summer (January).

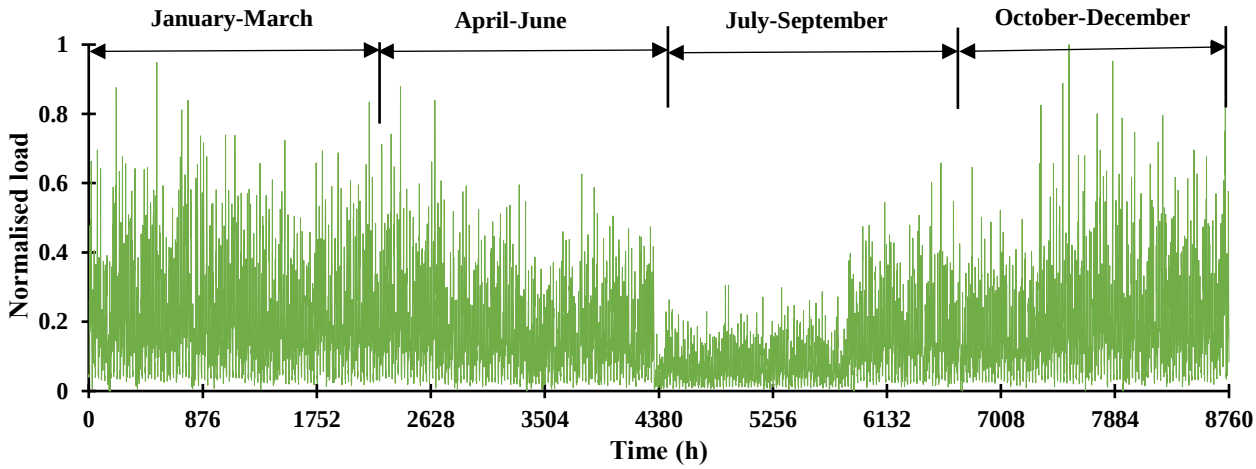

Fig 6.3(b): Yearly hourly load demand (normalised) for a 10–50 house micro-grid. Values shown are normalised by the peak load (kW) in any time interval.

Figure 6.3(b) presents an annual hourly resolved time series (normalised) of the total loads. In this study, the first scenario with 210 kWh/day and 76,650 kWh annual load demand is considered as the base-line scenario which is compared with the other scenarios.

Table 6.3: Estimation of load demand for a household in summer (January).

Appliances	Ratings (W)	Quantity	Approximate operating time (h/day)	Total demand (kWh/day)
Refrigerator	200/150	2	24	8.40
TV	150	2	4	1.20
Fan	30	3	8	0.72
Incandescent Lights	40/60	20	4	3.44
Dishwasher	1500	1	1.5	2.25
Washing Machine	500	1	1	0.50
Dryer	2000	1	1	2.00
Oven	2200	1	1	2.20
Miscellaneous *	N/A	N/A	24	0.29
Grand total				**21.00 kWh/day**

***** Includes small items such as charging electronic devices, small entertainment devices (e.g. sound systems), and small temporary use of other electronics (e.g. printers, kettles, radios).

6.2.2 PV modelling and meteorological data

Figures 6.4 shows data for yearly hourly global solar irradiance and ambient temperature (downloaded from NASA) within HOMER for a sample town in South Australia (Streaky Bay). As expected, since Australia is in the southern hemisphere, the daily radiation levels of the studied area are higher (7.54 kWh/m^2/day) in the summer months (December and January) and lower (3.61 kWh/m^2/day) in the winter months (May, June, and July). The average solar irradiation is 5.75 kWh/m^2/day and average clearness index is 0.83 whilst the monthly average wind speed and monthly average temperature are 5.61 m/s and 23 ˚C, respectively [57]. The hourly time resolved global solar irradiation data are checked with data from Australian Bureau of Meteorology (BOM) from Adelaide station [58]. The data obtained from BOM are slightly lower than the data downloaded from HOMER. This is because of the study area is around 700 km away from Adelaide and HOMER gives location based global solar irradiation data.

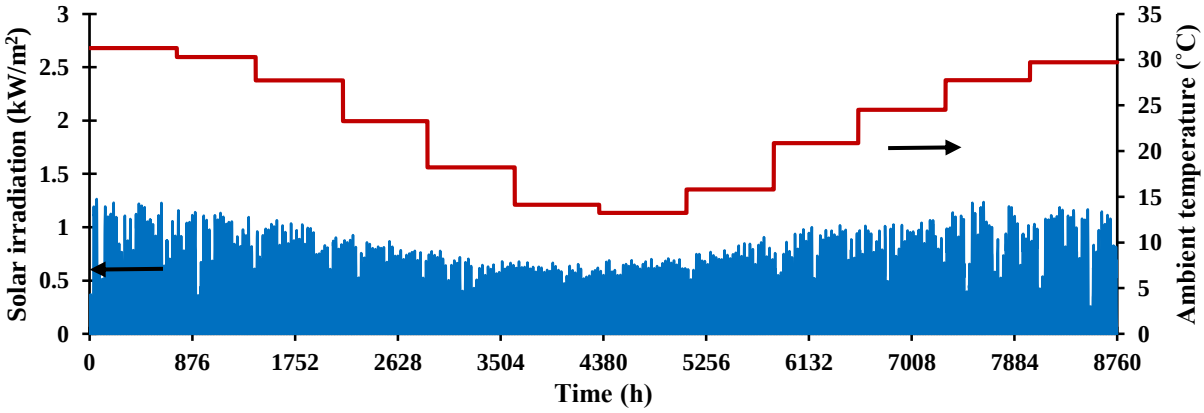

Fig. 6.4: Yearly time resolved (hourly) solar irradiation and ambient temperature for Streaky Bay, South Australia.

In HOMER based optimisations, the power output from the PV array ($P_{PV}(t)$) can be calculated using Equation 6.1, whereby Y_{PV} is the rated capacity of the PV array (0.25 kW, power output under standard test conditions), f_{PV} is the PV derating factor measured in percentage (90 %), which is a derating scaling factor that accounts for real-world conditions that reduce performance.

Additionally, $G(t)$ is the solar radiation incident on the PV array, G_{ref} is the solar radiation incident under standard test conditions (1kW/m^2), α_P is the temperature coefficient of power (-0.485%/°C), $T_{PV}(t)$ is the cell temperature in the PV array, T_{ref} is the cell temperature under the standard test conditions (25 °C) [59].

$$P_{PV}(t) = Y_{PV} f_{PV} \left(\frac{G(t)}{G_{ref}}\right)\left[1 + \alpha_P\left(T_{PV}(t) - T_{ref}\right)\right] \tag{6.1}$$

The PV cell temperature in any time interval $T_{PV}(t)$ can be calculated from Equation 6.2, where $T_{amb}(t)$ is the ambient temperature, $T_{PV,NOCT}$ is the Nominal Operating Cell Temperature (NOCT, 25 ˚C), $T_{amb,NOCT}$ is the ambient temperature at NOCT (20 ˚C), G_{NOCT} is the solar radiation when NOCT is defined at 0.8 kW/m^2, η_{PV} is the panel efficiency (15.3 %), $\tau\alpha$ is the solar transmittance and solar absorptance of the PV array which HOMER assumes is 0.9 and taken from [60].

$$T_{PV}(t) = T_{amb}(t) + G(t)\left(\frac{T_{PV,NOCT} - T_{amb,NOCT}}{G_{NOCT}}\right)\left(1 - \frac{\eta_{PV}}{\tau\alpha}\right) \tag{6.2}$$

To obtain Equation 6.2, Equation 6.3 which is the energy balance for the PV array is rearranged into Equation 6.4, where U_L is the heat transfer coefficient. The term $\left(\frac{\tau\alpha}{U_L}\right)$ is difficult to measure and therefore, manufacturers provide the NOCT which is the cell temperature using a solar radiation incident of 0.8 kW/m^2, an ambient temperature of 20 °C, and no load operation (i.e. $\eta_{PV} = 0$).

$$\tau\alpha G(t) = \eta_{PV} G(t) + U_L(T_{PV}(t) - T_{amb}) \tag{6.3}$$

$$T_{PV}(t) = T_{amb}(t) + G(t)\left(\frac{\tau\alpha}{U_L}\right)\left(1 - \frac{\eta_{PV}}{\tau\alpha}\right) \tag{6.4}$$

Using these values, Equation 6.5 can be obtained.

$$\frac{\tau\alpha}{U_L} = \frac{T_{PV,NOCT} - T_{amb,NOCT}}{G_{NOCT}} \tag{6.5}$$

Substituting Equation 6.5 into Equation 6.4 yields Equation 6.2 to calculate the cell temperature. The system modelled does not consider any solar tracking optimisation mechanisms (i.e. typical of household rooftop PV systems) and a 90 % de-rating factor for each panel reflects changing conditions in regard to temperature and accumulation of debris on the solar panels.

6.2.3 ICE modelling

In HOMER, the fuel curve which resolves fuel consumption (l/h) over the dynamic range of diesel generators output power (kW) is as shown in Figure 6.5. Equation 6.6 gives the fuel consumption rate for electrical output [59], whereby F_1 is the fuel curve intercept coefficient, Y_{ICE} is the rated capacity of

the generator, F_2 is the fuel curve slope, and P_{ICE} (t) is the electrical output of the generator. The considered lower heating value of diesel fuel is 43,200 kJ/kg with a density of 820 kg/m^3.

$$C_{fuel_{ICE}}(t) = F_1 Y_{ICE} + F_2 P_{ICE}(t) \quad (6.6)$$

The ICE efficiency is calculated using Equation 6.7 [59].

$$\eta_{ICE}(t) = \frac{3600 \times P_{ICE}(t)}{\rho \times C_{fuel_{ICE}}(t) \times LHV} \quad (6.7)$$

The ICE supplies the necessary load requirements when both renewables and battery storage are unable to satisfy the demand. In this study, a 48 kW rated capacity diesel engine with a fuel intercept coefficient of 0.0165 l/h/kW and fuel curve slope of 0.267 l/h/kW is considered. This is selected as it is close to the peak load demand in the base-line scenario (55.20 kW). The minimum load ratio of 30 % is considered for the diesel generator, which is recommended by manufacturers due to the efficiency of diesel generator under this is much lower [61, 62] as shown in Figure 6.5. Multiple units of the same 48 kW ICE are used when meeting higher magnitudes of load (10 house micro-grid at 210 kWh/day to a 50 house micro-grid of 1,050 kWh/day).

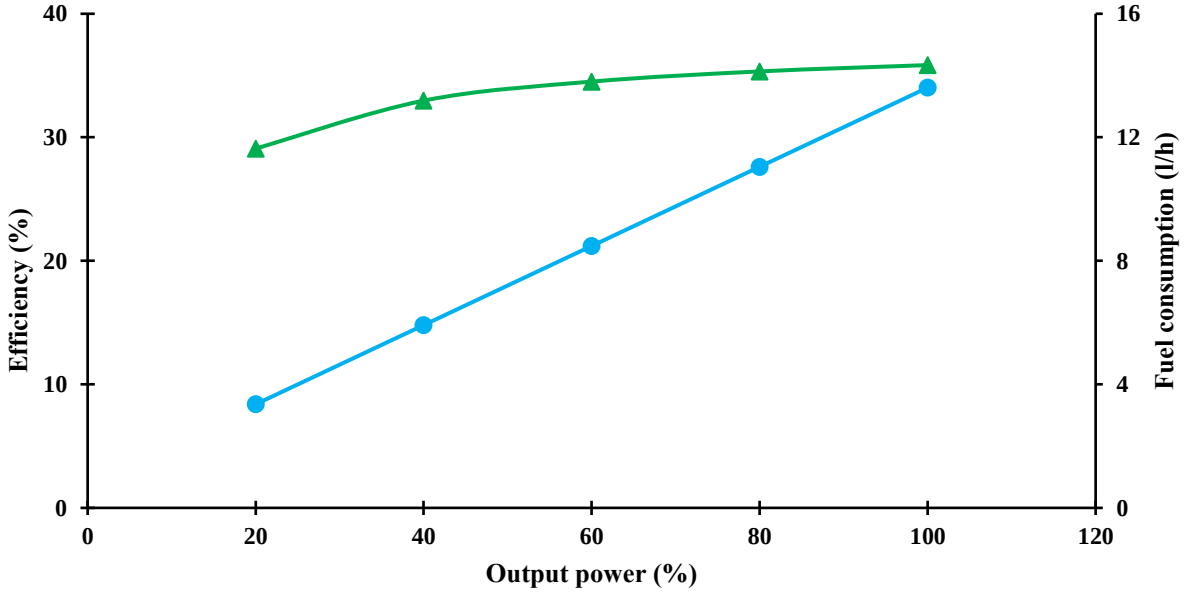

Fig. 6.5: Internal Combustion Engine efficiency and fuel consumption over output power.

6.2.4 Battery modelling

In this study, three different types of battery storage technologies are modelled (lead acid, Li-ion, and VRF). HOMER uses several equations to determine the charge and discharge power as well as the amount of energy into, and out of, the battery storage at any given time step (1 h). Equation 6.8 is used to determine the maximum battery charge power, whereby $Q_1(t)$ refers to the available energy at the beginning of the time step and above minimum state of charge level (BOC_{min}=20 % for LAB, BOC_{min}=0 % for Li-ion and VRF), $Q(t)$ refers to the total energy at the beginning of the time step, c is the storage capacity ratio, k is the storage rate constant, and Δt is the amount of time in the time step [59].

$$P_b(t) = \frac{kQ_1(t)e^{-k} + Q(t)kc\left(1 - e^{-k\Delta t}\right)}{1 - e^{-k\Delta t} + c(k\Delta t - 1 + e^{-k\Delta t})} \quad (6.8)$$

The maximum battery discharge power can be calculated with Equation 6.9, where Q_{max} is the total capacity of the storage [59].

$$P_b(t) = \frac{-kcQ_{max} + kQ_1(t)e^{-k\Delta t} + Q(t)kc\left(1 - e^{-k\Delta t}\right)}{1 - e^{-k\Delta t} + c(k\Delta t - 1 + e^{-k\Delta t})} \quad (6.9)$$

More detailed calculations can be found from HOMER help manual [59]. The total battery capacity to meet the load requirements of the differently scaled micro-grids is calculated by the HOMER considering the meteorological condition, number of cyclic charging/discharging etc. The study compares the storage depletion, which is the difference of state of charge at beginning of the year to the end of the year among the three systems. Homer calculates the battery lifetime based on the battery throughput which is the sum of the discharge energy measured after charging losses but before discharging losses.

6.2.5 Inverter modelling

An inverter is used to connect the AC and DC bus which converts the power from AC voltage to DC voltage. Equation 6.10 gives the actual power at the load side after the AC-DC voltage conversion, whereby P_o (t) is the power out of the inverter, P_i (t) is the power into the inverter, and η_{inv} is the inverter efficiency (95 %) [9]. The capacity of inverter is automatically selected by HOMER.

$$P_o(t) = P_i(t)\eta_{inv} \quad (6.10)$$

6.2.6 Economic analysis

The Cost of Energy (COE, $/kWh) which is defined as the average cost for one kWh of energy, can be calculated using Equation 6.11 [59], whereby C_{ta} is the total annualised cost of the system, and E_s is the total energy served in a year.

$$COE = \frac{C_{ta}}{E_s} \quad (6.11)$$

The total annualised cost of the system (C_{ta}) can be calculated using Equation 6.12 where C_{cap} is the capital cost, C_{rep} is the replacement cost, and $C_{O\&M}$ is the operation and maintenance cost

$$C_{ta} = C_{cap} + C_{rep} + C_{O\&M} \quad (6.12)$$

The study also calculates the NPC using Equation 6.13, where CRF is the capital recovery factor and can be calculated with Equation 6.14 [59], where *i* is the real annual interest rate and is calculated using Equation 6.15, *n* is the number of years, i' is the nominal interest rate, f is the annual inflation rate.

$$NPC = \frac{C_{ta}}{CRF(i,n)} \quad (6.13)$$

$$CRF(i,n) = \frac{i(1+i)^n}{(1+i)^n - 1} \quad (6.14)$$

$$i = \frac{i' - f}{1 + f} \tag{6.15}$$

Table 6.4: Hardware components cost and lifetime for stand-alone hybrid micro-grid.

Components	Description	Capital cost ($)	Replacement cost ($)	O & M cost ($)	Life time (yr)
PV Module [63]	250 W	930/kW	0	5/yr	25
ICE [64]	48 kW	370/kW	296/kW	0.05/h	15,000 h
LAB [65]*	2.8 kWh	325	325	10/yr	5
Li-ion battery**	13.5 kWh	6,500	6,000	0	10
VRF [66, 67]	20 kWh	15,800	0	0	25
Inverter [9]	1 kW	800	750	20/yr	15
ICE Fuel [10]	Diesel Fuel	0.91 $/l			
Discount rate [10]		10 %			

* It is assumed that battery is being fully replaced after its lifetime.

** Prices were provided within the HOMER Energy software.

An annual inflation rate of zero is used in the calculation of the interest rate. A 10 % interest rate is used in this study. Table 6.4 provides a summary of the characteristics, costs, and lifetime of different system components.

6.3 Results and discussion

In this study, the effects of different battery technologies (i.e. LAB, Li-ion, VRF) on the PV/ICE hybrid system are first analysed while meeting the power requirements of differently scaled micro-grids (10-50 households). Table 6.5 shows the summary results of the optimised hybrid baseline scenario for 10 houses (210 kWh/day). The analyses are then extended to examine the effects of upscaling the system whilst studying the effects on performance indicators such as COE ($/kWh), CO_2 emissions (kg/yr), Duty Factors (kWh/start-stop/yr), and Renewable Penetration (%). Finally, a sensitivity analysis is conducted for the baseline scenario to see the effect of variations in the input parameters on the COE ($/kWh).

6.3.1 Type of battery technology

In this section, optimised results of PV/ICE/LAB, PV/ICE/Li-ion, and PV/ICE/VRF systems are compared when meeting a household load demand of 7,6650 kWh/yr with the highest reliability (zero unmet load). From Table 6.5, it is evident that the COE for PV/ICE/Li-ion system is the lowest (0.31 $/kWh), albeit very comparable to that for the PV/ICE/LAB. A similar trend is true for NPC ($) as well. This is attributed to the overall lower replacement and maintenance costs associated with using fewer, but higher rated Li-ion batteries (13.5 kWh, Table 6.4) compared to the LAB (2.8 kWh, Table 6.4). Although the replacement cost is higher than the PV/ICE/VRF system, both the capital and the O&M cost is lower in PV/ICE/Li-ion system than VRF-based system. On the other hand, the COE (0.35 $/kWh) and NPC ($242,052) for PV/ICE/VRF-based hybrid system is higher than the other two because of the higher capital cost for VRF-based technology (Table 6.4). From Table 6.6 it is also obvious that

the annualised capital cost for the PV/ICE/LAB-based system is much lower than PV/ICE/VRF and PV/ICE/Li-ion option. This explains why (overall) the COE for both LAB and Li-ion based hybrid systems are comparable.

Table 6.5: Summary of optimised hybridised PV/ICE systems based on three different battery technologies when used in a 10 house micro-grid. Load demand met is 76,650 kWh (210 kWh/day and 55.20 kW peak load demand).

Characteristics	PV/ICE/LAB	PV/ICE/Li-ion	PV/ICE/VRF
COE ($/kWh)	0.32	0.31	0.35
NPC ($)	223,457	216,305	242,052
PV capacity (kW)/units	47.90/192	49.10/197	44.80/180
ICE generator capacity (kW)	48	48	48
Battery capacity (kWh)/units	229/82	108/8	100/5
Inverter capacity (kW)	23.30	23.40	19.60
PV energy (kWh/yr)	92,838	95,180	86,840
ICE energy (kWh/yr)	15,035	18,807	25,525
Renewable Penetration (RP, %)	80	76	67
Capital cost ($)	97,610	124,560	145,368
Replacement cost ($)	67,445	38,048	12,374
O&M cost ($)	16,863	2,273	9,600
Fuel cost ($)	4,890	6,050	8301
Fuel consumption (l/yr)	5,374	6,723	9,122
Excess energy (kWh/yr)	19,140	30,466	23,349
Unmet load (kWh/yr)	0	0	0
ICE generator operating time (h/yr)	1,011	1,265	1,715
Engine starts (nos/yr)	533	662	762
Duty Factor (kWh/start-stop/yr)	28.20	28.40	33.50

Table 6.6: Total annualised cost of hybridised PV/ICE systems based on three different battery technologies when used in a 10 house micro-grid.

System configurations	Capital cost ($)	O&M ($)	Replacement cost ($)	Salvage ($)	Resource ($)	Total cost ($)
PV/ICE/LAB	10,754	1,858	7,430	-314	4,891	24,619
PV/ICE/Li-ion	13,723	250	4,192	-452	6,118	23,831
PV/ICE/VRF	16,015	1,058	1,363	-70	8,301	26,667

The more interesting outcome relates to the way which battery technology affects the operational emissions, and in particular the combustion emissions from diesel fuel used in supplementary prime movers. The PV/ICE/LAB-based hybrid system produces less CO_2 emissions (14,064 kg/yr) despite having a comparable Duty Factor (28.20 kWh/start-stop/yr) to that for systems based on Li-ion (28.40 kWh/start-stop/yr). This may be explained by the lower operating time for the ICE in the PV/ICE/LAB (1,011 h/yr) compared to PV/ICE/Li-ion (1,265 h/yr). Further study is warranted to see whether this is

due to the unit size of each type battery type (Table 6.4). However, PV/ICE/VRF generates the highest CO_2 emissions (23,872 kg/yr) as shown in Table 6.7. A similar trend is evident for the other emissions. Another explanation for this is because the contribution of energy generation from the ICE in the PV/ICE/VRF system is greater (25,525 kWh/yr) than the contribution from the PV/ICE/LAB system (15,035 kWh/yr) and the PV/ICE/VRF system (18,807 kWh/yr) as shown in Table 6.5. However, the environmental impact of the VRF battery is lower than the LAB [68]. Additionally, lead is a hazardous metal with negative health implications [69], particularly in developing countries where outdated recycling process may cause serious health damage due to lead dust, fumes, and the discharge of hazardous waste from LAB [70, 71]. In relation to the life cycle GHG emissions, Li-ion has much lower life cycle emissions (0.00011 kg CO_2-eq/kWh) [72] than the life cycle emissions of LAB (0.028 kg CO_2-eq/kWh) [73].

Table 6.7: Operational emissions from hybridised PV/ICE systems based on three different battery technologies when used in a 10 house micro-grid.

Emissions (kg/yr)	PV/ICE/LAB	PV/ICE/Li-ion	PV/ICE/VRF
CO_2	14,064	17,594	23,872
CO	90.80	114	154
Unburn Hydro Carbon	3.87	4.84	6.57
Particulate Matters	0.54	0.67	0.91
SO_2	34.40	43.10	58.50
NO_x	84.20	105	143

Although the renewable energy contributions from the PV module is comparable for all three systems, the lower battery capacity for PV/ICE/VRF is attributed to the greater contribution of ICE energy for load meeting reliability. Therefore, the emissions for the PV/ICE/VRF hybrid system are relatively higher compared to the other two systems. As such the Renewable Penetration (RP) for PV/ICE/LAB is comparatively higher (80 %) among the systems. It is also evident from the outcomes that excess energy generation from the PV/ICE/LAB (19,140 kWh/yr) system is comparatively much lower than the PV/ICE/Li-ion (30,466 kWh/yr) and PV/ICE/VRF (23,349 kWh/yr) systems. This is due to the different battery capacity for these systems, which receives surplus energy produced by the PV modules during the charging process as presented in Table 6.8. It is also obvious from Table 6.8 that an LAB has a lower expected life time (3.47 years) than the Li-ion (10 years), and the VRF battery (25 years). More importantly, a Li-ion battery serves the same load demand with much lower nominal capacity with minimal losses compared to the other two batteries. However, a VRF battery, as reported earlier, has a higher lifetime of 25 years. This is because the LAB has a lower cycle life and is much more sensitive to the depth of discharge, discharge rate, and temperature than the Li-ion and VRF batteries.

Figures 6.6(a), (b), and (c) represent the state of charge for one year of LAB, Li-ion, and VRF, respectively. The minimum battery state of charge for a lead acid battery is considered as 20 % to

increase its longevity [10]. This is why the PV/ICE/LAB hybrid energy system requires a larger battery bank to meet the load demand. Additionally, both the Li-ion (Figure 6.6(b) and VRF (Figure 6.6(c)) batteries can be deep discharged down to 0 % and charged and discharged faster compared to the lead acid battery. Therefore, a smaller battery bank is required to meet the demand using Li-ion and VRF batteries.

Table 6.8: Battery performance for hybridised PV/ICE systems when used in a 10 house micro-grid.

Parameters	PV/ICE/LAB	PV/ICE/Li-ion	PV/ICE/VRF
Battery nominal capacity (kWh)	229	108	100
Usable nominal capacity (kWh)	183	108	100
Energy in (during charging, kWh/yr)	44,087	36,130	37,373
Energy out (during discharging, kWh/yr)	35,422	32,618	28,105
Storage depletion (kWh/yr)	170	106	87
Losses (kWh/yr)	8,835	3,618	9,355
Annual throughput (kWh/yr)	39,603	34,382	32,453
Lifetime throughput (kWh)	137,360	343,820	811,314
Expected lifetime (yr)	3.47	10	25

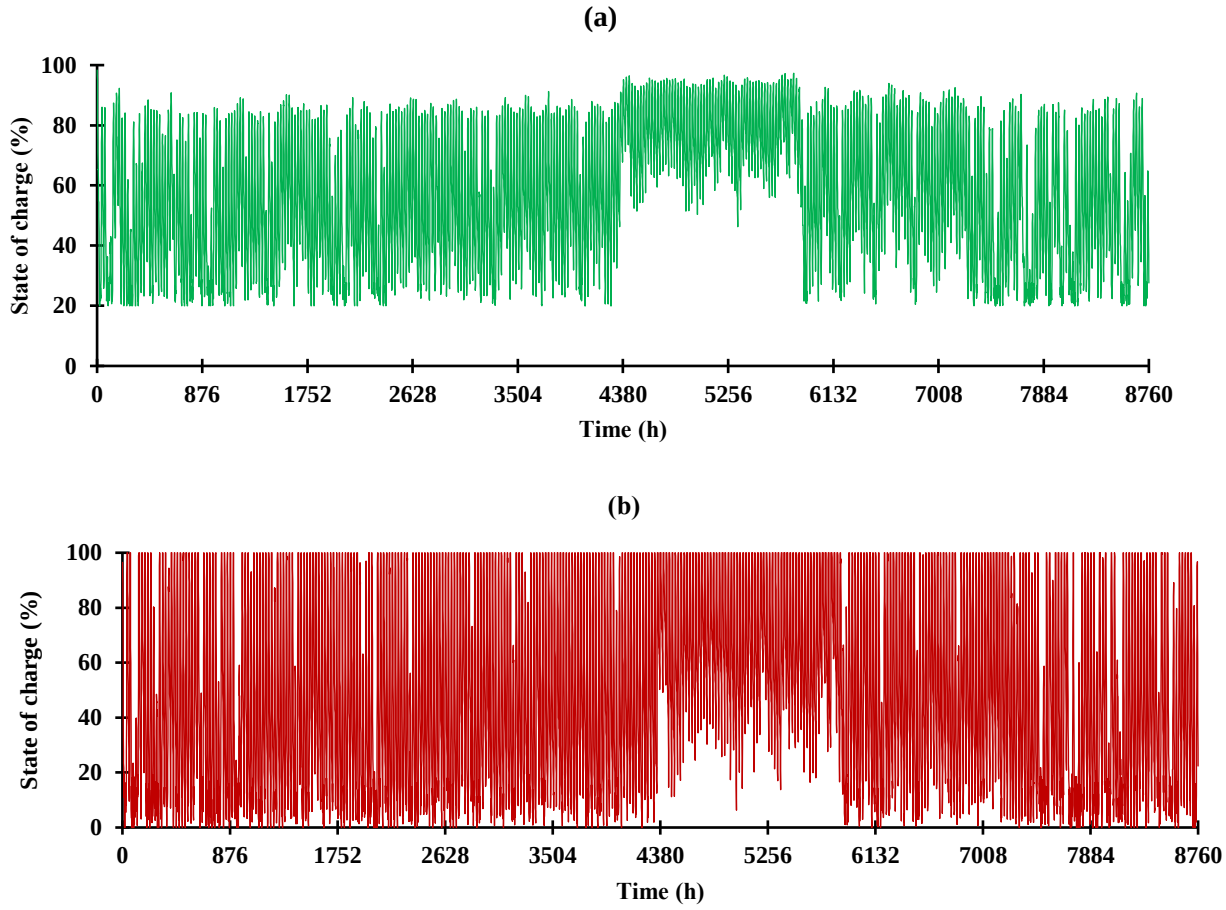

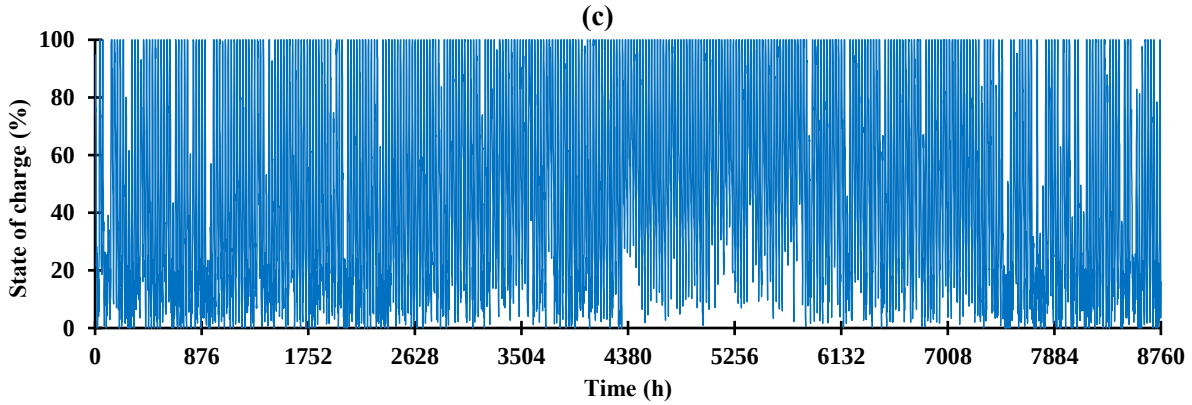

Fig. 6.6: Time resolved Battery state of charge for (a) LAB (229 kWh), (b) Li-ion (108 kWh), and (c) VRF (100 kWh) batteries over the period of one year in the baseline (10 houses) micro-grid.

The annual average battery state of charge for LAB, Li-ion, and VRF systems is 57 %, 50 %, and 49 %, respectively. From a technology perspective, the Li-ion batteries have shown accelerated progress in their capacity, energy density, cost reduction, and safety issues [74]. On the other hand, VRF batteries have also gained much attention for energy storage application, particularly as recent development of vanadium electrolyte technology makes them denser, reliable, and cost effective [75]. Therefore, it is expected that in near future, both Li-ion and VRF batteries could play vital role in stand-alone energy storage applications.

6.3.2 Scalability of daily load demand

Analysis takes into account different daily load demands, keeping the same fluctuation as the baseline scenarios. From Figure 6.7, it is evident that for a PV/ICE/LAB hybridised system, the COE changes almost 10% from the base load scenario of 10 houses to the 50 houses micro-grid. However, the COE changes 4~5 % and 7~8 % from the 10 houses base load demand to the 50 houses micro-grid for the PV/ICE/Li-ion and PV/ICE/VRF–based hybridised systems, respectively. This indicates that differences in COE between PV/ICE/LAB, PV/ICE/Li-ion, and PV/ICE/VRF increase at higher load demands.

Results from Figure 6.8 also indicate that the PV/ICE/LAB hybridised system generates relatively smaller amounts of excess energy compared to the PV/ICE/Li-ion and PV/ICE/VRF-based hybridised systems while meeting the same load demand. This is because of the HOMER optimisation algorithms choosing larger battery capacities for the PV/ICE/LAB system, which accepts a significantly larger amount of the surplus energy produced by the PV module than the rest of the system configurations. Additionally, PV module capacities for the PV/ICE/Li-ion and PV/ICE/VRF-based hybridised systems are greater than the PV/ICE/LAB system. The results also indicate that the excess energy decreases almost half from the 10 houses base case scenario to the 50 houses micro-grid for all the cases.

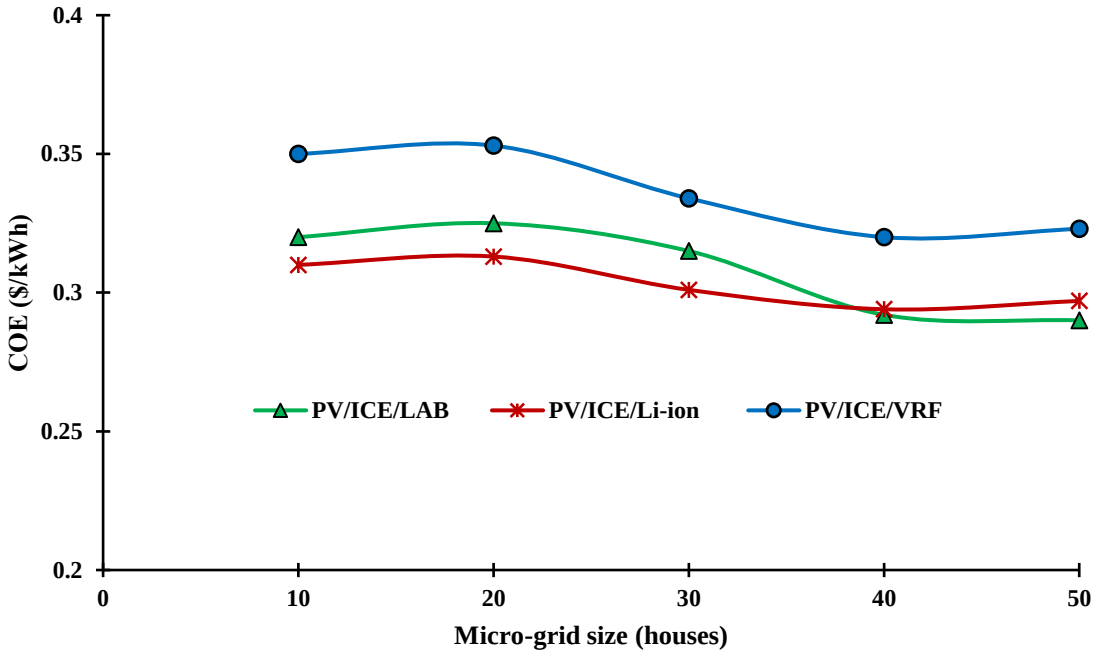

Fig. 6.7: COE ($/kWh) for hybridised systems with different batteries and changing load demands based on differently sized micro-grids (10–50 houses).

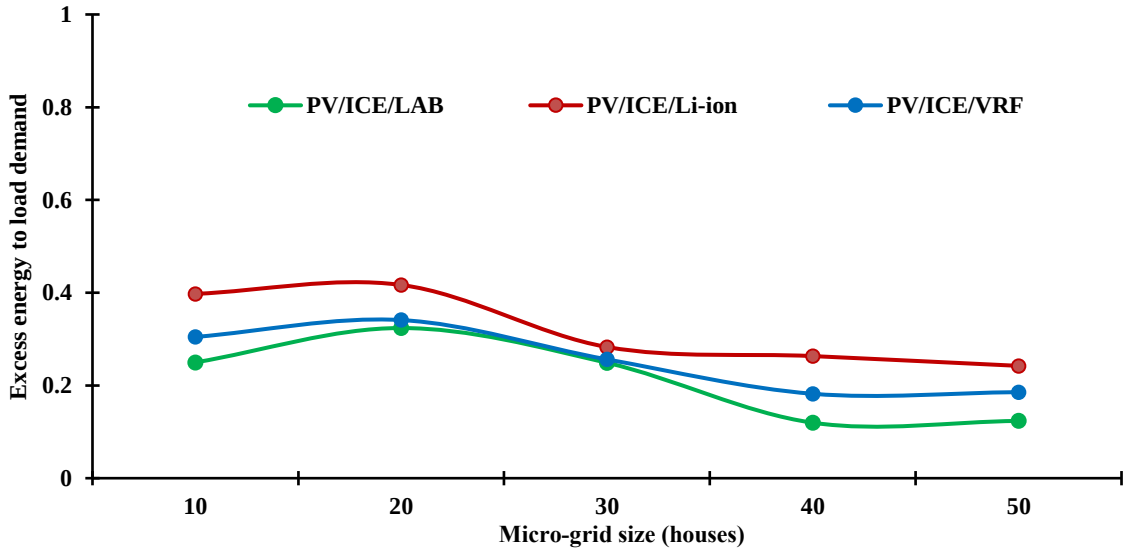

Fig. 6.8: Excess energy to load demand for hybridised systems with different batteries and changing load demands.

It is evident from Figure 6.9 that the DF rises significantly for all the system configurations as the load demand increases. For example, for the PV/ICE/LAB system meeting the 10 houses base load demand has a DF of 48 kWh/start-stops/yr whereas for a 50 houses micro-grid, the DF increases to 137 kWh/start-stops/yr. A similar trend is also apparent for the other systems. This is because when there is elevated load demand, the ICE meets a greater load in every start-up. The results from this outcome also

indicate that Renewable Penetration is higher for PV/ICE/LAB system regardless of how load demand changes, as shown in Figure 6.10. Additionally, RP decreases for all three systems as the load demand increases.

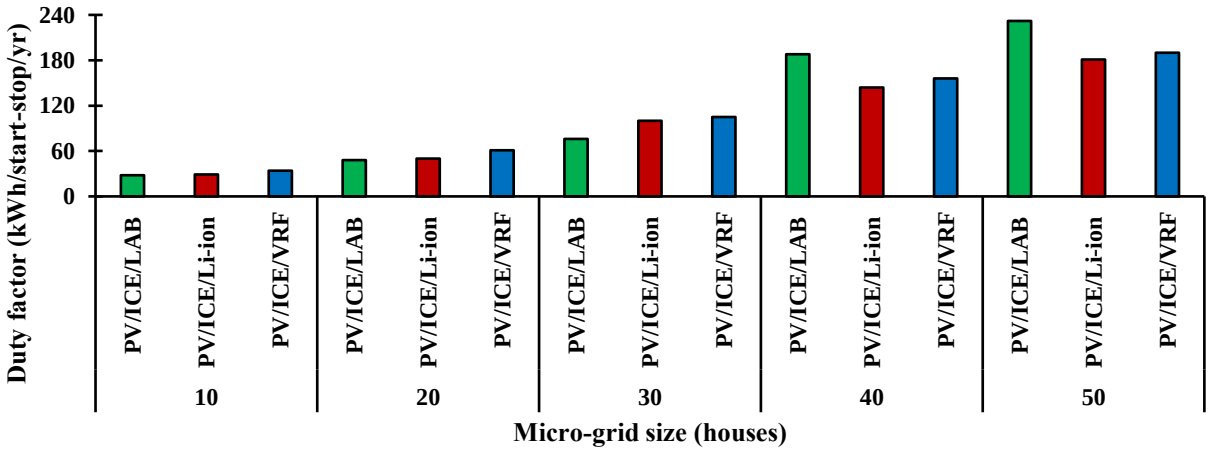

Fig. 6.9: Duty Factor (DF) for hybridised systems with different batteries and changing load demands.

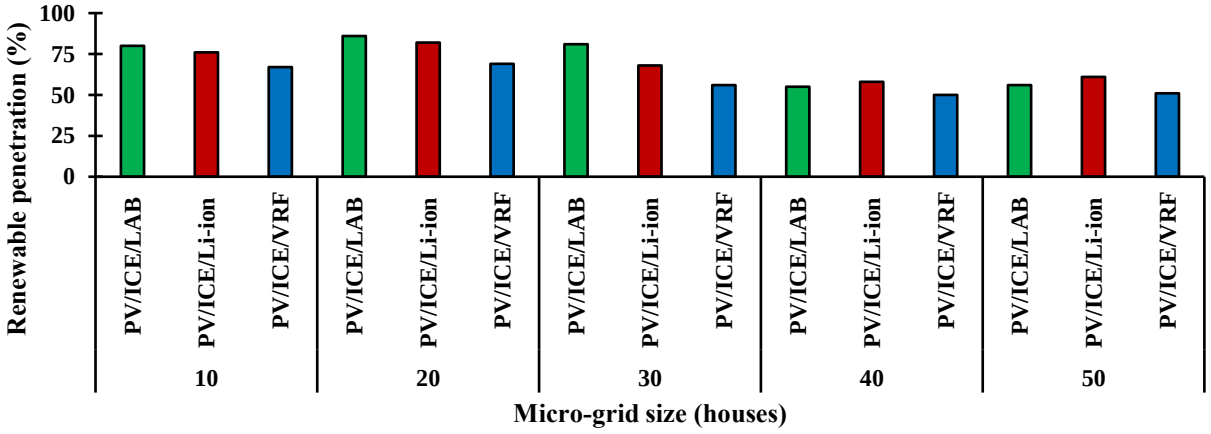

Fig. 6.10: Renewable Penetration (RP) for hybridised systems with different batteries and changing load demands.

6.3.3 Sensitivity to hardware and operational costs

The last part of this study examines whether changes to several cost components affects the likely COE. These varied parameters are capital cost, PV cost, battery cost, and fuel cost on the COE for the base-load scenario of 10 houses. It is clear from Figure 6.11(a) that the capital cost has significant effects on the COE for all the system configurations. A 40 % reduction in capital cost would decrease the COE

by 32 %, 31 %, and 24 %for PV/ICE/Li-ion, PV/ICE/LAB, and PV/ICE/VRF-based hybridised systems, respectively. The larger difference is appeared in VFR-based system because of the higher capital cost of the system components for the PV/ICE/VRF system compared to the former two systems. The results indicate that the variation of battery costs might have a considerable effect on the COE for the three different configurations. The COE of the PV/ICE/VRF system is more visibly affected by a variation in battery cost than the other two systems, as shown in Figure 6.11(b). A further 40 % in the cost of the battery for the both PV/ICE/Li-ion and PV/ICE/VRF-based hybridised systems would result in 17 % declines in the COE, whereas for the PV/ICE/LAB the decline would be 15 %. With recent progress in the development of Li-ion and VFR batteries, the capital cost of these batteries will drop considerably compared to the LAB, as the technology is now well-developed. Therefore, a 20 % reduction in VRF cost would match the base case COE of the PV/ICE/LAB–based hybridised system. This reduction of Li-ion battery cost however gives major boost for the application of stand-alone hybrid systems. Additionally, the replacement and operating cost for a LAB is much higher than the equivalent costs for Li-ion and VRF batteries as the lifetime of the LAB is lower than the costs for the Li-ion and VRF batteries. PV module cost also affects the COE to some extent in all cases. As the PV capacities for all the scenarios are similar, the changes are also alike, as shown in Figure 6.11(c). It is also evident from this analysis that variations in the fuel price have some effects on the COE for all system configurations. However, the changes are higher for the PV/ICE/VRF hybridised system compared to other two systems shown in Figure 6.11(d). This is because of the greater contribution of the ICE which is attributed to higher fuel consumption.

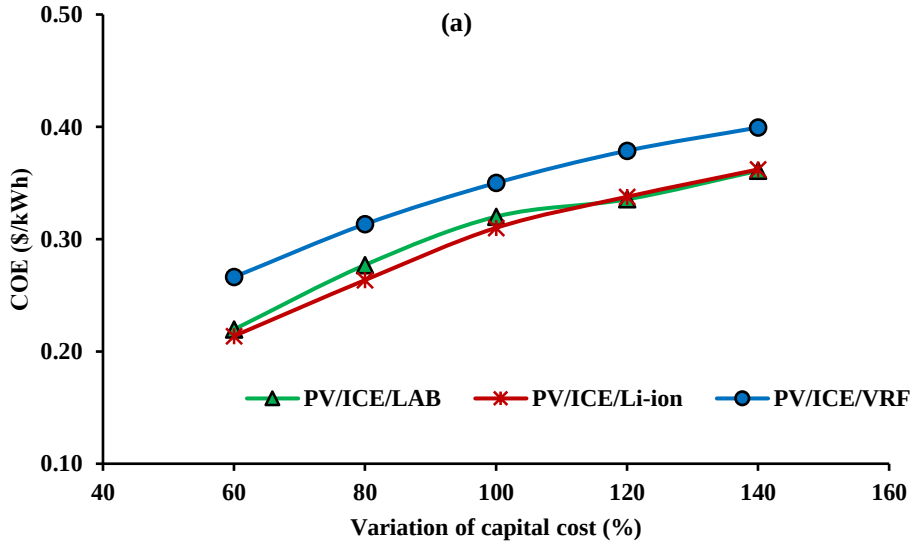

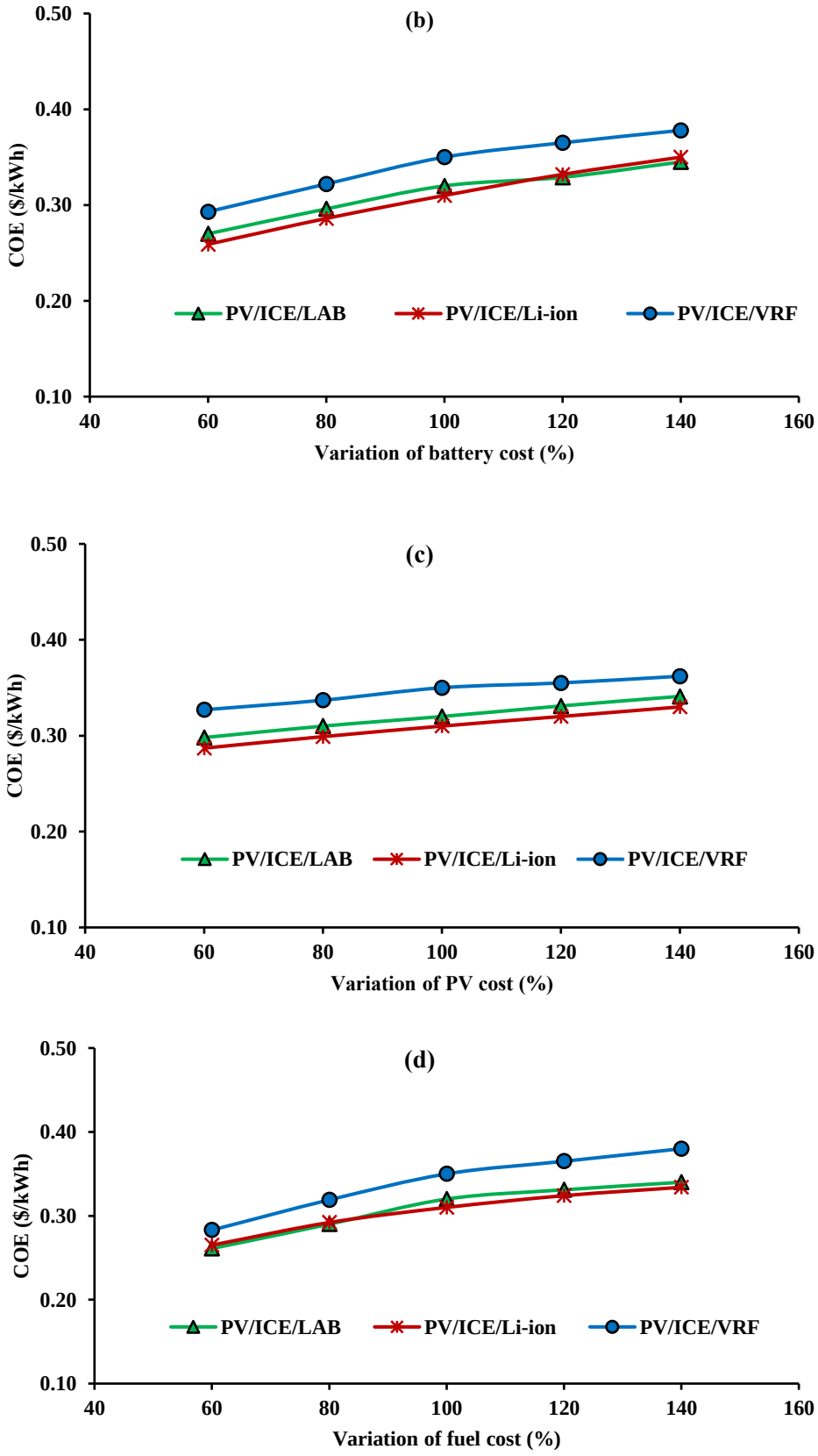

Fig. 6.11: Sensitivity analysis for variations to (a) capital cost (b) battery cost, (c) PV, and (d) fuel cost on COE for PV/ICE/LAB, PV/ICE/Li-ion, and PV/ICE/VRF–based hybrid systems for the baseline 10 house micro-grid.

6.4 Conclusions

The effects of three battery technologies (LAB, Li-ion, and VRF) and load scalability (10 to 50 houses) on the performance of a hybridised stand-alone micro-grid have been analysed. The main outcomes of this study are summarised as follows:

- The COE for both PV/ICE/LAB and PV/ICE/Li-ion systems is comparable. This appears true across all scales considered and even when up to ±40 % variations are applied to the baseline case (10 house micro-grid) in terms of changes to the cost of PV panels, batteries, and diesel fuels. The PV/ICE/VRF system is more sensitive to variations in capital and battery costs than the systems based on LAB and Li-ion batteries. The results also show that the COE is less sensitive to variations in PV module costs, while fuel costs have some effects on COE for all the three hybridised systems.
- Despite the higher replacement costs of PV/ICE/LAB, these appear to be offset by the much higher capital costs associated with PV/ICE/Li-ion and PV/ICE/VRF batteries. The net result appears as a relatively similar COE for both PV/ICE/LAB and PV/ICE/Li-ion systems.
- Whilst the study did not consider the lifecycle emissions associated with each battery technology, it appears that operational emissions (ICE fuel combustion) are lowest with PV/ICE/LAB systems compared to others. This is also reflected through these systems (based on LAB technology) having the best renewable energy penetration (80 %) compared to PV/ICE/Li-ion (76 %) and PV/ICE/VRF systems (67 %). Systems integrating LAB's also have the lowest excess (dumped) energy. Contributing to this may be the need to maintain higher overall (a range) battery state of charge in LAB systems.

The above summary observations indicate that optimisations which do not include life cycle emissions (within single- or multi-objectives) are unlikely to yield much variations in COE between LAB and Li-ion storage when integrated in hybridised systems. Additional research on stand-alone hybridised systems based on multi-objective optimisations that consider cradle-to-grave (life cycle) impacts of different battery technologies is warranted. This is supported by the significantly higher replacement costs and shorter lifetimes associated with LAB systems. To exemplify, the replacement and O&M costs for the PV/ICE/VRF-based system ($12,374 and $9,600, respectively) are lower than equivalent costs for the PV/ICE/LAB system and the PV/ICE/Li-ion system (replacement cost for PV/ICE/LAB is $67,445 and O&M cost is $16,863; replacement cost for PV/ICE/Li-ion is $38,048 and O&M cost is $2,273). However, the results presented in this study which are based on a limited number of constraints and hardware specifications may also indicate that where stand-alone hybrid systems are sized (without including life cycle emissions as an objective function), the impact of whether LAB or Li-ion batteries are used may have limited impact on the outcomes. Further research is warranted to resolve this.

Chapter references

[1] Vorrath, S. *Australia's top 20 greenhouse gas emitters*. 2015 [cited 2017 25.05]; Available from: 25.05.2017 https://reneweconomy.com.au/graph-of-the-day-australias-top-20-greenhouse-gas-emitters-98644/.

[2] Bajpai, P. and V. Dash, *Hybrid renewable energy systems for power generation in stand-alone applications: a review*. Renewable and Sustainable Energy Reviews, 2012. **16**(5): p. 2926-2939.

[3] Hoque, S.N. and B.K. Das, *Analysis of Cost, Energy and Emission of Solar Home Systems in Bangladesh*. International Journal of Renewable Energy Research 2013. **3**(2): p. 347-352.

[4] Kang, L., et al., *Effects of load following operational strategy on CCHP system with an auxiliary ground source heat pump considering carbon tax and electricity feed in tariff*. Applied Energy, 2017. **194**: p. 454-466.

[5] *Renewable energy investement opprtunities in South Australia*. [cited 2018 25.03]; Available from: 25.03.2018 https://invest.sa.gov.au/wp-content/uploads/2017/11/Renewable-energy.pdf.

[6] *State of the Energy Market, May 2017*. [cited 2018 10.03]; Available from: 10.03.2018 https://www.aer.gov.au/system/files/AER%20State%20of%20the%20energy%20market%202017%20-%20A4.pdf.

[7] *South Australian Electricity Report*. [cited 2018 10.01]; Available from: 10.01.2018 http://www.aemo.com.au/-/media/Files/Electricity/NEM/Planning_and_Forecasting/SA_Advisory/2017/South-Australian-Electricity-Report-2017.pdf.

[8] *Hornsdale Power Reserve* [cited 2018 12.01]; Available from: 25.01.2018 https://hornsdalepowerreserve.com.au/.

[9] Brka, A., Y.M. Al-Abdeli, and G. Kothapalli, *The interplay between renewables penetration, costing and emissions in the sizing of stand-alone hydrogen systems*. International Journal of Hydrogen Energy, 2015. **40**(1): p. 125-135.

[10] Das, B.K., Y.M. Al-Abdeli, and G. Kothapalli, *Optimisation of stand-alone hybrid energy systems supplemented by combustion-based prime movers*. Applied Energy, 2017. **196**: p. 18–33.

[11] Das, B.K. and Y.M. Al-Abdeli, *Optimisation of stand-alone hybrid CHP systems meeting electric and heating loads*. Energy Conversion and Management, 2017. **153**: p. 391-408.

[12] Mandal, S., B.K. Das, and N. Hoque, *Optimum sizing of a stand-alone hybrid energy system for rural electrification in Bangladesh*. Journal of Cleaner Production, 2018. **200**: p. 12-27.

[13] Brka, A., Y.M. Al-Abdeli, and G. Kothapalli, *Influence of neural network training parameters on short-term wind forecasting*. International Journal of Sustainable Energy, 2016. **35**(2): p. 115-131.

[14] Brka, A., Y.M. Al-Abdeli, and G. Kothapalli, *Predictive power management strategies for stand-alone hydrogen systems: Operational impact*. International Journal of Hydrogen Energy, 2016. **41**(16): p. 6685-6698.

[15] Brka, A., G. Kothapalli, and Y.M. Al-Abdeli, *Predictive power management strategies for stand-alone hydrogen systems: Lab-scale validation*. International Journal of Hydrogen Energy, 2015. **40**(32): p. 9907-9916.

[16] Nema, P., R. Nema, and S. Rangnekar, *A current and future state of art development of hybrid energy system using wind and PV-solar: A review*. Renewable and Sustainable Energy Reviews, 2009. **13**(8): p. 2096-2103.

[17] Vazquez, S., et al., *Energy storage systems for transport and grid applications*. Industrial Electronics, IEEE Transactions on, 2010. **57**(12): p. 3881-3895.

[18] Courtecuisse, V., et al., *A methodology to design a fuzzy logic based supervision of Hybrid Renewable Energy Systems*. Mathematics and Computers in Simulation, 2010. **81**(2): p. 208-224.

[19] Hadjipaschalis, I., A. Poullikkas, and V. Efthimiou, *Overview of current and future energy storage technologies for electric power applications*. Renewable and Sustainable Energy Reviews, 2009. **13**(6): p. 1513-1522.

[20] Kazempour, S.J., et al., *Electric energy storage systems in a market-based economy: Comparison of emerging and traditional technologies.* Renewable Energy, 2009. **34**(12): p. 2630-2639.
[21] Barote, L., et al. *Stand-alone wind system with vanadium redox battery energy storage*. in *Optimization of Electrical and Electronic Equipment, 2008. OPTIM 2008. 11th International Conference on*. 2008. IEEE.
[22] Li, W. and G. Joos. *A power electronic interface for a battery supercapacitor hybrid energy storage system for wind applications*. in *Power Electronics Specialists Conference, 2008. PESC 2008. IEEE*. 2008. IEEE.
[23] Chauhan, A. and R. Saini, *A review on integrated renewable energy system based power generation for stand-alone applications: configurations, storage options, sizing methodologies and control.* Renewable and Sustainable Energy Reviews, 2014. **38**: p. 99-120.
[24] Bernal-Agustín, J.L. and R. Dufo-López, *Simulation and optimization of stand-alone hybrid renewable energy systems.* Renewable and Sustainable Energy Reviews, 2009. **13**(8): p. 2111-2118.
[25] Bhattacharjee, S. and S. Acharya, *PV–wind hybrid power option for a low wind topography.* Energy Conversion and Management, 2015. **89**: p. 942-954.
[26] Ma, T., H. Yang, and L. Lu, *Study on stand-alone power supply options for an isolated community*. International Journal of Electrical Power & Energy Systems, 2015. **65**: p. 1-11.
[27] Shezan, S., N. Das, and H. Mahmudul, *Techno-economic analysis of a smart-grid hybrid renewable energy system for Brisbane of Australia.* Energy Procedia, 2017. **110**: p. 340-345.
[28] Das, B.K., et al., *A techno-economic feasibility of a stand-alone hybrid power generation for remote area application in Bangladesh.* Energy, 2017. **134**: p. 775-788.
[29] Yilmaz, S. and F. Dincer, *Optimal design of hybrid PV-Diesel-Battery systems for isolated lands: A case study for Kilis, Turkey.* Renewable and Sustainable Energy Reviews, 2017. **77**: p. 344-352.
[30] Rehman, S. and L.M. Al-Hadhrami, *Study of a solar PV–diesel–battery hybrid power system for a remotely located population near Rafha, Saudi Arabia.* Energy, 2010. **35**(12): p. 4986-4995.
[31] Deshmukh, M.K. and S.S. Deshmukh, *Modeling of hybrid renewable energy systems.* Renewable and Sustainable Energy Reviews, 2008. **12**(1): p. 235-249.
[32] Shaahid, S. and M. Elhadidy, *Optimal sizing of battery storage for stand-alone hybrid (photo-voltaic+ diesel) power systems.* International Journal of Sustainable Energy, 2005. **24**(3): p. 155-166.
[33] Hiendro, A., et al., *Techno-economic analysis of photovoltaic/wind hybrid system for onshore/remote area in Indonesia.* Energy, 2013. **59**: p. 652-657.
[34] Li, C., et al., *Techno-economic feasibility study of autonomous hybrid wind/PV/battery power system for a household in Urumqi, China.* Energy, 2013. **55**: p. 263-272.
[35] Rohani, G. and M. Nour, *Techno-economical analysis of stand-alone hybrid renewable power system for Ras Musherib in United Arab Emirates.* Energy, 2014. **64**: p. 828-841.
[36] Suresh Kumar, U. and P.S. Manoharan, *Economic analysis of hybrid power systems (PV/diesel) in different climatic zones of Tamil Nadu.* Energy Conversion and Management, 2014. **80**: p. 469-476.
[37] Halabi, L.M., et al., *Performance analysis of hybrid PV/diesel/battery system using HOMER: A case study Sabah, Malaysia.* Energy Conversion and Management, 2017. **144**: p. 322-339.
[38] Nandi, S.K. and H.R. Ghosh, *Prospect of wind–PV-battery hybrid power system as an alternative to grid extension in Bangladesh.* Energy, 2010. **35**(7): p. 3040-3047.
[39] Testa, A., et al. *Optimal design of energy storage systems for stand-alone hybrid wind/PV generators*. in *Power Electronics Electrical Drives Automation and Motion (SPEEDAM), 2010 International Symposium on*. 2010. IEEE.
[40] Garimella, N. and N.-K.C. Nair. *Assessment of battery energy storage systems for small-scale renewable energy integration*. in *TENCON 2009-2009 IEEE Region 10 Conference*. 2009. IEEE.
[41] Fabjan, C., et al., *The vanadium redox-battery: an efficient storage unit for photovoltaic systems.* Electrochimica Acta, 2001. **47**(5): p. 825-831.

[42] Kear, G., A.A. Shah, and F.C. Walsh, *Development of the all-vanadium redox flow battery for energy storage: a review of technological, financial and policy aspects.* International Journal of Energy Research, 2012. **36**(11): p. 1105-1120.
[43] Merei, G., C. Berger, and D.U. Sauer, *Optimization of an off-grid hybrid PV–Wind–Diesel system with different battery technologies using genetic algorithm.* Solar Energy, 2013. **97**: p. 460-473.
[44] Nair, N.-K.C. and N. Garimella, *Battery energy storage systems: Assessment for small-scale renewable energy integration.* Energy and Buildings, 2010. **42**(11): p. 2124-2130.
[45] Rezzouk, H. and A. Mellit, *Feasibility study and sensitivity analysis of a stand-alone photovoltaic–diesel–battery hybrid energy system in the north of Algeria.* Renewable and Sustainable Energy Reviews, 2015. **43**: p. 1134-1150.
[46] Haghighat Mamaghani, A., et al., *Techno-economic feasibility of photovoltaic, wind, diesel and hybrid electrification systems for off-grid rural electrification in Colombia.* Renewable Energy, 2016. **97**: p. 293-305.
[47] Shezan, S.A., et al., *Performance analysis of an off-grid wind-PV (photovoltaic)-diesel-battery hybrid energy system feasible for remote areas.* Journal of Cleaner Production, 2016. **125**: p. 121-132.
[48] Ramli, M.A.M., A. Hiendro, and Y.A. Al-Turki, *Techno-economic energy analysis of wind/solar hybrid system: Case study for western coastal area of Saudi Arabia.* Renewable Energy, 2016. **91**: p. 374-385.
[49] Ramli, M.A.M., A. Hiendro, and S. Twaha, *Economic analysis of PV/diesel hybrid system with flywheel energy storage.* Renewable Energy, 2015. **78**: p. 398-405.
[50] Khan, M.R.B., et al., *Optimal combination of solar, wind, micro-hydro and diesel systems based on actual seasonal load profiles for a resort island in the South China Sea.* Energy, 2015. **82**: p. 80-97.
[51] Ma, T., et al., *Technical feasibility study on a standalone hybrid solar-wind system with pumped hydro storage for a remote island in Hong Kong.* Renewable Energy, 2014. **69**: p. 7-15.
[52] Halabi, L.M. and S. Mekhilef, *Flexible hybrid renewable energy system design for a typical remote village located in tropical climate.* Journal of Cleaner Production, 2017.
[53] Baneshi, M. and F. Hadianfard, *Techno-economic feasibility of hybrid diesel/PV/wind/battery electricity generation systems for non-residential large electricity consumers under southern Iran climate conditions.* Energy Conversion and Management, 2016. **127**: p. 233-244.
[54] Singh, S., M. Singh, and S.C. Kaushik, *Feasibility study of an islanded microgrid in rural area consisting of PV, wind, biomass and battery energy storage system.* Energy Conversion and Management, 2016. **128**: p. 178-190.
[55] Ngan, M.S. and C.W. Tan, *Assessment of economic viability for PV/wind/diesel hybrid energy system in southern Peninsular Malaysia.* Renewable and Sustainable Energy Reviews, 2012. **16**(1): p. 634-647.
[56] Woolridge, M., *Modelling of stand-alone hybrid renewable energy systems (Bachelor thesis in School of Engineering).* 2017, Edith Cowan University: Joondalup, Australia.
[57] *HOMER Pro*. [cited 2017 12.03]; Available from: 12.03.2017 https://www.homerenergy.com/products/pro/index.html.
[58] *BOM.South Australia weather and warnings* Available from: 12.12.2018. http://reg.bom.gov.au/climate/reg/oneminsolar/.
[59] *HOMER's Calculations*. [cited 2018 12.01]; Available from: 12.01.2018 https://www.homerenergy.com/products/pro/docs/3.11/homers_calculations.html.
[60] Duffie, J.A. and W.A. Beckman, *Solar engineering of thermal processes*. 2013: John Wiley & Sons.
[61] Dufo-López, R., et al., *Multi-objective optimization minimizing cost and life cycle emissions of stand-alone PV–wind–diesel systems with batteries storage.* Applied Energy, 2011. **88**(11): p. 4033-4041.
[62] Arun, P., R. Banerjee, and S. Bandyopadhyay, *Optimum sizing of battery-integrated diesel generator for remote electrification through design-space approach.* Energy, 2008. **33**(7): p. 1155-1168.
[63] *Euro Solar*. [cited 2017 25.10]; Available from: 25.10.2017 https://www.eurosolar.com.au/.

[64] Rajbongshi, R., D. Borgohain, and S. Mahapatra, *Optimization of PV-biomass-diesel and grid base hybrid energy systems for rural electrification by using HOMER.* Energy, 2017. **126**: p. 461-474.
[65] *Wholesale Solar. Trojan Battery Company L16P-AC Trojan Deep Cycle battery Battery*. [cited 2017 10.12]; Available from: 12.10.2017 https://www.wholesalesolar.com/9921655/trojan-battery-company/batteries/trojan-battery-company-l16p-ac-trojan-deep-cycle-battery-battery.
[66] *redT Energy Storage*. [cited 2017 28.10]; Available from: 20.10.2017 https://redtenergy.com/.
[67] Lee, J. *Vanadium Batteries to Power $27 billion Off-Grid Energy Market.* [cited 2017 28.09]; Available from: 28.09.2017 http://www.kitco.com/commentaries/2017-01-24/Vanadium-Batteries-to-Power-27-billion-Off-Grid-Energy-Market.html.
[68] Badrinarayanan, R., et al., *Extended dynamic model for ion diffusion in all-vanadium redox flow battery including the effects of temperature and bulk electrolyte transfer*. Journal of Power Sources, 2014. **270**: p. 576-586.
[69] Tian, X., et al., *The lead-acid battery industry in China: outlook for production and recycling.* Waste Management & Research, 2015. **33**(11): p. 986-994.
[70] Gottesfeld, P. and A.K. Pokhrel, *Lead exposure in battery manufacturing and recycling in developing countries and among children in nearby communities.* Journal of occupational and environmental hygiene, 2011. **8**(9): p. 520-532.
[71] Tian, X., et al., *Environmental impact and economic assessment of secondary lead production: Comparison of main spent lead-acid battery recycling processes in China.* Journal of cleaner production, 2017. **144**: p. 142-148.
[72] Peters, J.F., et al., *The environmental impact of Li-Ion batteries and the role of key parameters–A review.* Renewable and Sustainable Energy Reviews, 2017. **67**: p. 491-506.
[73] Katsigiannis, Y., P. Georgilakis, and E. Karapidakis, *Multiobjective genetic algorithm solution to the optimum economic and environmental performance problem of small autonomous hybrid power systems with renewables.* Renewable Power Generation, IET, 2010. **4**(5): p. 404-419.
[74] Blomgren, G.E., *The development and future of lithium ion batteries.* Journal of The Electrochemical Society, 2017. **164**(1): p. A5019-A5025.
[75] Choi, C., et al., *A review of vanadium electrolytes for vanadium redox flow batteries.* Renewable and Sustainable Energy Reviews, 2017. **69**: p. 263-274.

Chapter 7: General Discussions

The study focuses on several key issues related to optimally sizing stand-alone hybridised power, power and heat (CHP), and power, heating, and cooling (CCHP) systems. The significance of the study is presented in **Section 1.5**. Although earlier research on stand-alone hybridised power systems has been conducted, very few of the studies available in the literature focus on stand-alone hybridised CHP, and CCHP systems. Moreover, the study also investigates the effects of various parameters while sizing the optimal power, CHP, and CCHP systems when meeting reliability constraints, which is unnoticed in a number of studies in the literature. The primary objective of this project is to investigate the optimal system configurations using Genetic Algorithms (GA) whilst examining the effects of a number of parameters which influence sizing while satisfying a dynamic load profiles (i.e. electric, heating, and cooling). The PhD project also includes an extension to identify the impact of different battery technologies on optimisation conducted using HOMER.

The specific results of each chapter have already been discussed. This chapter is focused on the overall representation of fundamental outcomes from this study and their integration. In this regard, the key research questions presented in **Chapter 1** are also addressed in the subsequent sections.

7.1 Stand-alone systems meeting electric load only

When using single objective Genetic Algorithms (GAs) to optimally size systems satisfying highly dynamic electric load, the study first analyses the effects of several key factors on the Cost of Energy, reliability of meeting demand, renewable penetration, duty factors, and environmental impact (**Chapter 2**). The study also includes the optimisation of a hybrid system using HOMER with different battery technology (**Chapter 6**). In the following discussion, the issues related to research questions RQ 1 and RQ 5 have been addressed.

- **Cost of Energy:** The results of this study show in **Chapter 2** that the type of prime movers (i.e. ICE or MGT) and their configurations have significant effect on Cost of Energy (Table 2.4). The cost for renewably-based system with battery storage is comparable with the ICE-based hybrid energy systems regardless of a single large unit or multiple units used in tandem. However, the COE for ICE-based hybrid system is considerably lower than the MGT-based system. From the sensitivity analysis it can be said that the changes of interest rate and overall capital costs of components have noticeable effect on the COE for both scenarios while the other parameters (fuel cost, PV costs, and capital costs of ICE) have the least effect (Figure 2.9).
- **Performance indicators:** Combustion based hybridised systems produce significant amounts of waste heat as well as CO_2 (operational) and life cycle emissions, even though the COE may

be similar to PV/Batt systems. This is likely to be exacerbated if a thermal load (through cogeneration or trigeneration) also needs to be met, which then impacts overall efficiency not just COE. The results of this study indicate that the ICE-based system is more environmentally sustainable than the MGT-based hybrid system (Table 2.4). Although, the COE for the MGT based hybrid system is much higher than the hybrid ICE system, the MGT produces 316% waste heat to the electric power supplied by it. This figure is considerably lower for the ICE (129% waste heat to supplied electric power) and could possibly make the MGT system a more favourable supplementary device for cogeneration applications (Table 2.4).

- **Hardware parameters:** The COE for system consisting single unit supplementary prime mover is comparable to the similar capacity multiple prime movers operating in tandem (Table 2.4). However, the waste heat generation from the multiple units of supplementary prime movers is significantly higher than a single capacity engine at the cost of LCE. This is because of lower starting threshold constraints of ICEs or MGTs, which force to start engines when the load demand is lower (i.e. 9kW for 30kW engine) than the larger single capacity engine (i.e.18kW for 60-65kW). The transient start-up of supplementary prime movers have insignificant effects on sizing for both PV/Batt/ICE and PV/Batt/MGT-based hybrid systems, which account missed load 35kWh and 210kWh, respectively, over the year. The loss of load demand due to the transient behaviour of prime movers are well below the loss of power supply constraints (760kWh, LPSP: 0.01±0.005) considered in this analysis for system sizing. Although the minimum starting threshold ($P_{sup,\ min}$) of supplementary prime movers has no considerable effects (4–7%) on COE, it does on the LCE and operational CO_2 emissions (Figure 2.7) because of the higher running at lower $P_{sup,\ min}$. From this study in **Chapter 2** indicate that the effects of $P_{sup,\ min}$ for the system involves ICE is less pronounce in relation to the waste heat generation to the supplied power. However, this effect is more significant for MGT-based hybrid system that ICE-based system (Figure 2.7 (d)). This is due to the engine characteristics that produce more heat to power for MGT than the ICE.
- **Optimisation methods:** The study presented above is carried out using population size 10 as there appears no appreciable further improvement of objective function (Cost of Energy) but the time is considerable higher at larger population size than 10 (**Appendix E**). The effects of temporal resolution (60min vs 15min) of meteorological (i.e. solar irradiation, wind velocity, and ambient temperature) and electric load data have been discussed in **Chapter 2** (Figure 2.8). The results from this indicate that this effect is insignificant on the COE and the waste heat generation. However, there are noticeable effects on emissions for both PV/Batt/ICE and PV/Batt/MGT-based hybrid systems which lead to further investigation of this study using 15min resolution for CHP (**Chapter 3**) and CCHP (**Chapters 4** and **5**) systems. **Chapter 6** investigates a stand-alone PV/ICE system with different battery technologies (i.e. Lead acid, Li-ion, Vanadium redox flow) both economically and environmentally. Optimisation of this

study reveals that both Lead Acid Battery (LAB) and Li-ion-based hybridised system has comparable COE, whereas, the system involves Vanadium Redox Flow (VRF) battery cost is relatively higher because of the higher capital cost of battery (Table 6.5). Although capital and annualised costs associated with PV/ICE/Li-ion and PV/ICE/VRF-based systems are higher than the PV/ICE/LAB-based systems, the replacement and O & M costs are considerably lower in systems involves in Li-ion and VRF than the LAB (Tables 6.5 and 6.6). Although the COE and NPC for the PV/ICE/Li-ion is comparable to the PV/ICE/LAB, the affordability (lower battery capital cost) availability across the world, and extensive study of using lead acid battery (Table 6.2) encourages further study with lead acid battery.

7.2 Stand-alone energy system meeting electric and heating loads (CHP)

When using both single- and double-objective GA optimisations applied to systems featuring waste heat (generated by the supplementary prime movers), the project also considered two types of Power Management Strategies, namely Following Electric Load (FEL) and Following Electric and Thermal Load (FEL/FTL). These studies are carried out using multiple units of supplementary prime movers. The results reported in **Chapter 2** showed waste heat generation from combustion based prime movers (ICE and MGT) differs based on their capacity (using larger units compared to smaller capacity engines, for similar overall capacity). All analyses were undertaken while sizing the optimised hybridised CHP systems when satisfying a specified reliability (LPSP: 0.01±0.005). The research further considers relative magnitude of electric and heating loads to examine the seasonal effects on system sizing. In this section, **RQ 2** has been identified.

- **Cost of Energy:** The results presented in **Chapter 3** indicate that the load following strategies have marginal effects on COE. This is also true when the system is sizing using single- or multi-objective optimisation techniques. Additionally, the COE is comparable for PV/Batt/ICE and PV/Batt/MGT regardless of Power Management Strategies and optimisation techniques (Figure 3.6 (a)).
- **Performance indicators:** The PMS has significant effects on overall CHP system efficiency. The hybridisation of PMS (FEL/FTL) results in considerably higher overall CHP efficiency than the FEL type PMS. This outcome is more articulated for PV/Batt/ICE-based hybridised CHP system (32% higher in FEL/FTL than FEL strategies). The overall efficiency for hybridised system involves ICE is higher compared to MGT-based hybrid system. This is due to the higher electric efficiency of ICE (~35%) than the MGT (~25%). Results also indicate that the type of PMS affects the Life Cycle Emissions and waste heat generation (Figure 3.6). The biggest improvements in relation to meeting thermal demand achieved when the system is operating in FEL/FTL type PMS. This is also true for both single- and multi-objective

optimisations and the type of prime movers. Similar outcomes also appear for emissions. The relative changes of electric and thermal loads do not affects COE for the PV/Batt/ICE-based systems but have considerable effects for MGT-based systems. However, the overall efficiency is consistently better in higher thermal demand (i.e. lower ETLR) compared to higher electric demand. The higher environmental benefits attained in a system where the thermal demand is bigger than the electric demand (Figure 3.8). The energy generation from supplementary prime mover at lower ETLR is relatively lesser due to the constraints considered ($P_{sup,min}$) in which the electric load is more likely to fall below this threshold. In this context, the PMS forces to select large number of PV modules and battery bank up to the constraints (Table 3.2) and then the number of supplementary prime movers to meet the specified reliability (LPSP: 0.01±0.005). This is also attributed to the higher cost for MGT-based systems as the capital cost of MGT is substantially higher than the ICE (Table 3.5). The ETLR has insignificant effects on the Renewable Penetration (RP) (Table 3.4). However, there are notable effects on satisfying load demands (LPSP) as the ETLR decreases, the LPSP also declines. This is more likely to be occurred at lower ETLR because the GA optimisation cannot select the components beyond the constraints.

- **Optimisation methods:** Whilst the system operating FEL/FTL type PMS have no significant improvement in COE and overall efficiency between single- and multi-objective optimisation techniques, the recovered waste to meet the thermal demand is marginally higher in multi-objective optimisation (Table 3.3). In this process of optimisation, the algorithm attempts to make the most use of recovered waste heat generation so as to maximize the overall CHP efficiency. This is attributed to the higher contribution of energy from the supplementary prime movers in multi-objective optimisation compared to the single objective technique. Therefore, the optimisation techniques affect sizing of CHP system components.

7.3 Stand-alone energy systems meeting electric, heating, and cooling loads (CCHP)

The results discussed above largely based on the stand-alone systems sizing meeting electric and heating loads only using largely single objective Genetic Algorithms (GAs). The outcomes presented in **Chapter 4** analyses the effects of different load following strategies (i.e. FEL/FTL and FEL), hardware components, and changing the relative magnitudes of heating and cooling loads with same electric load using multi-objective optimisation (i.e. Cost of Energy and overall CHP/CCHP efficiency). This project uses a reliability constraint while meeting highly dynamic electric, heating, and cooling loads reported in Equation 4.15 and a detailed PMS to optimise the system configurations (Figure 4.5). The results compare CHP system with a system adding absorption thus meeting the cooling load through it. In **Chapter 5**, the research is investigated considering three objective functions of Cost of Energy ($/kWh), overall system energy efficiency (%) and exergy efficiency (%) of a stand-alone hybridised system

(PV/Batt/MGT) of power only (electric load only), CHP (electric and heating loads), and CCHP (electric, heating, and cooling) systems. The loads and meteorological data taken in this study are highly dynamic and a specific load demand reliability (LPSP) is considered while meeting the load requirements. A hybrid type PMS of FEL/FTL is used for analysis. A sensitivity of using double- vs triple-objective functions is carried out. Further analysis is done with changing relative magnitude of heating and cooling loads on sizing optimisation of a hybridised CCHP systems. The analysis presented in the subsequent sections is addressed the research questions **RQ 3** and **RQ 4**.

- **Cost of Energy:** The results presented in **Chapter 4** indicate that there is significant difference of COE for stand-alone hybrid CCHP systems operating between FEL/FTL and FEL strategies (Figure 4.7). However, the system operating CHP mode achieves marginal improvements (11%) in COE than the CCHP systems for both PV/Batt/ICE and PV/Batt/MGT-based configurations while operating FEL/FTL type PMS. The results indicate that a stand-alone hybridised system meeting electric load only (Power only system) has a lower COE than a CHP (meeting electric and heating loads) a CCHP (meeting electric, heating, and cooling loads) systems (Figure 5.7(a)). Although the cost is higher in a CCHP system, this system would benefit with higher efficiency, higher renewable penetration, and lower operational emissions than a CHP system and a power only system (Table 5.4 and Figure 5.7). However, Figure 5.7(c) indicates that the overall exergy efficiency in a CCHP system is lower than a CHP system and comparable with the power only system configuration. These trends are also true for systems with higher capacity supplementary prime movers (MGT 65kW). Even though the overall system energy and exergy efficiency for all configurations are comparable with MGT 65kW and MGT 30kW-based systems, the COE for the MGT 65kW-based systems is higher than MGT 30kW-based systems (Figure 5.7).
- **Performance indicators:** The interesting result evident from this study (Figure 4.7) is that the operational emissions (fuel dependant emissions) are lower in CHP compared to CCHP system unlike the other studies found in literature. This is because meeting cooling demand through electric chillers (powered by PV or battery) means the equivalent electric demand is higher compared to the cooling demand satisfying by the absorption chiller. In this context, the supplementary prime movers can run less frequently (the range constraints tested in GA modelling) in CHP systems compared to CCHP systems. It is also evident from Table 4.4 that the CHP systems have higher Renewable Penetration, lower fuel usage, and lower recovered waste heat to thermal demand in CHP than the CCHP systems. For both PV/Batt/ICE and PV/Batt/MGT-based hybridised CCHP systems, the lower COE and the higher overall efficiency in FEL/FTL are achieved at the expense of operational emissions (i.e. CO_2, NO_x) than the FEL type PMS (Figure 4.7). This is due to the higher running hour under FEL/FTL strategy which is attributed to higher fuel consumption and consequently the greater operational

emissions than FEL. However, the CCHP systems in FEL/FTL strategy have higher Duty Factor and lower transient start-ups than FEL. This indicates that once the supplementary prime movers start, it runs maximum time in FEL/FTL mode. It is also observed that the Renewable Penetration (RP) is significantly higher in the FEL strategy for both PV/Batt/ICE and PV/Batt/MGT-based CCHP systems compared to the FEL/FTL. This is marginally higher in CHP than the CCHP systems operating in FEL/FTL strategies. Additionally, the RP is slightly higher in PV/Batt/MGT than the PV/Batt/ICE -based systems for both CHP and CCHP configurations irrespective of operating strategies. The results are further extended to examine the effects of changing the relative proportions of heating ($P_{ther,\ h}$) and cooling ($P_{ther,c}$) loads keeping the electric load same. For PV/Batt/ICE-based hybrid CCHP systems, the changing relative ratio of $P_{ther,\ h}$:$P_{ther,c}$ has no significant effects on the COE. These changes have considerable effects on cost for PV/Batt/MGT-based hybrid CCHP systems due to the higher capital cost of MGT and lower electrical efficiency requires larger PV and battery bank than ICE. For both PV/Batt/ICE and PV/Batt/MGT-based CCHP systems, the relative changes of heating and cooling loads has no appreciable effects on the overall CCHP efficiency (Figure 4.8). However, this considerably affects the system sizing as the heating load increases for 30% to 70% of total thermal demands. This increased heating demands lead to smaller proportion of heating demand is met by recovered waste heat and the rest heating demand is satisfied through using PV and battery bank. Thus requires larger number of PV modules and battery bank with the increased heating demand. Additionally, the systems with higher heating than the cooling load have higher Renewable Penetration, lower recovered waste heat to thermal demand, inferior operational emissions, and smaller Duty Factor than the systems with higher cooling demands (Figure 4.8 and Table 4.5). Alternatively, for the larger cooling demand compared to heating demand needs smaller number of PV modules and battery bank because of higher co-efficient of performance of electric chiller (COP=3.5) compared to the electric heater efficiency ($\eta_{wh,sys}$=0.97). It is evident from the results present in **Chapter 5** that changing the relative magnitude of heating and cooling loads of a CCHP system has no significant effects on the COE and the overall energy efficiency. However, the overall exergy efficiency and renewable penetration are increased where the system has higher heating load than the cooling load. Additionally, the CCHP system with higher heating value would be environmentally benefited at the expense of duty factor.

- **Hardware parameters:** The results indicate that the CCHP systems (using an absorption chiller) in FEL/FTL have some developments in overall system efficiency compared to CHP systems. This difference is less appreciable when the CCHP systems operate FEL and compare with the CHP operate FEL/FTL type PMS (Figure 4.7). The systems involve MGT have always higher COE compared to ICE-based hybridised CHP and CCHP systems regardless of operating strategies. This is because of the higher capital cost of MGT and lower electrical efficiency

compared to ICE (Tables 2.2 and 4.5). Results from **Chapter 5** indicate that the overall energy and exergy efficiencies are higher in CHP and/or CCHP systems than the power only systems.

- **Optimisation methods:** The results achieved with triple-objectives (COE, η, η_{ex}) are comparable to those with double-objective functions (COE, η; or COE, η_{ex}).

In summary, this PhD project has investigated many factors affecting the sizing optimisation of a stand-alone power, CHP, and CCHP systems while meeting highly dynamic load and meteorological data within a specific load reliability. These systems have barely investigated in the current literature where detailed of PMSs are studied and dynamic electric, heating, and cooling loads within a specific load reliability are reported. The proposed system could be benefited to the remote community by improving the overall system efficiency through recovering waste heat and integrating renewable penetration lessen the dependency of fossil fuels with limited application of battery bank. In this way, a stand-alone hybridised CCHP system could reliably supply electric, heating, and cooling demand which is cost-effective and at the same time environmentally sustainable.

Chapter 8: Conclusions and Future Recommendations

8.1 Concluding remarks

This thesis investigates the effects of different types prime movers (i.e. ICE and MGT) when integrated into hybridised systems with PV modules and satisfying highly dynamic electric, heating, and cooling demand in a stand-alone community. The study analyses the impact of incremental increases to simulation complexity and different hardware components on the optimised systems. The meteorological data used in GA part of this work is from a remote location of Western Australia (Broome: 17˚56'S latitude and 122˚14'E longitude) and load profiles from a stand-alone application are incorporated. The load profiles are scaled and post-processed to allow different overall scales to be investigated. The research has been largely focused on using MATLAB-based single- and multi-objective Genetic Algorithms (GA) to address the research questions presented in Chapter 1. The optimisation results of stand-alone hybridised power, CHP, and CCHP systems are reported with several key performance indicators under the specific set of constraints tested. The findings reported in this thesis are summarized as follows:

- **Cost of Energy:** The Cost of Energy is comparable when hybridised systems are sized between a single large capacity and multiple prime movers operating in tandem meeting an electric demand. The other factors such as start-up thresholds, temporal resolution and transient time have insignificant effects on COE when the hybridised system is optimised using single objective optimisation. However, the PV/Batt/ICE-based hybrid system is more cost effective than the PV/Batt/MGT-based system because of higher capital cost of MGT than ICE. When the hybridised system is sized meeting electric and heating loads, the load following strategies have marginal effects on COE. The COE is comparable between PV/Batt/ICE and PV/Batt/MGT regardless of optimisation techniques used. With changing the relative magnitude of electric and heating loads, the COE is comparable for PV/Batt/ICE-based system whereas the COE is higher in larger heating demand for PV/Batt/MGT-based system. The COE for hybridised CHP system is slightly lower compared to the stand-alone CCHP system because of the additional hardware component (absorption chiller) in CCHP. The FEL/FTL type PMS leads to better economic benefits compared to FEL strategy for all system configurations. Additionally, COE is comparable for PV/Batt/ICE system while changing the magnitude of heating and cooling loads. The COE however increases considerably for PV/Batt/MGT-based hybrid CCHP system at the higher thermal load compared to the cooling load. Whilst the system (PV/Batt/MGT) is sized meeting electric, heating, and cooling loads, the COE for power only system is lower than the CHP and the CCHP system configurations. However, the COE is comparable with changing the magnitude of heating and cooling loads. The COE and NPC for

a lead acid battery (PV/ICE) based stand-alone hybridised system meeting power demand only are comparable with the Li-ion based system and lower than a vanadium redox flow based system while the system is optimised using HOMER. The similar trend is appeared when system is sized while changing the scalability of load demand. However, the availability and the lower capital cost of lead acid battery attributed to the extensive use in the hybridised system applications.

- **Overall system efficiency:** The Power Management Strategies strongly affect the system overall efficiency for both PV/Batt/ICE- and PV/Batt/MGT-based hybridised CHP systems using single or multi-objective optimisation techniques. Higher heating loads lead to greater overall CHP efficiency for all hybridised CHP systems. The overall system efficiency is also hardware specific because of their operating characteristics. The stand-alone hybridised CHP system achieves lower cost at the expense of overall system efficiency. The overall system efficiency (CHP/CCHP) is noticeably higher in FEL/FTL type PMS than FEL for both PV/Batt/ICE and PV/Batt/MGT-based hybrid CHP/CCHP systems. However, the system efficiency is not affected by the magnitude of heating and cooling loads. Although a stand-alone CCHP system (PV/Batt/MGT) has higher overall system efficiency than power only and CHP systems, the overall exergy efficiency is lower than the CHP system and comparable with power only system. However, changing the relative magnitude of heating and cooling loads has insignificant effects on overall system energy efficiency; however, these changes affect the overall system exergy efficiency.
- **Consequential performance:** Higher Renewable Penetration in a single larger capacity engine-based hybridised system leads to lower Life Cycle Emissions as well as operational emissions than multiple engine-based hybrid system. However, the waste heat generation is considerable higher in the systems with multiple engine than a single engine. Waste heat generation and emissions are also larger with the lower minimum starting threshold. It is also evident that finer temporal resolution attributed to better environmental benefits. The use of hybrid PMS in CHP system sizing leads to lower LCE compared to FEL type PMS. The system with higher heating load has environmental benefits in single optimisation sizing. Although no significant improvements can be achieved in terms of COE and overall efficiency between single- and multi-objective optimisations, the biggest merits of multi-objective functions are to meeting higher heating demand through recovered waste heat. Higher renewable penetration in CHP system leads to lower operational emissions than CCHP system when operating in FEL/FTL strategy. PV/Batt/MGT-based hybrid CHP/CCHP systems produce lower operational emissions compared to PV/Batt/ICE. Power Management Strategies have significant effects on operational emissions. Additionally, the systems with relatively higher heating demand generate smaller amount of emissions than larger cooling loads. A stand-alone hybridised PV/Batt/MGT power system has higher DF at the expense of operational emissions than a CHP

and a CCHP systems when the systems operating on FEL/FTL type PMS. Lower operational emissions and higher renewable penetration are achieved in a hybridised CCHP system with a higher heating load than a cooling load at the cost of DF. In HOMER optimisation, the PV/ICE/LAB-based system has lower operational emissions and higher renewable penetration than the PV/ICE/Li-ion and the PV/ICE/VRF-based hybridised systems. Both Li-ion and VRF batteries require lower capacity to meet the load demand as they can discharge down to zero and have lower annual depletion rate than a lead acid battery.

8.2 Future recommendations

This PhD project has considered a number of factors, which are contributed to knowledge in designing reliable, cost-effective stand-alone power, CHP, and CCHP systems. However, there are still several areas where further study is warranted bearing in mind the following factors:

- Lab- or pilot-scale application of different Power Management Strategies as discussed in this thesis through experimentation to analyse the COE and system overall efficiency.
- Studies with different system configurations such as wind turbine, solar thermal, hydrogen fuel cells, geothermal energy, heat pump etc.
- Experimentation of energy storage for power quality, voltage stabilisation and integration of number of charging/discharging cycles, and environmental effects on modelling of energy storage system.
- The effects of advanced economical modelling, inflation rates, adding carbon tax, and hourly maintenance cost of hardware components on Cost of Energy.
- Exergy analysis to understand the effect of exergy destruction in each component (both avoidable and unavoidable parts) and optimise the system components to minimise the avoidable exergy destruction.
- Optimised the systems using other intelligent techniques such as Particle Swarm Optimisation (PSO), improved Hybrid Optimisation by Genetic Algorithm (iHOGA), Ant Colony Optimisation (ACO), Simulated Annealing (SA), Differential Evaluation (DE) etc. and compare results with this study. The future works can be extended using different objective functions such as Life Cycle Emissions, exergetic sustainability etc.
- Utilization of Alternative Energy websites as a tool to communicate the trends and findings are identified in this research to further elaborate on trends and statistics studies on the most relevant criteria for the involved stakeholders such as end users, and both public and private investors.

- Analysing the hybridised Power, CHP, and CCHP systems with innovative PV modules including tracking systems, advanced storage devices, and integrated building energy system, and electric vehicle deployment with the system.
- Integrating desalination with the hybridised systems for multi-generation (i.e. power, chilled water, hot water, and drinking water) for the remote coastal area application in developing and underdeveloped countries.
- The impact Predictive Power Management Strategies on economical and operational characteristics of stand-alone power, CHP, and CCHP systems.
- The effects of using advanced Load Following Strategies such as in sizing stand-alone hybridised CCHP systems.
- Analysing the systems with different temporal resolutions, climatic conditions, and a range of magnitudes of load demands.
- Optimised the systems satisfying different load demands such as electric, hot water, space heating, cold water, space cooling with integrating different hardware components and renewables are warranted for further study.

Appendices

Appendix A, B, C, D and F

are not included in this version of the thesis

Appendix E Sensitivity analysis

Chapter 2 makes reference to a basic sensitivity analysis done to examine the effects of population size on the solutions for single objective optimisations. From Figure E.1, it appears that a population size 10 is chosen for system optimisation as no appreciable improvements in the COE (<1%) is achieved with further increase in population of 50, even though at the expense of computational time.

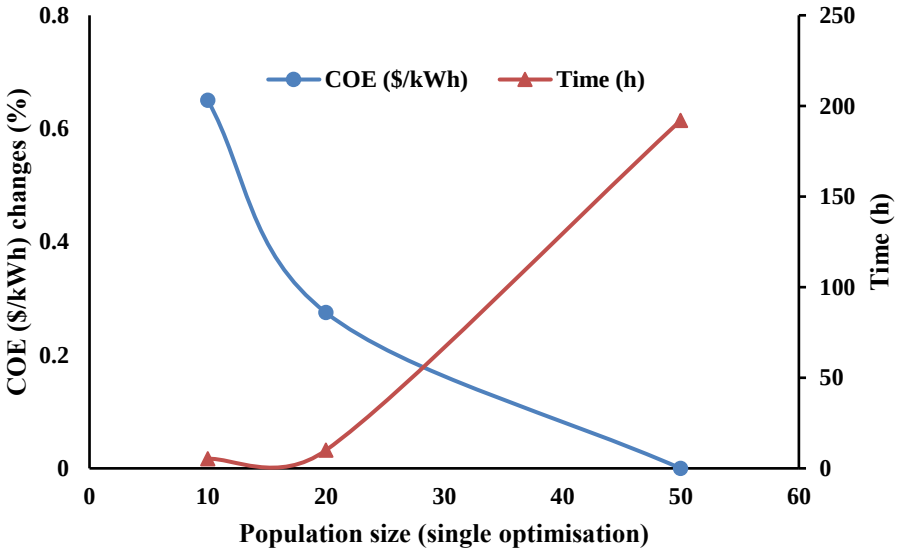

Fig. E.1: Effect of population size on system optimisation for PV/Batt system

Chapter 3 contains another sensitivity analysis to examine the susceptibility of up to two objective functions to GA population size. The reader is referred to that Chapter 3 Appendix for more details.